

HIGH TEMPERATURE GASIFICATION OF COAL CHAR  
IN CARBON DIOXIDE AND STEAM

by

MARK STEVEN DERSHOWITZ

SUBMITTED IN PARTIAL FULFILLMENT  
OF THE REQUIREMENTS FOR THE  
DEGREES OF

BACHELOR OF SCIENCE

and

MASTER OF SCIENCE

at the

© MASSACHUSETTS INSTITUTE OF TECHNOLOGY

MAY 1979

Signature of Author.....  
Department of Chemical Engineering, May 1979

Certified by.....  
Thesis Supervisor

Certified by.....  
Thesis Supervisor

Accepted by.....  
Chairman, Department Committee

ARCHIVES  
MASSACHUSETTS INSTITUTE  
OF TECHNOLOGY

AUG 8 1979

LIBRARIES

HIGH TEMPERATURE GASIFICATION OF COAL CHAR  
IN CARBON DIOXIDE AND STEAM

by

MARK STEVEN DERSHOWITZ

Submitted to the Department of Chemical Engineering  
in May, 1979, in partial fulfillment of the requirements  
for the Degrees of Bachelor of Science and Master of Science.

ABSTRACT

Weight losses and changes in physical properties of a pulverized Montana Rosebud coal char (particle diameter 75 to 150 microns) were measured during gasification in carbon dioxide and steam. Reactions were studied in a laminar flow furnace, at gas temperatures of 1473 to 2113°K, 1 atmosphere total pressure, with residence times between 115 and 330 msec.

Apparent reaction rates were calculated by an integral reactor analysis. The intrinsic kinetics governing the char reactions with carbon dioxide and steam were deduced by evaluating the effects of heat and mass transfer rate limitations, both within the porous particles and in the boundary layer surrounding them. External heat transfer effects and internal mass transfer (pore diffusional) effects were found to be significant for both reactions. Particle temperatures were between 30 and 270°K below the gas temperature. Pore diffusion effectiveness factors ranged between 0.16 and 1.0 for the char-CO<sub>2</sub> reaction, and between 0.11 and 0.57 for the char-steam reaction.

The intrinsic rates of carbon gasification, expressed per unit total char surface area, were determined in the form of a power law model:

$$\text{Rate} = \tilde{A}'' \exp \left\{ -\frac{E}{RT_p} \right\} C^n \frac{\text{moles (carbon)}}{\text{cm}^2 \text{ sec}}$$

where C is the concentration (mole/cm<sup>3</sup>) of the oxidizing gas (CO<sub>2</sub> or H<sub>2</sub>), T<sub>p</sub> is the particle temperature, n is the order of reaction and E is the activation energy. The kinetic parameters determined were:

	<u>n</u>	<u>E</u> (kcal/mole)	<u><math>\tilde{A}''</math></u>	
char - CO <sub>2</sub>	0	50.1	1.09	mole·cm <sup>-2</sup> ·sec <sup>-1</sup>
char - H <sub>2</sub> O	1	57.5	1.35 x 10 <sup>7</sup>	cm·sec <sup>-1</sup>

In determining the above rates, changes in char surface area with burnoff were accounted for. The specific (nitrogen adsorption) surface area of the char samples was found to increase significantly from an initial value of 81 m<sup>2</sup>/g. Values as high as 369 m<sup>2</sup>/g (after 30% gasification

on a dry, ash-free basis, in steam at 1473°K) and 255 m<sup>2</sup>/g (after 8 d.a.f.% burnoff in carbon dioxide at 1473°K) were measured. Particle bulk density was also found to change with burnoff. Char bulk density decreased from an initial value of 0.49 g/cc to as low as 0.28 g/cc after 81 d.a.f.% weight loss in steam at 1773°K.

Thesis Supervisors: Jack B. Howard, Professor of Chemical Engineering  
Adel F. Sarofim, Professor of Chemical Engineering

Department of Chemical Engineering  
Massachusetts Institute of Technology  
Cambridge, Massachusetts 02139  
May 11, 1979

Professor George C. Newton, Jr.  
Secretary of the Faculty  
Massachusetts Institute of Technology  
Cambridge, Massachusetts 02139

Dear Professor Newton:

In accordance with the regulations of the Faculty, I herewith submit a thesis, entitled "High Temperature Gasification of Coal Char in Carbon Dioxide and Steam," in partial fulfillment of the requirements for the degrees of Bachelor of Science and Master of Science in Chemical Engineering at the Massachusetts Institute of Technology.

Respectfully submitted,

Mark S. Dershowitz

## ACKNOWLEDGEMENTS

I would like to thank Professor Howard and Professor Saroffm for providing the guidance for this work, and lending their insight toward solving the various problems which arose. I also thank them for a swift, but meaningful review of the draft of this thesis.

I offer special thanks to Ted Bush and Mike Serio, who designed the gas burner and provided invaluable assistance in the lab. Without their aid, the experimental work would never have been completed so quickly and efficiently. My appreciation also goes to Tony Modestino, who did much of the work preparing the furnace for operation, and provided much information regarding the experimental apparatus.

I am indebted to the Phillips Petroleum Company for funding this research, and for providing the analyses of the char physical properties. My contact at Phillips, Vic Giroux, was very helpful and thoroughly pleasant to work with.

I extend gratitude to Patty Rich and Pat Coakley, who helped guide me through the rigors of the thesis format. I also thank George Paganis for his assistance in proofreading.

My most sincere appreciation goes to Pegg Hunter at the M.I.T. Graduate Student Council, who allowed me free use of her office and typewriter, and provided the humor that is needed during an undertaking such as a thesis.

Lastly, I'd like to mention collectively all of my past and present colleagues at the Head Table of the Muddy Charles, who thought I would never finish. I'm glad you are all wrong.

TABLE OF CONTENTS

1.	INTRODUCTION AND BACKGROUND . . . . .	15
1.1	Motivation . . . . .	15
1.2	Overview of Coal Gasification Processes . . . . .	20
1.3	Overview of Heterogeneous Reactions . . . . .	27
1.4	Reactivity of Coal Char . . . . .	31
1.4.1	Effects of Chemical Structure . . . . .	31
1.4.2	Effects of Inorganic Impurities . . . . .	35
1.4.3	Effects of Pore Structure; Changes During Gasification . . . . .	37
1.5	Mechanisms and Kinetic Studies . . . . .	39
1.5.1	Carbon - Carbon Dioxide Systems . . . . .	42
1.5.2	Carbon - Steam Systems . . . . .	49
1.6	Objectives and Scope of Study . . . . .	55
2.	APPARATUS AND PROCEDURES . . . . .	57
2.1	Feed Material . . . . .	57
2.2	Experimental Apparatus - General Description . . . . .	57
2.2.1	Furnace/Reaction Zone Assembly . . . . .	61
2.2.2	Char Feeder . . . . .	63
2.2.3	Particle Collector and Vacuum System . . . . .	65
2.2.4	Gas Burner Assembly . . . . .	67
2.2.5	Gas Flow Control and Measurement . . . . .	69
2.2.6	Temperature Measurements . . . . .	69
2.2.7	Weight Measurements . . . . .	73

TABLE OF CONTENTS (Cont'd)

2.3	Procedure for Laminar Flow Furnace Experiments . . . . .	73
2.4	Ash Determination . . . . .	77
2.5	System Evaluation . . . . .	78
2.5.1	Main Gas Temperature and Velocity . . . . .	78
2.5.2	Char Particle Velocity . . . . .	82
2.5.3	Residence Time . . . . .	85
2.5.4	Particle Collection Efficiency . . . . .	86
2.5.5	Particle Heating Rate . . . . .	86
2.5.6	Reaction Quenching Efficiency . . . . .	87
2.5.7	Effect of Char Feed Rate . . . . .	87
2.5.8	Pyrolysis Effects . . . . .	88
2.5.9	Burner-Generated Main Gas Streams . . . . .	90
3.	RESULTS . . . . .	93
3.1	Overview . . . . .	93
3.2	Weight Loss Data . . . . .	94
3.2.1	Char - Carbon Dioxide Reaction . . . . .	94
3.2.2	Char - Steam Reaction . . . . .	97
4.	DISCUSSION OF RESULTS . . . . .	100
4.1	Power Law Kinetics . . . . .	100
4.2	Apparent Kinetics . . . . .	101
4.2.1	Char - Carbon Dioxide Reaction . . . . .	108
4.2.2	Char - Steam Reaction . . . . .	113
4.3	Changes in Physical Properties . . . . .	113

TABLE OF CONTENTS (Cont'd)

4.4	Effects of External (Interphase) Gradients . . .	122
4.4.1	Surface Temperature . . . . .	123
4.4.2	Surface Concentration . . . . .	130
4.5	Effects of Internal (Intraphase) Gradients . . .	131
4.5.1	Particle Temperature . . . . .	131
4.5.2	Reactant Concentration . . . . .	133
4.6	Correction for Surface Area . . . . .	140
4.7	Intrinsic Kinetics . . . . .	144
4.7.1	Char Gasification in Carbon Dioxide . . .	147
4.7.2	Char Gasification in Steam . . . . .	151
5.	CONCLUSIONS . . . . .	156
5.1	Intrinsic Kinetics of Char Gasification in Carbon Dioxide and Steam . . . . .	156
5.2	Physical Properties of the Char . . . . .	157
6.	RECOMMENDATIONS FOR FUTURE WORK . . . . .	159
Appendix A.	Char Gasification in Carbon Dioxide . . . . .	160
Appendix B.	Char Gasification in Steam . . . . .	164
Appendix C.	Char Pyrolysis . . . . .	167
Appendix D.	Calculation of Main Gas Stream Properties . . . . .	169
Appendix E.	Main Gas Viscosity . . . . .	171
Appendix F.	Main Gas Kinematic Viscosity . . . . .	175
Appendix G.	Main Gas Thermal Conductivity . . . . .	177



TABLE OF CONTENTS (Cont'd)

Appendix H.	Bulk Diffusion Coefficients . . . . .	183
Appendix I.	Pore Diffusivities . . . . .	187
Appendix J.	Particle Terminal Velocity . . . . .	191
Appendix K.	Ash Content of the Initial Char . . . . .	196
Appendix L.	Fitting Data to Linear Equations by the Method of Least Squares . . . . .	198
Appendix M.	Evaluation of $I(T_0, \bar{E}, \bar{n}, L)$ . . . . .	200
Appendix N.	Physical Changes During Gasification . . . . .	214
Appendix O.	Listing of Computer Programs . . . . .	217
LITERATURE REFERENCES . . . . .		238

LIST OF FIGURES

1.1	U.S. Gross Energy Consumption by Primary Energy Source . . . . .	17
1.2	Effect of Intrinsic Heterogeneous Reaction Rate on Reactant Gas Concentration Within Porous Char Particles . . . . .	29
1.3	Arrhenius Plot for Heterogeneous Reactions Showing the Three Regimes of Rate Controlling Mechanisms . . . . .	30
1.4	A Representation of Bituminous Coal Structure . . . . .	32
2.1	Schematic of Flow System for Char Gasification Studies . . . . .	60
2.2	Reactor Tube Assembly . . . . .	62
2.3	Char Feeder . . . . .	64
2.4	Particle Collection Probe . . . . .	66
2.5	Gas Burner Assembly . . . . .	68
2.6	Axial Temperature Profile . . . . .	71
2.7	Analytic Expression for Furnace Temperature Profile . . . . .	72
2.8	Estimation of Furnace Setting for High Temperature Experiments . . . . .	74
2.9	Developing Laminar Velocity Profile for Flow Through an Isothermal Tube . . . . .	81
2.10	Centerline Velocity for Developing Laminar Profile in an Isothermal Tube . . . . .	83
2.11	Effect of Char Feed Rate . . . . .	89
2.12	Effect of Burner-Generated CO <sub>2</sub> Main Gas Stream . . . . .	92
3.1	Char Weight Loss (d.a.f.) in CO <sub>2</sub> . . . . .	96
3.2	Char Weight Loss (d.a.f.) in Steam . . . . .	99
4.1	Differential Analysis of Apparent Rate of Char Gasification in Carbon Dioxide (Isothermal Reaction Zone) . . . . .	104
4.2	Differential Analysis of Apparent Rate of Char Gasification in Steam (Isothermal Reaction Zone) . . . . .	105

LIST OF FIGURES (Cont'd)

4.3	Comparison of Experimental Weight Loss Data with Values Predicted by Linear Regression Model for Char Gasification in Carbon Dioxide . . . . .	111
4.4	Comparison of Experimental Weight Loss Data with Values Predicted by Linear Regression Model for Char Gasification in Steam . . . . .	115
4.5	Specific Surface Area After Partial Gasification in Carbon Dioxide . . . . .	118
4.6	Specific Surface Area After Partial Gasification in Steam . . . . .	119
4.7	Char Density After Partial Gasification in Carbon Dioxide and Steam . . . . .	121
4.8	Initial Montana Rosebud Char Particles . . . . .	124
4.9	Char Particles After 8% Burnoff in Carbon Dioxide at 1473°K . . . . .	125
4.10	Char Particles After 50% Burnoff in Steam at 1773°K . . . . .	126
4.11	Mass Transfer Coefficients for Bulk Diffusion . . . . .	132
4.12	Intraphase (Isothermal) Effectiveness Factors as a Function of Thiele Modulus (Spherical Geometry) . . . . .	136
4.13	Intraphase (Isothermal) Effectiveness Factors as a Function of Weisz Modulus . . . . .	139
4.14	Char Gasification in Carbon Dioxide: Test for First Order Kinetics . . . . .	148
4.15	Char Gasification in Carbon Dioxide: Test for Zeroth Order Kinetics . . . . .	149
4.16	Char Gasification in Steam: Test for Zeroth Order Kinetics . . . . .	152
4.17	Char Gasification in Steam: Test for First Order Kinetics . . . . .	153
E.1	Pure Component Viscosities . . . . .	173
E.2	Main Gas Viscosities . . . . .	174
F.1	Main Gas Kinematic Viscosities . . . . .	176

LIST OF FIGURES (Cont'd)

G.1	Pure Component Thermal Conductivities ( $H_2O$ and $H_2$ ) . . . . .	178
G.2	Pure Component Thermal Conductivities ( $CO_2$ , $CO$ and $N_2$ ) . . . . .	179
G.3	Main Gas Thermal Conductivities . . . . .	182
H.1	Bulk Diffusion Coefficients for $CO_2-N_2$ and $H_2O-N_2$ Mixtures . . .	185

LIST OF TABLES

1.1	U.S. Gross Energy Consumption by Primary Source . . . . .	13
1.2	U.S. Energy Reserves and Resources . . . . .	19
1.3	Coal Gasification Processes . . . . .	22
1.4	Equilibrium Constants of Common Gasification Reactions . . . . .	25
1.5	Heat of Reaction of Common Gasification Reactions . . . . .	26
1.6	Basic Chemical Structures in Coal . . . . .	33
1.7	Investigations of Intrinsic Global Kinetic Parameters for Gasification of Carbon in Carbon Dioxide . . . . .	47
1.8	Investigations of Intrinsic Global Kinetic Parameters for Gasification of Carbon in Steam . . . . .	54
2.1	Properties of the Initial Char . . . . .	58
3.1	Summary of Gasification Results in CO <sub>2</sub> . . . . .	95
3.2	Summary of Gasification Results in Steam . . . . .	98
4.1	Apparent Kinetics of Char Gasification in Carbon Dioxide: Least Square Linear Regression Model . . . . .	110
4.2	Apparent Reaction Rates: Char Gasification in Carbon Dioxide. . . . .	112
4.3	Apparent Kinetics of Char Gasification in Steam: Least Square Linear Regression Model . . . . .	114
4.4	Apparent Reaction Rates: Char Gasification in Steam . . . . .	116
4.5	Char Gasification in Carbon Dioxide: Surface Temperatures and Reactant Concentrations . . . . .	128
4.6	Char Gasification in Steam: Surface Temperatures and Reactant Concentrations . . . . .	129
4.7	Intraphase Effectiveness Factors for Char Gasification in Carbon Dioxide . . . . .	141
4.8	Intraphase Effectiveness Factors for Char Gasification in Steam . . . . .	142

LIST OF TABLES (Cont'd)

4.9	Char Gasification in Carbon Dioxide: Tests for Zeroth Order and First Crder Intrinsic Kinetics . . . . .	145
4.10	Char Gasification in Steam: Tests for Zeroth Order and First Order Intrinsic Kinetics . . . . .	146
4.11	Intrinsic Kinetics of Montana Rosebud Char Gasification in Carbon Dioxide . . . . .	150
4.12	Intrinsic Kinetics of Montana Rosebud Char Gasification in Steam . . . . .	155
A.1	Results of Char Gasification Experiments in Carbon Dioxide . . .	161
B.1	Results of Char Gasification Experiments in Steam . . . . .	165
C.1	Results of Char Pyrolysis Experiments . . . . .	168
D.1	Nominal Compositions for Calculation of Main Gas Properties . .	170
E.1	Pure Component Boiling Point Data . . . . .	172
I.1	Pore Diffusion Coefficients for Char - Carbon Dioxide Systems. .	189
I.2	Pore Diffusion Coefficients for Char - Steam Systems . . . . .	190
J.1	Char Particle Terminal Velocities . . . . .	193
K.1	Results of Ash Determination Tests . . . . .	197
M.1	Numerical Integration of $I(T_o, \bar{E}, \bar{n}, L)$ for CO <sub>2</sub> Gasification Experiments . . . . .	201
M.2	Numerical Integration of $I(T_o, \bar{E}, \bar{n}, L)$ for Steam Gasification Experiments . . . . .	207
M.3	Linearization of $I(T_o, \bar{E}, \bar{n}, L)$ . . . . .	213
N.1	Physical Properties of Char Samples After Partial Gasification in Carbon Dioxide . . . . .	215
N.2	Physical Properties of Char Samples After Partial Gasification in Steam . . . . .	216

## Chapter 1

### INTRODUCTION AND BACKGROUND

#### 1.1 Motivation

From 1960 to 1972, world energy consumption increased at an annual rate of 4.9 percent. The projected rate of increase<sup>21</sup> through the year 1990 is 3.3 percent per year.

Energy consumption in the United States increased at a rate of 3.7 percent per year over the period of 1960 to 1973. Petroleum and natural gas consumption increased at rates of 4.2 and 4.8 percent per year, while consumption of coal increased at only 1.7 percent per year. Although domestic energy consumption declined<sup>76</sup> by two percent in 1974 and 1975, recent forecasts by the U.S. Department of Energy<sup>77</sup> predict total annual energy consumption to increase some forty percent by 1980 (to 106 quadrillion BTU per year). The fraction of energy supplied by petroleum and natural gas (49 and 26 percent, respectively, in 1977)<sup>76</sup> is expected to decrease (to 41 and 19 percent in 1990), while coal will supply 26 percent of our energy in 1990, compared with 19 percent in 1977. Figure 1.1 summarizes energy consumption in the United States over the period 1947 to 1977, with predictions to 1985 and 1990. Statistics from the United States Department of Energy<sup>19,77</sup> used to generate Figure 1.1

are presented in Table 1.1.

It seems preferable to meet our energy demand by using domestic sources of energy. Therefore, the projected increase in coal consumption in the United States is hardly unexpected, since some seventy percent of our energy reserves and resources<sup>21</sup> are in the form of coal deposits (see Table 1.2).

Depending on the end-use and environmental constraints, coal may be utilized in four major ways - gasification, combustion, liquefaction and pyrolysis. Gaseous fuels are easier to handle and distribute than are solid fuels. Environmental advantages of gaseous fuels include ease of sulfur removal and ability to burn without formation of particulate solids.<sup>78</sup>

Production of high-BTU gas from coal (synthetic natural gas, SNG) is projected<sup>21</sup> to increase at an annual rate of 29 percent between 1985 and 1990, with production reaching 1.3 trillion cubic feet per year in 1990 (1975 estimate, given oil priced at \$11 per barrel, under "business as usual" strategy). If the Federal Government takes actions to increase domestic supply of energy, production of SNG is projected at 2.8 trillion cubic feet per year by 1990. In light of the current price of imported oil (\$15 per barrel for oil from OPEC countries), these production estimates are



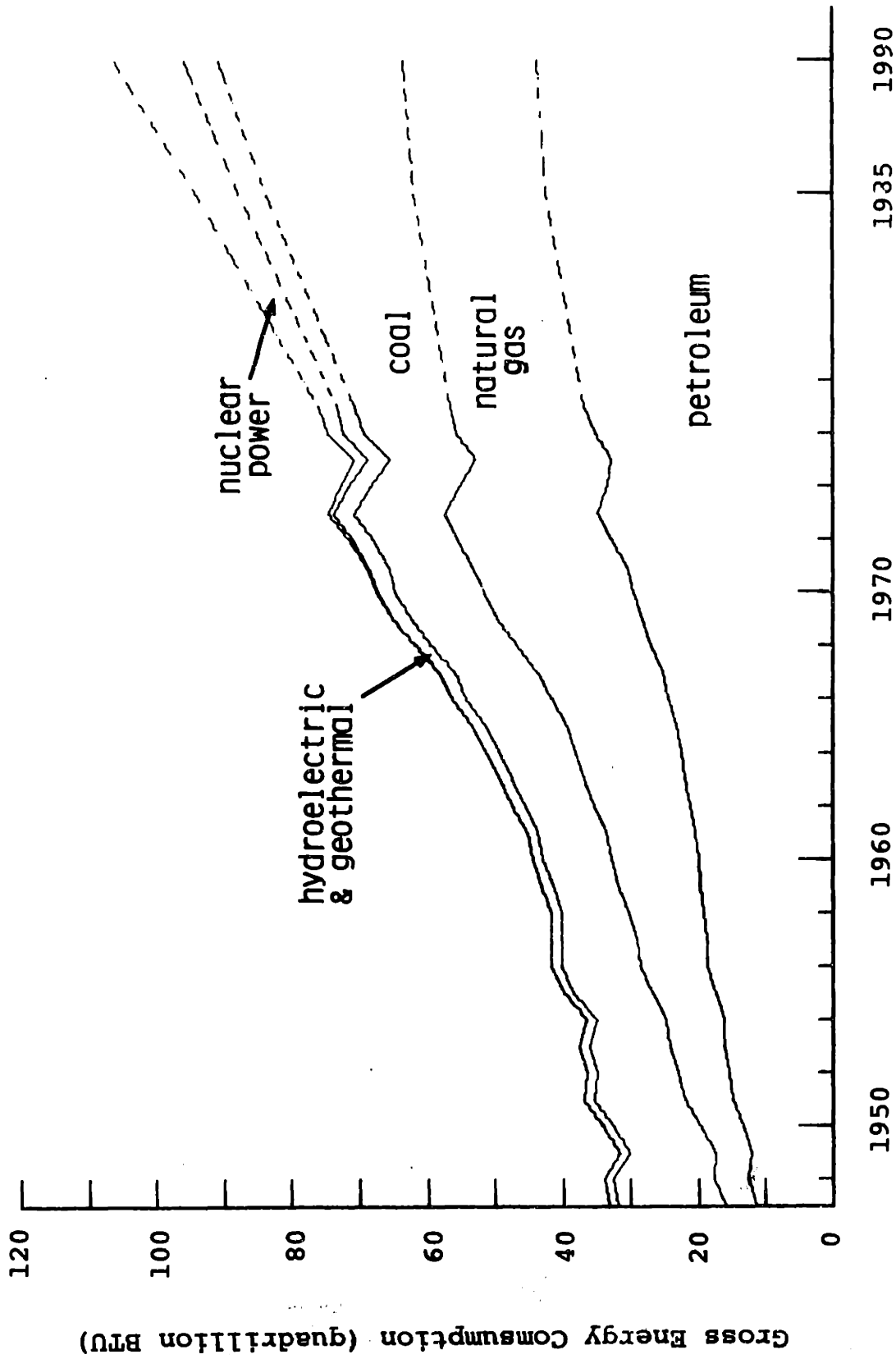


Figure 1.1 U.S. Gross Energy Consumption by Primary Energy Source <sup>21,77</sup>

Table 1.1

U.S. Gross Energy Consumption By Primary Energy Source <sup>21,77</sup>

<u>Year</u>	<u>Coal</u>	<u>Natural Gas (dry)</u>	<u>Petroleum<sup>a</sup></u>	<u>Hydroelectric &amp; Geothermal Power</u>	<u>Nuclear Electric Power</u>	<u>TOTAL</u>
(Quadrillion BTU)						
1947	15.824	4.518	11.367	1.326	-	33.035
1948	14.897	5.033	12.557	1.393	-	33.880
1949	12.631	5.289	12.119	1.449	-	31.488
1950	12.913	6.150	13.489	1.440	-	33.992
1951	13.225	7.248	14.848	1.454	-	36.775
1952	11.868	7.760	15.334	1.496	-	36.458
1953	11.893	8.156	16.098	1.439	-	37.586
1954	10.195	8.548	16.132	1.388	-	36.263
1955	11.540	9.232	17.524	1.407	-	39.703
1956	11.752	9.834	18.627	1.487	-	41.700
1957	11.168	10.416	18.570	1.551	0.001	41.706
1958	9.849	10.995	19.214	1.636	0.002	41.696
1959	9.810	11.990	19.747	1.591	0.002	43.140
1960	10.140	12.699	20.067	1.657	0.006	44.569
1961	9.906	13.228	20.487	1.680	0.018	45.319
1962	10.189	14.121	21.267	1.821	0.024	47.422
1963	10.714	14.843	21.950	1.767	0.034	49.308
1964	11.264	15.648	22.386	1.907	0.035	51.240
1965	11.908	16.098	23.241	2.058	0.038	53.343
1966	12.495	17.393	24.394	2.073	0.057	56.412
1967	12.256	18.250	25.335	2.344	0.080	58.265
1968	12.659	19.580	27.052	2.342	0.130	61.763
1969	12.733	21.020	28.421	2.659	0.146	64.979
1970	12.922	22.029	29.614	2.650	0.229	67.444
1971	12.560	22.734	30.492	2.833	0.391	69.010
1972	12.396	22.699	32.966	2.978	0.576	71.615
1973	13.286	22.512	34.852	3.048	0.888	74.586
1974	12.948	21.732	33.468	3.362	1.215	72.725
1975	12.828	19.948	32.742	3.289	1.839	70.646
1976	13.751	20.345	35.123	3.153	2.037	74.409
1977	14.129	19.613	36.947	2.591	2.674	75.953
1985	21.7	19.4	42.4	4.2	6.2	93.9
1990	27.3	19.9	43.6	5.0	10.4	106.2

<sup>a</sup> includes natural gas liquids

Table 1.2 U.S. Energy Reserves and Resources  
 (Source: Enzer et al, U.S. Dept. of the Interior, 1975)<sup>21</sup>

<u>Source</u>	<u>Reserves</u> <sup>a,b,c</sup>	<u>Resources</u> <sup>a,b,d</sup>
Coal	10400 <sup>e</sup>	21000
Petroleum <sup>f</sup>	424 - 540	1584 - 2860
Natural Gas	409 - 533	1441 - 2597
Shale Oil <sup>g</sup>	460 - 1160	2424
Uranium <sup>h</sup>	1920	3360
Geothermal	10	70 - 130
<b>TOTAL</b>	<b>13600 - 14600</b>	<b>29900 - 32400</b>

- a All figures are in quadrillion ( $10^{15}$ ) BTU.
- b Two values given represent minimum and maximum estimates.
- c Reserves are defined as identified deposits known to be recoverable with current technology under present economic conditions.
- d Resources include reserves as well as materials that have been identified, but cannot now be extracted because of economic or technological limitations, as well as economic or subeconomic materials that have not as yet been discovered.
- e U.S. Demonstrated Coal Reserve Base, January 1974. Recoverability varies between 40 and 90 percent for individual deposits. Fifty percent or more of the overall reserve is recoverable.
- f Including natural gas liquids.
- g From oil shale yielding at least 25 gallons of shale oil per ton of oil shale.
- h Using lightwater reactor, producing 400 billion BTU per ton of  $U_3O_8$ .

probably conservative.

Over the past 100 years or so, coal gasification techniques have been developed on a purely empirical basis.<sup>9</sup> In contrast, the present need to develop new, high performance gasifiers has led to a close examination of the basic principles of the processes involved:

- heat and mass transfer
- chemical equilibria
- kinetics of the heterogeneous chemical reactions involved.

## 1.2 Overview of Coal Gasification Processes

Coal gasification processes may be characterized by several different criteria, including the following:

1. Quality of product gas -
  - a. Low-BTU fuel                      100-200 BTU/scf
  - b. Medium-BTU fuel                 200-300 BTU/scf
  - c. High-BTU fuel (SNG)            900-1000 BTU/scf

Medium-BTU gas can be upgraded to SNG quality via catalytic methanation.

2. Gasifying medium. So-called "gasification" processes use steam and carbon dioxide (sometimes with hydrogen) as the oxidizing medium. "Hydrogasification" involves formation of methane by direct reaction of

coal or char with hydrogen.

3. Operating conditions (temperature and pressure).
4. Method of gas-solids contact (fixed bed, fluidized bed or entrained flow reactor, etc.).<sup>60</sup>
5. Allowable coal feedstocks.
6. Method of heat supply for the endothermic steam-carbon or CO<sub>2</sub>-carbon reactions -
  - a. Partial combustion of char
  - b. Limestone or dolomite "acceptor" (CO<sub>2</sub> Acceptor Process<sup>24</sup>)
  - c. Electrical energy
  - d. Molten baths<sup>75,79</sup>

Table 1.3 is a summary of several gasification and hydro-gasification processes.

Coal behavior during most gasification processes can be considered in two stages:

1. Pyrolysis (thermal decomposition), generally in the 400-900°C temperature range:

Coal  $\xrightarrow{\text{heat}}$  Solid (char) + Liquid (tar) + Gases

2. Heterogeneous reaction with oxidizing gases - see equations (1.1) through (1.6).

Table 1.3

Coal Gasification Processes

<u>Process (Developer)</u>	<u>Gas Quality (a)</u>	<u>Type of Reactor</u>	<u>Operating Conditions</u>		<u>Current Status (c)</u>
			<u>Pres. (b)</u>	<u>T(°K)</u>	
<u>Gasification</u>					
CO <sub>2</sub> Acceptor (Consolidation Coal Co.) <sup>2,73</sup>	m,h	fluidized	m	{ gasifier 1100 regenerator 1300	PP (1977)
Koppers-Totzek (Heinrich Koppers GmbH of Issen) <sup>60</sup>	m,h	entrained	1	1200-1550	Commercial
Lurgi (Lurgi Mineralotechnik GmbH) <sup>62,73</sup>	l,m,h	fixed bed	m	900-1050	Commercial
Molten Salt (Rockwell Intl.) <sup>73</sup>	l	molten salt bath	m	1250	1 t/hr PDU (1977)
Synthane (Lummus Co.) <sup>36,73</sup>	h	fluidized	h	{ preheater 700 gasifier 1250	72 t/d PP (1977)
U-GAS <sup>TM</sup> (Institute of Gas Technology) <sup>59</sup>	l	fluidized	m	{ preheater 700 gasifier 1300	PP (1975)
Wellman-Galusha (Wellman Eng. Co.) <sup>73</sup>	l	fixed bed	1	800-900	Commercial
Westinghouse (Westinghouse) <sup>66,73</sup>	l	fluidized	m	{ devolatilizer 1050 gasifier 1150-1400	15 t/d PDU (1977)
Winkler (Davy Power Gas, Inc.) <sup>4,60</sup>	l,m,h	fluidized	1	1100-1250	Commercial
<u>Hydrogasification</u>					
BI-GAS (Bituminous Coal Research, Inc.) <sup>73</sup>	h	entrained	h	{ 1st stage 1500 2nd stage 1200	120 t/d PP (1977)
Hydrane (Dept. of Energy) <sup>32,60</sup>	m,h	fluidized	h	{ upper zone 1100 hydrogasifier 950	1/2 t/d PP (1974)
HYGAS <sup>®</sup> (Institute of Gas Technology) <sup>68,73</sup>	h	fluidized	h	{ preheater 700 gasifying stages 900-1300	75 t/d PP (1977)

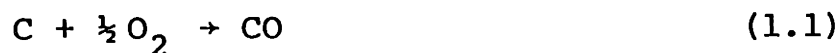
Table 1.3 continued

Notes to Table 1.3

- (a) Product gas quality:
- |   |            |                        |
|---|------------|------------------------|
| l | low-BTU    | 100-200 BTU/scf        |
| m | medium-BTU | 200-300 BTU/scf        |
| h | high-BTU   | 900-1000 BTU/scf (SNG) |
- (b) Operating pressure:
- |   |        |                            |
|---|--------|----------------------------|
| l | low    | < 3 atm                    |
| m | medium | up to approximately 35 atm |
| h | high   | above 35 atm               |
- (c) Current status:
- |     |                            |
|-----|----------------------------|
| PP  | pilot plant                |
| PDU | process demonstration unit |

The principal chemical reactions related to coal gasification are as follows:

Char combustion



CO<sub>2</sub> and steam gasification



Water-Gas shift reaction



Direct methanation (hydrogasification)



Gasification reactions (1.3) and (1.4) are endothermic. The heat required to sustain them is often provided by supplying oxygen to the gasifier to promote the exothermic reactions (1.1) and (1.2). At low pressures and high temperatures, reaction (1.6) is of little importance. The water-gas shift, reaction (1.5), is not a primary gasification reaction (i.e., it does not directly involve the carbon in the coal/char). The extent of reaction (1.5) is determined by equilibrium considerations within the gasifier.

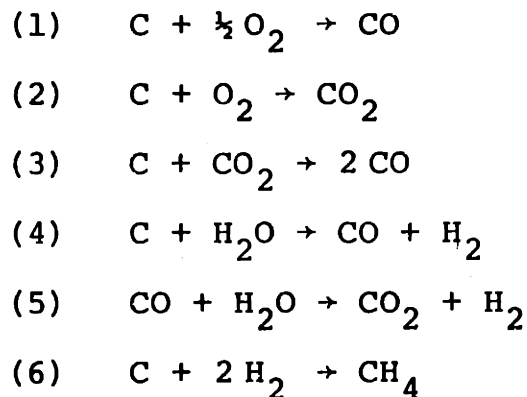


Table 1.4  
Equilibrium Constants of Common Gasification Reactions  
 (Source: Von Fredersdorff and Elliott, 1963)<sup>80</sup>

	(1)	(2)	(3)	(4)	(5)	(6)
	$C + \frac{1}{2} O_2 \rightarrow CO$	$C + O_2 \rightarrow CO_2$	$C + CO_2 \rightarrow 2CO$	$C + H_2O \rightarrow CO + H_2$	$CO + H_2O \rightarrow CO_2 + H_2$	$C + 2H_2 \rightarrow CH_4$
Temperature (°K)	$\log_{10} K_p$ (a)					
	(1)	(2)	(3)	(4)	(5)	(6)
300	24.05	69.09	-21.00	-16.00	4.996	8.899
600	14.34	34.40	-5.729	-4.297	1.432	2.000
800	11.93	25.83	-1.963	-1.357	0.606	0.150
900	11.13	22.97	-0.716	-0.372	0.344	-0.488
1000	10.48	20.68	0.278	0.418	0.139	-1.007
1100	9.945	18.80	1.087	1.064	-0.023	-1.435
1200	9.498	17.24	1.756	1.601	-0.154	-1.794
1300	9.118	15.92	2.319	2.057	-0.262	-2.101
1400	8.790	14.78	2.798	2.446	-0.352	-2.363
1500	8.504	13.80	3.210	2.784	-0.426	-2.592
1750	7.926	11.83	4.024	3.455	-0.569	-
2000	7.486	10.35	4.622	3.956	-0.667	-
2250	7.138	9.197	5.079	4.341	-0.738	-
2500	6.854	8.277	5.432	4.647	-0.785	-

(a) Carbon as  $\beta$ -Graphite  
 Partial pressures measured in atmospheres

Table 1.5  
Heat of Reaction of Common Gasification Reactions  
 (Source: Von Fredersdorff and Elliott, 1963)<sup>80</sup>



Temperature (°K)	Heat of Reaction (kcal/mole) (carbon as $\beta$ -graphite)					
	(1)	(2)	(3)	(4)	(5)	(6)
0	-27.20	-93.97	39.56	29.91	-9.66	-15.99
298	-26.42	-94.05	41.22	31.38	-9.84	-17.89
600	-26.33	-94.12	41.46	32.16	-9.30	-19.89
900	-26.64	-94.27	40.99	32.42	-8.58	-21.17
1200	-27.06	-94.41	40.30	32.44	-7.86	-21.79
1500	-27.55	-94.56	39.47	32.30	-7.17	-22.06
1750	-27.99	-94.68	38.70	32.08	-6.62	-
2000	-28.46	-94.83	37.91	31.80	-6.11	-
2250	-28.94	-94.98	37.10	31.49	-5.61	-
2500	-29.45	-95.14	36.24	31.14	-5.10	-

### 1.3 Overview of Heterogeneous Reactions

Heterogeneous reactions occur by way of both diffusional and chemical steps:

1. Diffusion of reactants from the bulk gas stream through a relatively stagnant film to the solid surface and to available capillary areas or pore structure.
2. Adsorption of reactants on the solid.
3. Surface chemical reaction (which may be preceded by reactant dissociation).
4. Desorption of surface reaction products (which contain one or more of the underlying atoms previously part of the solid).
5. Diffusion of the gaseous product into the bulk gas stream.

A study of the gas-carbon(char) reaction kinetics must necessarily consider both diffusional and chemical kinetic effects.

The rate at which a particular char sample reacts at a given temperature should be proportional to the total surface area of the sample, provided that all unit areas are equally reactive and are exposed to the same concentration of reactant gas molecules. Under these conditions, a reaction is said to be chemically controlled, and the observed reaction rate is in fact the intrinsic chemical reaction rate.

Rates of the adsorption, surface reaction and desorption steps are slow compared with rates of diffusion (both bulk phase and pore diffusion). The reactant gas concentration is uniform throughout the particle, and equal to  $C_0$ , the bulk phase concentration. This is shown in Figure 1.2 as curve I. The observed activation energy, shown by an Arrhenius plot (Figure 1.3), is of course, the intrinsic (true) activation energy for the reaction, for that particular char.

As temperature increases, the intrinsic reaction rate increases to such an extent that the rate of diffusion of reactant gas molecules through the internal pore structure of the char particles limits the rate at which the reaction may proceed. As shown by curve II in Figure 1.2, the concentration of reactant gases within the porous structure of the particle falls below the bulk gas concentration, and hence the observed reaction rate decreases. The observed activation energy in this regime (section II in Figure 1.3) is approximately one-half of the intrinsic value. The transition from regime I to regime II would be represented by curve a in Figure 1.2.

At still higher temperatures, the reaction rate becomes limited by the rate at which reactant gas molecules can diffuse through the stagnant gas film surrounding the particle (curve III in Figure 1.2). Shown in regime III of Figure 1.3, the observed activation energy for the reaction

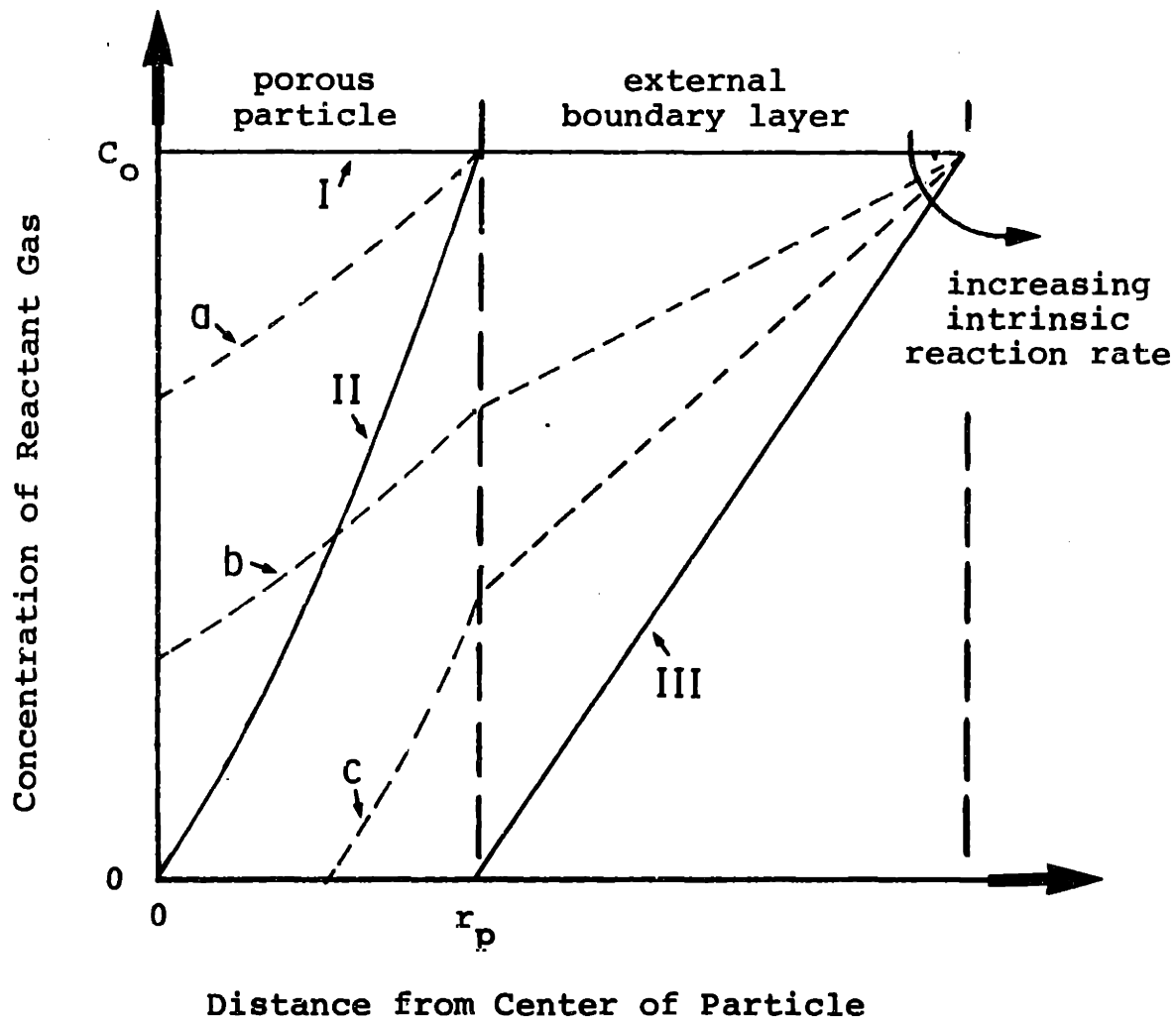


Figure 1.2 Effect of Intrinsic Heterogeneous Reaction Rate on Reactant Gas Concentration Within a Porous Char Particle

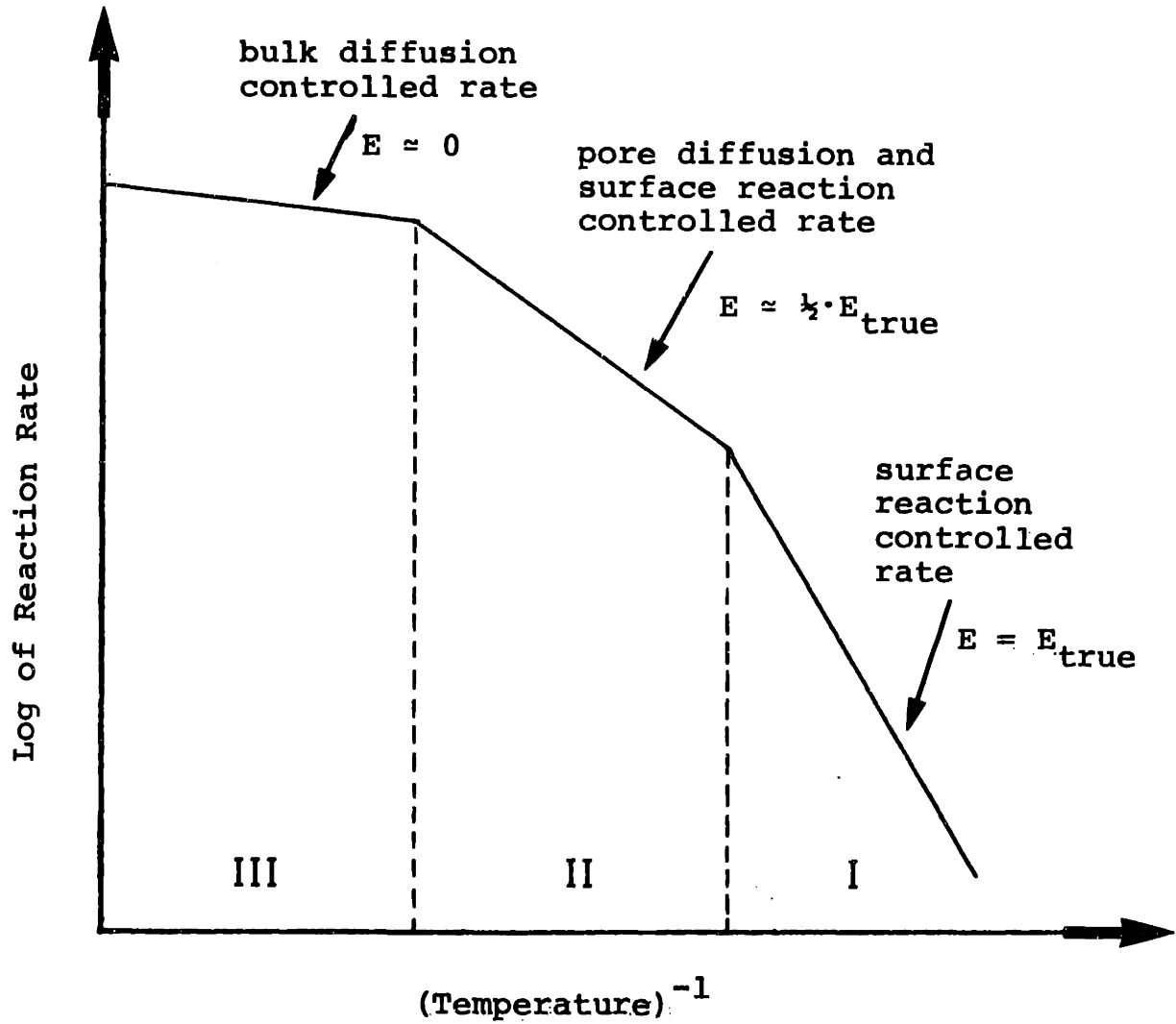


Figure 1.3 Arrhenius Plot for Heterogeneous Reactions Showing the Three Regimes Of Rate Controlling Mechanisms

equals the activation energy for bulk phase diffusion, which is generally in the range of 0 to 5 kcal/mole.

#### 1.4 Reactivity of Coal Char

Char usually accounts for 30 to 70 percent (by weight) of the original coal, following pyrolysis. It consists mostly of carbon and ash, with small amounts of hydrogen, oxygen, nitrogen and sulfur. The amount and composition of the char depends on such parameters as parent coal type, pyrolysis temperature and heating rate, pressure and particle size.

Char reactivity depends on three characteristics of the sample:

1. Chemical structure
2. Inorganic constituents
3. Pore structure

The effects of each of these factors will now be examined.

##### 1.4.1 Effects of Chemical Structure

The complex coal structure (Figure 1.4) requires analysis in terms of its characteristic functional groups. These fundamental groups, typifying the atomic species C, H, O, N and S, are summarized in Table 1.6.

A typical coal structure consists of aromatic/hydroaromatic clusters (average 2 to 5 rings per cluster) loosely

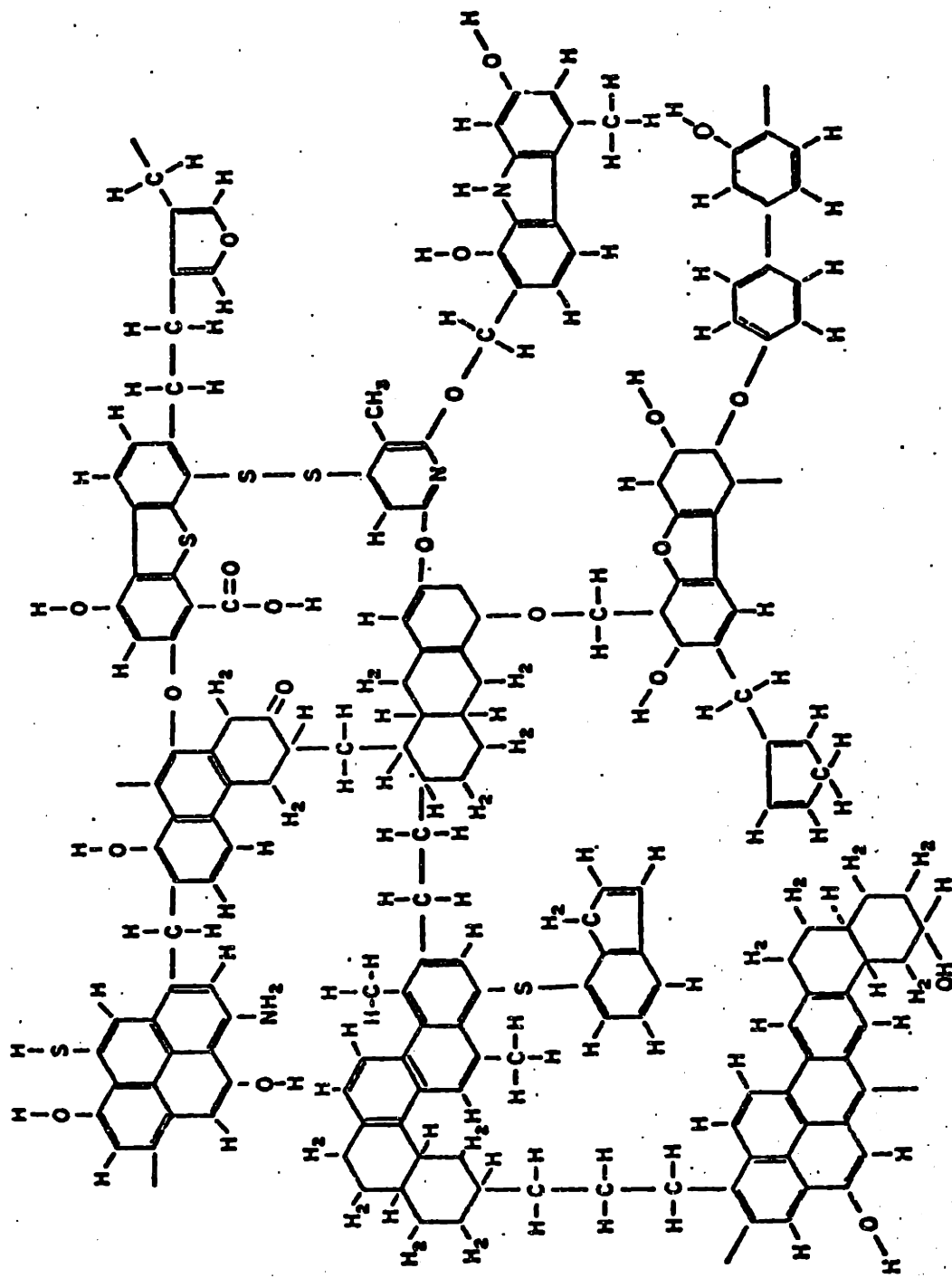
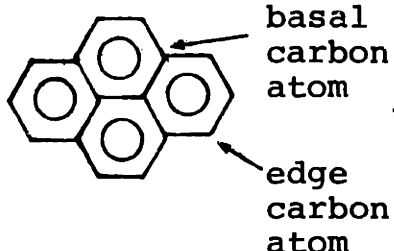
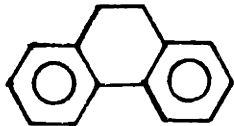

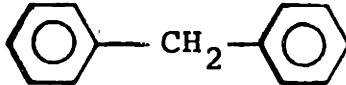
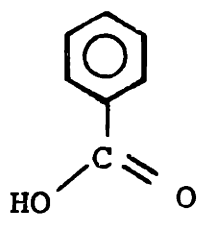




Figure 1.4 A Representation of Bituminous Coal Structure <sup>64</sup>



Table 1.6  
Basic Structures In Coal

<u>Atomic Species</u>	<u>Fundamental Group</u>	<u>Typical Examples</u>
<b>C</b>	polynuclear aromatics	
	hydroaromatics	
<b>H</b>	aliphatics	
		
<b>O</b>	hydroxyl - OH	
	carboxyl - C(=O)OH	
	carbonyl >C=O	
<b>N</b> <b>S</b>	substituted aromatics	
	heterocyclics	

joined together by methylene, ether and sulfide linkages, 1 to 3 carbon atoms in length.<sup>47</sup> The loose aliphatic linkages allow cross-linking between clusters on different planes, and hence the development of an extensive pore structure.<sup>29</sup> Aliphatic, hydroaromatic and heterocyclic bonds are quite susceptible to bond breakage at pyrolysis temperatures.<sup>29</sup>

Chars are characterized by highly carbon-rich, polynuclear aromatic structures. Edge carbon atoms are at least one order of magnitude more reactive than basal carbon atoms.<sup>81</sup> Increased activity at carbon edges is presumed to be due to the availability of unpaired  $\sigma$  electrons which are available to form bonds with chemisorbed species.<sup>45</sup> The  $\sigma$  electrons of basal carbon atoms are tied up in chemical bonds with adjacent carbon atoms. Furthermore, impurities which may catalyze certain carbon reactions (section 1.4.2) tend to diffuse and concentrate at crystallite edges.<sup>81</sup> Enhanced activity found at defects in the char structure (such as vacancies) is probably due to geometric or charge imbalances.<sup>71</sup>

Oxygen and hydrogen sites also promote char reactivity since chemisorption on non-aromatic sites is usually favored to aromatic sites.<sup>47</sup> Oxygen sites are thought to influence reactivity via electron exchanges.<sup>47</sup> Hydrogen sites are presumed to increase char reactivity by preferential oxidation.<sup>40,47</sup> Nitrogen and sulfur could promote ring structure

attack since  $\pi$  electrons are most available at heterocyclic sites.

#### 1.4.2 Effects of Inorganic Impurities

Inorganic impurities in coal char occur in two forms - mineral matter and trace metals. Mineral matter is typically 10 to 30 percent by weight in raw coals, consisting of four major types:

1. Alumino-silicates (clays), such as kaolinite ( $\text{Al}_2\text{Si}_2\text{O}_5(\text{OH})_4$ ) and illite ( $\text{KAl}_3\text{Si}_3\text{O}_{10}(\text{OH})_2$ ).
2. Oxides, such as silica ( $\text{SiO}_2$ ) and hematite ( $\text{Fe}_2\text{O}_3$ ).
3. Carbonates, such as calcite ( $\text{CaCO}_3$ ), siderite ( $\text{FeCO}_3$ ), dolomite ( $\text{CaCO}_3 \cdot \text{MgCO}_3$ ) and ankerite ( $2\text{CaCO}_3 \cdot \text{MgCO}_3 \cdot \text{FeCO}_3$ ).
4. Sulfides and sulfates, such as pyrite ( $\text{FeS}$ ) and gypsum ( $\text{CaSO}_4 \cdot 2\text{H}_2\text{O}$ ).

Typically, mineral matter is randomly distributed in coal as inclusions on the order of 2 microns in diameter. During pyrolysis, gasification or combustion, mineral matter is transformed to ash ( $\text{SiO}_2$ ,  $\text{Al}_2\text{O}_3$ ,  $\text{Fe}_2\text{O}_3$ ,  $\text{CaO}$ ,  $\text{MgO}$ ).

Some 20 to 30 trace metals are also distributed throughout the coal structure. They are either organically bound to the coal molecule (e.g., boron), bonded inorganically to mineral matter (e.g., zirconium, manganese) or occur in both

organic and inorganic forms (e.g., copper). Typical concentrations of trace metals in coal are 5 to 500 ppm, although some elements (e.g., B, Ba, Sr, Cu, Mn, Sn, Zr) often appear at the 500 to 1000 ppm level.<sup>47</sup>

Mineral matter and trace elements can provide direct catalytic activity (particularly iron, calcium and manganese compounds). Laine et al<sup>45</sup> discuss findings that as little as 100 ppm iron can increase carbon reactivity in CO<sub>2</sub> by a factor of 150. Kayembe and Pulsifer<sup>43</sup> found that 10 percent (by weight) of K<sub>2</sub>CO<sub>3</sub> reduced the activation energy of the steam gasification of a Bear coal char from 61 to 35 kcal/mole, at 600-850°C and 1 atm total pressure. Other salts found to have catalytic effects at those conditions were (in decreasing order of effectiveness) Na<sub>2</sub>CO<sub>3</sub>, Li<sub>2</sub>CO<sub>3</sub>, KCl, NaCl and CuO. Surface impurities can also affect secondary reactions, such as the water-gas shift.

There are several theories for the effects of mineral matter and trace metals on char reactivity. The geometric or transfer theory<sup>71</sup> suggests that an oxidative intermediate formed by reactant dissociation at a nearby catalytic site migrates to react with carbon. The electronic theory<sup>71</sup> suggests that chemisorption and desorption are favored at covalent or ionic carbon-metal bonds generated by electron transfer. Long and Sykes<sup>50</sup> suggest that catalytic effects

are due to interaction with the  $\pi$  electrons of the carbon (graphite) lattice, causing changes in bond order which facilitate reaction at the active edge sites.

#### 1.4.3 Effects of Pore Structure; Changes During Gasification

The pore structure of a char particle determines the local concentration of reactant gas molecules within the particle. Pore structure is characterized by three parameters:

1. Specific internal surface area ( $S_g$ ,  $m^2/g$ )
2. Specific internal pore volume ( $V_g$ ,  $cm^3/g$ )
3. Distribution of internal volume or area over the range of pore diameters,  $\delta$ .

Pores may be roughly classified as micropores ( $\delta > 20$  angstroms), mesopores ( $20 < \delta < 500 \text{ \AA}$ ) or macropores ( $\delta > 500 \text{ \AA}$ ). Classification by pore diameter,  $\delta$  would imply cylindrical geometry of pores. Electron microscopy studies by Harris and Yost<sup>35</sup> indicate both cylindrical and conical pores, as well as flat cavities. X-ray studies by Hirsch<sup>38</sup> indicate that macropores reflect weak cross-linking among condensed aromatic and hydroaromatic clusters.

Pore size distribution determines the accessibility of internal surface area to reactant gases. Large surface area of the smallest pores may not be accessible to a reactant unless large feeder pores exist, or the reaction kinetics are

slow enough to allow time for diffusion into these micropores. Dutta et al<sup>20</sup> found that only pores with  $\delta > 20$  to  $40 \text{ \AA}$  were available for reaction with  $\text{CO}_2$  at  $840\text{--}1100^\circ\text{C}$ .

Typically, average pore diameter  $\bar{\delta}$  decreases with increasing rank of parent coals. Hippo and Walker<sup>37</sup> studied the reactivities of sixteen chars in  $\text{CO}_2$  at  $900^\circ\text{C}$ . A char from a Pennsylvania low volatile bituminous coal was over 150 times less reactive than a Montana lignite char. This was attributed to a relative absence of large feeder pores, resulting in poor utilization of the total surface area.

The pore structure of a coal char changes during gasification. Turkdogan et al<sup>73</sup> suggest that, depending on the type of carbon, up to 50 percent of the volume is initially isolated by micropores, and is unavailable for reaction. (The surface areas investigated ranged from  $0.1$  to  $1100 \text{ m}^2/\text{g}$ ). During early stages of gasification, specific surface area (and therefore reaction rate) increases. Walker et al<sup>85</sup> concluded that the reaction develops new surface area by (to a small extent) enlarging micropores, but principally by opening up pore volume not previously accessible to reactants because the microcapillaries were too small or because existing pores were unconnected. As the reaction proceeds, surface area and reaction rate increase until the rate of formation of new area equals the rate of destruction of old

area. After that point, surface area tends to remain constant or decrease slightly.

The activity of char reaction sites is also subject to change, either during gasification or as a result of heat pretreatment. Duval<sup>80</sup> reported that active sites disappear spontaneously due to a thermal healing or annealing of the surface. This annealing process increases rapidly with temperature. Strickland-Constable<sup>70</sup> studied reactions of carbon filaments in CO<sub>2</sub> and steam at 900-2000°C. He explained this effect above 1200°C as a straightening of the molecular plane edges, whereby protruding atoms can move along the edge to fill vacancies, thus reducing reactivity. Goring et al<sup>30</sup> observed a decrease in reactivity of a Pittsburgh seam coal in CO<sub>2</sub> and steam at 875°C by pretreating the char up to 24 hours in nitrogen at 875°C.

### 1.5 Mechanisms and Kinetic Studies

The mechanism and kinetics of the carbon-carbon dioxide reaction (1.3) and carbon-steam reaction (1.4) have been studied extensively. The carbon in these studies varied from high purity graphites to coals and chars. Most of the studies have found the reactions to follow the Langmuir-Hinshelwood kinetics model,

$$\text{Rate of Carbon Gasification} = \frac{k_1 P_1}{1 + k_2 P_2 + k_3 P_1} \quad (1.7)$$

where  $P_1$  and  $P_2$  are the partial pressures of  $\text{CO}_2$  and  $\text{CO}$  (carbon- $\text{CO}_2$  system) or  $\text{H}_2\text{O}$  and  $\text{H}_2$  (carbon-steam system). (Often, concentrations are used instead of partial pressures.) The constants  $k_1$ ,  $k_2$  and  $k_3$ , functions of temperature and the particular carbon being studied, can be related to the rate constants of the individual steps in the reaction mechanisms. Note that equation (1.7) predicts that carbon monoxide will inhibit gasification rates in carbon dioxide, and that hydrogen will inhibit steam gasification rates.

The constants  $k_1$ ,  $k_2$  and  $k_3$  in equation (1.7) can be calculated by considering:

$$\frac{1}{\text{Rate}} = \left\{ \frac{1 + k_2 P_2}{k_1} \right\} \cdot \frac{1}{P_1} + \frac{k_3}{k_1} \quad (1.8)$$

$$= \left\{ \frac{k_2}{k_1 P_1} \right\} \cdot P_2 + \left\{ \frac{1 + k_3 P_1}{k_1 P_1} \right\} \quad (1.9)$$

Thus, at a given temperature, the constants may be determined by performing two sets of experiments:

1. Vary  $P_1$  while holding  $P_2$  constant; plot the reciprocal rate against  $(1/P_1)$ , as in equation (1.8).
2. Vary  $P_2$  while holding  $P_1$  constant; plot the reciprocal rate against  $P_2$ , as in equation (1.9).



Equation (1.7) represents a wide range of conditions.

Two cases should be noted:

Case I. For the conditions

$$k_2 P_2 \ll 1 \quad \text{and} \quad k_3 P_1 \ll 1 \quad (1.10)$$

the rate of gasification becomes

$$\text{Rate} \longrightarrow k_1 P_1 \quad (1.11)$$

and the reaction appears to be first order with respect to component 1 ( $\text{CO}_2$  or  $\text{H}_2\text{O}$ ) partial pressure. Conditions (1.10) may be expected at low pressure (on the order of 1 atm) and high temperature<sup>20</sup> ( $k_2$  and  $k_3$  generally decrease rapidly with temperature).

Case II. For the conditions

$$k_2 P_2 \ll 1 \quad \text{and} \quad k_3 P_1 \gg 1 \quad (1.12)$$

the rate of gasification becomes

$$\text{Rate} \longrightarrow k_1/k_3 \quad (1.13)$$

and the reaction appears to be independent (0th order) of the oxidizing gas partial pressure. Conditions (1.12) are expected at high pressure (>15 atm).<sup>20</sup> The exact conditions for which either (1.11) or (1.13) can be expected to apply will depend largely on the particular type of carbon being investigated.

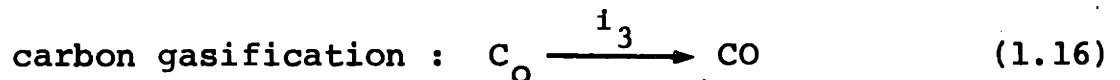
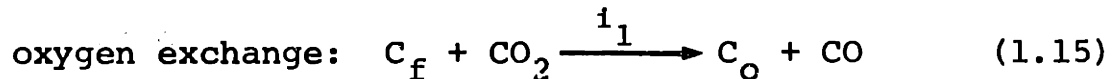
### 1.5.1 Carbon - Carbon Dioxide Systems

For carbon-CO<sub>2</sub> studies, equation (1.7) becomes

$$\text{Rate} = \frac{k_1 P_{\text{CO}_2}}{1 + k_2 P_{\text{CO}} + k_3 P_{\text{CO}_2}} \quad (1.14)$$

Two mechanisms have been postulated to justify equation (1.14).

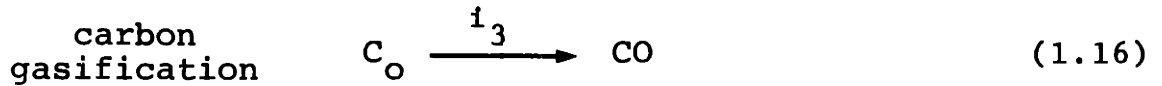
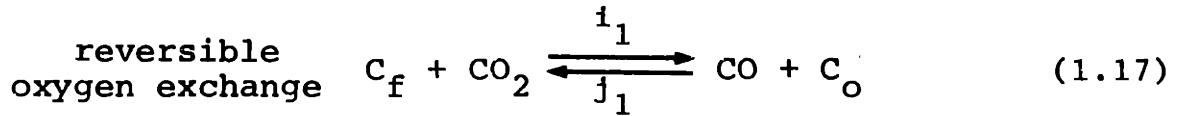
Both mechanisms propose chemical bonding of an oxygen atom (from a CO<sub>2</sub> molecule) to a free surface carbon atom (denoted by C<sub>f</sub>), forming a surface oxide (denoted by C<sub>o</sub>) and a gaseous molecule of carbon monoxide. This is followed by a slow desorption of the surface oxide as a second CO molecule. These steps are represented by,



Brown,<sup>14</sup> using a C<sup>14</sup>O<sub>2</sub> tracer, showed that some CO<sub>2</sub> molecules are able to enter into the surface, leaving two oxygen atoms to remove two free surface carbon sites, but that this accounted for only 1 to 2 percent of the total number of reaction sites.

The proposed mechanisms differ in explaining the retarding effect of CO on the overall reaction. Ergun<sup>22</sup> suggests (mechanism A) that the retarding effect is due to the reverse

of reaction (1.15), and hence the complete mechanism is,



whereby carbon monoxide reduces the concentration of the surface oxide complex, thereby reducing the rate of reaction (1.16). Equations (1.15), (1.16) and (1.17) may be used to derive equation (1.14). The rate of carbon transfer to the gas phase, given by equation (1.16), is

$$\text{Rate} = i_3 \cdot [C_o] \quad (1.18)$$

where  $[C_o]$  is the concentration of the surface oxide complex. Assume that the total number of active sites,  $C_t$  is constant, and that all sites are equivalent:

$$C_t = C_f + C_o \quad (1.19)$$

Using the steady state approximation for the surface oxide,

$$\begin{aligned} \frac{d}{dt} [C_o] &= i_1 [C_f] P_{CO_2} - j_1 P_{CO} [C_o] - i_3 [C_o] \\ &= i_1 P_{CO_2} [C_t] + [C_o] (i_3 + j_1 P_{CO} + i_1 P_{CO_2}) = 0 \end{aligned} \quad (1.20)$$

$[C_o]$  may be calculated:

$$[C_o] = \frac{i_1 [C_t] P_{CO_2}}{i_3 + j_1 P_{CO} + i_1 P_{CO_2}} \quad (1.21)$$

Combining equations (1.18) and (1.21), the rate of carbon gasification becomes:

$$\text{Rate} = \frac{i_1 [C_t] P_{\text{CO}_2}}{1 + \frac{j_1}{i_3} P_{\text{CO}} + \frac{i_1}{i_3} P_{\text{CO}_2}} \quad (1.22)$$

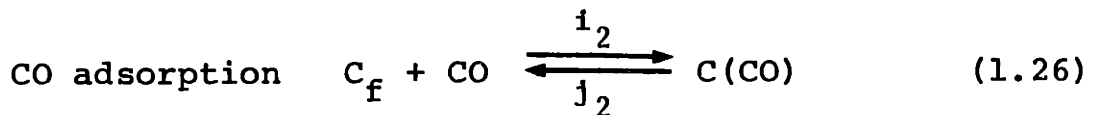
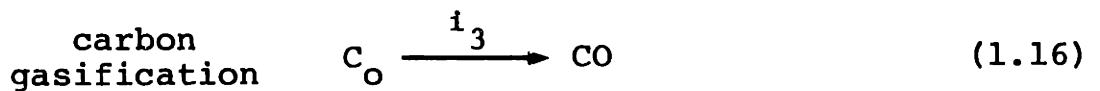
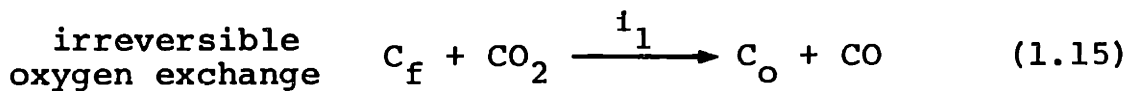
and the Langmuir-Hinshelwood constants in equation (1.14) are seen to be (Mechanism A):

$$k_1 = i_1 [C_t] \quad (1.23)$$

$$k_2 = j_1 / i_3 \quad (1.24)$$

$$k_3 = i_1 / i_3 \quad (1.25)$$

An alternate formulation (Mechanism B) supported by Gadsby et al<sup>27</sup> suggests that adsorption of carbon monoxide on free surface sites is the rate hindering step:



The Langmuir-Hinshelwood constants in equation (1.14) become (Mechanism B):

$$k_1 = i_1 [C_t] \quad (1.27)$$

$$k_2 = i_2 / j_2 \quad (1.28)$$

$$k_3 = i_1 / i_3 \quad (1.29)$$

Long and Sykes<sup>51</sup> and Blakeley and Overholser<sup>11,58</sup> found that hydrogen, in addition to carbon monoxide, inhibited carbon gasification in carbon dioxide. This cannot be explained by an expression of the form (1.14).

Mechanism A is the most widely accepted explanation for gasification in CO<sub>2</sub>, near or below atmospheric pressure.<sup>80</sup> Menster and Ergun,<sup>56</sup> using C<sup>14</sup>O<sub>2</sub> to follow oxygen exchange on a carbon black at 750-859°C, found no definitive evidence for CO adsorption, equation (1.26).

Literature values of the activation energy for carbon - carbon dioxide systems vary considerably (see Table 1.7). Often, a global value (i.e., for equation (1.3)) is reported, rather than three separate values corresponding to the constants  $k_1$ ,  $k_2$  and  $k_3$  in equation (1.14). Notice that if the activation energy is simply evaluated from the temperature dependence of  $k_1$ :

$$k_1 = i_1 [C_t] \quad (1.23)$$

so

$$E = E_{i_1} + E_t \quad (1.30)$$

If  $[C_t]$  is approximately independent of temperature,  $E_t \approx 0$  and  $E \approx E_{i_1}$ , so the activation energy is that of the forward step of the oxygen exchange reaction (1.17).

The kinetics of gasification of many different carbons in CO<sub>2</sub> have been investigated. Rather than being related to coal

and char gasification, most of the previous studies have been motivated by applications of so-called "pure" forms of carbon, such as the use of graphites as electrodes, structural carbons and moderators in atomic reactors. In the latter instances, the motivation is to determine conditions for which carbon reactivity is minimized. Nonetheless, insight into the char gasification reactions can be obtained from the pure carbon gasification studies. In particular, it is interesting to note the temperatures of changing regimes of rate control (i.e., transition from intrinsic kinetic control to pore diffusional control to bulk diffusional control of the reaction rate). Table 1.7 is a summary of some of these studies. Notice the wide range of activation energies (33 to 104 kcal/mole), in part attributable to variations in the types of carbon investigated. It is also possible that some of the earlier investigators neglected to account for all diffusional effects. (Recall that in the temperature range of pore diffusional rate limitations,  $E_{\text{observed}} \approx \frac{1}{2} E_{\text{true}}$ .) Global kinetic parameters are listed since not all studies were correlated with the three-parameter ( $k_1, k_2, k_3$ ) Langmuir-Hinshelwood equation.

Gray and Kimber<sup>33</sup> found the rates of charcoal gasification in both carbon dioxide and steam at 2300°K were two orders of magnitude lower than the bulk diffusion controlled rate.

Ergun<sup>22</sup> found no diffusional limitations up to 1670°K. However,

Table 1.7

**Investigations of Intrinsic Global Kinetic Parameters  
For Gasification of Carbon in Carbon Dioxide**

Investigator	Type of Carbon	Range of Investigation		Activation Energy (kcal/mole)	Order of Reaction with respect to CO <sub>2</sub>
		T (°K)	P (atm)		
Clement (1911) <sup>17</sup>	charcoal	1075-1375	1	42	
"	coke	1175-1575	1	58	
"	anthracite	1375-1575	1	34	
Drakeley (1931) <sup>60</sup>	several cokes	1225-1375		50-70	
Mayers (1934) <sup>60</sup>	spectroscopic carbon	1225-1575		35-50	
Meyer (1938) <sup>57</sup>	graphite filament	up to 2500	~10 <sup>-4</sup>	~90	0
Mayers (1939) <sup>60</sup>	Acheson graphite	1125-1425		52	
Gadsby et al (1948) <sup>27</sup>	coconut shell charcoal	1000-1100	1	59	1
Lewis et al (1949) <sup>60</sup>	New England coke	1075-1365	1.1	48	
"	anthracite	1075-1365	1.1	33	
Long and Sykes (1950) <sup>60</sup>	coconut shell charcoal	975-1175		59,68	
Walker et al (1953) <sup>60</sup>	graphite	1175-1475	1	48	
"	gas-baked carbon	1175-1375	1	47	
Tyler and Smith (1955) <sup>78</sup>	petroleum coke	1025-1185	1	51-57	0.6
Wicke (1955) <sup>60</sup>	activated charcoal	1125-1275	0.1-1	86	
Ergun (1956) <sup>22</sup>	3 different carbons	975-1675	1	59	
Walker and Rasts (1956) <sup>60</sup>	graphitized carbon	1240-1400	1	66	1
Blakeley and Overholser (1965) <sup>11</sup>	ATJ graphite	1150-1250	1	60	0.6
Overholser and Blakeley (1965) <sup>60</sup>	Speer Mod-2 graphite	1150-1250	1	55	0.7
Gulbransen et al (1965) <sup>78</sup>	graphite	1275-1475	~10 <sup>-2</sup>	88	
Blake et al (1967) <sup>10</sup>	coke	1125-1175	1	57	
Turkdogan and Vinters (1969) <sup>72</sup>	graphite, coconut charcoal	940-1475	10 <sup>-3</sup> -10	68	0.5
Fuchs and Yavorsky (1975) <sup>67</sup>	coal chars	1025-1175	18-35	55	0
Biederman et al (1976) <sup>6</sup>	graphite	1235-1395	~10 <sup>-4</sup>	104	1
Strangs and Walker (1976) <sup>60</sup>	graphite	1175-1280	10 <sup>-2</sup> -10 <sup>-1</sup>	99	
Wen and Wu (1976) <sup>60</sup>	activated charcoal	1135-1365	1	69	1
Detts et al (1977) <sup>60</sup>	coal chars	1115-1375	1	59	1

Gulbransen et al<sup>34</sup> (graphite-CO<sub>2</sub>) and Strickland-Constable<sup>70</sup> (carbon filaments-CO<sub>2</sub>) observed that reaction rates leveled off near 1470°K, and remained constant up to ca. 2300°K. This was attributed<sup>34</sup> to the rate being controlled by bulk diffusion. Walker and Raats<sup>84</sup> reported a decrease in activation energy from 66 kcal/mole below 1400°K to 44 kcal/mole over the range 1400 to 1665°K, which they discussed in terms of an increase in pore diffusional resistance within graphitized carbon rods at the higher temperatures. Walker et al<sup>85</sup> (graphite-CO<sub>2</sub>) reported an activation energy of 26 kcal/mole at 1470 to 1670°K, compared with 48 kcal/mole at 1170 to 1470°K, certainly indicative of the transition from chemical control to pore diffusional control in the higher temperature range.

Gray and Kimber<sup>33</sup> pointed out that CO<sub>2</sub> and H<sub>2</sub>O gasification studies at temperatures above ca. 2000°K may be complicated by the concurrent reaction of carbon with molecular oxygen formed by the dissociation of CO<sub>2</sub> and H<sub>2</sub>O:

<u>Dissociation Reactions</u>	<u>log<sub>10</sub> K<sub>a</sub></u>			
	<u>1500°K</u>	<u>2000°K</u>	<u>2500°K</u>	
CO <sub>2</sub> ⇌ CO + ½ O <sub>2</sub>	-5.3	-2.9	-1.4	(1.31)
H <sub>2</sub> O ⇌ H <sub>2</sub> + ½ O <sub>2</sub>	-5.7	-3.5	-2.2	(1.32)

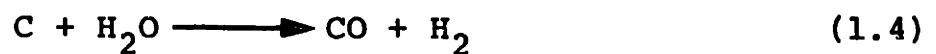
Mandel<sup>52</sup> found that at 1500°K, the rate of coal char gasification in CO<sub>2</sub> (P<sub>CO<sub>2</sub></sub> = 0.2 atm) was two orders of magnitude lower than



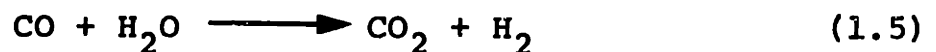
the rate of reaction in oxygen ( $P_{O_2} = 0.2$  atm). Gulbransen et al<sup>34</sup> found that the rate of graphite gasification in  $CO_2$  was only one percent of the rate of reaction in oxygen at  $1425^\circ K$ , and 0.1 percent of the rate of oxidation at  $1275^\circ K$ . Therefore, even small amounts of molecular oxygen can affect observed gasification rates in carbon dioxide or steam. Golovina reported that the rate of graphite gasification in carbon dioxide increased up to  $1500^\circ K$ , decreased between  $1500$  and  $2300^\circ K$ , then once again increased above  $2300^\circ K$ .<sup>52</sup> The latter increase in rate is thought to be due to reaction of graphite with molecular oxygen formed by  $CO_2$  dissociation. Strickland-Constable<sup>70</sup> attributed a similar increase in the rate of reaction between carbon filaments and  $N_2O$  above  $1900^\circ K$  to dissociation of nitrous oxide.

### 1.5.2 Carbon - Steam Systems

There is considerable uncertainty in the literature regarding the mechanism of the carbon-steam reaction, although most investigators<sup>7,26,41,57,...</sup> agree that carbon monoxide and hydrogen are the primary products:



A secondary reaction, the water-gas shift,



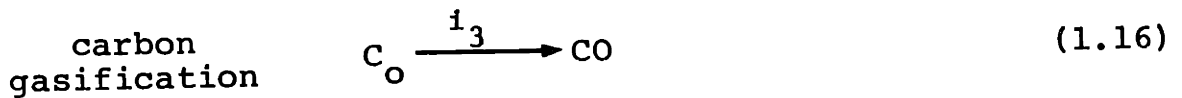
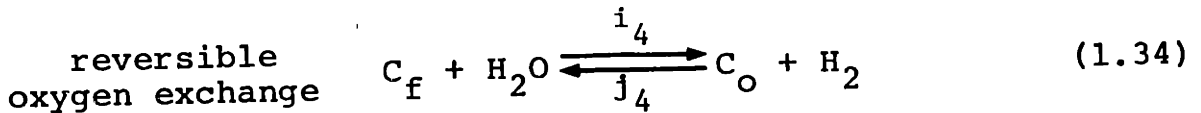
is catalyzed by the carbon surface or impurities in the

carbon.<sup>41</sup> The Langmuir-Hinshelwood expression for reaction (1.4) is

$$\text{Rate} = \frac{k_1 P_{H_2O}}{1 + k_2 P_{H_2} + k_3 P_{H_2O}} \quad (1.33)$$

where "rate" refers to carbon transfer from the solid to the gas phase.

Ergun<sup>23</sup> has proposed a mechanism (A-1) analogous to Mechanism A for carbon dioxide gasification, involving a reversible oxygen exchange reaction forming a surface oxide ( $C_O$ ), followed by release of the surface oxide from the carbon surface, as carbon monoxide:



Analogous to equations (1.23) through (1.25), the Langmuir-Hinshelwood constants in (1.33) become (Mechanism A-1)

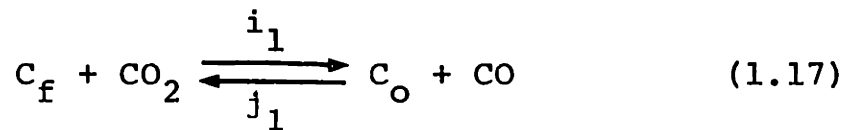
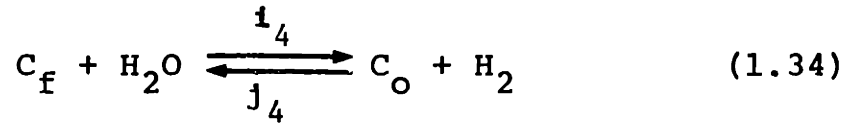
$$k_1 = i_4 [C_t] \quad (1.35)$$

$$k_2 = j_4 / i_3 \quad (1.36)$$

$$k_3 = i_4 / i_3 \quad (1.37)$$

Hydrogen retardation of the overall reaction (1.4) from this mechanism is due to reduction of the surface oxide concentration via the reverse step of equation (1.34).

If extensive conversion via equation (1.4) occurs, carbon dioxide arises as a secondary product. Water-gas equilibrium is often achieved.<sup>23,41,80</sup> This suggests the following (Mechanism A-2):



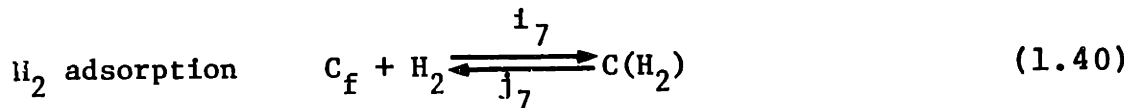
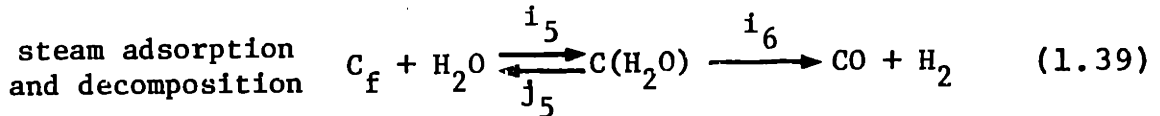
Reactions (1.34) and (1.17) provide for CO<sub>2</sub> formation and water-gas equilibrium. Combination of the oxygen exchange reactions (1.17) and (1.34) and the surface oxide desorption step (1.16), along with the assumption of C<sub>t</sub> being constant (equation (1.19)) and steady state for the species C<sub>o</sub> (analogous to equation (1.20)) results in the global rate expression for Mechanism A-2:<sup>23</sup>

$$\text{Rate} = \frac{(i_4^P H_2O + i_1^P CO_2) [C_t]}{i_3 + j_4^P H_2 + i_4^P H_2O + i_1^P CO_2 + j_1^P CO} \quad (1.38)$$

obviously not of the form of equation (1.33). According to equation (1.38), both carbon monoxide and hydrogen can inhibit the carbon-steam reaction, as reported by Ergun<sup>23</sup> and Blakeley and Overholser.<sup>11,58</sup> However, Long and Sykes<sup>51</sup> claim that CO does not inhibit the carbon-steam reaction. They suggest that CO<sub>2</sub>

and  $H_2O$  prefer different reaction sites, implying that equation (1.38) is an oversimplification of mechanism A-2.

Several investigators<sup>25,51</sup> have suggested that hydrogen inhibition is due to chemisorption at gasification temperatures (Mechanisms B-1 and B-2). Mechanism B-1, postulated by Johnstone et al,<sup>41</sup> involves adsorption of steam on active sites:



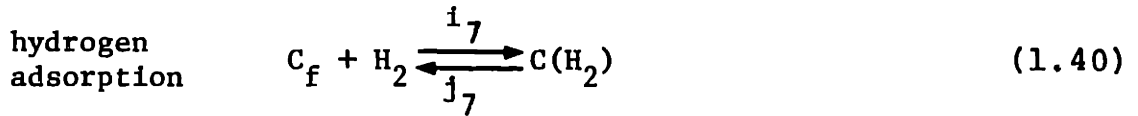
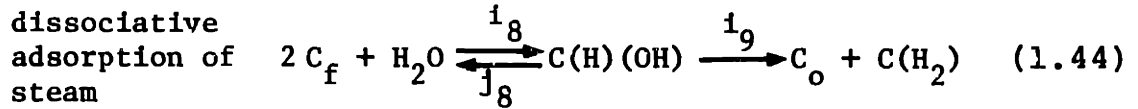
where  $C(H_2O)$  and  $C(H_2)$  denote adsorbed molecules of steam and hydrogen. If all active sites are equivalent and can be occupied by only one molecule, the constants in equation (1.33) are (Mechanism B-1):

$$k_1 = \left\{ \frac{i_5 i_6}{j_5 + i_6} \right\} \cdot [C_t] \quad (1.41)$$

$$k_2 = i_7/j_7$$

$$k_3 = \frac{i_5}{j_5 + j_6} \quad (1.43)$$

Long and Sykes<sup>51</sup> suggest that water molecules dissociate upon adsorption. Assuming still that adsorption accounts for rate hindrance by hydrogen, we have Mechanism B-2:



where C(H)(OH) denotes a dual-site surface complex formed by the dissociative adsorption of an H<sub>2</sub>O molecule. The Langmuir-Hinshelwood constants for equation (1.33) become

(Mechanism B-2):

$$k_1 = \frac{i_8 i_9}{j_8 + i_9} \cdot [C_t] \quad (1.45)$$

$$k_2 = i_7 / j_7 \quad (1.46)$$

$$k_3 = \left\{ \frac{1}{i_3} + \frac{1}{j_7} + \frac{1}{i_9} \right\} \cdot \left\{ \frac{i_8 i_9}{j_8 + i_9} \right\} \quad (1.47)$$

Table 1.8 is a summary of past investigations of the kinetics of steam-carbon systems. As was the case in section 1.5.1, most of the studies involved pure carbons (e.g., graphite), rather than coals or chars. Reported activation energies range from 32 to 112 kcal/mole in studies not involving addition of catalysts. Values from zero to unity have been reported (as expected) for the order of reaction with respect to H<sub>2</sub>O.

Table 1.8  
Investigations of Intrinsic Global Kinetic Parameters  
for Gasification of Carbon in Steam

Investigator	Type of Carbon	Range of Investigation		Activation Energy (kcal/mole)	Order of Reaction with respect to H <sub>2</sub> O
		T (°K)	P (atm)		
Mayers (1934) <sup>23</sup>	graphite	1125-1435		35-50	
Fleer and White (1936) <sup>25</sup>	coke (Na <sub>2</sub> CO <sub>3</sub> catalyst)	1175-1275		27	
Meyer (1938) <sup>27</sup>	graphite filament	up to 2500	~ 10 <sup>-4</sup>	~ 90	0
Loag and Sykes (1948) <sup>51</sup>	charcoal	975-1075		42-65	
Johnstone et al (1952) <sup>41</sup>	graphite tube: 0% burnoff	1135-1210	1	112	
	7.5% burnoff	1135-1210	1	96	
Hunt et al (1953) <sup>39</sup>	pitch coke	1255-1425		45	
Jolley and Pohl (1953) <sup>42</sup>	coal cokes	1075-1225	1	40	
Wicke and Rossberg (1953) <sup>76</sup>	coal	1275-1475		56	
Pilcher et al (1955) <sup>53</sup>	graphitized coke	1275-1375		41	
Binford and Eyring (1956) <sup>7</sup>	graphite	1175-1575	10 <sup>-9</sup> -10 <sup>-7</sup>	60	{ 0 (1175-1375°K) 1 (1475-1575°K)
Zielke and Gorin (1957) <sup>50</sup>	Disco char	1100-1200	1-30	40-75	0.1-0.5
Blyholder and Eyring (1959) <sup>12</sup>	electrode graphite	1175-1575		36	
Ergun (1962) <sup>23</sup>	metallurgical coke	1175-1475	1	59	
Blakeley and Overholser (1965) <sup>11</sup>	ATJ graphite	1050-1200	1	~ 50	0.7
Stewart and Diehl (1972) <sup>47</sup>	coal chars	1175-1275	1	34-40	0.6
Van Heek et al (1973) <sup>78</sup>	coal chars	875-1375	1-70	32-50	0
Fuchs and Yavorsky (1975) <sup>47</sup>	coal chars	1025-1175	18-70	~ 50	0
Kaftanov and Fedoseev (1976) <sup>47</sup>	graphite	1175-1475		70	1
Knyambe and Pulsifer (1976) <sup>48</sup>	coal chars	875-1125	1	61	0
Linares et al (1977) <sup>49</sup>	lignite char	1025-1200	~ 10 <sup>-2</sup>	42	0.6

## 1.6 Objectives and Scope of Study

The following objectives were set for this investigation:

1. Obtain data on the rate of gasification of a coal char in carbon dioxide and steam, under the following conditions:

Type of char - a Montana Rosebud (see section 2.1)

Temperature - ca. 1500 to 2100°K

Total pressure - 1 atm

Char residence time - ca. 100 to 300 msec

2. Evaluate the effect of pyrolysis on the observed gasification rates.

3. Determine apparent (global) kinetic parameters governing the observed gasification rates.

4. Deduce the intrinsic kinetics governing the char-CO<sub>2</sub> and char-H<sub>2</sub>O reactions.

5. Examine physical changes, if any (surface area, porosity, etc.) in the char as a result of gasification.

To fulfill the above objectives, experiments in a laminar flow furnace (described in Chapter 2) were conducted. The rate of char weight loss under gasifying conditions was studied.

Bush et al<sup>15</sup> reported preliminary results of these experiments.

Further analysis is included in this report.

The conditions set during the experiments were:

1. Nominal temperature - 1473, 1773 and 2113°K
  2. Char residence times, corresponding to the distance through the furnace reaction zone which the char particles were allowed to fall (i.e., the distance between the char feeder and particle collection probe):
    - Feeder-collector separation - 3, 4.5 and 6 inches
    - Residence times (also determined by the main gas flow rate, see below) -
      - at 1473°K, ca. 160 to 330 msec
      - at 1773°K, ca. 125 to 285 msec
      - at 2113°K, ca. 120 to 240 msec
  3. Partial pressure (atm) of the oxidizing gas in the main gas stream (total pressure of 1 atm):
    - CO<sub>2</sub> gasification -  $P_c \approx 0.26$  and  $0.6$
    - H<sub>2</sub>O gasification -  $P_w \approx 0.34$  and  $0.65$
- For pyrolysis experiments, the main gas stream consisted of pure argon.
4. Main gas flow rate - approximately 6 l/min STP. The exact conditions under which each experimental run was conducted (residence times are estimated, see section 2.4.3) are given in Appendix A (CO<sub>2</sub> gasification), Appendix B (H<sub>2</sub>O gasification) and Appendix C (pyrolysis).



## Chapter 2

### APPARATUS AND PROCEDURES

#### 2.1 Feed Material

The char used in these experiments was provided by Foster-Wheeler Corporation of Livingston, New Jersey. It was produced from a pulverized Montana Rosebud coal in a muffle tube furnace at 1365°K and 1 atm total pressure. The gas composition in the furnace was approximately 41 mole percent CH<sub>4</sub>, 45% H<sub>2</sub>O and 14% CO<sub>2</sub>. Residence time was on the order of 150 milliseconds (msec). The char, as provided by Foster-Wheeler, was divided into three size fractions. The fraction containing particles of diameters between 75 and 150 microns was used in this study. (This fraction will hereafter be referred to as the initial char.) Properties of the initial char are listed in Table 2.1.

#### 2.2 Experimental Apparatus - General Description

The apparatus chosen for the required experiments had to meet the following requirements:

1. Materials resistant to high temperatures (ca. 2000°K) and test atmospheres (steam and carbon dioxide).
2. Accurate char feeding and collection systems.

Table 2.1

Properties of the Initial Char

Particle diameter <sup>(a)</sup>	75 - 150 $\mu\text{m}$
Bulk density, $\rho_p$ <sup>(b)</sup>	0.49 $\text{g/cm}^3$
Skeletal density, $\rho_t$ <sup>(b)</sup>	1.73 $\text{g/cm}^3$
Porosity, $\xi = 1 - (\rho_p/\rho_t)$	0.72
Total (nitrogen) surface area, $S_g^\circ$ <sup>(b)</sup>	81 $\text{m}^2/\text{g}$
Ash content, $f_{\text{ash}}^\circ \times 100\%$	20.5 wt%
Ultimate Analysis <sup>(b,c)</sup>	
Carbon	75.0 wt%
Hydrogen	0.8 wt%
Nitrogen	0.7 wt%
Sulfur	0.5 wt%

- (a) An average particle diameter,  $d_p$ , of 100  $\mu\text{m}$  is assumed for calculations.
- (b) Analysis by Phillips Petroleum Company, Bartlesville, Oklahoma.
- (c) Includes size fractions below 75  $\mu\text{m}$  and above 150  $\mu\text{m}$ . The fraction used in experiments (75-150  $\mu\text{m}$ ) is approximately 60 wt% of the entire char.

3. Furnace capabilities to insure rapid heating of both char and reactant gases to the desired reaction temperature.

The system used is depicted in Figure 2.1. The basic design is given by Kobayashi.<sup>44</sup> In brief, the apparatus consists of a vertical tube furnace (section 2.2.1) through which a steady, laminar flow of preheated reactant gas (the main gas stream) is maintained. A preweighed amount of char is injected into the furnace "hot zone" via a water-cooled feeder tube (section 2.2.2) which extends through the furnace shell. The particle stream emerging from the feeder is rapidly heated to the reaction temperature while being entrained along the furnace centerline by the main gas stream. After falling for the desired distance, the particles are collected and the reaction is quenched in a water-cooled probe (section 2.2.3) which is raised into the reaction zone from below. A sintered bronze filter is positioned at the tip of the collection probe. The main gas stream and char are drawn into the filter by means of a vacuum system. Cooling water injected directly into the filter insures rapid quenching of the reaction.

The high temperature main gas stream ( $\text{CO}_2\text{-N}_2$  or  $\text{H}_2\text{O-N}_2$ ) is generated in a burner (section 2.2.4) mounted atop the

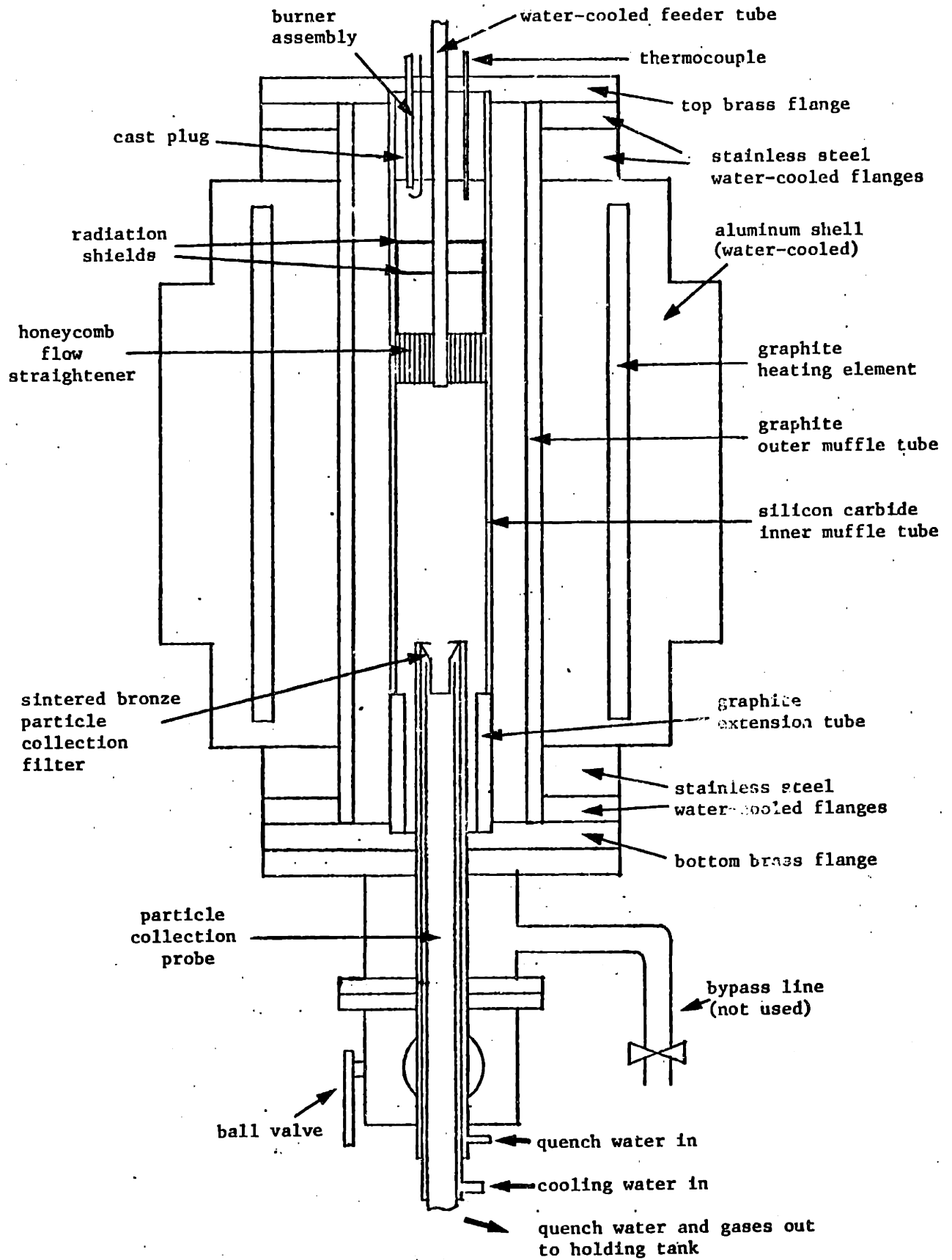


Figure 2.1 Schematic of Flow System for Char Gasification Studies

furnace assembly. This eliminates the need to preheat the main gas stream. Gas distribution plates and a honeycomb flow straightener, positioned between the burner exit and the tip of the char feeder tube, insure a flat velocity profile for the main gas stream at the point of char injection into the reaction zone. (Kobayashi<sup>44</sup> showed that the thin boundary layer due to the presence of the feeder tube may be ignored.)

### 2.2.1 Furnace/Reaction Zone Assembly

The furnace used in this study is an ASTRO model 1000A (ASTRO Industries, Inc., Santa Barbara, California). The furnace is equipped with an ASTRO model 50 KVA power supply connected to a 3.5 in. (8.9 cm) inner diameter (I.D.), 12 in. (30.5 cm) long tubular graphite heating element enclosed in an 11 in. (27.9 cm) diameter water-jacketed aluminum shell. The heating element is isolated on the inside by a 3 in. (7.6 cm) outer diameter (O.D.), 2.625 in. (6.7 cm) I.D., 24 in. (61.0 cm) long graphite muffle tube, which is located top and bottom by O-ring seals between two stainless steel water-cooled flanges. The volume surrounding the heating element is continuously purged with argon.

The reactor tube assembly, Figure 2.2, is fitted inside the graphite muffle tube and is seated between brass flanges at the top and bottom of the furnace. The silicon carbide (SiC)

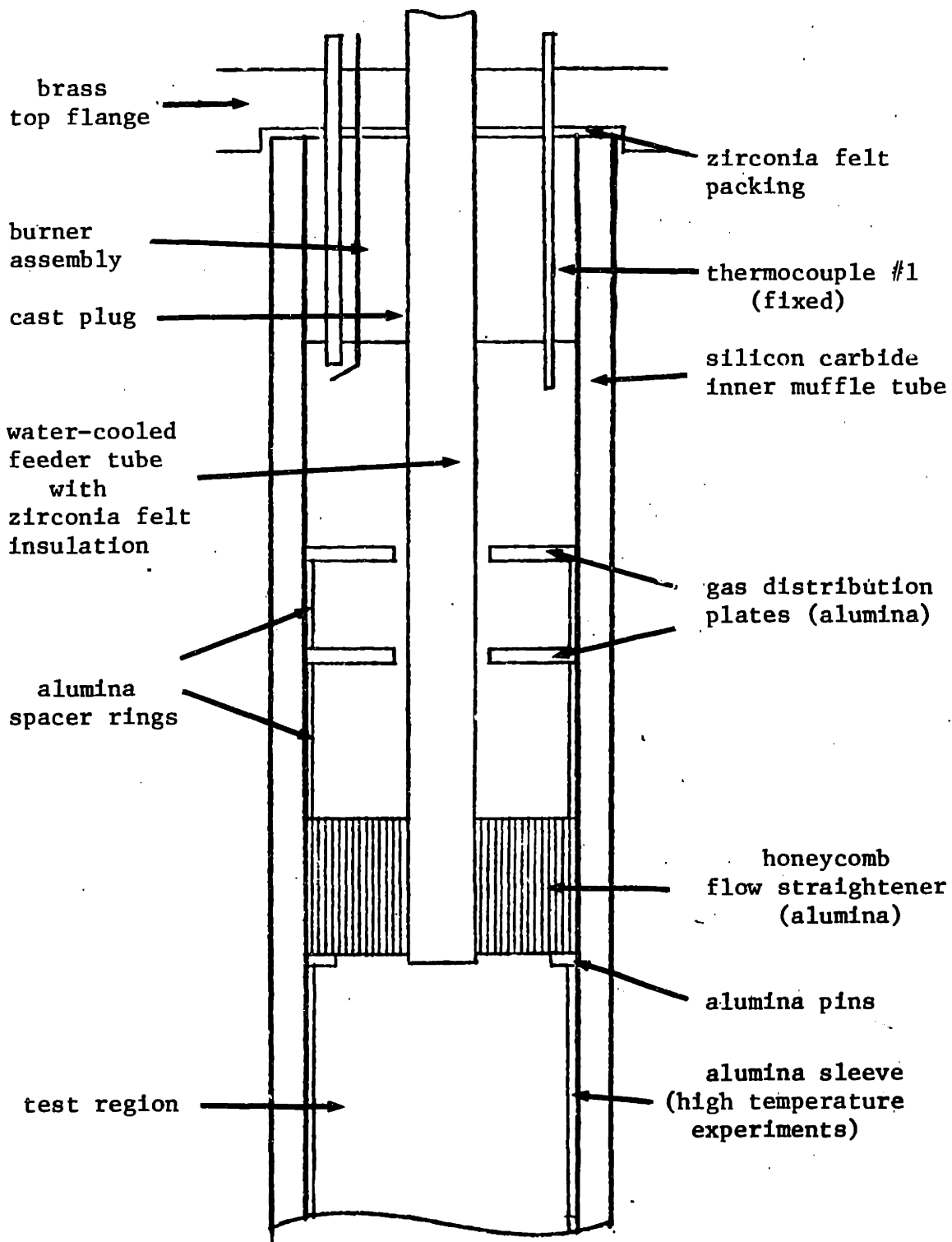


Figure 2.2 Reactor Tube Assembly

inner muffle tube, which is 18 in. (45.7 cm) long, 2 in. (5.1 cm) I.D., 2.5 in. (6.4 cm) O.D., rests on the 6.5 in. (16.5 cm) long, 2.5 in. (6.4 cm) O.D., 1.75 in. (4.5 cm) I.D. graphite extension tube. For all experiments below 1800°K, the SiC muffle tube is fitted with alumina pins on which the alumina honeycomb flow straightener is supported. The honeycomb hole size is 1/16 in. (1.6 mm) diameter, and the distance between holes is 0.083 in. (2.1 mm). Two thin alumina spacer rings, resting on the flow straightener, are used to support the gas distribution plates, which are alumina disks with 1/8 in. (3.2 mm) holes drilled on a circle which divides the disk into two sections of equal area. For experiments above 1800°K, an alumina sleeve, 8.25 in. (21.0 cm) long, is used to protect the SiC surface from erosion by the main gas stream.

### 2.2.2 Char Feeder

The char feeder system is shown in Figure 2.3. The feeder body consists of a plexiglas chamber, 3 in. (7.6 cm) long by 0.5 in. (1.3 cm) I.D., fitted with a charge port and needle valve. Carrier gas (helium), introduced through the hollow needle valve at high velocity (ca. 20 cm/sec) but low flow rate (ca. 30 cm<sup>3</sup>/min STP), fluidizes the char particles to prevent plugging. An external electric vibrator provides additional agitation. Thus, the feed rate is

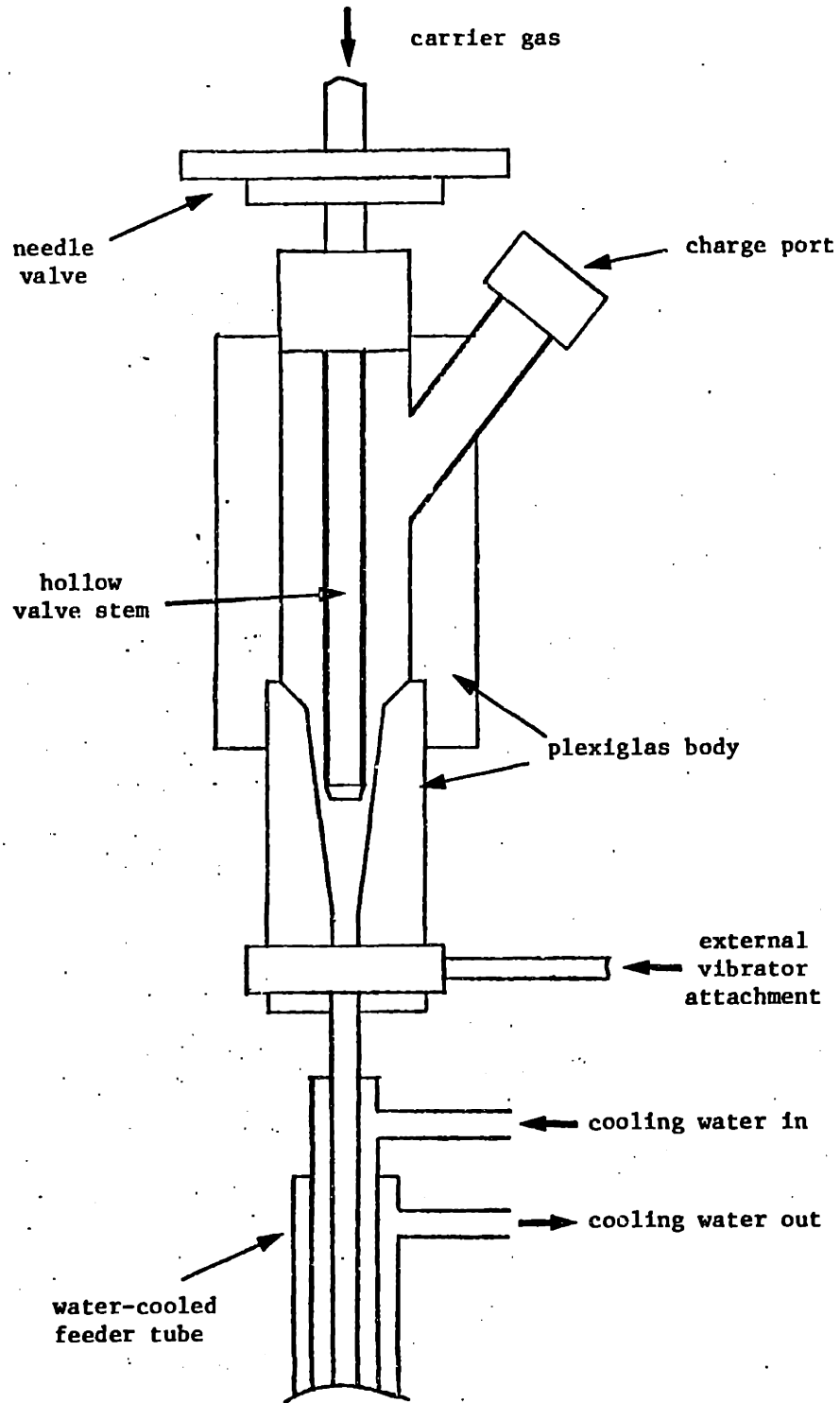


Figure 2.3 Char Feeder



controlled by adjusting the needle valve opening, vibrator strength and carrier gas flow rate. Although the char feed rate is not easily reproduced, varying feed rate has no effect on reaction rate (section 2.5.7).

The feeder body is epoxied to the 0.125 in. (3.2 mm) O.D., 0.0625 in. (1.6 mm) I.D. stainless steel feeder tube, jacketed (0.375 in. O.D.) for water cooling. A 0.0625 in. (1.6 mm) layer of zirconia felt is bonded to the feed tube for insulation. The water-cooled feed tube extends slightly (< 0.25 in.) below the honeycomb flow straightener into the reaction zone.

### 2.2.3 Particle Collector and Vacuum System

The particle collection probe, shown in Figure 2.4, is a 1.375 in. (3.5 cm) O.D., 0.5 in. (1.3 cm) I.D. tubular copper assembly. It is fully jacketed for cooling water, and includes a line to provide distilled water which is directly injected around the periphery of the sintered bronze filter in the probe tip, thus cooling the char particles and quickly quenching the reaction. The filter (manufactured by Thermet Inc., Gloucester, Massachusetts) has a 0.75 in. (1.9 cm) O.D. at the open end, and a 0.375 in. (9.5 cm) O.D. along the straight section. Nominal pore size is 5 microns. Injection (quench) water and reaction gases are drawn through the

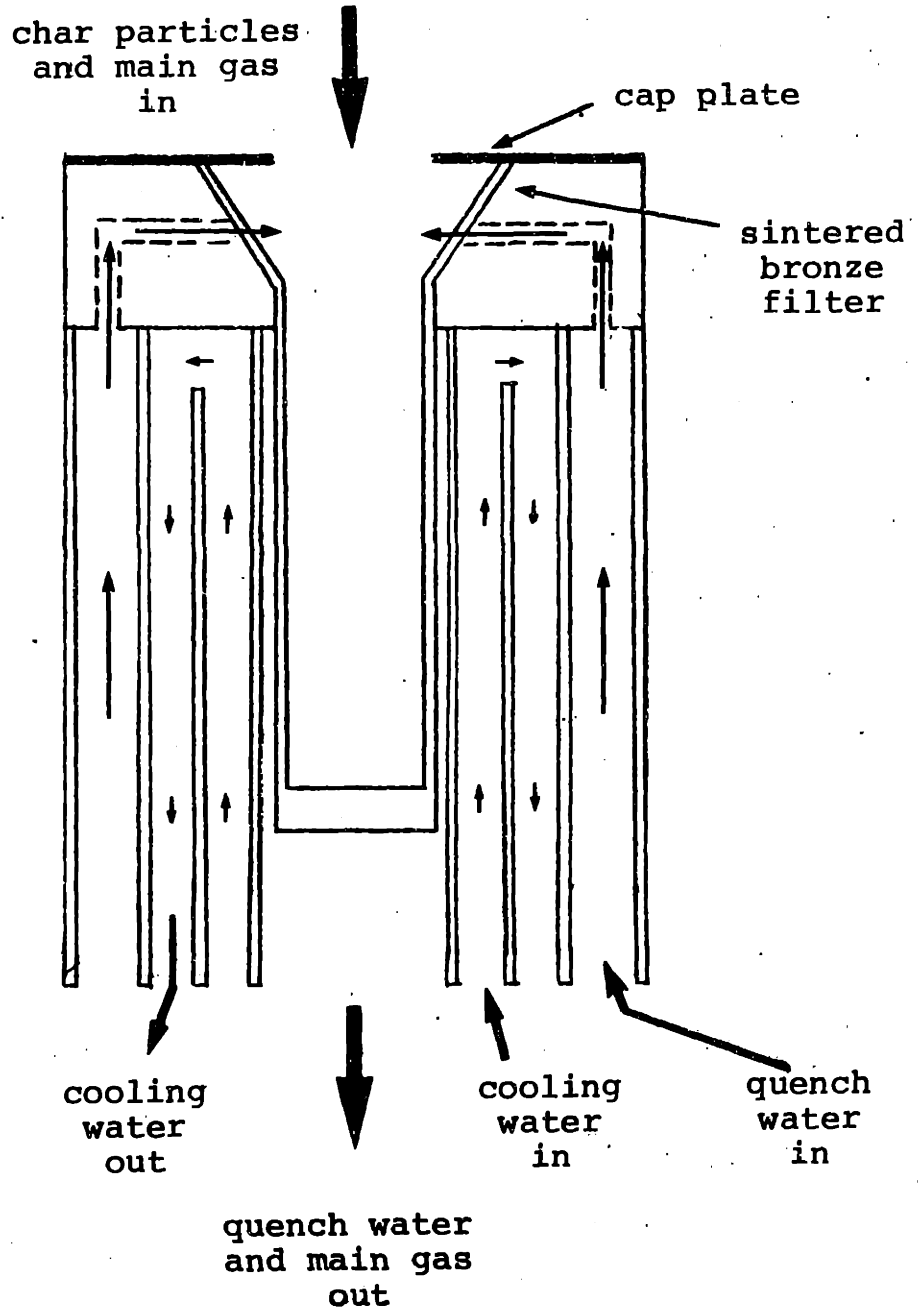


Figure 2.4 Particle Collection Probe

filter into a large collection tank, while char particles are retained in the filter. Suction is provided by two Cenco Megavac vacuum pumps connected in parallel, each rated at a capacity of 57 l/min at 0 psig. The collection tank must be periodically pressurized and drained during normal operation.

#### 2.2.4 Gas Burner Assembly

Figure 2.5 depicts the burner assembly which is used to generate the main gas streams ( $\text{CO}_2\text{-N}_2$  or  $\text{H}_2\text{O-N}_2$  mixtures). It is mounted in the 3 in. (7.6 cm) long by 2 in. (5.1 cm) O.D. plug of alumina castable cement attached to the furnace top flange, as shown in Figure 2.2.

To prevent explosions, fuel ( $\text{CO}$  or  $\text{H}_2$ ) and oxidant (air or oxygen-enriched air) enter the burner separately, with check valves and flashback arrestors fitted to each gas line. The fuel line is a 0.125 in. (3.2 mm) O.D., 0.0625 in. (1.6 mm) I.D. electrically grounded stainless steel tube, extending approximately 0.25 in. (6.4 mm) below the lower face of the cast plug. The oxidant line is a 0.25 in. (6.4 mm) O.D., 0.1875 in. (4.8 mm) I.D. tube enclosing the fuel line, extending approximately 0.25 in. (6.4 mm) into the cast plug. An annulus about the fuel line allows transport of the oxidant into the furnace. A molybdenum electrode, insulated by alumina tubing, is used to ignite the fuel/oxidant mixture below the end of

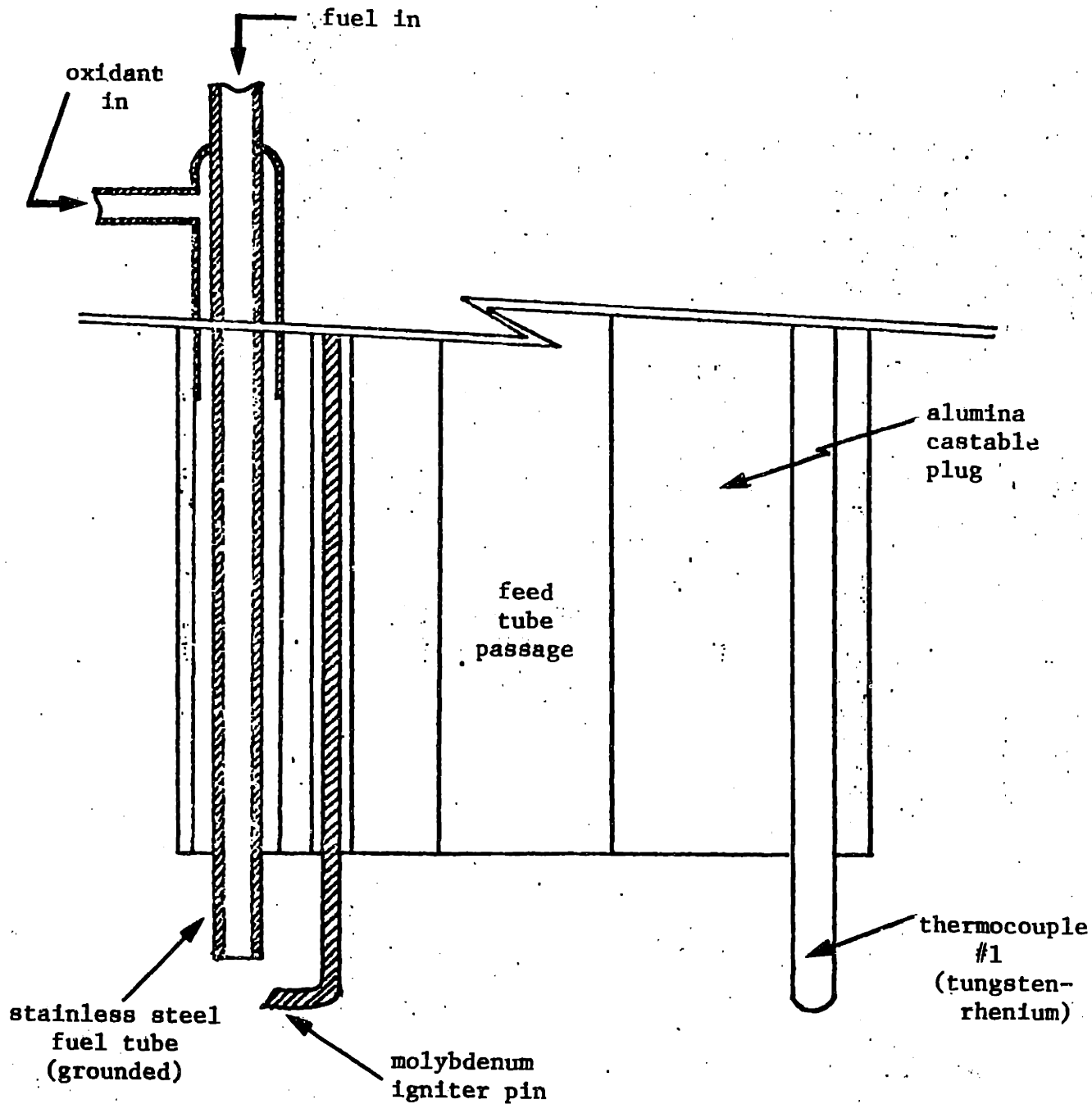
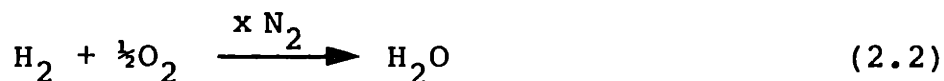
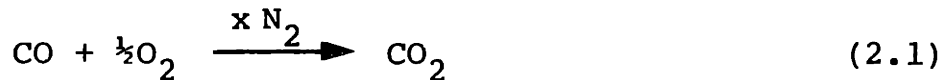


Figure 2.5 Gas Burner Assembly

the fuel line. When energized, a tesla coil connected to the electrode causes a spark to jump from the electrode to the end of the fuel line, igniting the mixture. The pertinent reactions are:



where x depends on the degree of oxygen-enrichment of the air used as the oxidant. Changes in thermocouple readings indicate that ignition has occurred. Fuel/oxidant mixtures are adjusted to slightly fuel-rich, to insure that molecular oxygen is not present in the main gas stream during char reaction experiments.

#### 2.2.5 Gas Flow Control and Measurement

Flow rates for the fuel and oxidant lines to the burner, helium carrier gas and argon streams are controlled by Matheson (Gloucester, Massachusetts) rotameters. Calibration of the rotameters is verified with a wet test meter (Precision Scientific Company, Chicago, Illinois).

#### 2.2.6 Temperature Measurements

Temperature is measured using tungsten 5% rhenium - tungsten 26% rhenium thermocouples, manufactured by ARI Industries, Inc., Franklin Park, Illinois. Their millivolt

output is displayed on a Doric 400A digital indicator, with readings to within  $\pm 0.1$  mv (corresponding to approximately  $\pm 5^\circ\text{K}$ ). Thermocouple #1 is fixed in the burner assembly, as shown in Figure 2.5. Thermocouple #2 is very long, and can be raised into the reaction zone from below when the collection probe is not in place, to measure the SiC muffle tube wall temperature ( $T_w$ ) in the reaction zone. Temperature profiles in the reaction zone, measured at experimental nominal temperatures ( $T_o$ ) of 1473 and 1773 $^\circ\text{K}$ , are shown in Figure 2.6. Using an average of the two curves in Figure 2.6, the data are fit to the expression (see Figure 2.7)

$$\theta_w(z) = 1.0 - \alpha z^\beta \quad (2.3)$$

where

$$\alpha = 1.08 \times 10^{-4} \quad (2.4)$$

$$\beta = 2.71 \quad (2.5)$$

$z$  is the distance (cm) from the water-cooled char feeder tube exit (approximately level with the bottom of the honeycomb flow straightener), and  $\theta_w(z)$  is the ratio ( $^\circ\text{K}/^\circ\text{K}$ ) of the muffle tube wall temperature at a distance  $z$ , to the wall temperature at  $z=0$  (which is  $T_o$ , the nominal temperature of the experiment).

[Although attempts were made to protect the thermocouple wires from the corrosive effects of the high-temperature main gas streams, thermocouple #2 (the long probe) was destroyed

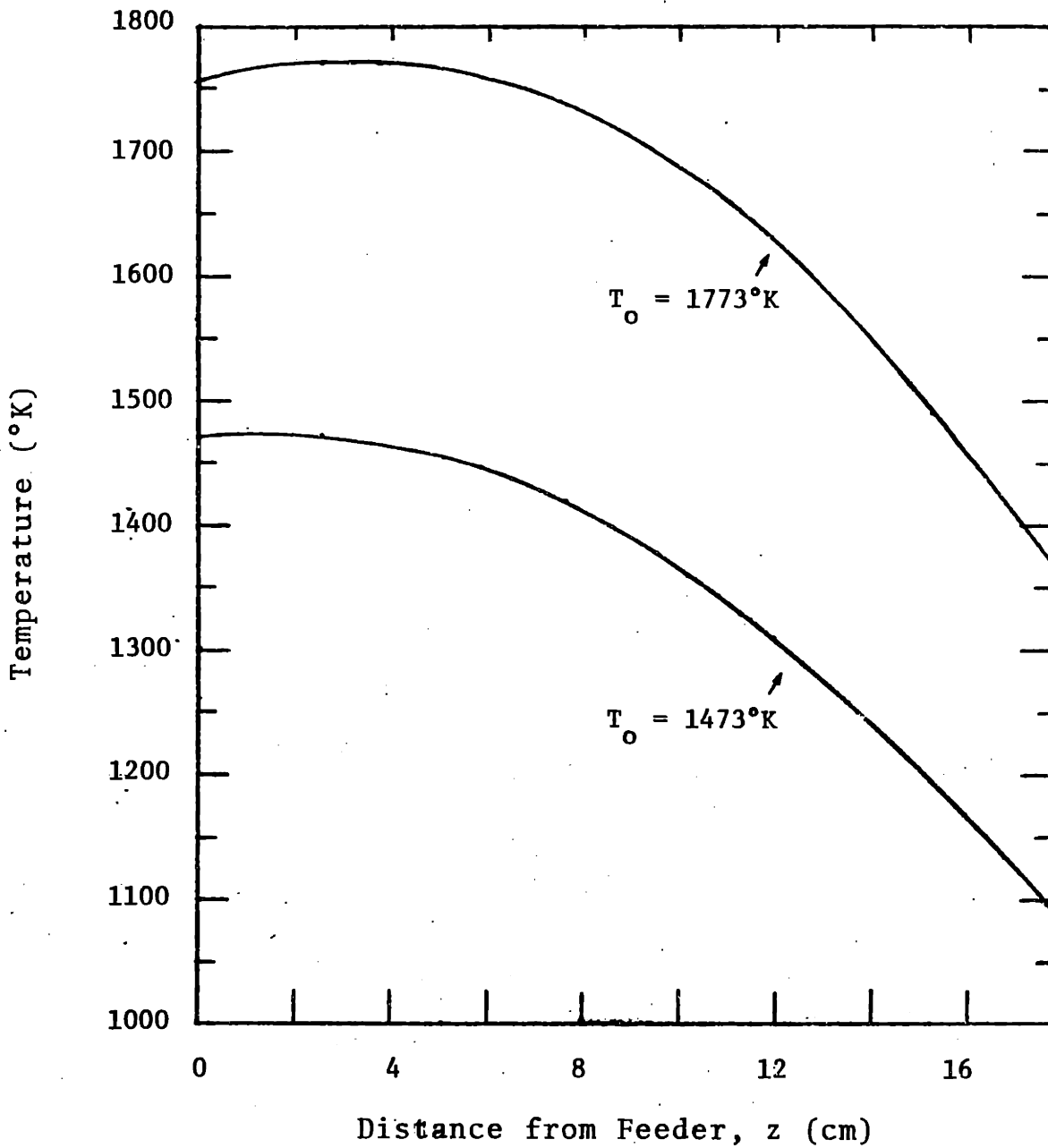


Figure 2.6 Axial Temperature Profile

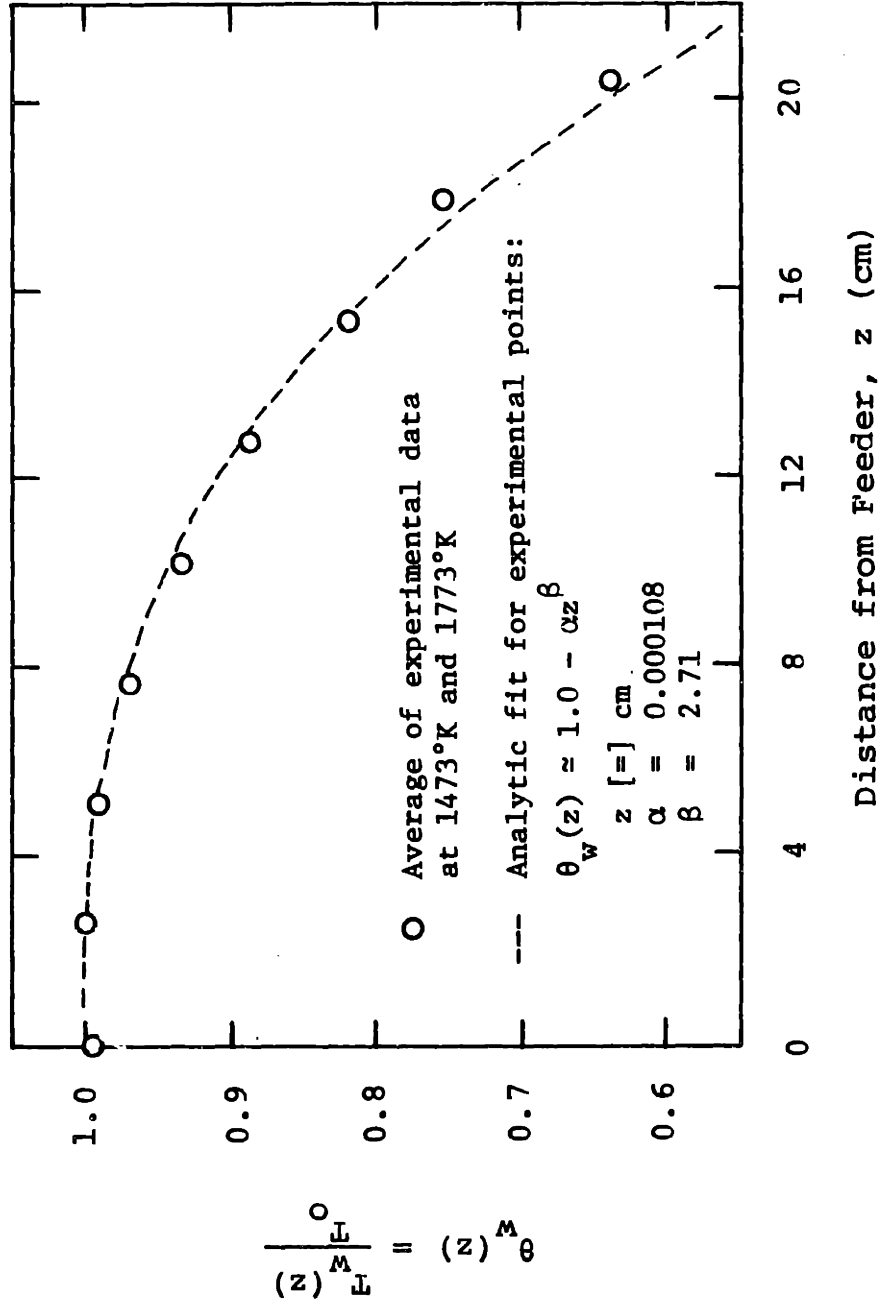


Figure 2.7 Analytic Expression for Furnace Temperature Profile



before the high temperature experiments (nominal temperature ca. 2100°K) could be attempted. Thus, direct temperature measurements during these high temperature runs became impossible. The correct setting for the furnace power supply was inferred by extrapolating results from experiments at lower temperatures (see Figure 2.8) which were performed before the thermocouple was destroyed. Thus, it was estimated that a furnace setting of 220 would result in a temperature of 2113°K near the top of the furnace reaction zone.]

#### 2.2.7 Weight Measurements

Weights are measured using a Mettler model H34 analytical balance, having an accuracy of  $\pm 0.1$  mg. Weights of char samples and collection filters, both before and after reaction, are measured while the samples are in equilibrium with the laboratory air.

#### 2.3 Procedure for Laminar Flow Furnace Experiments

In preparation for experimental runs, the cooling water for the furnace flanges, furnace shell, feeder tube and collection probe is turned on, and argon streams through the silicon carbide muffle tube and the region surrounding the graphite heating element are started. The furnace power supply is turned on and regulated so the furnace gradually (2 to 5

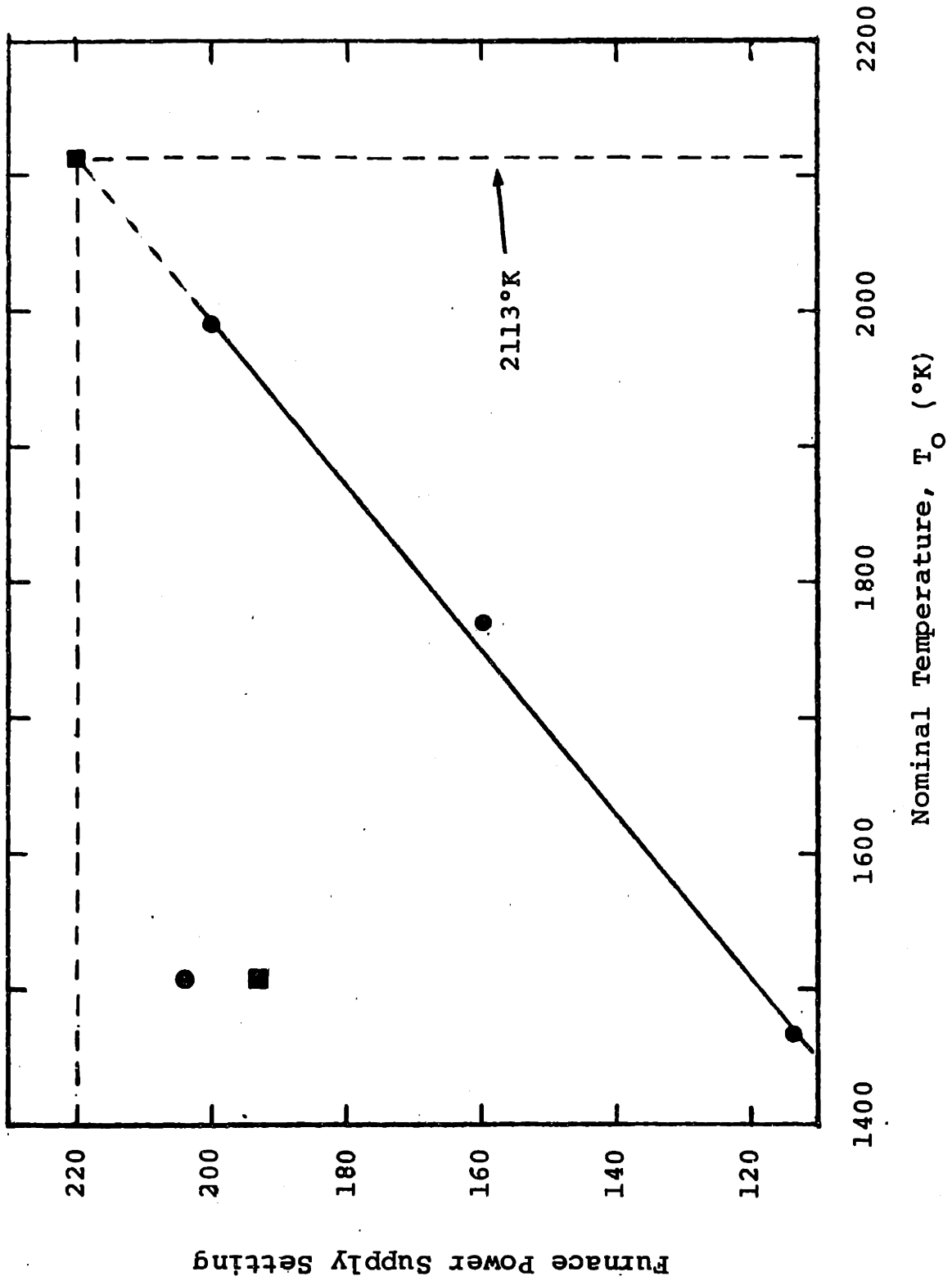


Figure 2.8 Estimation of Furnace Setting for High Temperature Experiments

hours) reaches the desired operating temperature. The temperature is continuously monitored during heat-up with thermocouple #2. Once the furnace temperature has stabilized, argon flow through the SiC tube is discontinued and the gas burner is ignited using a fuel-rich mixture of hydrogen and air. The fuel and oxidant flows into the burner are adjusted to produce the desired main gas composition (see sections 2.2.4 and 2.5.9), with the total main gas flow rate constant at approximately 6 l/min STP. (For pyrolysis experiments, with an argon main gas stream, the burner is not used.) Temperature is allowed to stabilize again for about 30 minutes.

Char samples (100 to 200 mg) are weighed in porcelain crucibles, and transferred to the feeder. A preweighed sintered bronze filter is secured in the collection probe, and the quench water flow and vacuum pumps are turned on. The probe is raised to the desired height in the furnace. Char residence time is varied by adjusting the position of the collection probe with respect to the feeder tube exit. An O-ring through which the probe is pushed secures the probe and isolates the furnace from the laboratory atmosphere. Suction is maintained at 1 to 6 inches vacuum at the probe tip. The feeder needle valve is opened, feeder carrier gas turned on and vibrator activated, causing the char particles to enter and fall through the furnace, into the collection filter.

After all of the char is fed (determined visually), the vibrator is switched off, needle valve closed and carrier gas stopped. The collection probe is removed from the furnace and the vacuum pumps and quench water flow turned off. The filter is removed from the probe and dried overnight at room temperature before weighing. The weight of char collected is calculated from the increase in filter weight. After weighing, the samples are removed from the filters and stored in glass vials.

The following data are recorded for each run:

1. Furnace power supply setting.
2. Feed sample number.
3. Weight of the crucible used to charge the feeder, both before and after charging. The weight of char fed is calculated by difference.
4. Reading (mv) of thermocouple #1.
5. Flow rates of gases entering the burner.
6. Filter weight (dried) before and after the run.
7. Feeder-collection probe separation (inches).

Usually 3 to 5 runs are made at a given set of conditions (temperature, main gas composition, feeder-collector separation), after which the quench water holding tank is pressurized and drained.

At the completion of the last run of the day, the gas burner is turned off and argon flow through the SiC muffle

tube is resumed. The furnace power supply is regulated to obtain a furnace cooling rate of approximately 10°K per minute. When the furnace temperature drops below approximately 350°K, the power supply, argon flows and cooling water are turned off.

#### 2.4 Ash Determination

A modified version of the A.S.T.M.<sup>91</sup> procedure for determination of the ash content of a coal or char is used to determine the ash content (percent by weight) of the initial char. Preweighed char samples in porcelain crucibles are placed in a home-made brick-insulated furnace having four silicon carbide electrodes connected in parallel to a variac. The furnace is continuously purged with air, and the temperature is set to 500°C. After one hour, the temperature is set to 750°C. Samples are left at 750°C (for at least one hour) until they reach constant weight. Samples are cooled in a dessicator before weighing. Using this procedure, the initial char is found to have an ash content of 20.4 wt% (see Appendix K). [The moisture content of the initial char is neglected since Mandel<sup>52</sup> reports it to be under one percent by weight.]

## 2.5 System Evaluation

### 2.5.1 Main Gas Temperature and Velocity

The temperature and velocity profiles of the main gas stream are very complicated because of end effects due to the feeder tube (and carrier gas) and collection probe, and because of the non-isothermal nature of the furnace muffle tube. Simplifying assumptions are made to allow approximate calculation of the gas temperature and velocity.

#### Temperature

It is assumed that the gas temperature equals the SiC muffle tube wall temperature, and is independent of radial position in the furnace tube:

$$\theta_g(z) = \frac{T_g(z)}{T_o} = \frac{T_w(z)}{T_o} = \theta_w(z) \quad (2.6)$$

where the SiC wall temperature is given approximately by equations (2.3) through (2.5). Measurements indicate that this assumption is justified except in the regions just below the feeder tube exit and just above the collection probe.

Near the feeder tube, there is a radial temperature gradient, caused by the feeder tube and mixing of the carrier gas and main gas. Hence, in the region up to approximately 5 cm below the exit of the feeder tube, the gas near the furnace centerline is cooler (perhaps 50 to 100°K) than the gas near the SiC tube wall. To minimize the effects of this in the

calculation of reaction rates (section 4.2), an integral analysis is used, with the lower limit of integration chosen as a point in the furnace below this heat-up region.

Conductive cooling due to the presence of the water-cooled collection probe and due to the reaction quench water (which is injected directly into the collection filter) results in a large axial temperature gradient (ca. 400 °K/cm) in the gas approximately 1 to 2 cm above the collection probe. A correction for this narrow cooling region is not included in the calculation of reaction rates.

### Velocity

The velocity profile of the main gas stream can be approximated by making the following simplifying assumptions:

- A-1. Consider only the velocity component in the  $\hat{z}$  direction (i.e., along the furnace axis).
- A-2. Neglect end effects due to the feeder tube and carrier gas.
- A-3. Neglect the effects of the char particles falling along the furnace centerline.
- A-4. Assume a flat velocity profile at the point  $z=0$  due to the honeycomb flow straightener, with a laminar ( $Re \sim 100$ ), Newtonian (parabolic) velocity profile developing for  $z \geq 0$ .

A-5. Separate the effects of the laminar profile development from the effects of the non-isothermal axial temperature profile.

An approximate solution to the Navier-Stokes equations describing the steady state development of laminar flow in the inlet section of an isothermal tube (axial velocity component,  $u_g$ ), with a flat velocity profile at the entrance of the tube, is given by Langhaar<sup>46</sup> (Figure 2.9):

$$u_g^* = u_g^*(r^*, z^*, \theta_g = 1) \quad (2.7)$$

where  $u_g^*$  is a dimensionless axial velocity ( $u_{g,avg}$  is the average gas velocity):

$$u_g^* = u_g / u_{g,avg} \quad (2.8)$$

$r^*$  is a dimensionless radial coordinate, measured from the tube centerline ( $R_w$  is the radius of the tube):

$$r^* = r / R_w \quad (2.9)$$

and  $z^*$  is a dimensionless axial coordinate, measured from the entrance of the tube ( $\nu$  is the gas kinematic viscosity):

$$z^* = \frac{\nu z}{R_w^2 u_{g,avg}} \quad (2.10)$$

$\theta_g$  is set to unity to indicate that equation (2.7) is for an isothermal tube. In order to use these results in calculating the main gas velocity profile, assumption A-5 must be made.

Hence,  $u_{g,avg}$  and  $\nu$  are calculated at the nominal temperature,



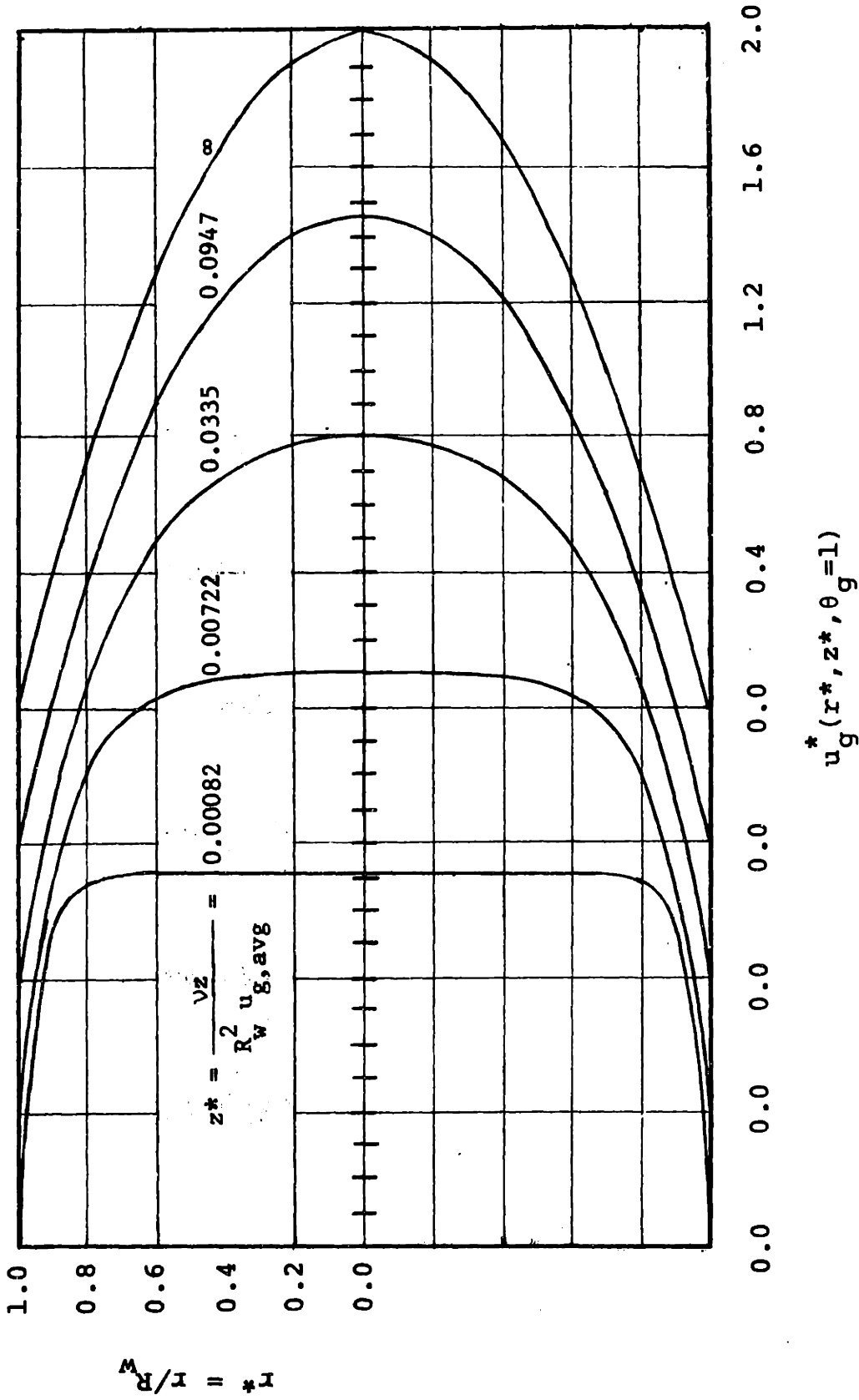


Figure 2.9 Developing Laminar Velocity Profile For Flow Through an Isothermal Tube

$T_0$ . (Calculation of  $v$  is shown in Appendix F.)

It is apparent from Figure 2.7 that the reaction zone is far from isothermal. As the main gas cools, it proportionately decelerates. To account for this, the following is assumed:

$$u_g^*(r^*, z^*, \theta_g) = \theta_g \cdot u_g^*(r^*, z^*, 1) \quad (2.11)$$

Hence, by assumption A-5, an isothermal laminar profile development and non-isothermal furnace temperature profile are considered separately to arrive at an approximate main gas velocity profile.

### 2.5.2 Char Particle Velocity

The char particles leave the feeder tube, fall along the furnace centerline under the combined action of gravity and entrainment by the main gas, and are collected in the filter in the collection probe. The isothermal main gas velocity,  $u_g^*(r^*=0, z^*, 1)$  is shown in Figure 2.10. An approximate analytic expression for  $u_g^*(0, z^*, 1)$  is given by:

$$u_g^*(r^*=0, z^*, \theta_g=1) \approx 2.0 - a \exp(-bz^*) \quad (2.12)$$

where the constants  $a$  and  $b$  are chosen as:

$$a = 0.762 \quad (2.13)$$

and

$$b = 16.30 \quad (2.14)$$

Both gravity and entrainment effects must be accounted

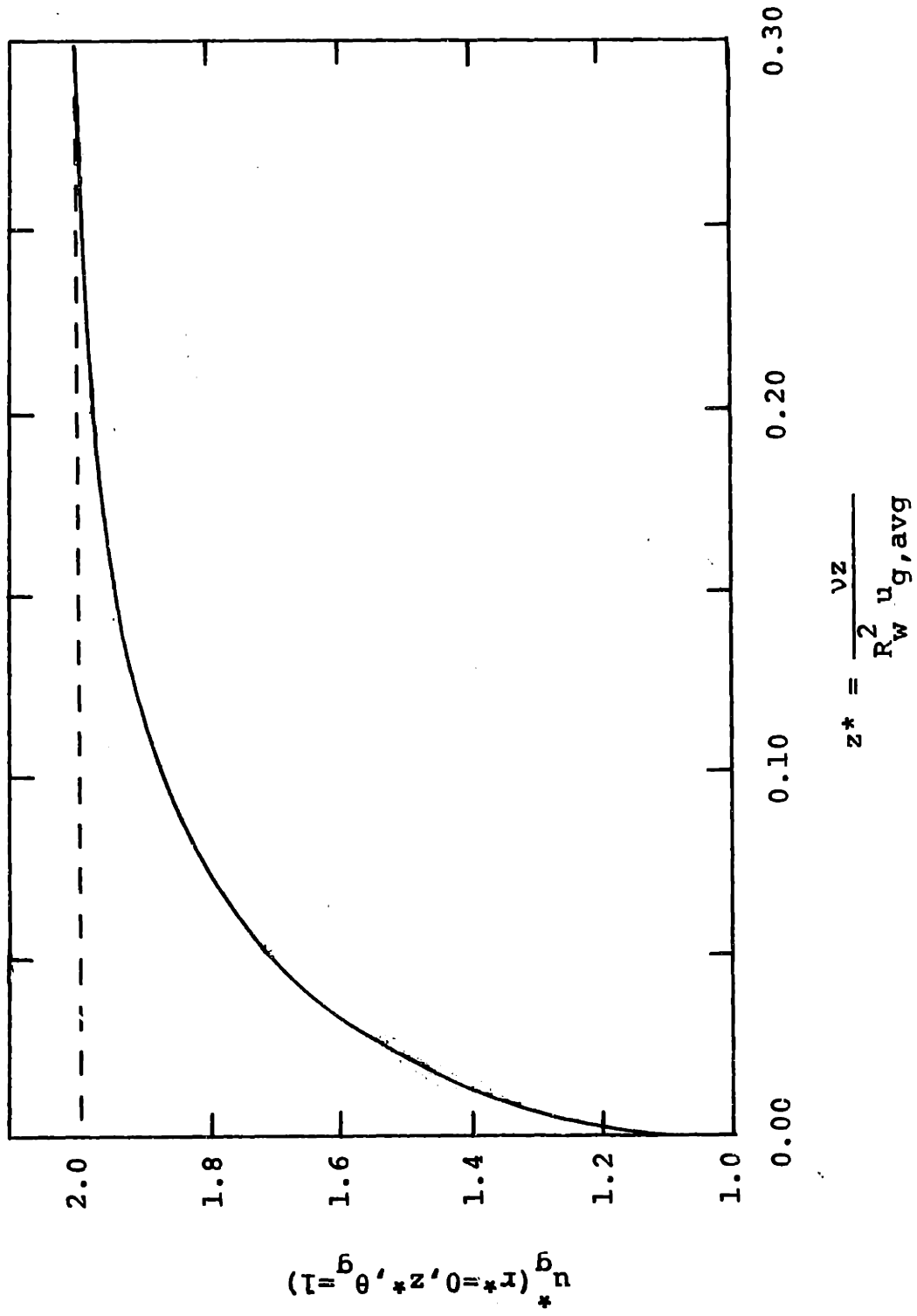


Figure 2.10 Centerline Velocity for Developing Laminar Profile in an Isothermal Tube

for in an expression for the char particle velocity. This is shown as:

$$u_p(z) = u_g(0, z, \theta_g) + [u_p - u_g] \quad (2.15)$$

where  $u_p(z)$  is the particle velocity as a function of distance from the feeder tube (axial velocity component). The second term on the right side of equation (2.15) is the relative velocity of a particle with respect to the main gas. This term reflects the action of gravity on the particle. Following initial velocity changes, this term approaches a constant, namely, the terminal velocity of the char particle with respect to the main gas:

$$u_p(z) - u_g(0, z, \theta_g) \rightarrow u_{\text{term}} \quad (2.16)$$

where  $u_{\text{term}}$  is a function of the properties of both the gas and solid (see Appendix J). Calculated values of  $u_{\text{term}}$  for the experimental conditions of this study are listed in Table J.1.

It is also shown in Appendix J that the time required for a particle to reach this terminal velocity is small compared with overall particle residence times in the furnace reaction zone. Therefore, equation (2.16) is assumed to apply for all  $z \geq 0$ , and the char velocity becomes:

$$\begin{aligned} u_p(z) &= u_g(0, z, \theta_g) + u_{\text{term}} \\ &= [\theta_g \cdot u_{g, \text{avg}} \cdot u_g^*(0, z, 1)] + u_{\text{term}} \end{aligned} \quad (2.17)$$

It is also assumed that the value of  $u_{\text{term}}$ , calculated at an experimental nominal temperature of  $T_0$ , may be used in equation (2.17) at all values of  $z$ , even though  $\theta_g(z)$  varies from unity.

[Calculations in Appendix J are for single, independent char particles. It is more reasonable to believe that the char particles fall as a stream rather than as isolated particles, with each particle exerting some influence on the velocity of neighboring particles. Although this effect is well known, quantitative estimation is difficult. Qualitatively, it can be said that particle velocities are likely to be greater than those calculated by equation (2.17).]

### 2.5.3 Residence Time

Using the results of section 2.4.2, the residence time ( $\tau$ ) of a char particle in the furnace test region may be estimated:

$$\tau = \int_0^L \frac{dz}{u_p(z)} \quad (2.18)$$

where  $z$  is the axial distance from the exit of the feeder tube,  $L$  is the distance of separation between the feeder and particle collection probe, and the particle velocity,  $u_p(z)$ , can be approximated by equation (2.17). Residence times calculated by equation (2.18) are shown in Appendix A

(CO<sub>2</sub> gasification), Appendix B (H<sub>2</sub>O gasification) and Appendix C (pyrolysis experiments).

#### 2.5.4 Particle Collection Efficiency

It is imperative that all particles passing through the reaction zone of the furnace are trapped in the filter/collection probe. The efficiency of this collection system is checked periodically, particularly after equipment modifications or adjustments. This check is done by feeding a pre-weighed amount of char into the furnace under non-reactive conditions (room temperature, argon main gas stream), and collecting the char in a sintered bronze filter in the collection probe, using the usual procedure. Efficiencies of 98 to 105 percent are consistently obtained. Although the conditions during the efficiency tests are not quite the same as for gasification experiments, this range of collection efficiencies is indicative of the error involved in gasification tests.

#### 2.5.5 Particle Heating Rate

Upon entering the reaction zone, the particles must heat up from the laboratory temperature to the reaction (gas) temperature. Kobayashi<sup>44</sup> estimated heat-up times of 15 to 50 msec (heating rate ca.  $10^5$  °K/sec) for coal particles in an argon main gas stream in the same apparatus

used in this study. This finite heat-up time is accounted for in the integral reaction rate analysis (section 4.2).

#### 2.5.6 Reaction Quenching Efficiency

The temperature of the main gas passing through the collection filter in the collection probe is measured as approximately 500 to 600°K, at a distance of about 1 cm below the top edge of the filter. If the reaction rate constant can be approximated by an Arrhenius expression:

$$k = A \exp \left\{ - \frac{E}{RT} \right\} \quad (2.19)$$

then a reaction rate inside the filter may be determined. The rate of reaction in the filter ( $k_f$ ) relative to the reaction rate at 1473°K ( $T_o$ ) is given by:

$$\frac{k_f}{k} = \exp \left\{ - \frac{E}{R} \left[ \frac{1}{T_f} - \frac{1}{T_o} \right] \right\} \quad (2.20)$$

where R is the gas constant. Assuming a filter temperature ( $T_f$ ) of 550°K and an activation energy (E) of 40 kcal/mole:

$$k_f / k \sim 10^{-10} \quad (2.21)$$

Therefore, even if the particles remain in the filter for several minutes at temperature  $T_f$ , a negligible amount of reaction occurs.

#### 2.5.7 Effect of Char Feed Rate

As mentioned in section 2.2.2, the feed rate of char

into the furnace reaction zone is not precisely controlled. Fortunately, changes in feed rate are found to have no regular effect on reaction rate, for both the char-CO<sub>2</sub> and char-H<sub>2</sub>O reactions. In Figure 2.11, for several sets of duplicate runs (i.e., all conditions the same except feed rate), it is seen that feed rate has no apparent effect. Therefore, the feed rate is not included as a variable in the reaction rate analysis (chapter 4).

#### 2.5.8 Pyrolysis Effects

Mandel,<sup>52</sup> studying the same coal char (except that all particles under ca. 200 μm diameter were used), reports the following data for pyrolysis experiments:

<u>Residence Time (msec)</u>	<u>Dry, Ash-free (d.a.f.) Weight Loss (percent)</u>	
	<u>1500°K</u>	<u>1750°K</u>
60-70	9	7
175-225	10-12	9
275-375	8-19	13
400-500	8-17	14
5 minutes	15	23-28

(A residence time of 5 minutes was obtained by placing the sample in a crucible which was raised into the furnace reaction zone.)

The above results must be questioned, in light of the following:



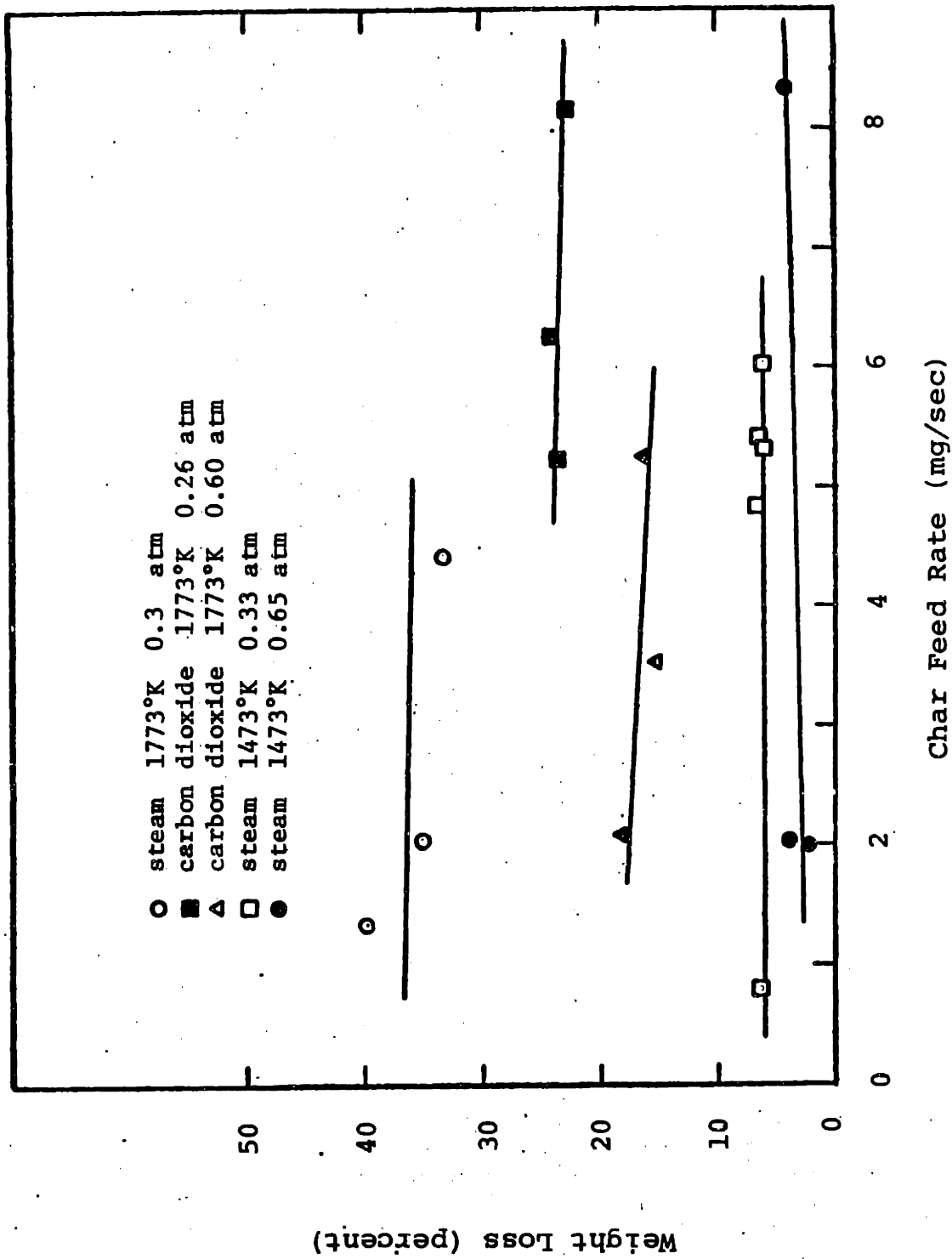


Figure 2.11 Effect of Char Feed Rate

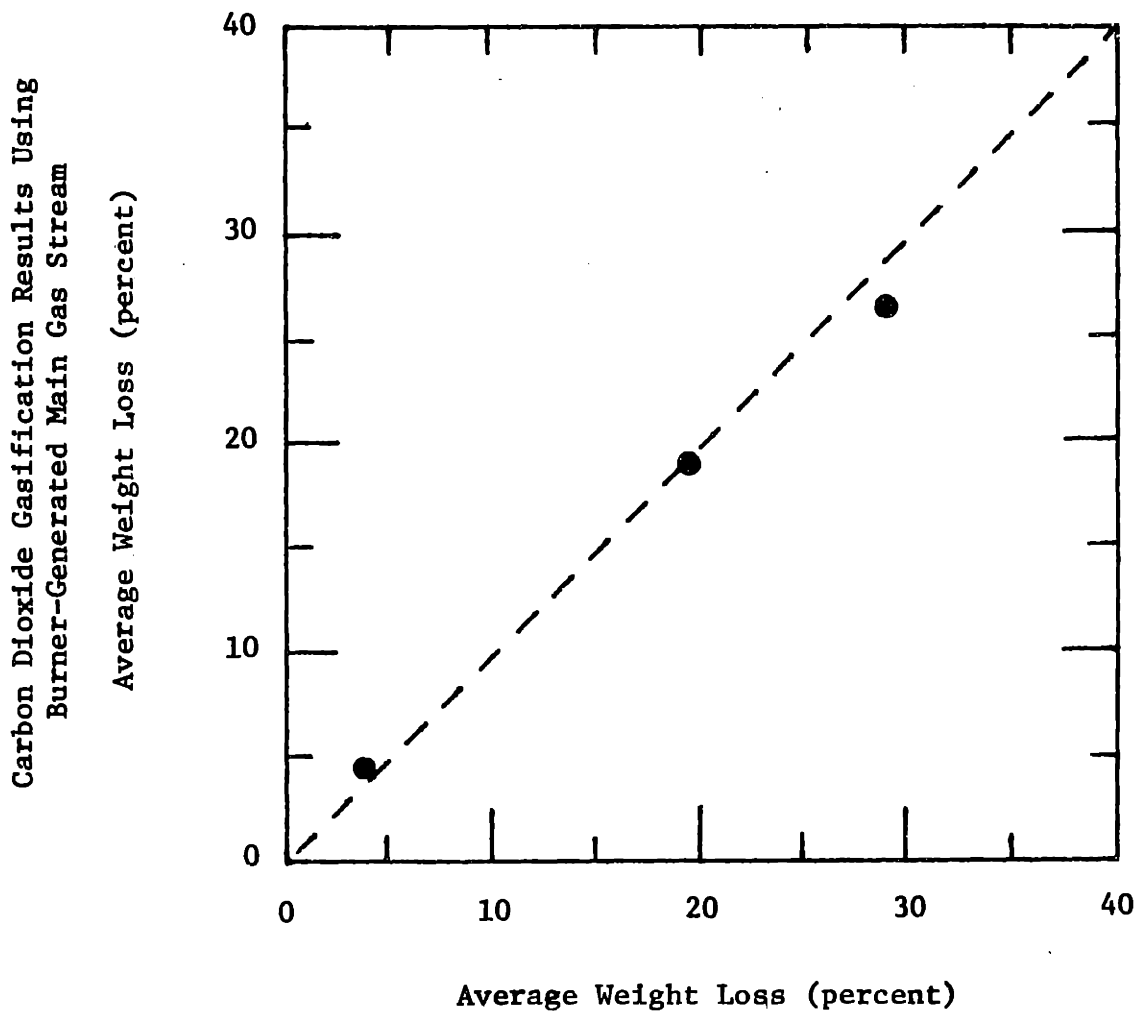
1. Particle heat-up times on the order of 50 msec are expected.
2. The initial char was prepared in a gasifier at 1365°K with residence times on the order of 150 msec.

In this study, a maximum d.a.f. weight loss of 5.1 percent is reported (Appendix C) under pyrolysis conditions at 1773°K, with residence time up to approximately 300 msec. In some runs, the char collected is several percent over 100 percent of the char fed. This range of apparent pyrolysis weight loss data (95 to 100+ percent) corresponds closely to the collection efficiencies discussed in section 2.5.4, implying that weight loss due to pyrolysis at temperatures below 1773°K is negligible. Bush et al<sup>15</sup> showed that pyrolysis effects at higher temperatures and comparable residence times are also expected to be negligible.

#### 2.5.9 Burner-Generated Main Gas Streams

The main gas stream for gasification experiments in both carbon dioxide and steam is generated in the gas burner described in section 2.2.4. For both studies, the burner is ignited using a fuel-rich hydrogen-air mixture. For CO<sub>2</sub> gasification, the hydrogen fuel supply is gradually replaced by carbon monoxide. However, a small amount (ca. 5 mole%) of hydrogen is found to be required in order to maintain a stable

CO - air/O<sub>2</sub> flame. Equilibrium considerations indicate that essentially all of this H<sub>2</sub> appears as H<sub>2</sub>O in the main gas stream. To determine the effect of this steam on reaction rates, several CO<sub>2</sub> gasification experiments are repeated using main gas streams of carbon dioxide from a compressed gas cylinder and argon diluent, instead of the CO<sub>2</sub>-H<sub>2</sub>O-N<sub>2</sub> burner-generated main gas stream. Carbon dioxide partial pressure and run temperature are approximately the same in both instances. As shown in Figure 2.12, significant effects are not observed.



Carbon Dioxide Gasification Results Using  
Main Gas Stream of Pure CO<sub>2</sub> with Argon Diluent

Figure 2.12 Effect of Burner-Generated  
CO<sub>2</sub> Main Gas Stream

## Chapter 3

## RESULTS

3.1 Overview

Experiments were conducted to determine the kinetics of the gasification of a Montana Rosebud coal char in carbon dioxide and steam, at temperatures up to approximately 2100°K. The rate of weight loss of char samples as a function of residence time in various oxidizing atmospheres was observed. Weight loss due to pyrolysis was negligible (section 2.5.8).

Weight loss data are reported on a dry, ash-free (d.a.f.) basis, for easier comparison of this work with studies on different types of carbon. Neglecting the small moisture content (less than 1 wt%) of the initial char, the d.a.f. weight loss (percent) is calculated as:

$$\begin{array}{l} \text{d.a.f.} \\ \text{weight loss} \\ \text{(percent)} \end{array} = \begin{array}{l} \text{observed} \\ \text{weight loss} \\ \text{(percent)} \end{array} \div (1 - f_{\text{ash}}^{\circ})$$

or

$$x \cdot 100\% = \frac{1 - (G_f/G_o)}{1 - f_{\text{ash}}^{\circ}} \cdot 100\% \quad (3.1)$$

where  $G_o$  and  $G_f$  are the initial and final char sample weights, and  $f_{\text{ash}}^{\circ}$  is the fractional ash content in the initial char.

Each reaction (char-CO<sub>2</sub> and char-H<sub>2</sub>O) was studied at three different nominal main gas temperatures ( $T_o$ ), namely

1473, 1773 and 2113°K. The nominal temperature is the maximum temperature in the nonisothermal furnace reaction zone. At each temperature, experiments were conducted in two different test atmospheres (i.e., different partial pressure, P, of the oxidizing gas in the main gas stream). The partial pressures were:

char-CO<sub>2</sub> reaction            P<sub>CO<sub>2</sub></sub> = 0.26, 0.53-0.63 atm

char-H<sub>2</sub>O reaction            P<sub>H<sub>2</sub>O</sub> = 0.32-0.35, 0.65 atm

Total pressure was constant at 1 atm. For each set of conditions {T<sub>0</sub>, P}, three char residence times (τ) were studied. Residence times were governed by the distance (L) between the exit of the char feeder tube and the top of the char collection probe. The feeder-collector separations were:

$$L_1 = 3.0 \text{ in.} = 7.6 \text{ cm} \quad (3.2)$$

$$L_2 = 4.5 \text{ in.} = 11.4 \text{ cm} \quad (3.3)$$

$$L_3 = 6.0 \text{ in.} = 15.2 \text{ cm} \quad (3.4)$$

resulting in residence times up to approximately 350 msec at 1473°K, 300 msec at 1773°K and 250 msec at 2113°K.

### 3.2 Weight Loss Data

#### 3.2.1 Char - Carbon Dioxide Reaction

Results of gasification experiments in CO<sub>2</sub> test atmospheres are summarized in Table 3.1 and Figure 3.1. Note that

Table 3.1  
Summary of Gasification Results in CO<sub>2</sub>

Nominal Bulk Gas Conditions			Average d.a.f. Weight Loss (percent) as a function of Feeder - Collector Separation		
<u>T<sub>O</sub></u> (°K)	<u>P<sub>C</sub></u> (atm)	<u>C<sub>O</sub> x 10<sup>6</sup></u> (mole/cm <sup>3</sup> )	<u>7.6 cm</u>	<u>11.4 cm</u>	<u>15.2 cm</u>
1473	0.26	2.15	- 1.5	1.8	4.3
1473	0.53	4.38	4.8	7.3	12.9
1773	0.26	1.79	14.5	23.8	29.4
1773	0.57-0.63	4.12	11.5	22.9	33.4
2113	0.26	1.50	20.9	41.2	48.5
2113	0.57	3.29	25.0	44.6	64.0

Notes

1. Total pressure = 1 atm
2. Main gas flow rate varies between 6.13 and 6.59 l/min (STP)
3. Excludes the results of runs C-10 and C-16 (Table A.1)
4. P<sub>C</sub> is the partial pressure of carbon dioxide in the main gas stream.

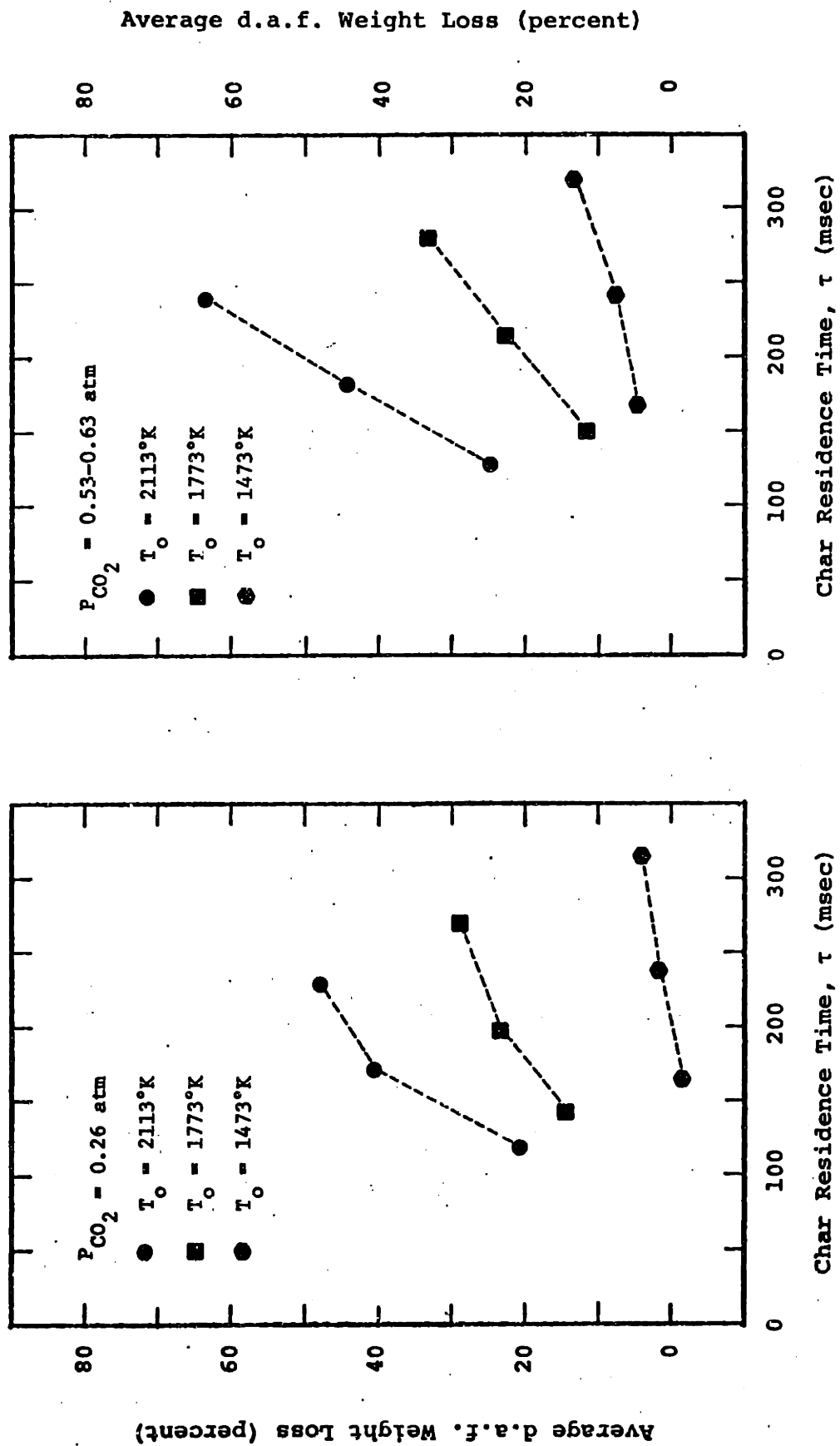


Figure 3.1 Char Weight Loss (d.a.f.) in CO<sub>2</sub>



$C_o$  (Table 3.1) is the concentration of  $CO_2$  in the main gas, evaluated at the nominal temperature,  $T_o$ . Run data are shown in detail in Table A.1 (Appendix A). Calculations in Chapter 4, based on data at 1773°K,  $P_{CO_2} = 0.57-0.63$  atm, use the average value of 0.60 atm as the carbon dioxide partial pressure.

The negative d.a.f. weight loss observed at 1473°K,  $P_{CO_2} = 0.26$  atm, is probably due to inefficiencies in the char feeding and collection systems. Also of note is the fact that the weight loss at 1773°K,  $P_{CO_2} \sim 0.60$  atm, is slightly less than the weight loss at the same nominal gas temperature, with  $P_{CO_2} = 0.26$  atm, for feeder-collector separations of 7.6 and 11.4 cm. This could be attributed to collection inefficiencies, and to the difference in the main gas heat capacity (which would result in a slightly longer heat-up time for the main gas at the higher  $CO_2$  partial pressure), although similar effects are not seen at the other experimental temperatures. The maximum d.a.f. weight loss observed was 64.0 percent at 2113°K,  $P_{CO_2} = 0.57$  atm, residence time of 240 msec.

### 3.2.2 Char - Steam Reaction

Results of char gasification experiments in steam test atmospheres are summarized in Table 3.2 and Figure 3.2. Details of experimental data are in Table B.1 (Appendix B). A maximum of 78.1 percent d.a.f. weight loss was observed at 2113°K,  $P_{H_2O} = 0.65$  atm, residence time of 224 msec.

Table 3.2

Summary of Gasification Results in Steam

Nominal Bulk Gas Conditions			Average d.a.f. Weight Loss (percent) as a function of Feeder - Collector Separation		
$T_o$ (°K)	$P_w$ (atm)	$C_o \times 10^6$ (mole/cm <sup>3</sup> )	<u>7.6 cm</u>	<u>11.4 cm</u>	<u>15.2 cm</u>
1473	0.32-0.35	2.73	1.1	4.5	7.5
1473	0.65	5.38	5.0	11.6	26.6
1773	0.32	2.20	22.4	34.5	44.9
1773	0.65	4.47	27.2	51.2	72.2
2113	0.32	1.85	31.9	55.7	66.7
2113	0.65	3.75	28.5	59.6	78.1

Notes

1. Total pressure = 1 atm
2. Main gas flow rate varies between 5.94 and 6.28 l/min (STP)
3. Excludes the results of runs S-33, S-34, S-39, S-41 and S-58 (Table B.1)
4.  $P_w$  is the partial pressure of steam in the main gas stream

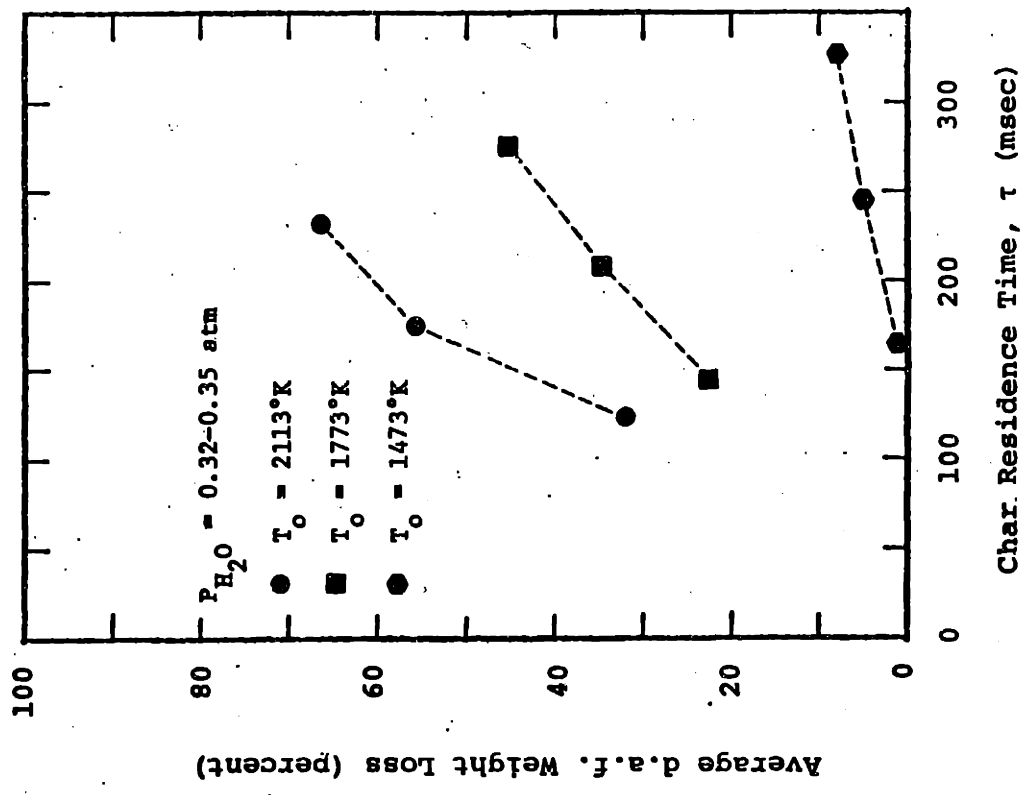
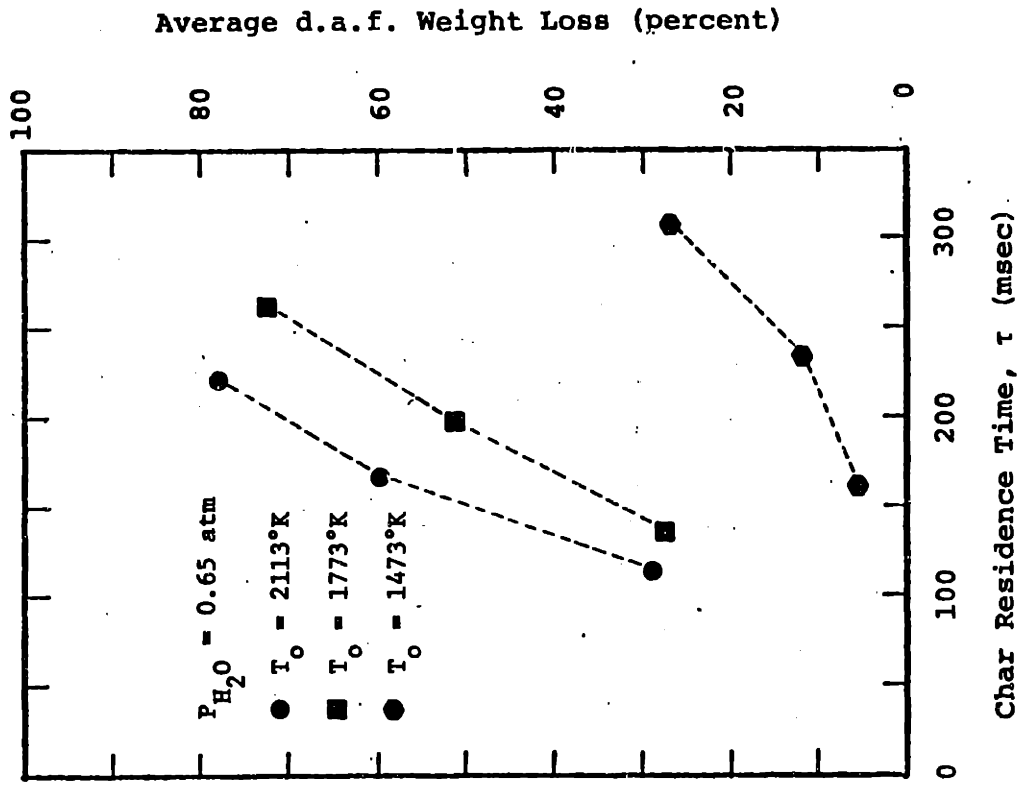


Figure 3.2 Char Weight Loss (d.a.f.) in Steam

## Chapter 4

### DISCUSSION OF RESULTS

#### 4.1 Power Law Kinetics

The intrinsic kinetics of the char gasification reactions with carbon dioxide and steam are expressed by a power law kinetic model:

$$R' = - \frac{1}{W} \frac{dW}{dt} = k' C^n \quad (4.1)$$

where  $R'$  is the intrinsic rate of char (carbon) gasification ( $\text{g sec}^{-1} \text{g}^{-1}$ ),  $W$  is the d.a.f. weight (g) of a char sample after time  $t$  (sec) in the reaction zone,  $C$  is the oxidizing gas ( $\text{CO}_2$  or  $\text{H}_2\text{O}$ ) concentration ( $\text{mole/cm}^3$ ),  $n$  is the intrinsic order of reaction with respect to the oxidizing gas, and  $k'$  is the intrinsic rate constant ( $\text{sec}^{-1}(\text{mole/cm}^3)^{-n}$ ). The temperature dependence of the rate constant is assumed to be of the Arrhenius form:

$$k' = A' \exp \left\{ - \frac{E}{RT_p} \right\} \quad (4.2)$$

where  $E$  is the intrinsic activation energy,  $T_p$  is the absolute particle temperature,  $A'$  is the Arrhenius frequency (or pre-exponential) factor (same units as  $k'$ ) and  $R$  is the gas constant.

It is sometimes convenient to define reaction rates on the basis of a unit total surface area or unit volume of

char particles:

$$R'' = - \frac{1}{S_g W} \frac{dW}{dt} = \frac{1}{S_g} R' \quad (4.3)$$

$$R''' = \rho_p \left\{ - \frac{1}{W} \frac{dW}{dt} \right\} = \rho_p R' \quad (4.4)$$

where  $R''$  is the intrinsic reaction rate per unit total surface area ( $\text{g}\cdot\text{cm}^{-2}\cdot\text{sec}^{-1}$ ) and  $R'''$  is the intrinsic reaction rate per unit char volume ( $\text{g}\cdot\text{cm}^{-3}\cdot\text{sec}^{-1}$ ).

The steps to be followed in determining the intrinsic kinetic parameters  $E$ ,  $n$  and  $A'$  are as follows:

1. Calculate apparent (observed) reaction rates based on the experimental results presented in Chapter 3.
2. Evaluate the effects of interphase heat and mass transfer rate limitations. Calculate the temperature ( $T_s$ ) and oxidant concentration ( $C_s$ ) on the external surface of a reacting char particle.
3. Evaluate the effects of heat and mass transfer rate limitations within the porous structure of the char particles.

## 4.2 Apparent Kinetics

The apparent kinetics of a gas-solid reaction are calculated by assuming that the conditions (temperature, reactant concentration) throughout the solid particles are uniform and equal to the bulk gas phase conditions ( $T_g, C_g$ ). The intrinsic

kinetic parameters in equations (4.1) and (4.2) are replaced by apparent kinetic parameters (denoted by an overbar), resulting in the following rate expression:

$$\bar{R}' = -\frac{1}{W} \frac{dW}{dt} = \bar{A}' \exp\left\{-\frac{E}{RT_p}\right\} C_g^{\bar{n}} \quad (4.5)$$

where  $\bar{R}'$  is the apparent reaction rate. Recall that  $T_g$ , and therefore  $C_g$ , are functions of position,  $z$  (distance from the feeder tube), in the furnace reaction zone.

The following dimensionless parameters are defined:

$$\theta_g(z) = T_g(z) / T_o \quad (2.6)$$

$$x = 1 - (W/W_o) \quad (4.6)$$

$$\bar{\epsilon}_o = \frac{\bar{E}}{RT_o} \quad (4.7)$$

where  $W_o$  is the initial d.a.f. weight of a char sample. The gas concentration is expressed in terms of the nominal concentration,  $C_o$ :

$$C_o = \frac{P}{RT_o} = C_g(z) \cdot \theta_g(z) \quad (4.8)$$

where  $P$  is the oxidizing gas partial pressure in the main gas stream. Thus, equation (4.5) is rewritten as:

$$\bar{R}' = -\frac{d}{dt}[\ln(1-x)] \quad (4.9)$$

$$= \bar{A}' [\exp(-\bar{\epsilon}_o/\theta_g)] [C_o/\theta_g]^{\bar{n}} \quad (4.10)$$

If the reaction zone was isothermal at temperature  $T_o$ , the apparent reaction rate, denoted  $\bar{R}'_{iso}$ , could be determined via a differential analysis, by measuring the slope of a

straight line plot of the quantity  $\{\ln(1-x)\}$  versus time,  $t$ , as shown by equation (4.9). Note that the intercept of such a plot would not necessarily be at  $t=0$  since there is a finite heat-up time for the char particles. Plots of this form are shown in Figure 4.1 ( $\text{CO}_2$  gasification) and Figure 4.2 (steam gasification). Apparent reaction rates, determined by this method, are listed on Figures 4.1 and 4.2. Once apparent reaction rates are determined by equation (4.9), values of  $\bar{A}$ ,  $\bar{E}$  and  $\bar{n}$  could be determined which best fit these rates to equation (4.10).

Unfortunately, the reaction zone for the gasification experiments was not isothermal. Thus, the rates listed on Figure 4.1 and Figure 4.2 are for some average temperature in the reaction zone, rather than for the nominal temperature,  $T_0$ . The nonisothermal reaction zone suggests that an integral analysis be used to determine the apparent reaction rates. Time,  $t$ , is expressed in terms of particle velocity and distance traveled through the reaction zone:

$$dt = \frac{dz}{u_p(z)} \quad (4.11)$$

The right sides of equations (4.9) and (4.10) are equated and integrated, using equation (4.11):

$$-\ln \left\{ \frac{1-x(z_2)}{1-x(z_1)} \right\} = \bar{A} \bar{C}_o \bar{n} \int_{z_1}^{z_2} \frac{\theta_g^{-\bar{n}} \cdot \exp(-\bar{E}_o/\theta_g)}{[\theta_g \cdot u_{g,avg} \cdot u_g^*(0,z,1)] + u_{term}} dz \quad (4.12)$$

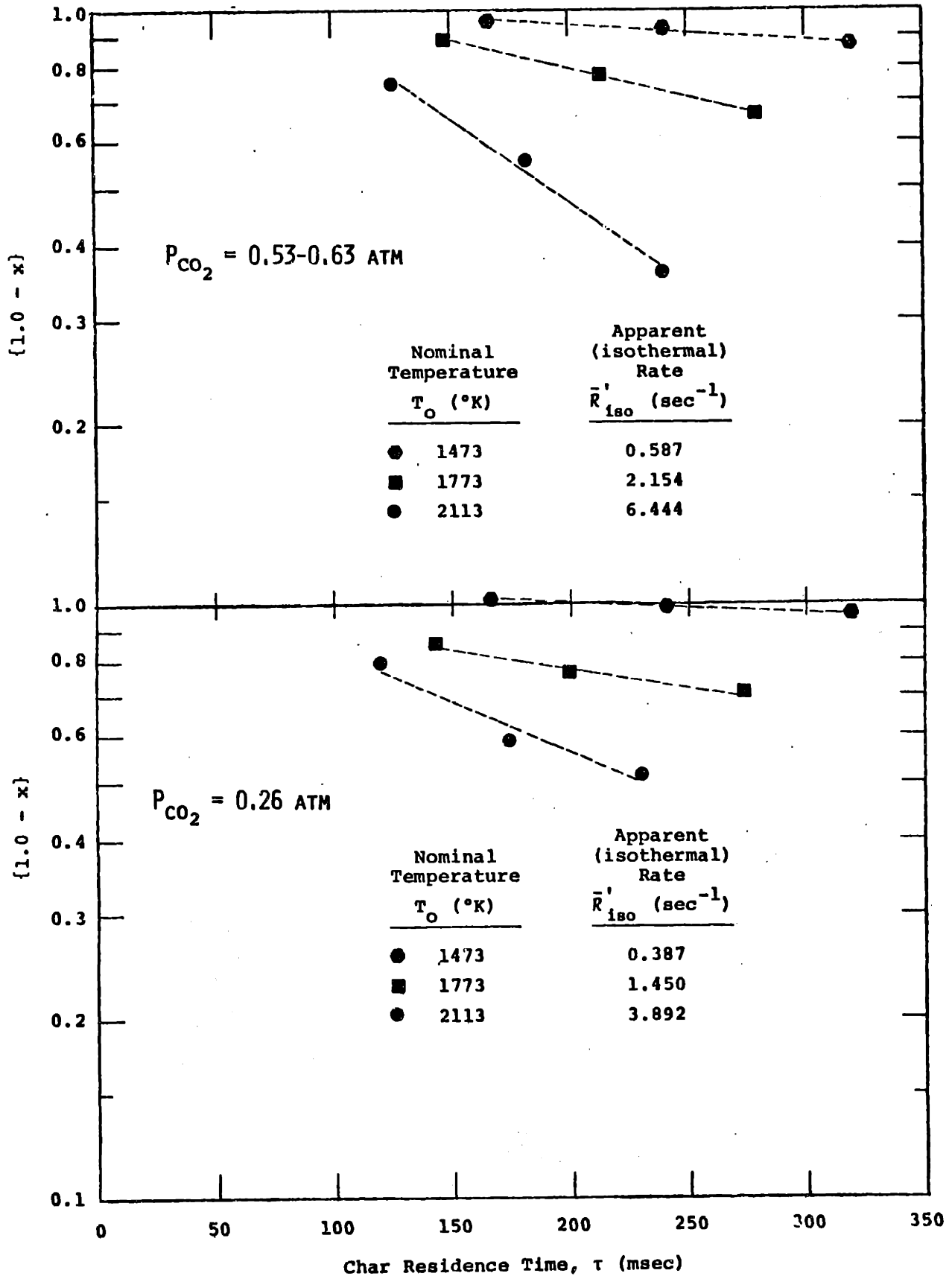


Figure 4.1 Differential Analysis of Apparent Rate of Char Gasification In Carbon Dioxide (Isothermal Reaction Zone)



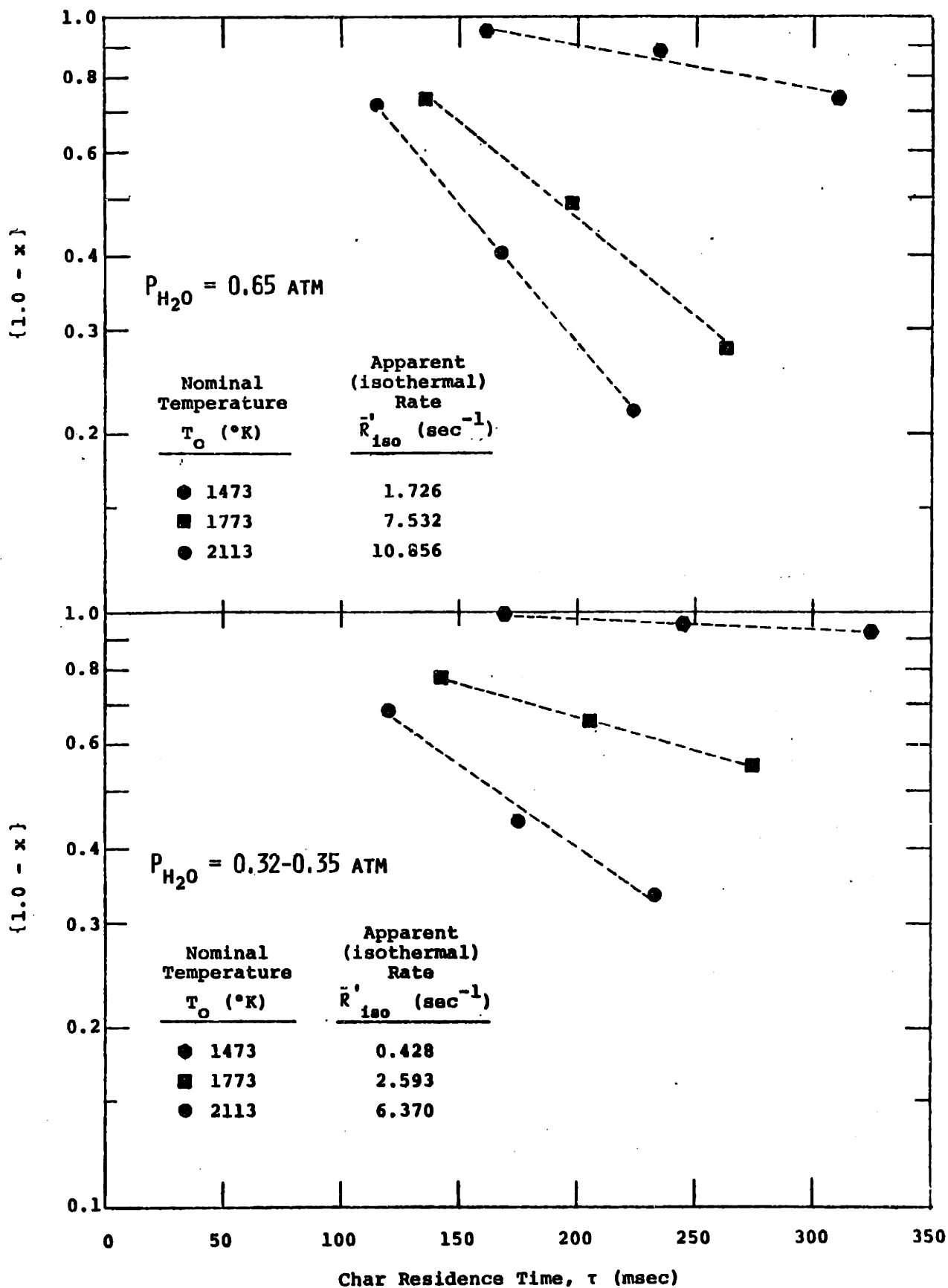


Figure 4.2 Differential Analysis of Apparent Rate of Char Gasification in Steam (Isothermal Reaction Zone)

where  $x(z)$  is the d.a.f. fractional char weight loss after falling a distance  $z$  through the furnace reaction zone, and equation (2.17) is used to express the char particle velocity. In order to avoid the uncertainties in the gas/char heat-up region of the furnace ( $z < L_1$ ), the lower limit of integration is chosen as  $L_1$ , and the upper limit may be either  $L_2$  or  $L_3$ :

$$z_1 = L_1 \quad (4.13)$$

$$z_2 = L = L_2 \text{ or } L_3 \quad (4.14)$$

where  $L_1$ ,  $L_2$  and  $L_3$  are defined in section 3.1. Replacing  $\theta_g$  by the experimentally measured  $\theta_w$  (see section 2.5.1), the integral on the right side of equation (4.12), denoted for simplicity by  $I(T_o, \bar{E}, \bar{n}, L)$ ,

$$I(T_o, \bar{E}, \bar{n}, L) = \int_{L_1}^L \frac{\theta_w^{-\bar{n}} \cdot \exp(-\bar{E}_o/\theta_w)}{[\theta_w \cdot u_{g,avg} \cdot u_g^*(0,z,1)] + u_{term}} dz \quad (4.15)$$

may be evaluated numerically for particular values of  $\bar{E}$  and  $\bar{n}$ , by approximating  $\theta_w$  by equations (2.3) through (2.5), and expressing  $u_g^*$  by equations (2.10), (2.12), (2.13) and (2.14). Numerical integration of equation (4.15) is shown in Tables M.1 and M.2 (Appendix M). Thus, the integrated rate expression, equation (4.12), becomes:

$$-\ln \left\{ \frac{1-x(L)}{1-x(L_1)} \right\} = \bar{A}' C_o^{\bar{n}} I(T_o, \bar{E}, \bar{n}, L) \quad (4.16)$$

The integral analysis above involves determining values

for  $\bar{A}'$ ,  $\bar{E}$  and  $\bar{n}$  which best fit the experimental weight loss data to equation (4.16). Once these values are obtained, apparent rates at each nominal temperature are calculated using equation (4.10), with  $\theta_g$  set equal to unity.

Further simplification is made by expressing  $I(T_o, \bar{E}, \bar{n}, L)$  in the linear form:

$$\ln I = I_1 \bar{E} + I_3 \bar{n} + I_4 \quad (4.17)$$

where the parameters  $I_1$ ,  $I_3$  and  $I_4$ , for a given main gas composition, are functions of  $T_o$  and  $L$ . The error involved in approximating  $I(T_o, \bar{E}, \bar{n}, L)$  by equation (4.17) is less than 3 percent. The linearization parameters  $I_1$ ,  $I_3$  and  $I_4$  are calculated using the least square fit method of Appendix L. They are listed in Appendix M, Table M.3.

Taking the natural logarithm of equation (4.16) and using equation (4.17) results in a linear form of the integrated rate equation:

$$\ln \left[ -\ln \left\{ \frac{1-x(L)}{1-x(L_1)} \right\} \right] - I_4 = \ln \bar{A}' + \bar{n} [\ln C_o + I_3] + I_1 \bar{E} \quad (4.18)$$

Equation (4.18) is particularly convenient because it is linear in the three unknowns,  $\ln \bar{A}'$ ,  $\bar{E}$  and  $\bar{n}$ . Thus, the method of least squares for fitting data to linear equations, may be used to fit the char weight loss data of Tables 3.1 and 3.2 to equation (4.18). The computer program AVFIT (Appendix O) is used to perform this correlation. The results are in section 4.2.1 (char-CO<sub>2</sub> reaction) and section 4.2.2 (char-H<sub>2</sub>O reaction).

After determining the least square values of  $\bar{A}'$ ,  $\bar{E}$  and  $\bar{n}$ , apparent reaction rates,  $R'_{reg}$ , are calculated at each set of conditions  $\{T_o, C_o\}$ , using equation (4.10) with  $\theta_g$  set to unity. There is no reason a priori to expect that the experimental data taken over the entire range of conditions studied (1473 to 2113°K) can be expressed by equation (4.16) in terms of a single set of apparent kinetic parameters,  $\{\bar{A}', \bar{E}, \bar{n}\}$ . Thus, the calculated rates must be corrected for the regression error in the least square fit model which is used to determine  $\{\bar{A}', \bar{E}, \bar{n}\}$ . Recalling that data for equation (4.18) are available at two residence times ( $L = L_2$  and  $L_3$ ) for each set of conditions  $\{T_o, C_o\}$ , the correction factor is:

$$\text{Apparent Rate Correction Factor} = \left[ \frac{1 - \hat{x}(L_2)}{1 - x(L_2)} + \frac{1 - \hat{x}(L_3)}{1 - x(L_3)} \right] \cdot \frac{1}{2} \quad (4.19)$$

where  $\hat{x}$  denotes the d.a.f. fractional weight loss value predicted by the least square fit linear regression model. Therefore, the apparent reaction rates to be used in the subsequent analysis of the intrinsic kinetics are:

$$\bar{R}' = \bar{R}'_{reg} \cdot \begin{matrix} \text{correction factor,} \\ \text{equation (4.19)} \end{matrix} \quad (4.20)$$

#### 4.2.1 Char - Carbon Dioxide Reaction

The char gasification data of Table 3.1 were analyzed via computer program AVFIT. The following observed kinetic parameters were determined:

$$\bar{E} \quad \text{activation energy} = 23.2 \text{ kcal/mole} \quad (4.21)$$

$$\bar{n} \quad \text{order of reaction} = 0.26 \quad (4.22)$$

$$\bar{A}' \quad \text{frequency factor} = 5.81 \times 10^4 \quad (4.23)$$

The units of the frequency factor are:

$$\bar{A}' \quad [=] \text{ g} \cdot \text{sec}^{-1} \cdot \text{g}^{-1} \cdot (\text{mole/cm}^3)^{-0.26}$$

The results of AVFIT for CO<sub>2</sub> gasification data are shown in Table 4.1. The correlation coefficient, "R squared", at the bottom of the "Analysis of Variance" Table, is indicative of the closeness of the fit of the experimental data to the linearized apparent rate expression (4.18). R squared equal to ±1.0 indicates an exact fit. A comparison of the weight loss data predicted by AVFIT with the experimental data is shown in Figure 4.3. The agreement is quite good, with the largest difference in values being less than 5 percent d.a.f. weight loss.

Apparent rates at each set of experimental conditions are calculated using equation (4.10) and the apparent kinetic parameters given by equations (4.21) through (4.23). These rates are shown in Table 4.2. Additionally, the correction factor, equation (4.19), has been applied to each of the rates, as shown in Table 4.2. Thus, the rates listed in the last column of Table 4.2,  $\bar{R}'$ , will be used in the analysis to follow. It is seen that the apparent gasification rate increases by approximately a factor of 10 between 1473 and 2113°K.

Table 4.1

Apparent Kinetics of Char Gasification in Carbon Dioxide:  
Least Square Linear Regression Model

$T_o$ (°K)	$P_{CO_2}$ (atm)	$C_o \times 10^6$ (mole/cm <sup>3</sup> )	$L$ (cm)	$x(L)$ (%)	$x(L_1)$ (%)	$\hat{x}(L)$ (%)	$Y^\dagger$	$(Y - \hat{Y})^\dagger$
1473	0.26	2.15	11.4	1.8	-1.5	1.9	-0.802	-0.037
1473	0.26	2.15	15.2	4.2	-1.5	3.9	-0.931	0.056
1473	0.53	4.38	11.4	7.3	4.8	8.7	-1.017	-0.440
1473	0.53	4.38	15.2	12.9	4.8	10.9	-0.497	0.302
1773	0.26	1.79	11.4	23.8	14.5	23.6	0.611	0.020
1773	0.26	1.79	15.2	29.4	14.5	29.0	0.420	0.028
1773	0.60	4.12	11.4	22.9	11.5	23.6	0.747	-0.063
1773	0.60	4.12	15.2	33.4	11.5	30.5	0.772	0.161
2113	0.26	1.50	11.4	41.2	20.9	40.2	1.711	0.056
2113	0.26	1.50	15.2	48.5	20.9	50.9	1.374	-0.104
2113	0.57	3.29	11.4	44.6	25.0	47.6	1.694	-0.167
2113	0.57	3.29	15.2	64.0	25.0	59.2	1.873	0.189

Analysis of Variance

<u>Source of Variation</u>	<u>Degrees of Freedom</u>	<u>Sum of Squares</u>	<u>Mean Square</u>	<u>F Ratio</u>
Total (uncorrected)	12	15.69		
Mean	1	2.96		
Total (corrected)	11	12.74		
Regression	2	12.34	6.17	} 139.
Residual	9	0.40	0.044	

R squared = 0.968

$$^\dagger Y = \ln \left[ -\ln \left\{ \frac{1 - x(L)}{1 - x(L_1)} \right\} \right] - I_4(T_o, L)$$

$\hat{Y}$  is the value of Y predicted by the linear regression model.

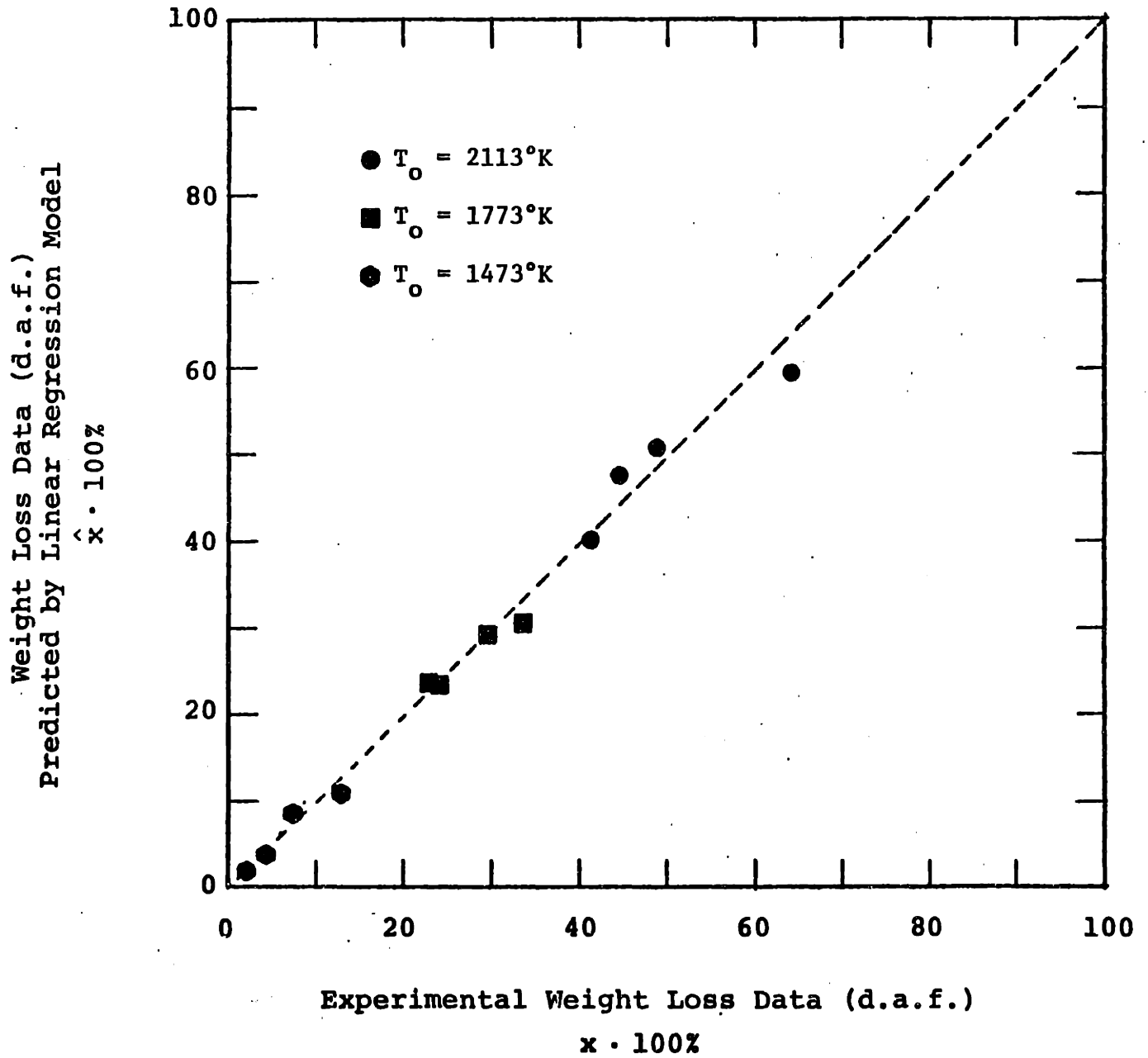


Figure 4.3 Comparison of Experimental Weight Loss Data with Values Predicted by Linear Regression Model for Char Gasification in Carbon Dioxide

Table 4.2

Apparent Reaction Rates:  
Char Gasification in Carbon Dioxide

Nominal Gas Conditions		$\bar{R}'_{iso}$	$\bar{R}'_{reg}$	Regression Correction Factor	$\bar{R}'$
$T_o$ (°K)	$P_C$ (atm)	(sec <sup>-1</sup> )	(sec <sup>-1</sup> )		(sec <sup>-1</sup> )
1473	0.26	0.387	0.688	1.001	0.689
1473	0.53	0.587	0.830	1.004	0.833
1773	0.26	1.450	2.499	1.004	2.509
1773	0.60	2.154	3.115	1.017	3.168
2113	0.26	3.892	6.871	0.985	6.769
2113	0.57	6.444	8.446	1.041	8.789



#### 4.2.2 Char - Steam Reaction

The apparent kinetic parameters for char gasification in steam, determined by the linear regression method of AVFIT, are:

$$\bar{E} \text{ activation energy} = 26.2 \text{ kcal/mole} \quad (4.24)$$

$$\bar{n} \text{ order of reaction} = 1.19 \quad (4.25)$$

$$\bar{A}' \text{ frequency factor} = 3.07 \times 10^{10} \quad (4.26)$$

The results of the linear regression model are shown in Table 4.3 and Figure 4.4. Comparing Figure 4.3 (char-CO<sub>2</sub>) with Figure 4.4 shows that the 3 parameter ( $\bar{A}'$ ,  $\bar{E}$ ,  $\bar{n}$ ) linear regression model is less successful in correlating the results of the steam gasification experiments than the CO<sub>2</sub> gasification experiments. The correction factors, equation (4.19), will be more significant for the char-H<sub>2</sub>O study. This is shown in Table 4.4, where apparent gasification rates in steam are summarized.

#### 4.3 Changes in Physical Properties

While exposed to gasifying atmospheres, the char particles undergo physical changes. As discussed in section 1.4.3, specific surface area ( $S_g$ ) is expected to change (initially increasing). Changes in porosity (i.e., changes in bulk density) are also expected.

The total surface area (N<sub>2</sub> adsorption) and bulk density

Table 4.3

Apparent Kinetics of Char Gasification in Steam:  
Least Square Linear Regression Model

$T_o$ (°K)	$P_{H_2O}$ (atm)	$C_o \times 10^6$ (mole/cm <sup>3</sup> )	L (cm)	x(L) (%)	x(L <sub>1</sub> ) (%)	$\hat{x}(L)$ (%)	$Y^\dagger$	$(Y - \hat{Y})^\dagger$
1473	0.33	2.73	11.4	4.5	1.1	5.9	-0.774	-0.352
1473	0.33	2.73	15.2	7.5	1.1	8.6	-0.824	-0.166
1473	0.65	5.38	11.4	11.6	5.0	14.6	-0.010	-0.392
1473	0.65	5.38	15.2	26.6	5.0	19.8	0.567	0.419
1773	0.32	2.20	11.4	34.5	22.4	33.8	0.971	0.062
1773	0.32	2.20	15.2	44.9	22.4	40.4	0.965	0.262
1773	0.65	4.47	11.4	51.2	27.2	49.0	1.867	0.117
1773	0.65	4.47	15.2	72.2	27.2	59.6	2.035	0.493
2113	0.32	1.85	11.4	55.7	31.9	53.7	2.064	0.109
2113	0.32	1.85	15.2	66.7	31.9	64.8	1.857	0.079
2113	0.65	3.75	11.4	59.6	28.5	69.8	2.385	-0.412
2113	0.65	3.75	15.2	78.1	28.5	83.7	2.396	-0.221

Analysis of Variance

<u>Source of Variation</u>	<u>Degrees of Freedom</u>	<u>Sum of Squares</u>	<u>Mean Square</u>	<u>F Ratio</u>
Total (uncorrected)	12	30.25		
Mean	1	15.19		
Total (corrected)	11	15.06		
Regression	2	14.01	7.01	60.3
Residual	9	1.05	0.116	

R squared = 0.930

$$^\dagger Y = \ln \left[ -\ln \left\{ \frac{1 - x(L)}{1 - x(L_1)} \right\} \right] - I_4(T_o, L)$$

$\hat{Y}$  is the value of Y predicted by the linear regression model.

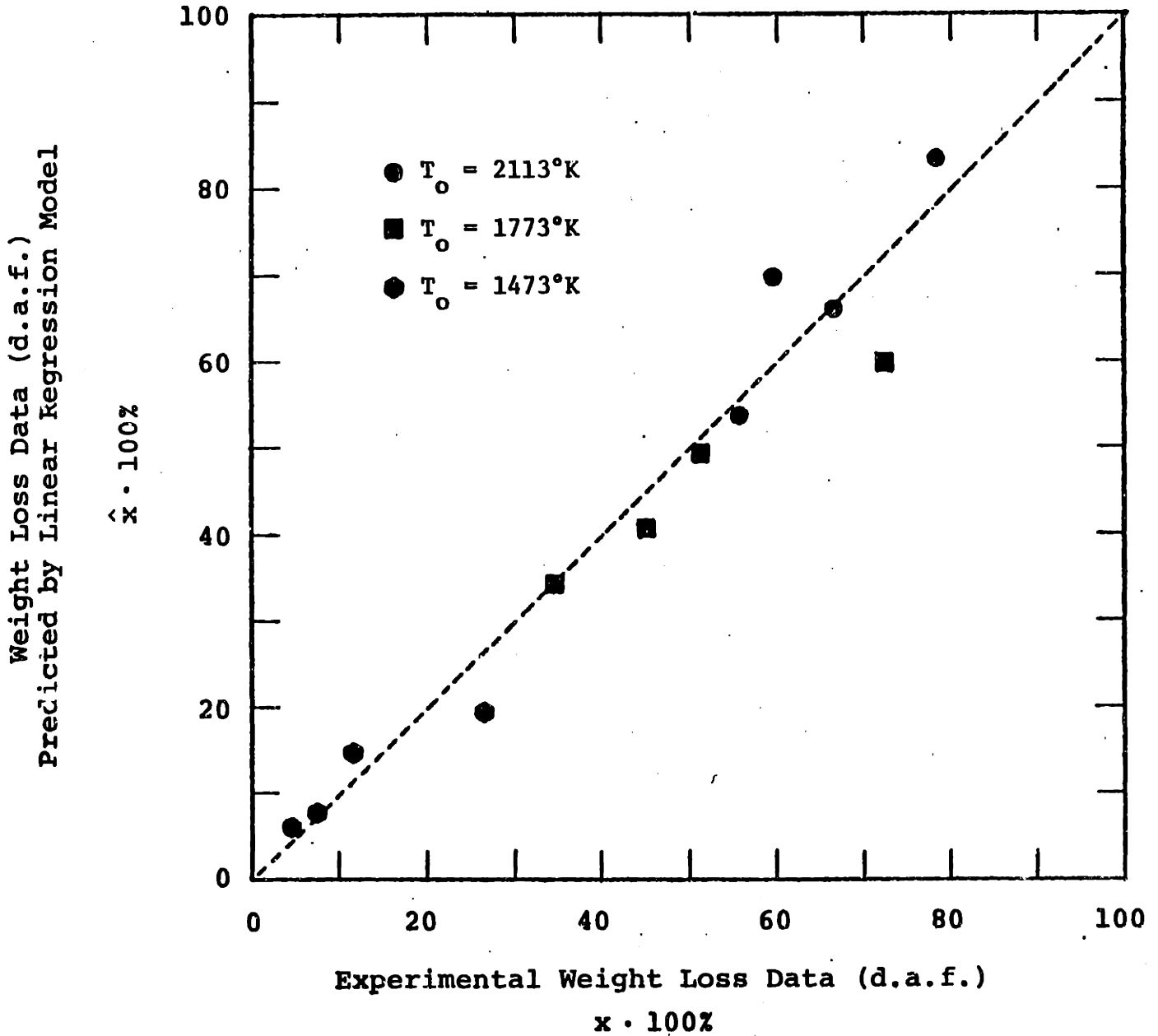


Figure 4.4 Comparison of Experimental Weight Loss Data With Values Predicted by Linear Regression Model For Char Gasification in Steam

Table 4.4

Apparent Reaction Rates:  
Char Gasification in Steam

Nominal Gas Conditions		$\bar{R}'_{iso}$	$\bar{R}'_{reg}$	Regression Correction Factor	$\bar{R}'$
$T_o$ (°K)	$P_w$ (atm)	( $sec^{-1}$ )	( $sec^{-1}$ )		( $sec^{-1}$ )
1473	0.33	0.428	0.982	0.987	0.969
1473	0.65	1.726	2.198	1.029	2.328
1773	0.32	2.593	3.451	1.046	3.611
1773	0.65	7.532	8.009	1.250	10.009
2113	0.32	6.370	9.261	1.051	10.229
2113	0.65	10.856	21.495	0.747	16.056

of several of the partially gasified char samples were measured (analysis by Phillips Petroleum Company, Bartlesville, Oklahoma). The results are detailed in Tables N.1 and N.2. The data of these tables may be compared with corresponding values for the initial char:

$$S_g = 81 \text{ m}^2/\text{g}$$
$$\rho_p = 0.49 \text{ g/cm}^3$$

Trends in the data of Tables N.1 and N.2 may be seen by plotting specific surface area and bulk density versus percent burnoff (d.a.f.), as shown in Figures 4.5 through 4.7.

### Surface Area

The specific (nitrogen) surface area of samples in  $\text{CO}_2$  (Figure 4.5) at  $1473^\circ\text{K}$  rises quickly (less than 1 percent weight loss) to a value of approximately 220 to 240  $\text{m}^2/\text{g}$ , then appears to level off. Similarly, the surface area of samples in  $\text{CO}_2$  at  $1773^\circ\text{K}$  appears to level off at approximately 170 to 180  $\text{m}^2/\text{g}$ , but begins to decrease after approximately 25 percent d.a.f. weight loss.

The surface area of samples in steam (Figure 4.6) at  $1473^\circ\text{K}$  rises quickly to approximately 200 to 250  $\text{m}^2/\text{g}$ , and continues to increase at a slower rate for continued burnoff. A maximum of 369  $\text{m}^2/\text{g}$  is reported at 30.4 percent d.a.f. weight loss. The surface area of samples in steam at  $1773^\circ\text{K}$  appears to level off at approximately 210 to 240  $\text{m}^2/\text{g}$ ,

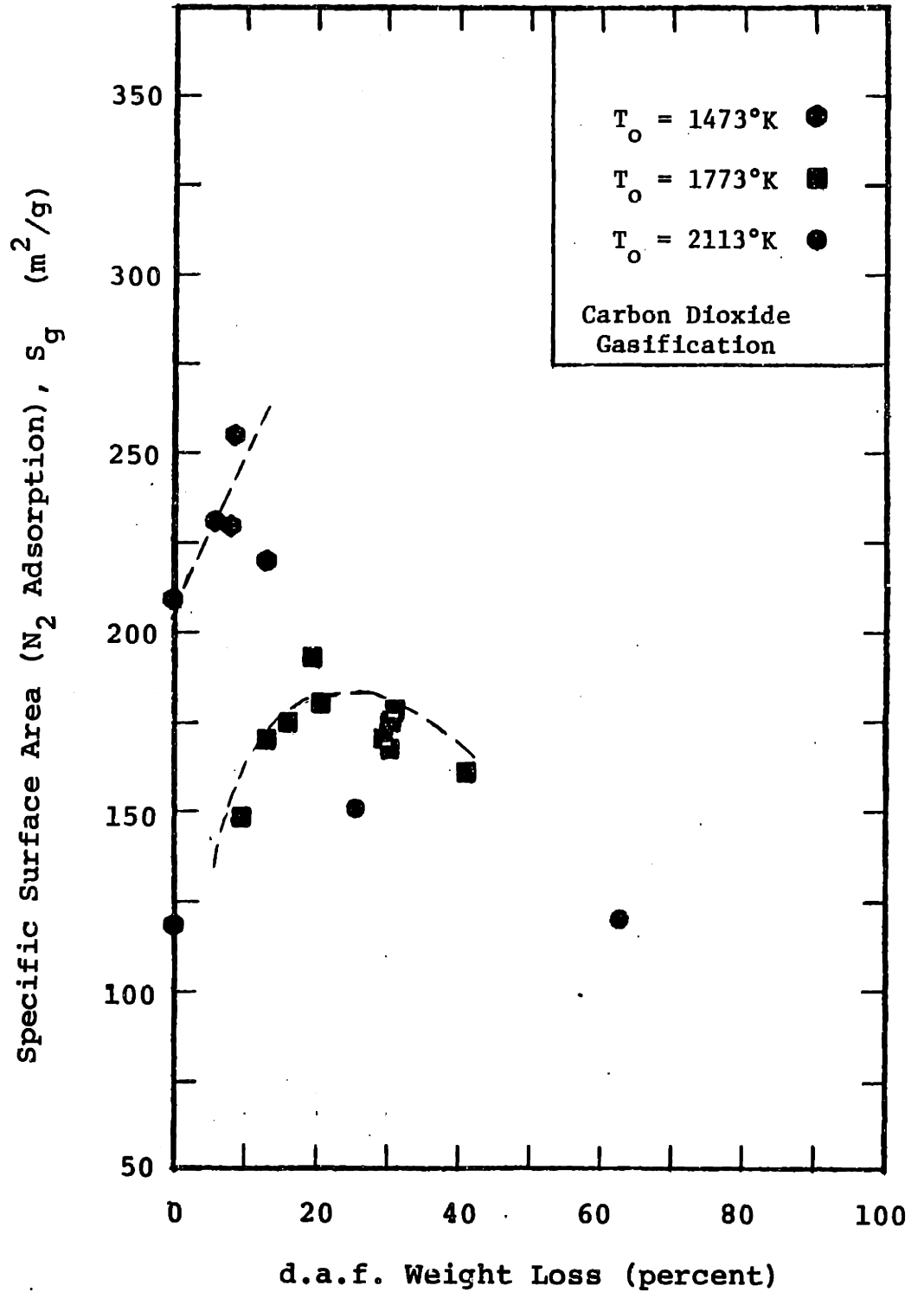


Figure 4.5 Specific Surface Area After Partial Gasification in Carbon Dioxide

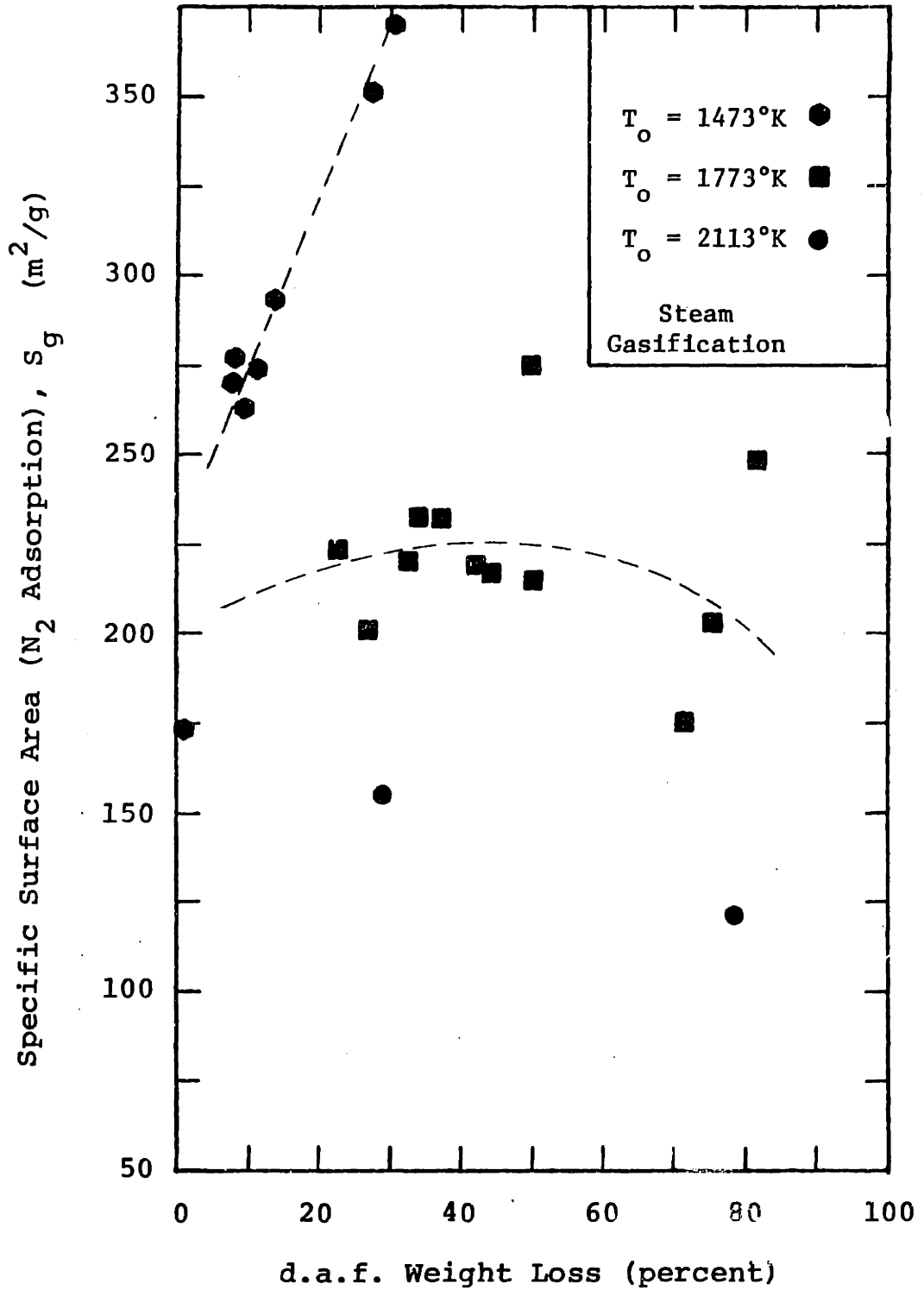


Figure 4.6 Specific Surface Area After Partial Gasification in Steam

although values as high as 279 m<sup>2</sup>/g (at 49.6% burnoff) and as low as 175 m<sup>2</sup>/g (at 71.3% burnoff) were measured.

The limited surface area data at 2113 °K are inconclusive. An average value of 135 to 140 m<sup>2</sup>/g is reported for each of the reactions studied.

For calculation of reaction rates on a unit total area basis (section 4.6) and for estimating pore diffusivities (Appendix I), the following values for specific surface area are assumed:

<u>Nominal Temperature</u>	<u>Specific Surface Area (m<sup>2</sup>/g)</u>	
	<u>Carbon Dioxide Gasification</u>	<u>Steam Gasification</u>
1473°K	230	300
1773°K	175	220
2113°K	135	135

It should be pointed out that surface areas measured by nitrogen adsorption may not accurately reflect the surface area that is actually available to carbon dioxide or steam molecules. Nonetheless, variation in N<sub>2</sub> surface area with burnoff should indicate corresponding changes in area open to CO<sub>2</sub> or H<sub>2</sub>O molecules.

#### Bulk Density

Although the data of Figure 4.7 are scattered, there is a general downward trend in particle density with increasing burnoff. The lowest value reported is 0.28 g/cm<sup>3</sup>, at 81.7%



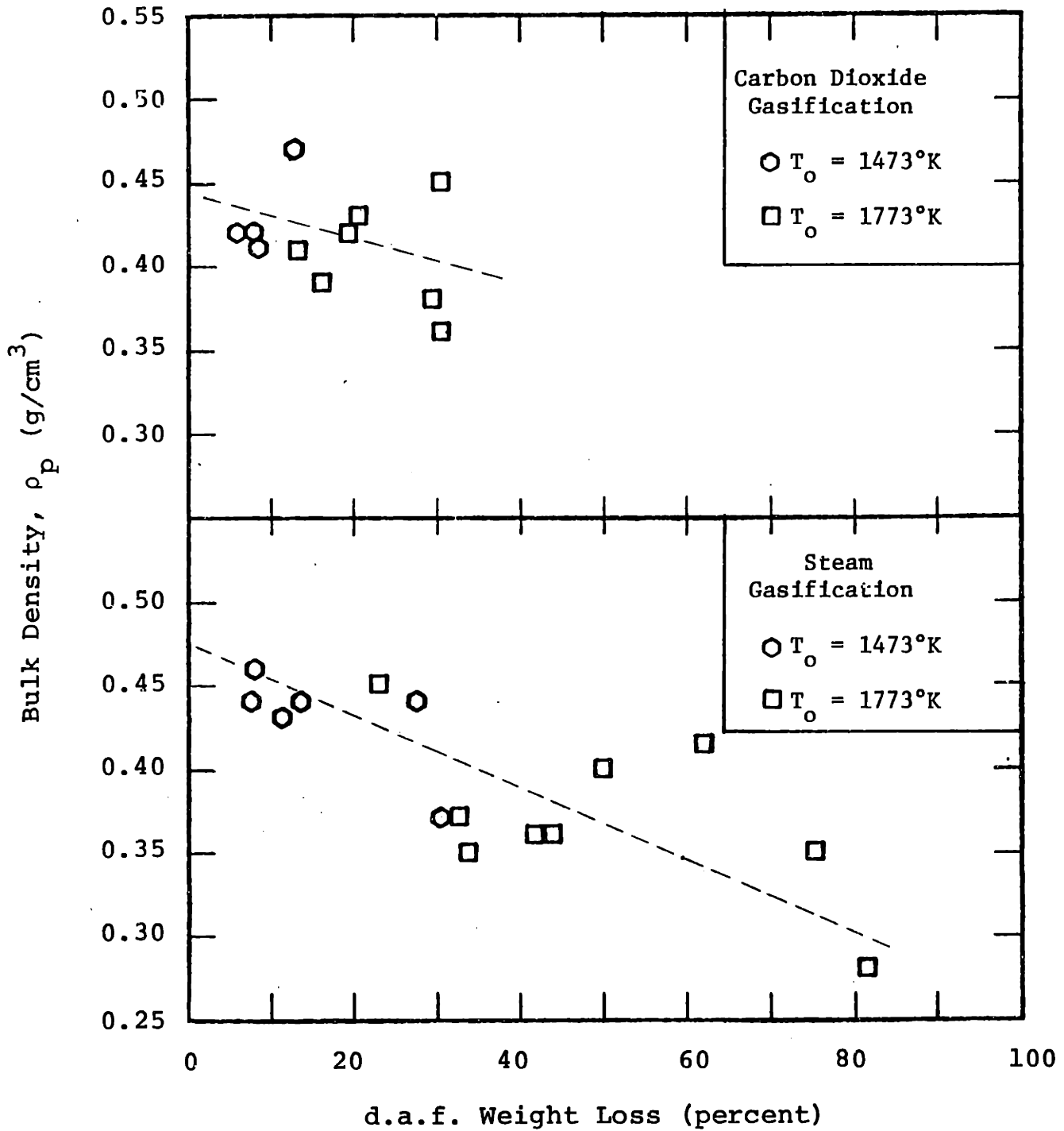


Figure 4.7 Char Density After Partial Gasification in Carbon Dioxide and Steam

d.a.f. weight loss in steam at 1773°K.

For the purpose of calculating reaction rates on a unit volume basis (section 4.4) and pore diffusivities (Appendix I), the initial char bulk density,  $0.49 \text{ g/cm}^3$ , is used. For calculation of particle terminal velocities (Appendix J), a value of  $0.43 \text{ g/cm}^3$  is chosen, to partially reflect the changes in the particle as it falls through the furnace reaction zone.

#### 4.4 Effects of External (Interphase) Gradients

As discussed in section 1.3, both chemical and diffusional effects must be considered when studying a heterogeneous reaction. At high temperatures, the intrinsic rate of reaction may be faster than the rate of reactant diffusion to the solid particle external surface and to active reaction sites within the char pore structure. Thus, the reactant concentration on the external surface,  $C_s$ , and within the porous particle,  $C(r)$ , may be less than the bulk gas concentration,  $C_g$ . Similarly, heat transfer limitations may result in the temperature on the particle external surface,  $T_s$ , being different from (less than for the endothermic gasification reactions) the bulk gas temperature,  $T_g$ . A temperature gradient within the reacting particle may also exist.

#### 4.4.1 Surface Temperature

To determine the surface temperature of a reacting char particle, an energy balance is made around the particle, assuming the temperature of the particle to be uniform and equal to the surface temperature,  $T_s$ :

$$\frac{\rho_p d_p}{6M_c} \bar{R}' (-\Delta\tilde{H}) = h(T_s - T_g) + \sigma(T_s^4 - T_g^4) \quad (4.27)^\dagger$$

where  $\Delta\tilde{H}$  is the heat of reaction,  $M_c$  is the molecular weight of carbon,  $d_p$  is the average particle diameter (assumed to be 0.01 cm),  $h$  is the heat transfer coefficient at the particle surface and  $\sigma$  is the Steffan-Boltzmann constant for radiative heat transfer. Note that  $\Delta\tilde{H}$  is evaluated at the particle temperature, and  $h$  is evaluated at  $T_{avg}$ , the average temperature in the boundary layer surrounding the particle:

$$T_{avg} = \frac{1}{2}(T_s + T_g) \quad (4.28)$$

[In writing equation (4.27), it is assumed that the char particles are spherical in shape. In fact, they are generally less regular in shape. A photograph of initial char particles (150x magnification) is shown in Figure 4.8. Similar photographs of char particles following partial gasification in carbon dioxide and steam are shown in Figures 4.9 and 4.10, respectively. The photos were furnished by the Phillips Petroleum Company, Bartlesville, Oklahoma.]

---

<sup>†</sup> A value of 1.0 is assumed for the emissivity of the char particle.



Figure 4.8 Initial Montana Rosebud Char Particles  
(150 X Magnification)

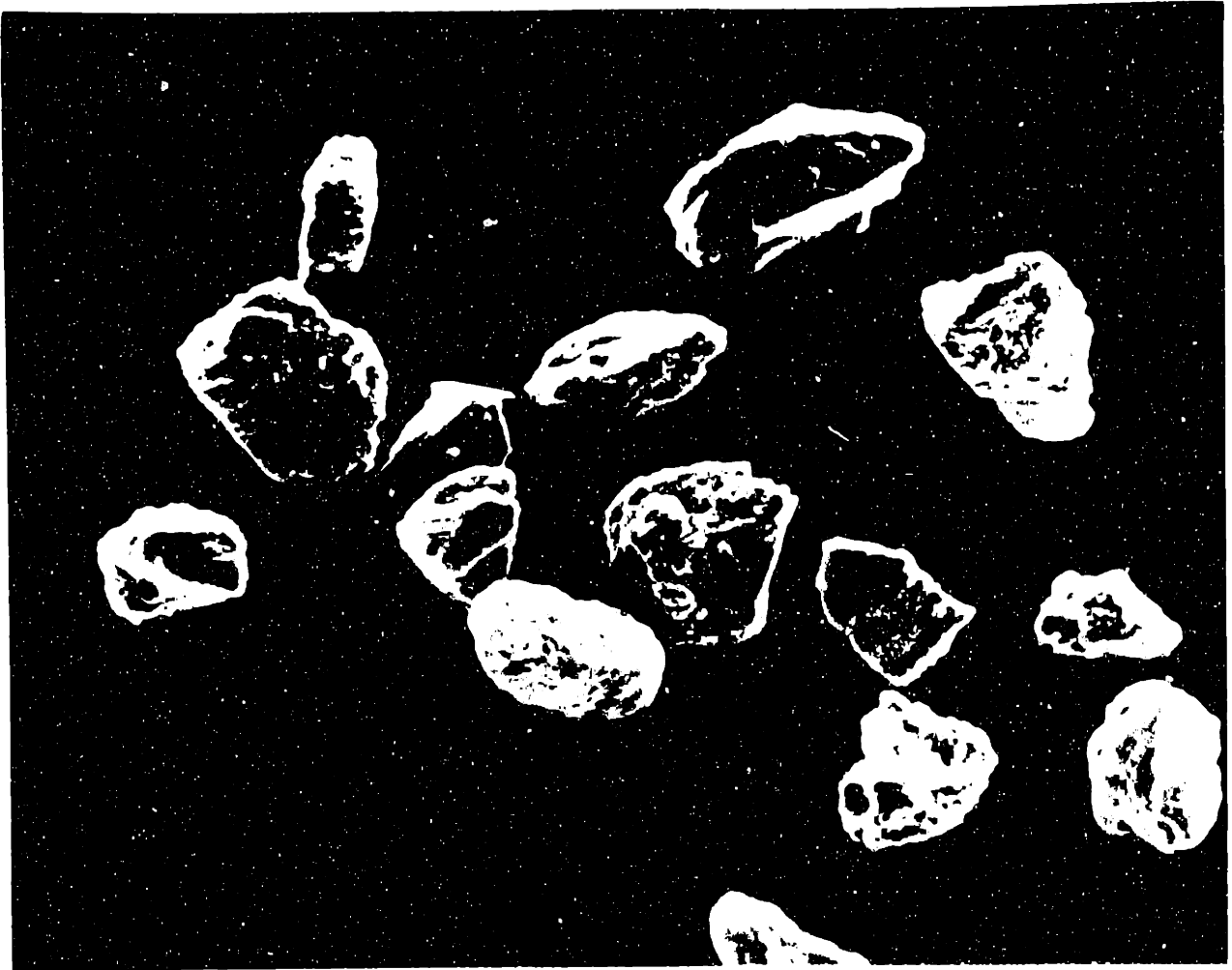


Figure 4.9 Char Particles After 8% Burnoff  
In Carbon Dioxide at 1473°K  
(150 X Magnification)

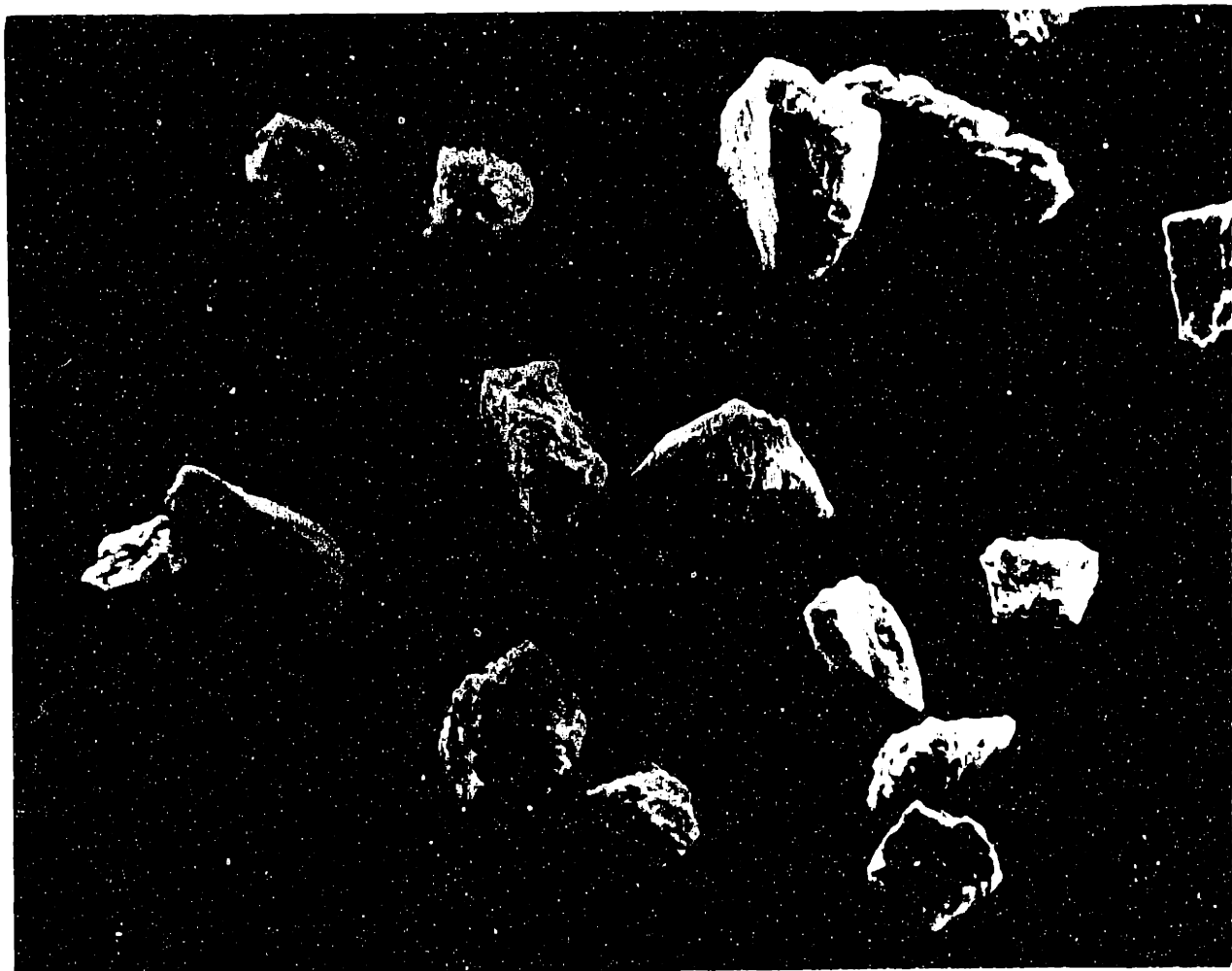


Figure 4.10 Char Particles After 50% Burnoff  
In Steam at 1773°K  
(150 X Magnification)

The heat transfer coefficient may be estimated by assuming a Nusselt number of two:

$$\text{Nu} = \frac{h d_p}{\lambda} = 2 \quad (4.29)$$

and thus

$$h = 2 \lambda / d_p \quad (4.30)$$

where  $\lambda$  is the main gas thermal conductivity, evaluated at  $T_{\text{avg}}$ . Heat of reaction data are presented in Table 1.5. Thermal conductivities of the main gas streams are calculated in Appendix G, and are expressed in the form of equation (G.8). The gas temperature,  $T_g$ , is taken to be the nominal temperature,  $T_o$ . The bulk density of the initial char ( $0.49 \text{ g/cm}^3$ ) is used for calculations. Values of  $\bar{R}'$  are taken from Table 4.2 and Table 4.4.

Equation (4.27) is solved via the Newton-Raphson iterative procedure. Calculated values of  $T_s$  are listed in Table 4.5 ( $\text{CO}_2$  gasification) and Table 4.6 (steam gasification). For the slowest reaction rates, the particle surface temperature is found to be over  $30^\circ\text{K}$  below the gas temperature. External temperature differences ( $T_o - T_s$ ) of up to  $230^\circ\text{K}$  ( $\text{CO}_2$  gasification) and  $270^\circ\text{K}$  (steam gasification) are calculated at a gas temperature of  $2113^\circ\text{K}$ .

Table 4.5  
Char Gasification in Carbon Dioxide:  
Surface Temperatures and Reactant Concentrations

$T_o$ (°K)	$P_{CO_2}$ (atm)	$C_o \times 10^6$ $\left\{ \frac{\text{mole}}{\text{cm}^3} \right\}$	$\bar{R}' \left( \frac{d\rho}{6M_c} \right) \times 10^4$ $\left\{ \frac{\text{mole}}{\text{cm}^2 \text{sec}} \right\}$	$T_s$ (°K)	$T_{avg}$ (°K)	$D_{12}$ $\left\{ \frac{\text{cm}^2}{\text{sec}} \right\}$	$\bar{R}''' / M_c$ $\left\{ \frac{\text{mole}}{\text{cm}^3 \text{sec}} \right\}$	$C_s / C_o$	$C_s \times 10^6$ $\left\{ \frac{\text{mole}}{\text{cm}^3} \right\}$
1473	0.26	2.15	0.469	1441	1457	2.33	0.0281	0.953	2.05
1473	0.53	4.38	0.567	1434	1454	2.32	0.0340	0.972	4.26
1773	0.26	1.79	1.708	1684	1729	3.10	0.103	0.846	1.51
1773	0.60	4.12	2.156	1661	1717	3.06	0.129	0.915	3.77
2113	0.26	1.50	4.61	1935	2024	4.03	0.276	0.619	0.928
2113	0.57	3.29	5.98	1880	1997	3.94	0.359	0.769	2.53



Table 4.6  
Char Gasification in Steam:  
Surface Temperatures and Reactant Concentrations

$T_o$ (°K)	$P_{H_2O}$ (atm)	$C_o \times 10^6$ $\left\{ \frac{\text{mole}}{\text{cm}^3} \right\}$	$\bar{r}' \left( \frac{d_{p,p}}{6M_c} \right) \times 10^4$ $\left\{ \frac{\text{mole}}{\text{cm}^2 \text{ sec}} \right\}$	$T_s$ (°K)	$T_{avg}$ (°K)	$D_{12}$ $\left\{ \frac{\text{cm}^2}{\text{sec}} \right\}$	$\bar{r}''' / M_c$ $\left\{ \frac{\text{mole}}{\text{cm}^3 \text{ sec}} \right\}$	$C_s / C_o$	$C_s \times 10^6$ $\left\{ \frac{\text{mole}}{\text{cm}^3} \right\}$
1473	0.33	2.73	0.660	1440	1457	3.82	0.0396	0.968	2.64
1473	0.65	5.38	1.584	1407	1440	3.75	0.0951	0.961	5.17
1773	0.32	2.20	2.457	1679	1726	5.07	0.147	0.890	1.96
1773	0.65	4.47	6.812	1546	1660	4.75	0.409	0.840	3.75
2113	0.32	1.85	6.961	1910	2012	6.56	0.418	0.712	1.31
2113	0.65	3.75	10.93	1845	1979	6.38	0.656	0.771	2.89

#### 4.4.2 Surface Concentration

The concentration of reactant ( $\text{CO}_2$  or  $\text{H}_2\text{O}$ ) molecules on the external surface of the char particles is determined by a mass balance around a particle:

$$\bar{R}''' / M_c = k_g a (C_g - C_s) \quad (4.31)$$

where  $\bar{R}'''$  is the reaction rate per unit solid volume ( $\text{g}\cdot\text{cm}^{-3}\cdot\text{sec}^{-1}$ ) defined by equation (4.4),  $k_g$  is a mass transfer coefficient for diffusion through the boundary layer surrounding the particle,  $a$  is the ratio of external surface area to particle volume ( $\text{cm}^{-1}$ ),

$$a = 6/d_p \quad (\text{spherical particles}) \quad (4.32)$$

and  $C_g$  and  $C_s$  are the reactant concentrations in the bulk gas phase and on the particle external surface, respectively.

Thus, the reactant concentration on the particle external surface is:

$$\frac{C_s}{C_g} = 1 - \frac{\bar{R}''' / M_c}{k_g a C_g} \quad (4.33)$$

To estimate the mass transfer coefficient  $k_g$ , a Sherwood number (Nusselt number for mass transfer) of two is assumed:

$$\text{Sh} = k_g d_p / D_{12} = 2 \quad (4.34)$$

where  $D_{12}$  is the appropriate ( $\text{CO}_2\text{-N}_2$  or  $\text{H}_2\text{O-N}_2$ ) bulk diffusion coefficient, evaluated at  $T_{\text{avg}}$ . Estimation of bulk diffusion coefficients is shown in Appendix H. The results are expressed

in the power law form of equation (H.2),  $D_{12}$  being proportional to temperature ( $^{\circ}\text{K}$ ) raised to the power 1.67. Thus, the mass transfer coefficient (Figure 4.11) becomes:

$$k_g = 2 D_{12} / d_p \quad (4.35)$$

and equation (4.33) may be solved for  $C_s$ .

The results are shown in Tables 4.5 and 4.6, where the gas concentration ( $C_g$ ) in equation (4.33) has been evaluated at  $T_o$  (i.e.,  $C_g = C_o$ ), and  $\rho_p$  is taken as  $0.49 \text{ g/cm}^3$  (the initial char density) in order to calculate values of  $\bar{R}'''$ . Although neither reaction becomes completely bulk diffusion rate limited (i.e.,  $C_s/C_o > 0$  for all experimental conditions), the surface reactant concentration drops to approximately two-thirds of the bulk gas concentration at the highest temperatures (fastest reaction rates) studied.

#### 4.5 Effects of Internal (Intraphase) Gradients

##### 4.5.1 Particle Temperature

The Biot modulus for heat transfer may be used to estimate the importance of intraphase temperature gradients:

$$Bi_h = hL/\lambda_p \propto \frac{\text{intraphase } \Delta T}{\text{interphase } \Delta T} \quad (4.36)$$

where  $h$  is the heat transfer coefficient,  $\lambda_p$  is the particle thermal conductivity and  $L$  is a characteristic length. For spherical particles:

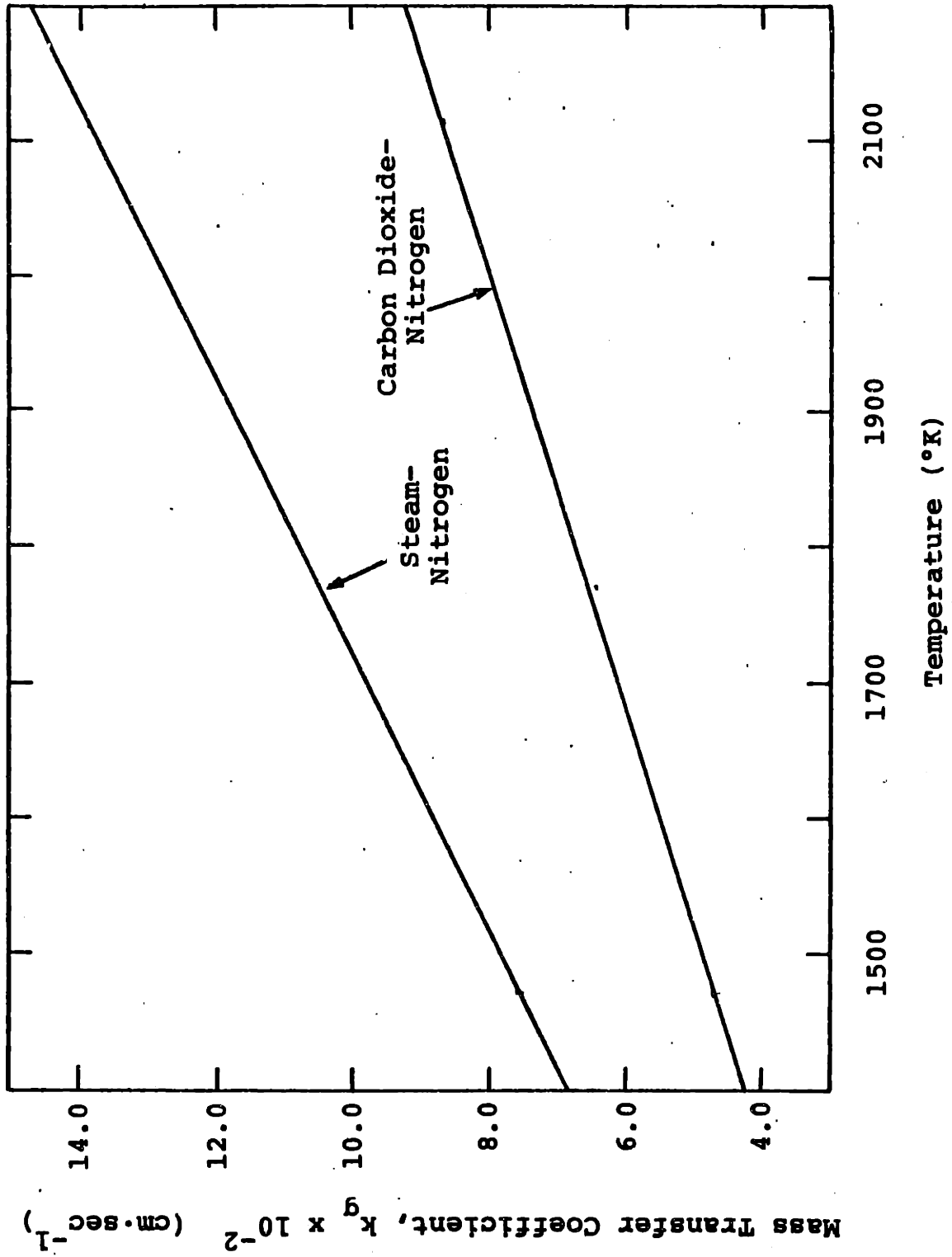


Figure 4.11 Mass Transfer Coefficients for Bulk Diffusion

$$L = \frac{1}{a} = \frac{1}{6} d_p \quad (4.37)$$

The heat transfer coefficient is estimated by assuming a Nusselt number of two (section 4.4.1). Thus,

$$Bi_h = \frac{1}{3} (\lambda/\lambda_p) \quad (4.38)$$

Taking  $\lambda$  and  $\lambda_p$  to be on the order of  $10^{-4}$  and  $10^{-3}$  calories per second per centimeter per degree Kelvin, respectively,

$$Bi_h \sim 0.1 \quad (4.39)$$

Therefore, it will be assumed that the particle temperature,  $T_p$ , is uniform, and equal to the surface temperature,  $T_s$ .

#### 4.5.2 Reactant Concentration

For all normal reactions (intrinsic order of reaction  $\geq 0$ ), pore diffusional rate limitations result in an observed rate less than the intrinsic reaction rate, since the concentration of reactant molecules as a function of position within the particle,  $C(r)$ , is less than the reactant concentration on the external surface of the particle. To handle this situation quantitatively, an effectiveness factor,  $\eta$ , is defined:

$$\eta = \frac{\text{observed rate}}{\text{rate in the absence of pore diffusion limitations}} \quad (4.40)$$

Consider the equation of continuity (spherical geometry) for the reactant species in an isothermal char particle at steady state, with the reaction rate expressed by the power

law model, equation (4.1):

$$\tilde{k}''' c^n = D_{\text{eff}} \left[ \frac{d^2 c}{dr^2} + \frac{2}{r} \frac{dc}{dr} \right] \quad (4.41)$$

where  $\tilde{k}'''$  is the intrinsic rate constant at the particle temperature on a unit volume basis (the superscript  $\sim$  indicates that the rate is measured in molar rather than weight units),  $n$  is the intrinsic order of reaction and  $r$  is the radial position within the particle. The following dimensionless parameters are defined:

$$C^* = C/C_s \quad (4.42)$$

$$\gamma = r/r_p \quad (4.43)$$

$$z = C^* \gamma \quad (4.44)$$

where  $r_p$  is the particle radius. Thus, equation (4.41) may be written as:

$$\frac{d^2 z}{d\gamma^2} = \phi_s^2 z^n \gamma^{1-n} \quad (4.45)$$

where the Thiele modulus for spherical geometry,  $\phi_s$ , is defined as:

$$\phi_s = r_p \left\{ \frac{\tilde{k}''' C_s^{n-1}}{D_{\text{eff}}} \right\}^{1/2} \quad (4.46)$$

The boundary conditions required to solve equation (4.45) are:

$$\text{B.C. 1} \quad \gamma = 0 \quad dC^*/d\gamma = 0 \quad (4.47)$$

$$\text{B.C. 2} \quad \gamma = 1 \quad z = 1 \quad (4.48)$$

Once the concentration profile,  $C(\gamma)$  is determined, the (isothermal) effectiveness factor may be calculated by integrating equation (4.40) over the particle volume:

$$\eta = \frac{4\pi \int_0^{r_p} [C(r)]^n r^2 dr}{\frac{4}{3}\pi r_p^3 C_s^n} \quad (4.49)$$

(For zeroth order reactions, the effectiveness factor is simply the fraction of particle volume in which the reactant concentration is non-zero.)

For first order reactions, equation (4.45), with boundary conditions (4.47) and (4.48), may be solved explicitly:

$$C^*(\gamma) = \frac{\sinh(\phi_s \gamma)}{\gamma \sinh \phi_s} \quad (4.50)$$

and thus the effectiveness factor becomes:

$$\eta_1 = \frac{3}{\phi_s} \left\{ \frac{1}{\tanh \phi_s} - \frac{1}{\phi_s} \right\} \quad (4.51)$$

where the subscript 1 indicates that equation (4.51) is for first order reactions. For large values of  $\phi_s$  (fast reactions):

$$\phi_s > 5: \quad \eta \rightarrow 3/\phi_s \quad (4.52)$$

The results of equation (4.51) are shown in Figure 4.12.

For a zeroth order reaction, the solution to equations (4.45), (4.47) and (4.48) is:

$$C^*(\gamma) = 1 - \left\{ \frac{1}{6} \phi_s^2 [1 - \gamma^2] \right\} \quad (4.53)$$

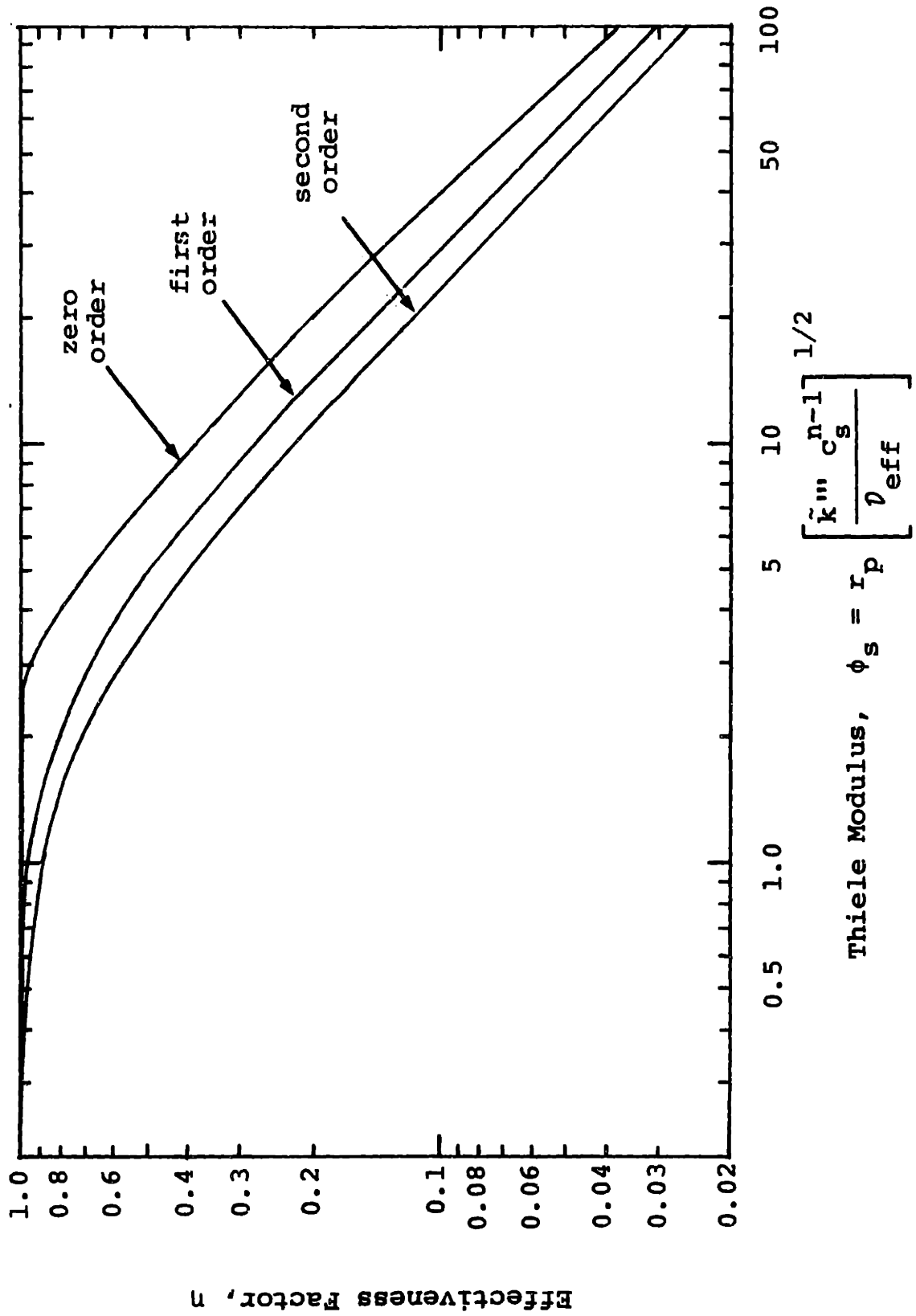


Figure 4.12 Intraphase (Isothermal) Effectiveness Factors as a Function of Thiele Modulus (Spherical Geometry)



Equation (4.53) predicts that for  $\phi_s^2 > 6$ , the reactant concentration will fall below zero at some point within the particle. Therefore, boundary condition (4.47) must be adjusted:

$$\text{B.C. 1} \quad \gamma = \gamma_0 \quad C^* = 0 \quad (4.54)$$

$$\text{B.C. 2} \quad \gamma = \gamma_0 \quad \frac{dC^*}{d\gamma} = 0 \quad (4.55)$$

$$\text{B.C. 3} \quad \gamma = 1 \quad z = 1 \quad (4.48)$$

where  $\gamma_0$ , a function of  $\phi_s$ , is the radial position in the particle where the reactant concentration just falls to zero (and remains zero for  $\gamma < \gamma_0$ ).

Thus, for zeroth order reactions,  $\phi_s^2 < 6$ ,  $C^*(r)$  is given by equation (4.53), and  $\eta$  is unity, since the reactant concentration never falls to zero within the particle. For  $\phi_s^2 > 6$ , the solution to equation (4.45), with boundary conditions (4.48), (4.54) and (4.55), is:

$$C^*(\gamma) = \frac{\phi_s^2}{\gamma} \left[ \frac{1}{6} - \frac{1}{2} \left( \frac{\gamma_0}{\gamma} \right)^2 + \frac{1}{3} \left( \frac{\gamma_0}{\gamma} \right)^3 \right] \quad (4.56)$$

where  $\gamma_0$ , as a function of  $\phi_s$ , is determined by solving equation (4.57):

$$\frac{6}{\phi_s^2} = 2\gamma_0^3 - 3\gamma_0^2 + 1 \quad (4.57)$$

Therefore, the effectiveness factor (isothermal particle) for zeroth order reactions is given by:

$$\eta_0 = \begin{cases} 1.0 & \phi_s^2 < 6 \\ 1.0 - \gamma_0^3 & \phi_s^2 > 6 \end{cases} \quad (4.58)$$

This result is shown in Figure 4.12, as is a similar result for second order reactions (from Satterfield<sup>67</sup>).

The drawback to the analysis presented above is that the Thiele modulus,  $\phi_s$ , is a function of the unknown intrinsic rate constant,  $\tilde{k}'''$ . This may be overcome by noting that from equation (4.40):

$$\frac{\bar{R}'''}{M_c} = \eta \tilde{k}''' C_s^n \quad (4.59)$$

where  $\tilde{k}'''$  is calculated at the particle temperature. Equations (4.46) and (4.59) are combined to eliminate the unknown rate constant, resulting in:

$$\Phi_s = \eta \phi_s^2 \quad (4.60)$$

where  $\Phi_s$  is the Weisz modulus,

$$\Phi_s = r_p^2 \left[ \frac{\bar{R}''' / M_c}{D_{\text{eff}} C_s} \right] \quad (4.61)$$

All of the variables in the definition of  $\Phi_s$  are known from experimental data. Thus, the data of Figure 4.12 are used with equation (4.60) to produce Figure 4.13, showing the dependence of  $\eta$  on  $\Phi_s$ , for zeroth, first and second order reactions.

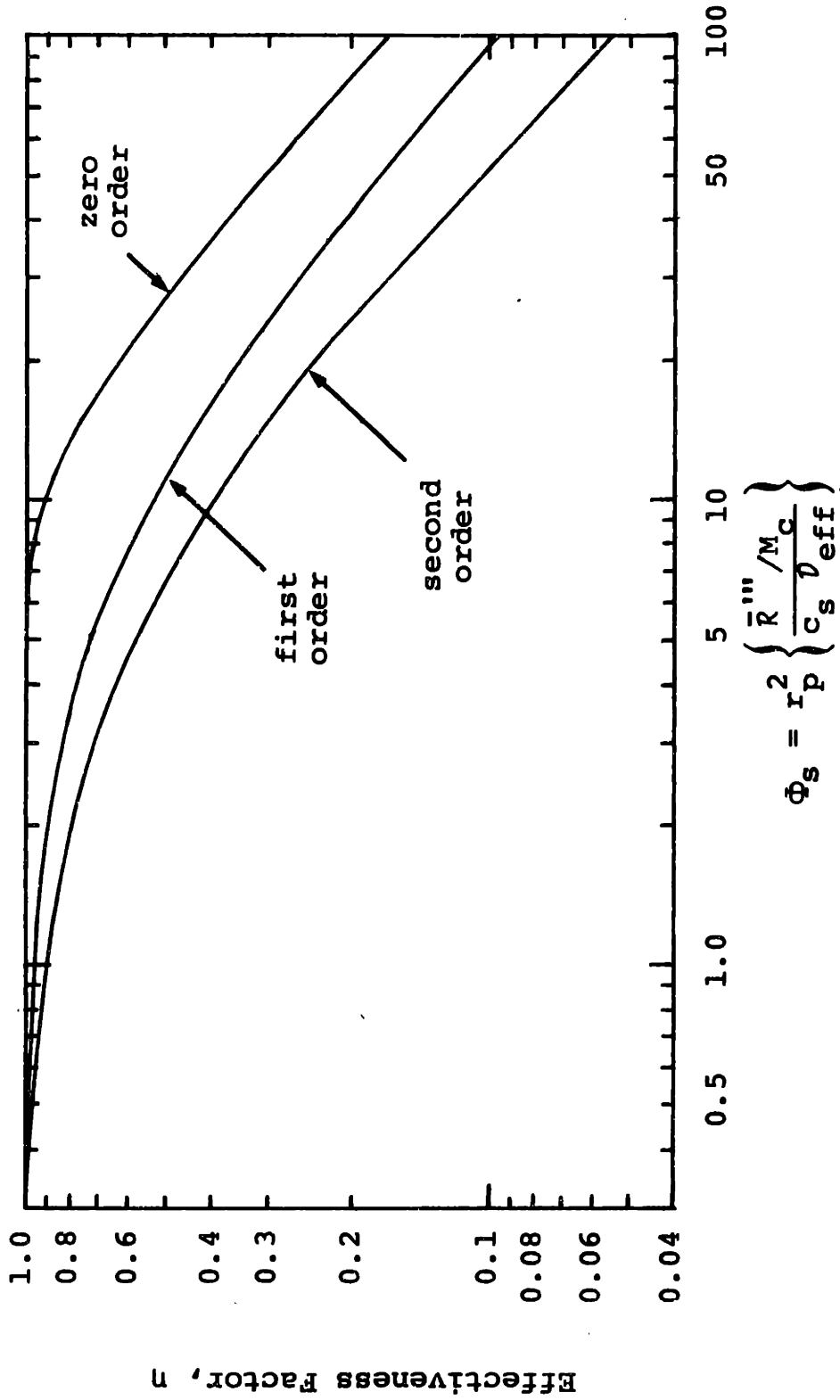


Figure 4.13 Intraphase (Isothermal) Effectiveness Factors As A Function of Weisz Modulus (Spherical Geometry)

For each of the experimental results in Tables 4.5 and 4.6, isothermal intraphase effectiveness factors are calculated, using equation (4.61) and Figure 4.13, for assumed orders of reaction of zero and unity. Effectiveness factors for char-CO<sub>2</sub> results are listed in Table 4.7. Effectiveness factors for char-H<sub>2</sub>O results are listed in Table 4.8. The effective diffusivities in these tables are calculated in Appendix I.

From the data in Tables 4.7 and 4.8, it is seen that pore diffusional effects are significant ( $\eta < 0.5$ ) even at the lowest temperatures (slowest reaction rates) studied. Effectiveness factors as low as 0.08 (1st order) and 0.16 (0th order) are calculated at particle temperatures near 1900°K, for both the char-CO<sub>2</sub> and char-H<sub>2</sub>O reactions. Therefore, it is expected that the apparent activation energies ( $\bar{E}$ ) of 23.2 kcal/mole (char-CO<sub>2</sub>) and 26.2 kcal/mole (char-H<sub>2</sub>O) reported in section 4.2 will be approximately one-half of the true (intrinsic) activation energies for these reactions.

#### 4.6 Correction for Surface Area

Specific (nitrogen adsorption) surface area of the partially gasified char samples is a function of gasification temperature, oxidizing medium and percent burnoff, as shown in Figures 4.5 and 4.6 (section 4.3). Therefore, it seems

Table 4.7

Intraphase Effectiveness Factors For  
Char Gasification in Carbon Dioxide

$T_O$ (°K)	$T_P$ (°K)	$C_S \times 10^6$ (mole/cm <sup>3</sup> )	$R''' / M_C$ (mole·cm <sup>-3</sup> ·sec <sup>-1</sup> )	$D_{eff}$ (cm <sup>2</sup> /sec)	$\Phi_s$	$\eta_O$	$\eta_I$
1473	1441	2.05	0.0281	0.0347	9.88	0.89	0.54
1473	1434	4.26	0.0340	0.0346	5.77	1.00	0.68
1773	1684	1.51	0.103	0.0492	34.5	0.41	0.22
1773	1661	3.77	0.129	0.0488	17.6	0.67	0.37
2113	1935	0.93	0.276	0.0681	109.3	0.16	0.078
2113	1880	2.53	0.359	0.0670	53.0	0.29	0.15

Table 4.8

Intraphase Effectiveness Factors for Char Gasification in Steam

$T_o$ (°K)	$T_p$ (°K)	$C_s \times 10^6$ (mole/cm <sup>3</sup> )	$\bar{R}''' / M_c$ (mole·cm <sup>-3</sup> ·sec <sup>-1</sup> )	$D_{eff}$ (cm <sup>2</sup> /sec)	$\Phi_s$	$\eta_o$	$\eta_1$
1473	1440	2.64	0.0396	0.0419	8.93	0.93	0.57
1473	1407	5.17	0.0951	0.0414	11.1	0.85	0.50
1773	1679	1.96	0.147	0.0616	30.6	0.46	0.24
1773	1546	3.75	0.409	0.0589	46.2	0.32	0.17
2113	1910	1.31	0.418	0.106	75.0	0.21	0.11
2113	1845	2.89	0.656	0.104	54.6	0.28	0.15

preferable to base intrinsic kinetics on normalized reaction rates (i.e., rates per unit area). Using equation (4.3), an intrinsic reaction rate (molar units) per unit total area may be defined:

$$\frac{\bar{R}''}{M_c} = -\frac{1}{S_g M_c} \frac{1}{W} \frac{dW}{dt} = \frac{1}{S_g} \tilde{k}' C^n \quad (4.62)$$

where

$$\tilde{k}' = k' / M_c \quad (4.63)$$

and  $k'$  is expressed in the Arrhenius form, equation (4.2).

Defining the rate constant on a moles per unit area basis,

$$\tilde{k}'' = \frac{k'}{S_g M_c} \quad (4.64)$$

and expressing this rate constant in an Arrhenius form,

$$\tilde{k}'' = \tilde{A}'' \exp \left\{ -\frac{E}{RT_p} \right\} \quad (4.65)$$

the observed rate of reaction (per unit total surface area) may be written in terms of the intraphase effectiveness factor and the intrinsic rate:

$$\frac{\bar{R}''}{M_c} = \eta \tilde{A}'' \exp \left\{ -\frac{E}{RT_p} \right\} C_s^n \quad (4.66)$$

where  $\tilde{A}''$ ,  $E$  and  $n$  are the intrinsic kinetic parameters, based on rates per unit total area.

#### 4.7 Intrinsic Kinetics

The intrinsic kinetic parameters may be deduced from equation (4.66) and the data of Table 4.7 (char-CO<sub>2</sub> reaction) or Table 4.8 (char-H<sub>2</sub>O reaction). Taking the natural logarithm of both sides of equation (4.66), and rearranging terms:

$$\ln \left[ \frac{\bar{R}'' / M_C}{\eta C_s^n} \right] = \ln \tilde{A}'' - \frac{E}{RT_p} \quad (4.67)$$

It is likely that the kinetics fall into one of the two cases discussed in section 1.5, and the order of reaction is either zero or unity (see equations (1.10) through (1.13)). Thus, equation (4.67) is considered for two cases:

##### I. first order kinetics

$$\ln \left[ \frac{\bar{R}'' / M_C}{\eta_1 C_s} \right] = \ln \tilde{A}'' - \frac{E}{RT_p} \quad (4.68)$$

##### II. zeroth order kinetics

$$\ln \left[ \frac{\bar{R}'' / M_C}{\eta_0} \right] = \ln \tilde{A}'' - \frac{E}{RT_p} \quad (4.69)$$

A plot of the left side of equation (4.68) or (4.69) versus the reciprocal particle temperature ( $1/T_p$ ) will yield a straight line (slope =  $-E/R$ ) fit of the data in Table 4.9 or Table 4.10, if the reaction shows first order (equation (4.68)) or zeroth order (equation (4.69)) behavior.



Table 4.9

Char Gasification in Carbon Dioxide:  
Tests for Zeroth Order and First Order Intrinsic Kinetics

$T_s$ (°K)	$C_g \times 10^6$ $\left(\frac{\text{mole}}{\text{cm}^3}\right)$	$\bar{R}$ ( $\text{sec}^{-1}$ )	$S_g$ ( $\text{m}^2/\text{g}$ )	$\frac{\bar{R}}{M_C} \times 10^8$ $\left(\frac{\text{mole}}{\text{cm}^2 \text{ sec}}\right)$	$\frac{\bar{R}}{M_C \eta_O} \times 10^8$ $\left(\frac{\text{mole}}{\text{cm}^2 \text{ sec}}\right)$	$\frac{\bar{R}}{M_C \eta_1 C}$ (cm/sec)
1441	2.05	0.689	230	2.495	2.794	0.0227
1434	4.26	0.833	230	3.020	3.020	0.0104
1684	1.51	2.509	175	11.95	28.86	0.3579
1661	3.77	3.168	175	15.09	22.66	0.1073
1935	0.928	6.769	135	41.78	266.1	5.770
1880	2.53	8.789	135	54.25	189.0	1.412

Table 4.10

Char Gasification in Steam:  
Tests for Zeroth Order and First Order Intrinsic Kinetics

$T_s$ (°K)	$C_s \times 10^6$ $\left(\frac{\text{mole}}{\text{cm}^3}\right)$	$\bar{R}$ (sec <sup>-1</sup> )	$S_g$ (m <sup>2</sup> /g)	$\frac{\bar{R}}{M_c} \times 10^8$ $\left(\frac{\text{mole}}{\text{cm}^2 \text{ sec}}\right)$	$\frac{\bar{R}}{M_{c_0} \eta} \times 10^8$ $\left(\frac{\text{mole}}{\text{cm}^2 \text{ sec}}\right)$	$\frac{\bar{R}}{M_{c_1} \eta C}$ (cm/sec)
1440	2.64	0.969	300	2.692	2.907	0.0180
1407	5.17	2.328	300	6.467	7.599	0.0249
1679	1.96	3.611	220	13.68	29.55	0.2865
1546	3.75	10.01	220	37.91	117.0	0.5876
1910	1.31	10.23	135	63.14	297.8	4.329
1845	2.89	16.06	135	99.11	355.2	2.301

#### 4.7.1 Char Gasification in Carbon Dioxide

The test for first order behavior of the char-CO<sub>2</sub> reaction is shown in Figure 4.14, where the left side of equation (4.68) is plotted against the reciprocal particle temperature, using the data in Table 4.9. The least square fit straight line shows a poor fit of the rate data to equation (4.68). Thus, first order kinetics are rejected.

Figure 4.15 shows the left side of equation (4.69) plotted against reciprocal particle temperature. The straight line correlates the data quite well (correlation coefficient,  $r^2 = 0.996$ ), so it is found that the char-CO<sub>2</sub> gasification reaction exhibits zeroth order behavior,

$$n = 0 \quad (4.70)$$

under the conditions studied. The slope of the line in Figure 4.15 is  $-2.52 \times 10^4 \text{ }^\circ\text{K}^{-1}$ , corresponding to an activation energy,

$$E = 50.1 \text{ kcal/mole} \quad (4.71)$$

The intrinsic kinetics of the char - carbon dioxide reaction are summarized in Table 4.11. The frequency factor is determined from the intercept of the line in Figure 4.15, at  $1/T_p = 0$ .

As discussed in section 1.5, reactions which obey the Langmuir-Hinshelwood kinetic model, equation (1.7), may appear to be first order [equations (1.10) and (1.11)] or zeroth order [equations (1.12) and (1.13)] with respect to

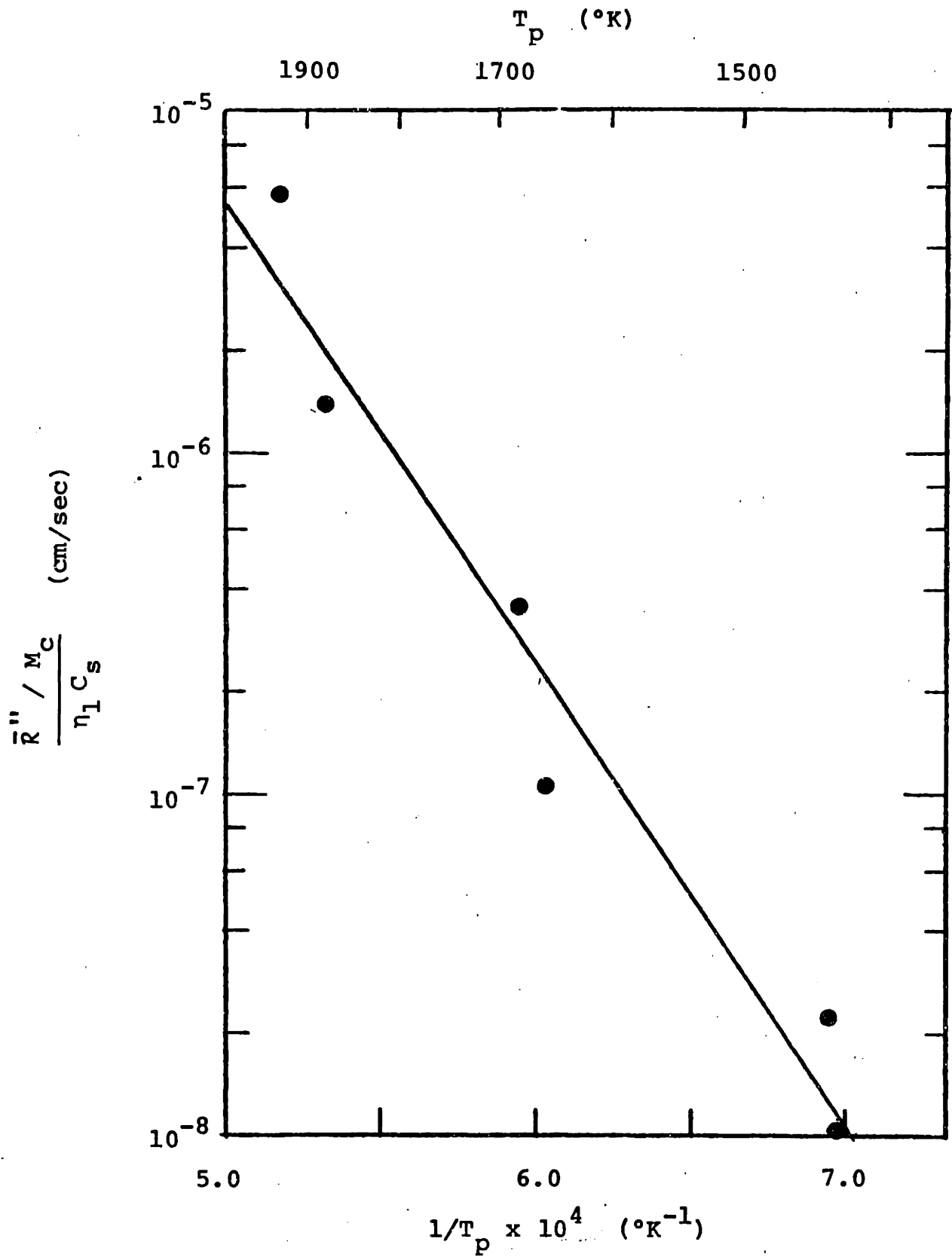


Figure 4.14 Char Gasification in Carbon Dioxide:  
Test for First Order Kinetics

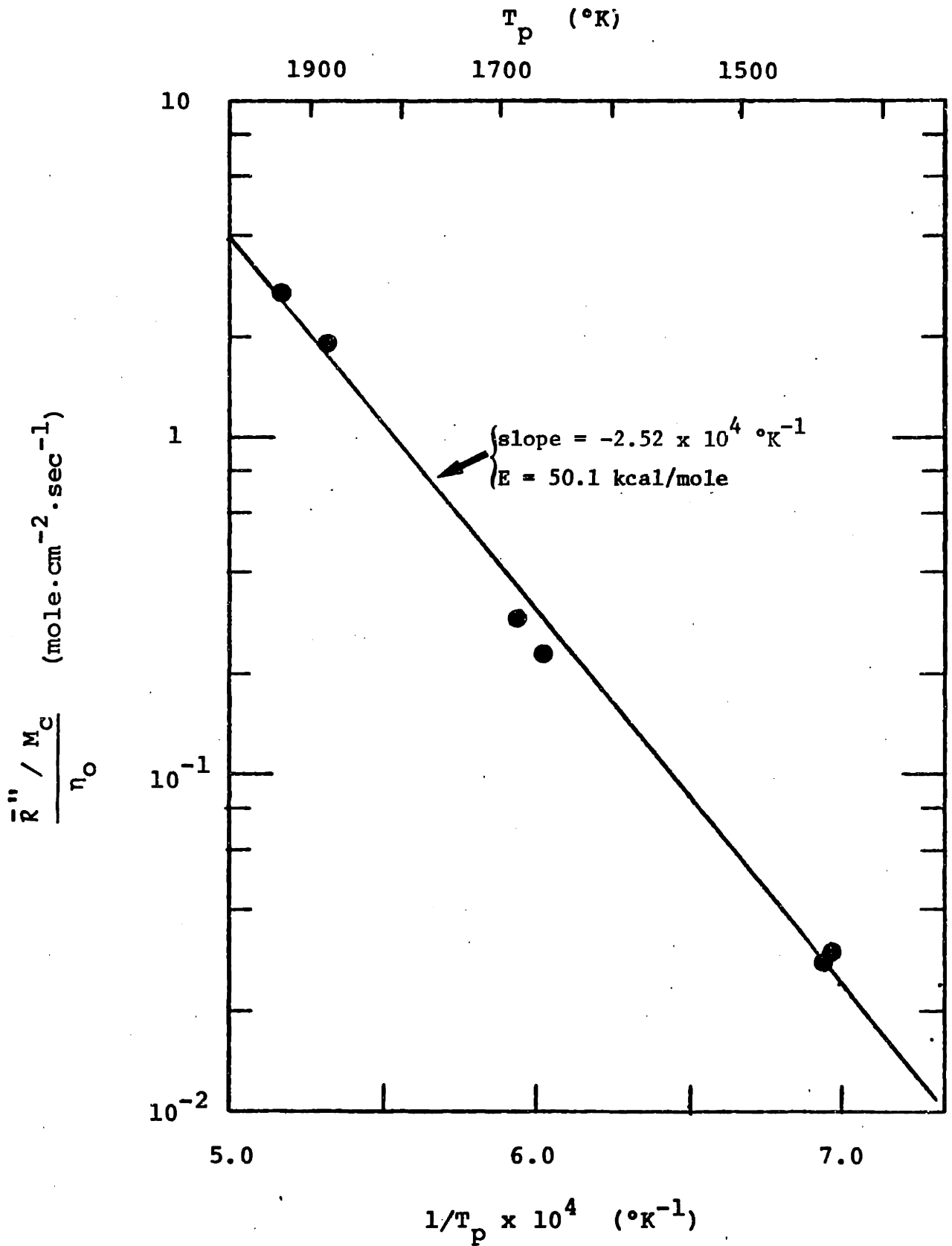


Figure 4.15 Char Gasification in Carbon Dioxide: Test for Zeroth Order Kinetics

Table 4.11

Intrinsic Kinetics of Montana Rosebud  
Char Gasification in Carbon Dioxide

$$\frac{R''}{M_c} = -\frac{1}{S_g M_c W} \frac{dW}{dt} = \tilde{A}'' \exp \left\{ -\frac{E}{RT_p} \right\} C_{CO_2}^n$$

n	order of reaction	zero
E	activation energy	50.1 kcal/mole
$\tilde{A}''$	frequency factor	1.09 $\frac{\text{mole}}{\text{cm}^2 \text{ sec}}$

the reactant gas. Generally, first order kinetics are expected at high temperatures and low pressures, since the coefficients  $k_2$  and  $k_3$  in equation (1.7) decrease with increasing temperature. Therefore, it is somewhat surprising that the char-CO<sub>2</sub> reaction in this study exhibited zeroth order intrinsic kinetic behavior. Of course, the kinetics of carbon reactions are largely dependent on the particular type of carbon being investigated.

#### 4.7.2 Char Gasification in Steam

The tests for zeroth order and first order kinetics for the char-steam reaction are shown in Figures 4.16 and 4.17, respectively. Figure 4.16 shows that the data do not fit (correlation coefficient = 0.871) the zeroth order theory, equation (4.69).

The least square fit straight line in Figure 4.17 (test for first order kinetics) is drawn for the case that the data point at  $T_p = 1546^\circ\text{K}$ ,  $C_s = 3.25 \times 10^{-6}$  mole/cm<sup>3</sup>, is neglected. A check of the data in Table B.1 shows that d.a.f. weight losses ranging from 43 to 82 percent were recorded at the experimental conditions ( $T_o = 1773^\circ\text{K}$ ,  $P_{\text{H}_2\text{O}} = 0.65$  atm) which this point represents. Therefore, the reliability of this point is seriously questioned. [Neglecting this point in the zeroth order test, Figure 4.16, does not significantly improve the zeroth order correlation.]

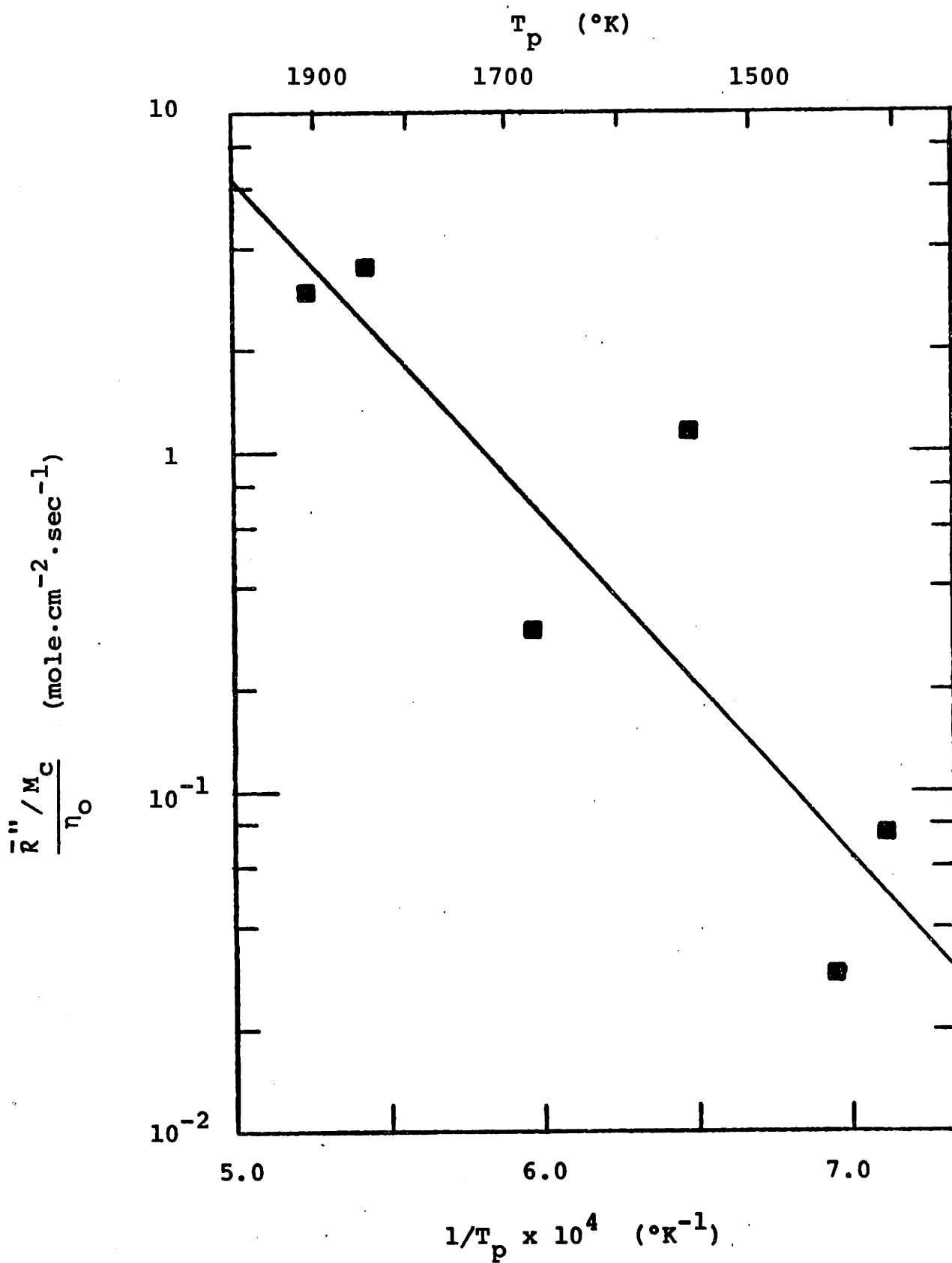


Figure 4.16 Char Gasification in Steam:  
Test for Zeroth Order Kinetics



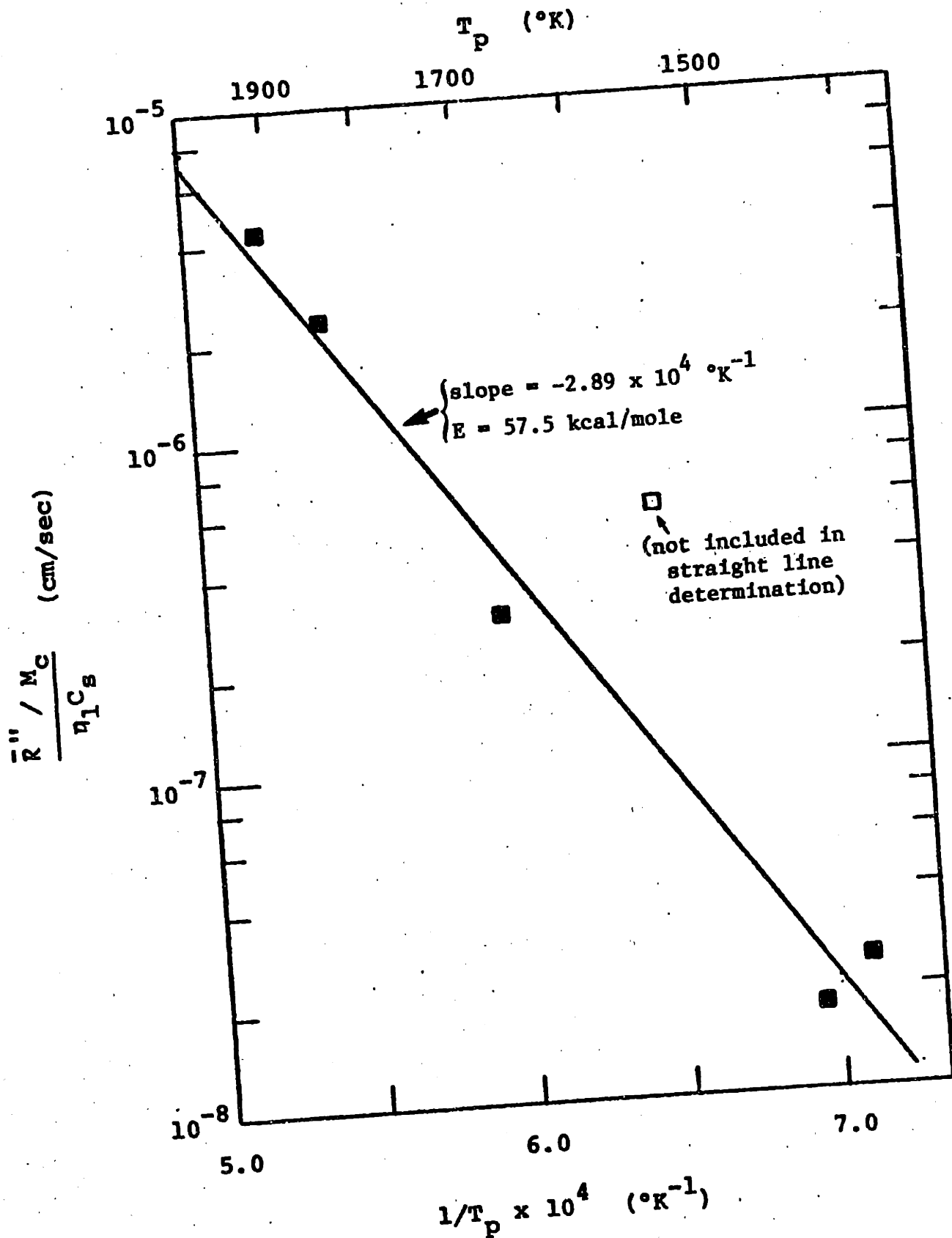


Figure 4.17 Char Gasification in Steam:  
Test for First Order Kinetics

The correlation coefficient of the least square fit line in Figure 4.17 is 0.989, and thus the order of reaction is reported as unity,

$$n = 1 \quad (4.72)$$

The slope of the line is  $-2.89 \times 10^4 \text{ } ^\circ\text{K}^{-1}$ , corresponding to an activation energy,

$$E = 57.5 \text{ kcal/mole} \quad (4.73)$$

The intercept at  $1/T_p \rightarrow 0$  determines the frequency factor, shown in Table 4.12 as  $1.35 \times 10^7 \text{ cm/sec}$ .

Table 4.12

Intrinsic Kinetics of Montana Rosebud  
Char Gasification in Steam

$$\frac{R''}{M_c} = -\frac{1}{S_g M_c W} \frac{dW}{dt} = \tilde{A}'' \exp \left( -\frac{E}{RT_p} \right) C_{H_2O}^n$$

n	order of reaction	unity
E	activation energy	57.5 kcal/mole
$\tilde{A}''$	frequency factor	$1.35 \times 10^7$ cm/sec

Chapter 5

CONCLUSIONS

5.1 Intrinsic Kinetics of Char Gasification in Carbon Dioxide  
And Steam

1. The intrinsic kinetics of the gasification of a Montana Rosebud coal char in carbon dioxide and steam, at temperatures of 1473 to 2113°K (gas temperature), 1 atm total pressure, and residence times up to 330 msec, are expressed by a power law model,

$$R'' / M_c = \tilde{A}'' \exp \left\{ -\frac{E}{RT_p} \right\} C^n \quad (5.1)$$

where the rate,  $R'' / M_c$ , is expressed in moles (carbon) per unit total char surface area per unit time, and C is the local concentration of the oxidizing gas. The kinetic parameters are:

	<u>n</u>	<u>E</u> (kcal/mole)	<u><math>\tilde{A}''</math></u>
char - CO <sub>2</sub>	0	50.1	1.09 $\frac{\text{mole}}{\text{cm}^2 \text{sec}}$
char - H <sub>2</sub> O	1	57.5	1.35 x 10 <sup>7</sup> cm/sec

2. Heat transfer limitations in the boundary layer surrounding the reacting char particles result in significant differences (up to 270°K) between the gas temperature and the particle temperature.

3. Bulk diffusional rate limitations in the external boundary layer are less pronounced, although the surface concentration of oxidizing gas drops to as low as approximately two-thirds of the bulk gas concentration.

4. The temperature of a reacting char particle is uniform throughout the particle, and equal to the temperature on the external surface of the particle.

5. Pore diffusional effects are significant. Intraphase effectiveness factors are below unity under all experimental conditions studied.

## 5.2 Physical Properties of the Char

1. The specific ( $N_2$  adsorption) surface area of the char increases significantly under all experimental conditions, even at less than 1 percent (d.a.f.) burnoff. The initial char has a specific surface area of approximately  $81 \text{ m}^2/\text{g}$ . The maximum surface areas measured for partially gasified char samples are:

<u>Nominal Temperature</u>	Carbon Dioxide Gasification		Steam Gasification	
	$S_g$ ( $\text{m}^2/\text{g}$ )	d.a.f. burnoff (%)	$S_g$ ( $\text{m}^2/\text{g}$ )	d.a.f. burnoff (%)
1473°K	255	8.4	369	30.4
1773°K	193	19.3	273	49.6
2113°K	151	25.6	155	28.8

2. Particle bulk density decreases slowly with burnoff, from an initial value of  $0.49 \text{ g/cm}^3$ . The lowest values measured are  $0.36 \text{ g/cm}^3$  after approximately 30 percent burnoff in  $\text{CO}_2$  at  $1773^\circ\text{K}$ , and  $0.28 \text{ g/cm}^3$  after 81 percent burnoff in steam at  $1773^\circ\text{K}$ .

## Chapter 6

### RECOMMENDATIONS FOR FUTURE WORK

1. The laminar flow furnace may be redesigned to provide a more isothermal reaction zone.
2. Methods may be introduced to accurately measure char particle velocities and temperatures.
3. Apparatus may be designed for experiments at pressures above 1 atmosphere.
4. Additional experiments may be conducted with char particles of different sizes, to check for mass transfer effects.
5. Additional experiments may be conducted to determine the Langmuir-Hinshelwood kinetics for the gasification reactions.
6. Evaluate the effect of the possible side reaction of the char with molecular oxygen, which might form from the dissociation of carbon dioxide or steam, particularly at the highest temperatures studied.

## Appendix A

### CHAR GASIFICATION IN CARBON DIOXIDE

The results of char gasification experiments in carbon dioxide are shown in Table A.1. Weight loss data on a dry, ash-free basis were calculated assuming an ash content of 20.5 percent by weight in the initial char. The small moisture content (ca. 1 wt%) was neglected. Residence times were approximated by the method discussed in sections 2.5.1 through 2.5.3. Data from runs C-10 and C-16 were not used in the calculation of reaction rates and intrinsic kinetics. Observed weight loss in these runs differed widely from observed weight loss in other runs conducted under the same experimental conditions.



Table A.1 Results of Char Gasification Experiments in Carbon Dioxide

Run Code	Nominal Temperature (°K)	Actual Max. T (°K)	Feeder - Collector Sep'n (cm)	Residence Time (msec)	Main Gas Stream			Char Fed (g)	Char Rec'd (g)	Char Wt. Loss (%)	d.a.f. Char Wt. Loss (%)		
					CO <sub>2</sub>	H <sub>2</sub> O	N <sub>2</sub>						
C-01	1773	1775	7.6	143	26	7	7	61	6.31	0.1131	0.1003	11.3	14.2
C-02	1773	1775	7.6	143	26	7	7	61	6.31	0.1394	0.1216	12.8	16.1
C-03	1773	1775	7.6	143	26	7	7	61	6.31	0.1071	0.0960	10.4	13.1
C-04	1773	1775	15.2	273	26	7	7	61	6.31	0.1392	0.1076	22.7	28.6
C-05	1773	1775	15.2	273	26	7	7	61	6.31	0.1575	0.1207	23.4	29.5
C-06	1773	1775	15.2	273	26	7	7	61	6.31	0.1445	0.1099	23.9	30.1
C-07	1773	1775	11.4	199	25	6	7	61	6.59	0.1381	0.1129	18.2	22.9
C-08	1773	1775	11.4	199	25	6	7	61	6.59	0.1460	0.1191	18.4	23.2
C-09	1773	1775	11.4	199	25	6	7	61	6.59	0.1460	0.1165	20.2	25.4
* C-10	1473	1460	15.2	319	26	7	7	61	6.45	0.1824	0.1621	11.1	14.0
C-11	1473	1460	15.2	319	26	7	7	61	6.45	0.1662	0.1600	3.7	4.7
C-12	1473	1460	15.2	319	26	7	7	61	6.45	0.1238	0.1201	3.0	3.8
C-13	1473	1460	7.6	167	26	7	7	61	6.45	0.1578	0.1602	-1.5	-1.9
C-14	1473	1460	7.6	167	26	7	7	61	6.45	0.1425	0.1437	-0.8	-1.0
C-15	1473	1460	7.6	167	26	7	7	61	6.45	0.1245	0.1260	-1.2	-1.5
* C-16	1473	1460	11.4	241	26	7	7	61	6.45	0.1244	0.1109	10.9	13.7
C-17	1473	1460	11.4	241	26	7	7	61	6.45	0.1410	0.1381	2.1	2.6
C-18	1473	1460	11.4	241	26	7	7	61	6.45	0.1298	0.1287	0.8	1.0
C-19	1473	1490	15.2	319	53	9	8	29	6.58	0.1598	0.1481	7.3	9.2
C-20	1473	1490	15.2	319	53	9	8	29	6.58	0.2138	0.1911	10.6	13.4
C-21	1473	1490	15.2	319	53	9	8	29	6.58	0.2111	0.1841	12.8	16.1
C-22	1473	1490	11.4	241	53	9	8	29	6.58	0.2040	0.1915	6.1	7.9
C-23	1473	1490	11.4	241	53	9	8	29	6.58	0.2026	0.1890	6.7	8.4
C-24	1473	1490	11.4	241	53	9	8	29	6.58	0.2059	0.1966	4.6	5.8
C-25	1473	1490	7.6	167	53	9	8	29	6.58	0.2193	0.2117	3.5	4.4
C-26	1473	1490	7.6	167	53	9	8	29	6.58	0.1802	0.1741	3.4	4.3
C-27	1473	1490	7.6	167	53	9	8	29	6.58	0.1273	0.1216	4.5	5.7
C-28	1773	1760	7.6	147	63	4	3	31	6.20	0.2155	0.1958	9.1	11.5
C-29	1773	1760	7.6	147	63	4	3	31	6.20	0.2100	0.1939	7.7	9.7
C-30	1773	1760	7.6	147	63	4	3	31	6.20	0.2004	0.1854	7.5	9.4

Table A.1 continued

Run Code	Nominal Temperature (°K)	Actual Max. T (°K)	Feeder - Collector Sep'n (cm)	Residence Time (msec)	Main Gas Stream			Char Fed (g)	Char Rec'd (g)	Char Wt. Loss (%)	d.a.f. Char Wt. Loss (%)		
					CO <sub>2</sub>	H <sub>2</sub> O	N <sub>2</sub>						
C-31	1773	1760	11.4	213	63	4	3	31	6.20	0.2479	0.2100	15.3	19.3
C-32	1773	1760	11.4	213	63	4	3	31	6.20	0.1468	0.1201	18.2	22.9
C-33	1773	1760	11.4	213	63	4	3	31	6.20	0.2372	0.1986	16.3	20.5
C-34	1773	1760	15.2	281	63	4	3	31	6.20	0.1686	0.1297	23.1	29.1
C-35	1773	1760	15.2	281	63	4	3	31	6.20	0.2208	0.1662	24.7	31.1
C-36	1773	1760	15.2	281	63	4	3	31	6.20	0.1884	0.1430	24.1	30.4
C-37	1773	-	15.2	276	57	6	7	30	6.36	0.1870	0.1288	31.1	39.2
C-38	1773	-	15.2	276	57	6	7	30	6.36	0.1995	0.1345	32.6	41.1
C-39	1773	-	15.2	284	57	3	9	31	6.13	0.1791	0.1410	21.3	26.8
C-40	1773	-	15.2	284	57	3	9	31	6.13	0.3227	0.2530	21.6	27.2
C-41	1773	-	15.2	284	57	3	9	31	6.13	0.1989	0.1382	30.6	38.5
C-42	1773	-	15.2	284	57	3	9	31	6.13	0.1704	0.1197	29.8	37.5
C-43	1773	-	11.4	215	57	3	9	31	6.13	0.1195	0.1002	16.2	20.4
C-44	1773	-	11.4	215	57	3	9	31	6.13	0.1091	0.0936	14.2	17.9
C-45	1773	-	11.4	215	57	3	9	31	6.13	0.1102	0.0855	22.4	28.2
C-46	1773	-	11.4	215	57	3	9	31	6.13	0.1162	0.0877	24.6	31.0
C-47	1773	-	7.6	149	57	3	9	31	6.13	0.0862	0.0791	8.2	10.3
C-48	1773	-	7.6	149	57	3	9	31	6.13	0.1268	0.1117	11.9	15.0
C-49	1773	-	7.6	149	57	3	9	31	6.13	0.1390	0.1232	11.4	14.4
C-50	1773	-	7.6	149	57	3	9	31	6.13	0.0750	0.0691	7.9	9.9
C-51	2113	-	15.2	230	26	7	7	61	6.32	0.1539	0.0953	38.1	48.0
C-52	2113	-	15.2	230	26	7	7	61	6.32	0.1402	0.0864	38.4	48.4
C-53	2113	-	15.2	230	26	7	7	61	6.32	0.1408	0.0858	39.1	49.2
C-54	2113	-	11.4	174	26	7	7	61	6.32	0.1481	0.1056	28.7	36.1
C-55	2113	-	11.4	174	26	7	7	61	6.32	0.1013	0.0639	36.9	46.5
C-56	2113	-	11.4	174	26	7	7	61	6.32	0.1072	0.0722	32.6	41.1
C-57	2113	-	7.6	120	26	7	7	61	6.32	0.1069	0.0862	19.4	24.2
C-58	2113	-	7.6	120	26	7	7	61	6.32	0.0954	0.0783	17.9	22.5
C-59	2113	-	7.6	120	26	7	7	61	6.32	0.1335	0.1168	12.5	15.7

Table A.1 continued

Run Code	Nominal Temperature (°K)	Actual Max. T (°K)	Feeder - Collector Sep'n (cm)	Residence Time (msec)	Main Gas Stream (Mole Percent) <sup>†</sup>			Flow Rate (l/min STP)	Char Fed (g)	Char Rec'd (g)	Char Wt. Loss (%)	d.a.f. Char Wt. Loss (%)	
					CO <sub>2</sub>	H <sub>2</sub> O	N <sub>2</sub>						
C-60	2113	-	15.2	240	57	3	9	31	6.13	0.1008	0.0505	49.9	62.8
C-61	2113	-	15.2	240	57	3	9	31	6.13	0.0957	0.0479	49.9	62.8
C-62	2113	-	15.2	240	57	3	9	31	6.13	0.0958	0.0454	52.6	66.2
C-63	2113	-	11.4	182	57	3	9	31	6.13	0.1338	0.0835	37.6	47.4
C-64	2113	-	11.4	182	57	3	9	31	6.13	0.1884	0.1248	32.3	40.7
C-65	2113	-	11.4	182	57	3	9	31	6.13	0.1253	0.0799	36.2	45.6
C-66	2113	-	7.6	126	57	3	9	31	6.13	0.1156	0.0923	20.2	25.4
C-67	2113	-	7.6	126	57	3	9	31	6.13	0.1351	0.1077	20.3	25.6
C-68	2113	-	7.6	126	57	3	9	31	6.13	0.1433	0.1161	19.0	23.9

Notes:

<sup>†</sup> The sum of mole percents of the main gas stream may not equal 100% due to round-off error.

\* Not included in the calculation of rates and kinetic parameters.

Appendix B

CHAR GASIFICATION IN STEAM

The results of char gasification experiments in steam are shown in Table B.1. Again, d.a.f. data are based on an initial ash content of 20.5 wt%, with the initial moisture content being neglected. Data from runs S-33, S-34, S-39, S-41 and S-58 were not used in kinetics calculations, due to unusually large variations in results when compared with other runs at the same conditions.

Table B.1 Results of Char Gasification Experiments in Steam

Run Code	Nominal Temperature (°K)	Actual Max. T (°K)	Feeder - Collector Sep'n (cm)	Residence Time (msec)	Main Gas Stream		Char Fed (g)	Char Rec'd (g)	Char Wt. Loss (%)	d.a.f. Char Wt. Loss (%)
					(Mole Percent)† (H <sub>2</sub> O H <sub>2</sub> N <sub>2</sub> )	Flow Rate (l/min STP)				
S-01	1473	1480	15.2	325	32	0 67	0.1757	0.1649	6.1	7.7
S-02	1473	1480	15.2	325	32	0 67	0.2981	0.2790	6.4	8.1
S-03	1473	1480	15.2	325	32	0 67	0.1456	0.1362	6.5	8.2
S-04	1473	1480	15.2	325	32	0 67	0.1950	0.1834	5.9	7.4
S-05	1473	1470	7.6	169	32	0 67	0.2138	0.2120	0.8	1.0
S-06	1473	1470	7.6	169	32	0 67	0.1676	0.1657	1.1	1.4
S-07	1473	1470	7.6	169	32	0 67	0.1904	0.1888	0.8	1.0
S-08	1473	1470	15.2	325	32	0 67	0.2176	0.2042	6.2	7.8
S-09	1773	1775	15.2	275	32	0 67	0.1063	0.0709	33.3	41.9
S-10	1773	1775	15.2	275	32	0 67	0.3110	0.2020	35.0	44.1
S-11	1773	1775	15.2	275	32	0 67	0.2355	0.1421	39.7	50.0
S-12	1773	1775	7.6	143	32	0 67	0.2021	0.1650	18.4	23.2
S-13	1773	1775	7.6	143	32	0 67	0.1957	0.1622	17.1	21.5
S-14	1773	1775	7.6	143	32	0 67	0.1929	0.1583	17.9	22.5
S-15	1773	1775	15.2	280	35	0 65	0.1511	0.0989	34.5	43.5
S-16	1473	1480	11.4	244	34	0 66	0.1533	0.1505	3.1	3.9
S-17	1473	1480	11.4	244	34	0 66	0.1543	0.1520	1.5	1.9
S-18	1473	1480	11.4	244	34	0 66	0.1386	0.1302	6.1	7.7
S-19	1773	1770	11.4	206	34	0 66	0.1957	0.1450	25.9	32.6
S-20	1773	1770	11.4	206	34	0 66	0.1497	0.1096	26.8	33.8
S-21	1773	1770	11.4	206	34	0 66	0.1279	0.0903	29.4	37.0
S-22	1473	1470	15.2	312	65	5 30	0.1199	0.0932	24.1	30.4
S-23	1473	1470	15.2	312	65	5 30	0.1459	0.1232	17.5	22.0
S-24	1473	1470	15.2	312	65	5 30	0.1054	0.1564	21.8	27.5
S-25	1473	1470	11.4	235	65	5 30	0.1651	0.1524	7.7	9.7
S-26	1473	1470	11.4	235	65	5 30	0.2155	0.1963	8.9	11.2
S-27	1473	1470	11.4	235	65	5 30	0.1221	0.1088	10.9	13.7
S-28	1473	1470	7.6	162	65	5 30	0.1471	0.1420	3.4	4.4
S-29	1473	1470	7.6	162	65	5 30	0.1539	0.1470	3.8	4.8
S-30	1473	1470	15.2	330	35	0 65	0.0820	0.0793	3.3	4.2
S-31	1473	1470	7.6	162	65	5 30	0.1588	0.1515	4.6	5.8
S-32	1473	1470	15.2	330	35	0 65	0.1216	0.1125	7.5	9.4

Table B.1 continued

Run Code	Nominal Temperature (°K)	Actual Max. T (°K)	Feeder - Collector Sep'n (cm)	Residence Time (msec)	Main Gas Stream			Char Fed (g)	Char Rec'd (g)	Char Wt. Loss (%)	d.s.f. Char Wt. Loss (%)
					(Mole Percent)†	Flow Rate (l/min STP)	Char Wt. Loss (%)				
					H <sub>2</sub>	H <sub>2</sub>	N <sub>2</sub>				
* S-33	1773	-	15.2	264	65	5	30	0.1840	0.1210	34.2	43.1
* S-34	1773	-	15.2	264	65	5	30	0.1755	0.1160	33.9	42.7
S-35	1773	-	15.2	264	65	5	30	0.2034	0.0884	56.5	71.3
S-36	1773	-	15.2	264	65	5	30	0.1944	0.1007	48.2	60.7
S-37	1773	-	11.4	198	65	5	30	0.1752	0.1062	39.4	49.6
S-38	1773	-	11.4	198	65	5	30	0.1911	0.1110	41.9	52.8
* S-39	1773	-	11.4	198	65	5	30	0.1668	0.0824	50.6	63.7
S-40	1773	-	7.6	136	65	5	30	0.1827	0.1427	21.9	27.6
* S-41	1773	-	7.6	136	65	5	30	0.1494	0.1289	13.7	17.3
S-42	1773	-	7.6	136	65	5	30	0.1284	0.1010	21.3	26.8
S-43	1773	-	15.2	264	65	5	30	0.2231	0.0783	64.9	81.7
S-44	1773	-	15.2	264	65	5	30	0.1628	0.0656	59.7	75.2
S-45	2113	-	15.2	233	32	0	67	0.0733	0.0384	47.6	59.9
S-46	2113	-	15.2	233	32	0	67	0.1050	0.0486	53.7	67.5
S-47	2113	-	15.2	233	32	0	67	0.0842	0.0358	57.5	72.4
S-48	2113	-	11.4	175	32	0	67	0.0729	0.0432	40.7	51.3
S-49	2113	-	11.4	175	32	0	67	0.1638	0.0946	42.2	53.1
S-50	2113	-	11.4	175	32	0	67	0.0724	0.0364	49.7	62.6
S-51	2113	-	7.6	121	32	0	67	0.1128	0.0841	25.4	32.0
S-52	2113	-	7.6	121	32	0	67	0.1078	0.0831	22.9	28.8
S-53	2113	-	7.6	121	32	0	67	0.1065	0.0771	27.6	34.8
S-54	2113	-	15.2	224	65	5	30	0.0889	0.0292	67.2	84.6
S-55	2113	-	15.2	224	65	5	30	0.0951	0.0360	62.1	78.2
S-56	2113	-	15.2	224	65	5	30	0.1128	0.0489	56.6	71.3
S-57	2113	-	11.4	168	65	5	30	0.0795	0.0405	49.1	61.8
* S-58	2113	-	11.4	168	65	5	30	0.1236	0.0758	38.7	48.7
S-59	2113	-	11.4	168	65	5	30	0.1094	0.0595	45.6	57.4
S-60	2113	-	7.6	115	65	5	30	0.1125	0.0866	23.0	29.0
S-61	2113	-	7.6	115	65	5	30	0.1016	0.0783	22.9	28.8
S-62	2113	-	7.6	115	65	5	30	0.0983	0.0767	22.0	27.7

Notes:

† The sum of mole percents of the main gas stream may not equal 100% due to round-off error.

\* Not included in the calculation of rates and kinetic parameters.

Appendix C  
CHAR PYROLYSIS

The results of pyrolysis experiments (argon main gas stream) are shown in Table C.1. A discussion of these results is found in section 2.5.8.

Table C.1

Results of Char Pyrolysis Experiments

<u>Run Code</u>	<u>T<sub>o</sub> (°K)</u>	<u>Feeder - Collector Sep'n(cm)</u>	<u>Char Fed (g)</u>	<u>Char Rec'd (g)</u>	<u>Char Wt. Loss (%)</u>
A-01	1473	7.6	0.3086	0.3064	0.7
A-02	1473	7.6	0.1030	0.1043	-1.2
A-03	1473	7.6	0.0955	0.0957	-0.2
A-04	1473	11.4	0.1605	0.1580	1.6
A-05	1473	11.4	0.0930	0.0926	0.4
A-06	1473	11.4	0.1128	0.1123	0.4
A-07	1473	15.2	0.0988	0.0979	0.9
A-08	1473	15.2	0.1248	0.1205	3.4
A-09	1473	15.2	0.1507	0.1458	3.3
A-10	1773	15.2	0.0747	0.0766	-2.5
A-11	1773	15.2	0.1513	0.1484	1.9
A-12	1773	15.2	0.1257	0.1205	4.1
A-13	1773	11.4	0.2337	0.2336	0.0
A-14	1773	11.4	0.2072	0.2263	-9.2
A-15	1773	7.6	0.1125	0.1220	-8.4
A-16	1773	7.6	0.1867	0.1833	1.8
A-17	1773	7.6	0.1400	0.1379	1.5

Note:

Main gas stream is pure argon,  $\dot{V} \approx 6$  l/min STP.



Appendix D

CALCULATION OF MAIN GAS STREAM PROPERTIES

Examination of Table A.1 (CO<sub>2</sub> gasification) and Table B.1 (steam gasification) reveals minor variations in the main gas composition about the two nominal partial pressures of the oxidizing gas (see section 1.6) in each study. For the purpose of calculating properties of the main gas stream, the "nominal" compositions in Table D.1 have been assumed. The following properties have been determined:

Appendix E - Viscosity,  $\mu$

Appendix F - Kinematic Viscosity,  $\nu$

Appendix G - Thermal Conductivity,  $\lambda$

Table D.1  
Nominal Compositions for Calculation of Main Gas Properties

Oxidizing Gas	Nominal Pressure (atm)	Variation in Nominal Pressure (atm)	Assumed Composition					Molecular Weight
			H <sub>2</sub> O	H <sub>2</sub>	CO <sub>2</sub>	CO	N <sub>2</sub>	
CO <sub>2</sub>	0.26	0.25 - 0.26	6	-	26	7	61	31.6
CO <sub>2</sub>	0.60	0.53 - 0.63	5	-	60	5	30	37.1
H <sub>2</sub> O	0.34	0.32 - 0.35	34	-	-	-	66	24.6
H <sub>2</sub> O	0.65	---	65	5	-	-	30	20.2

Appendix E

MAIN GAS VISCOSITY

Perry and Chilton<sup>61</sup> give the following formula for calculating the viscosity of a gas mixture at low pressures:

$$\mu = \frac{\sum_i y_i M_i^{1/2} \mu_i}{\sum_i y_i M_i^{1/2}} \quad (\text{E.1})$$

where  $\mu_i$  is the pure component viscosity,  $y_i$  is the mole fraction and  $M_i$  is the molecular weight of the  $i^{\text{th}}$  component in the mixture. Pure component viscosities at temperature  $T$  ( $^{\circ}\text{K}$ ) may be estimated from:

$$\mu_i \approx \frac{27.0 M_i^{1/2} T^{3/2}}{\tilde{V}_{b,i}^{2/3} (T + 1.47 T_{b,i})} \quad (\text{E.2})$$

where  $\mu_i$  is in micropoise ( $\text{g cm}^{-1} \text{sec}^{-1} \times 10^{-6}$ ),  $T_{b,i}$  is the normal boiling point ( $^{\circ}\text{K}$ ) and  $\tilde{V}_{b,i}$  is the liquid molar volume ( $\text{cm}^3/\text{mole}$ ) at  $T_{b,i}$ . Values of  $T_{b,i}$  and  $\tilde{V}_{b,i}$  for use in equation (E.2) are listed in Table E.1.

Using equation (E.2) and data in Table E.1, pure component viscosities may be calculated, as shown in Figure E.1. The main gas viscosities, Figure E.2, may be calculated using Figure E.1 and equation (E.1).

Table E.1  
Pure Component Boiling Point Data

<u>Component</u>	<u>Molecular Weight (g/mole)</u>	<u>Normal Boiling Point <math>T_b</math> (<math>^{\circ}</math>K)</u>	<u>Liquid Molar Volume (<math>\text{cm}^3/\text{mole}</math>)</u>
CO <sub>2</sub>	44	195	34.0
CO	28	81	30.7
H <sub>2</sub> O	18	373	18.9
H <sub>2</sub>	2	20	14.3
N <sub>2</sub>	28	77	31.2

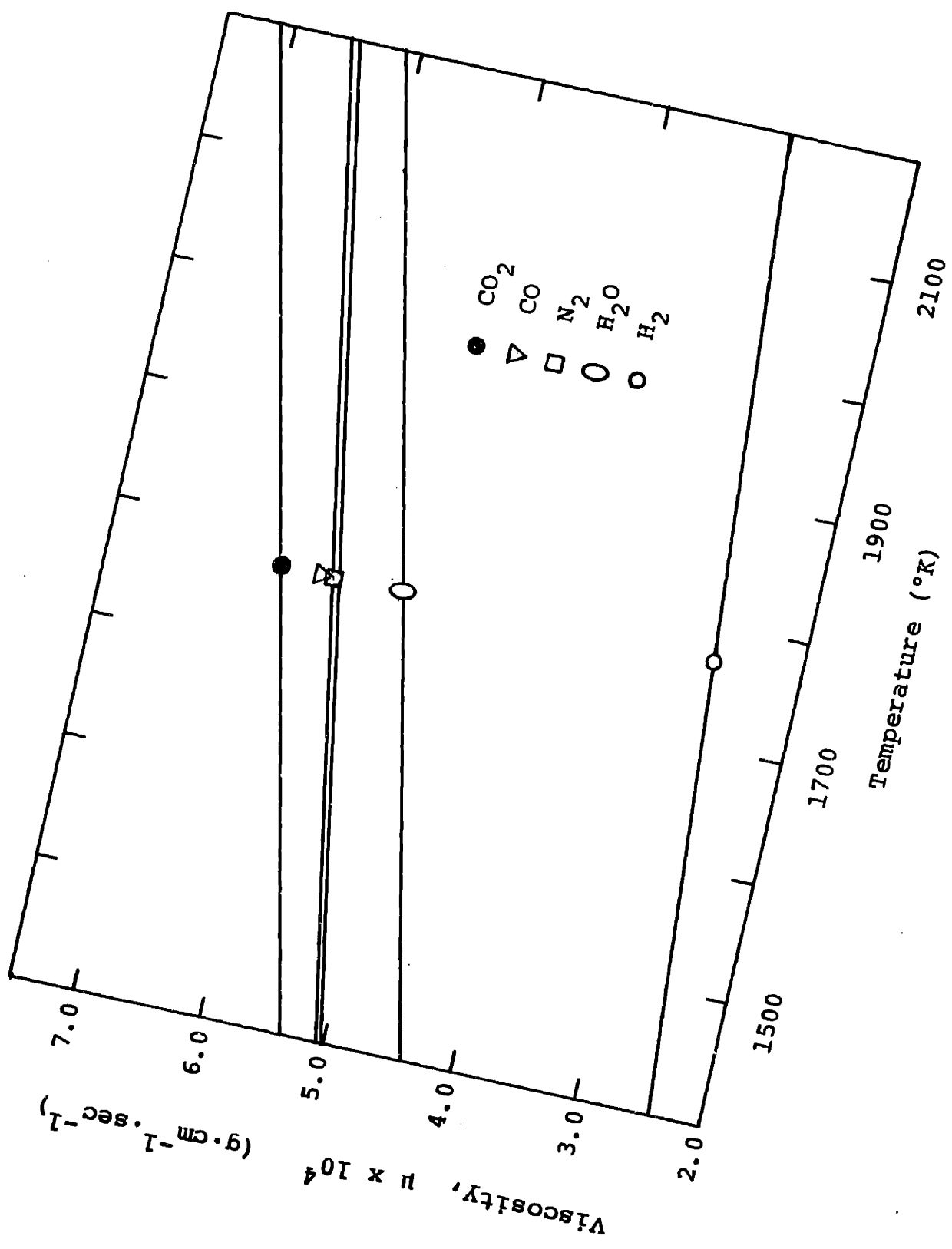


Figure E.1 Pure Component Viscosities

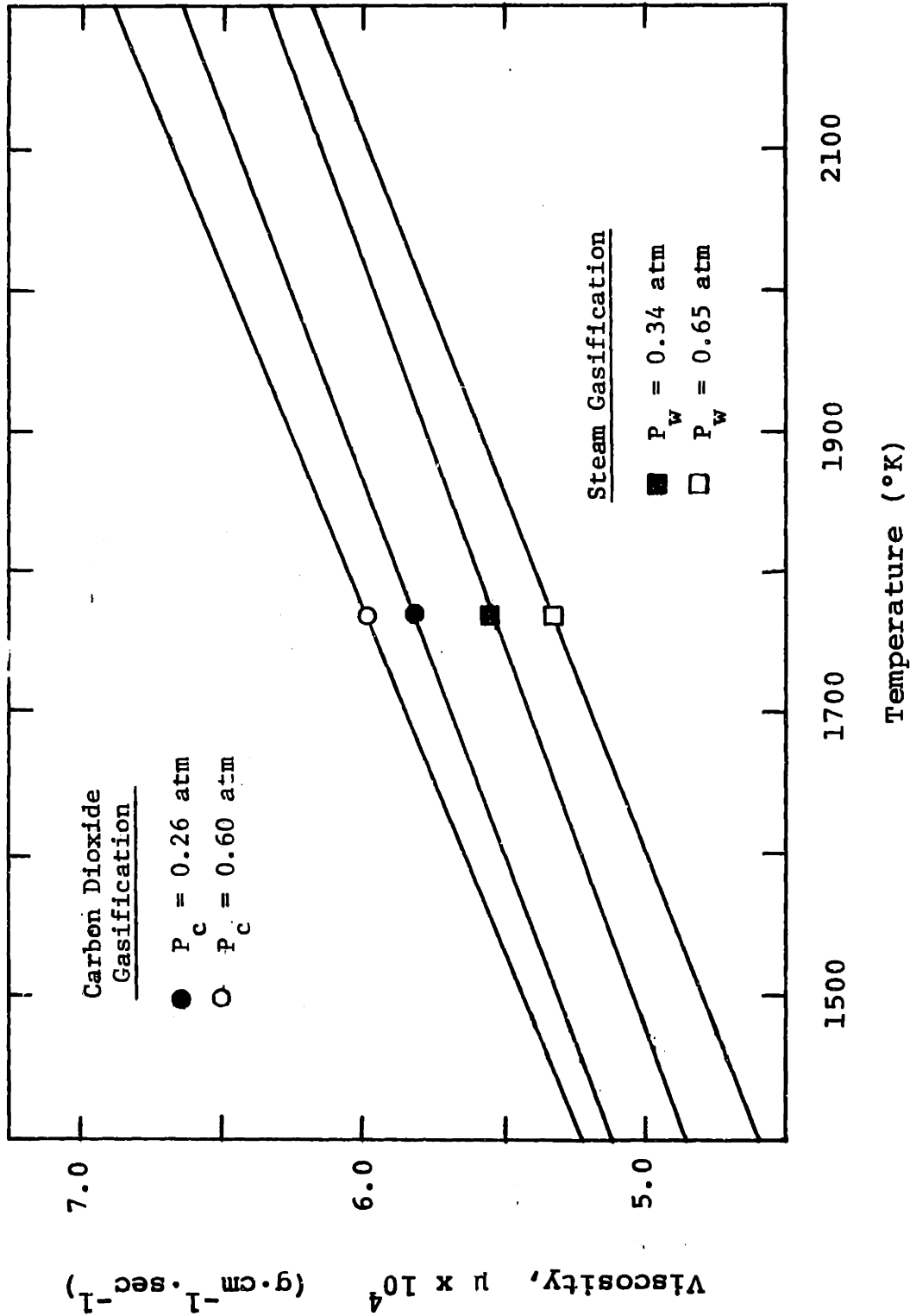


Figure E.2 Main Gas Viscosities

Appendix F

MAIN GAS KINEMATIC VISCOSITY

The kinematic viscosity is defined as the ratio of viscosity ( $\text{g cm}^{-1} \text{sec}^{-1}$ ) to density ( $\text{g/cm}^3$ ), and hence has the (CGS) units of square centimeters per second:

$$\nu = \mu / \rho \quad (\text{F.1})$$

The density of an ideal gas may be calculated as:

$$\rho = \left[ \frac{P}{RT} \right] \cdot M \quad (\text{F.2})$$

where M is the molecular weight, P is the total pressure and R is the gas constant. Using the viscosity data from Figure E.2 and the main gas molecular weights listed in Table D.1, Figure F.1 was constructed, showing the variation of the main gas kinematic viscosity,  $\nu$ , with temperature.

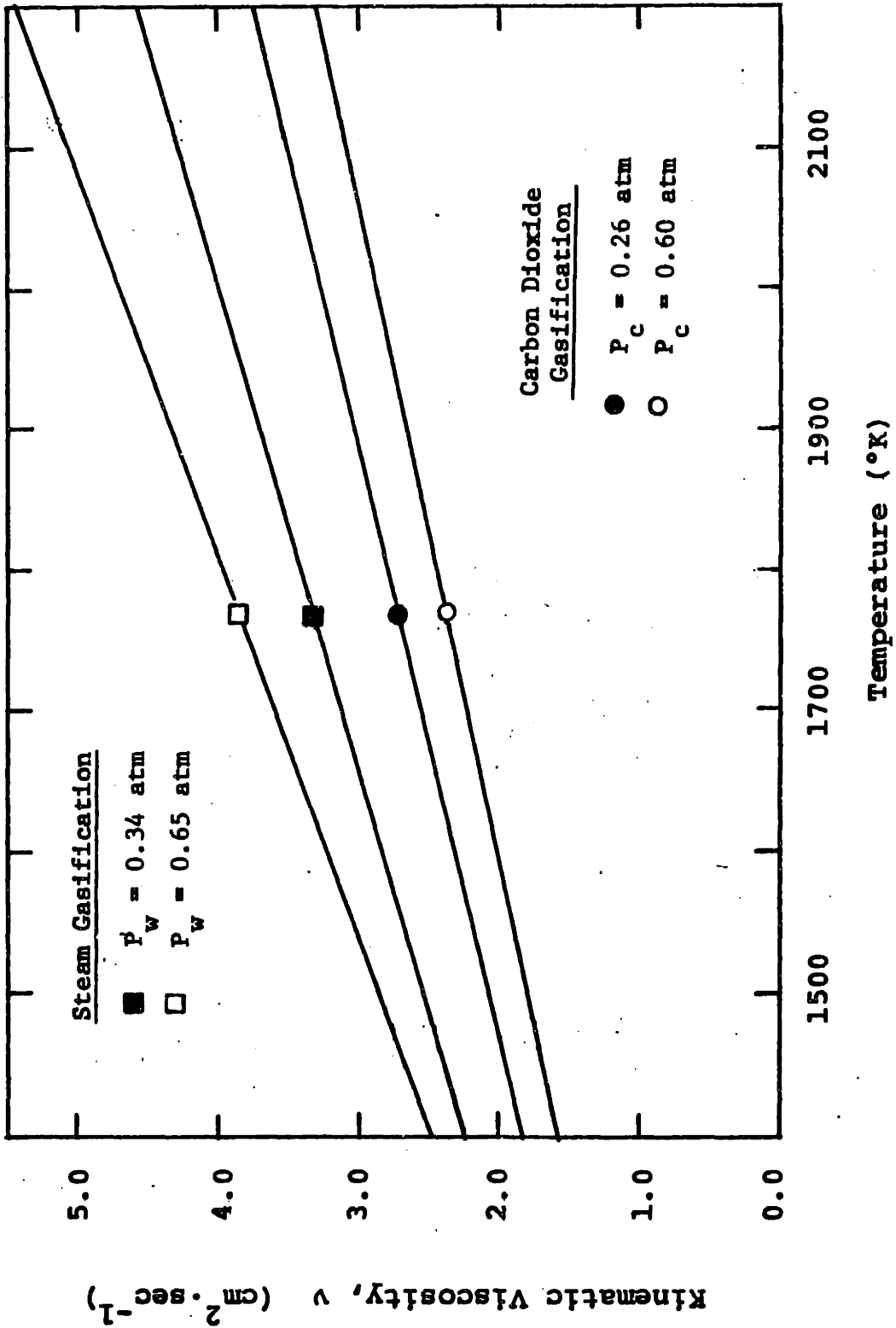


Figure F.1 Main Gas Kinematic Viscosities.



Appendix G

MAIN GAS THERMAL CONDUCTIVITY

Perry and Chilton<sup>61</sup> suggest the following formula for estimating the thermal conductivity of a pure gas at low pressures:

$$\lambda_i = \mu_i \left[ \hat{C}_{p,i} + \frac{2.48}{M_i} \right] \quad (G.1)$$

where the units of each term in equation (G.1) are:

$$\begin{aligned} \lambda_i & [=] \text{ cal} \cdot \text{sec}^{-1} \cdot \text{cm}^{-1} \cdot \text{°K}^{-1} \\ \mu_i & [=] \text{ g} \cdot \text{cm}^{-1} \cdot \text{sec}^{-1} \\ \hat{C}_{p,i} & [=] \text{ cal} \cdot \text{g}^{-1} \cdot \text{°K}^{-1} \end{aligned}$$

To estimate the thermal conductivity of a gas mixture, Perry and Chilton suggest:

$$\lambda = \frac{\sum_i y_i M_i^{1/3} \lambda_i}{\sum_i y_i M_i^{1/3}} \quad (G.2)$$

where  $y_i$  and  $M_i$  are the mole fraction and molecular weight of the  $i^{\text{th}}$  component in the mixture, respectively. Pure component viscosity data are shown in Figure E.1. Pure component molar heat capacities ( $\text{cal} \cdot \text{mole}^{-1} \cdot \text{°K}^{-1}$ ) may be estimated as follows:

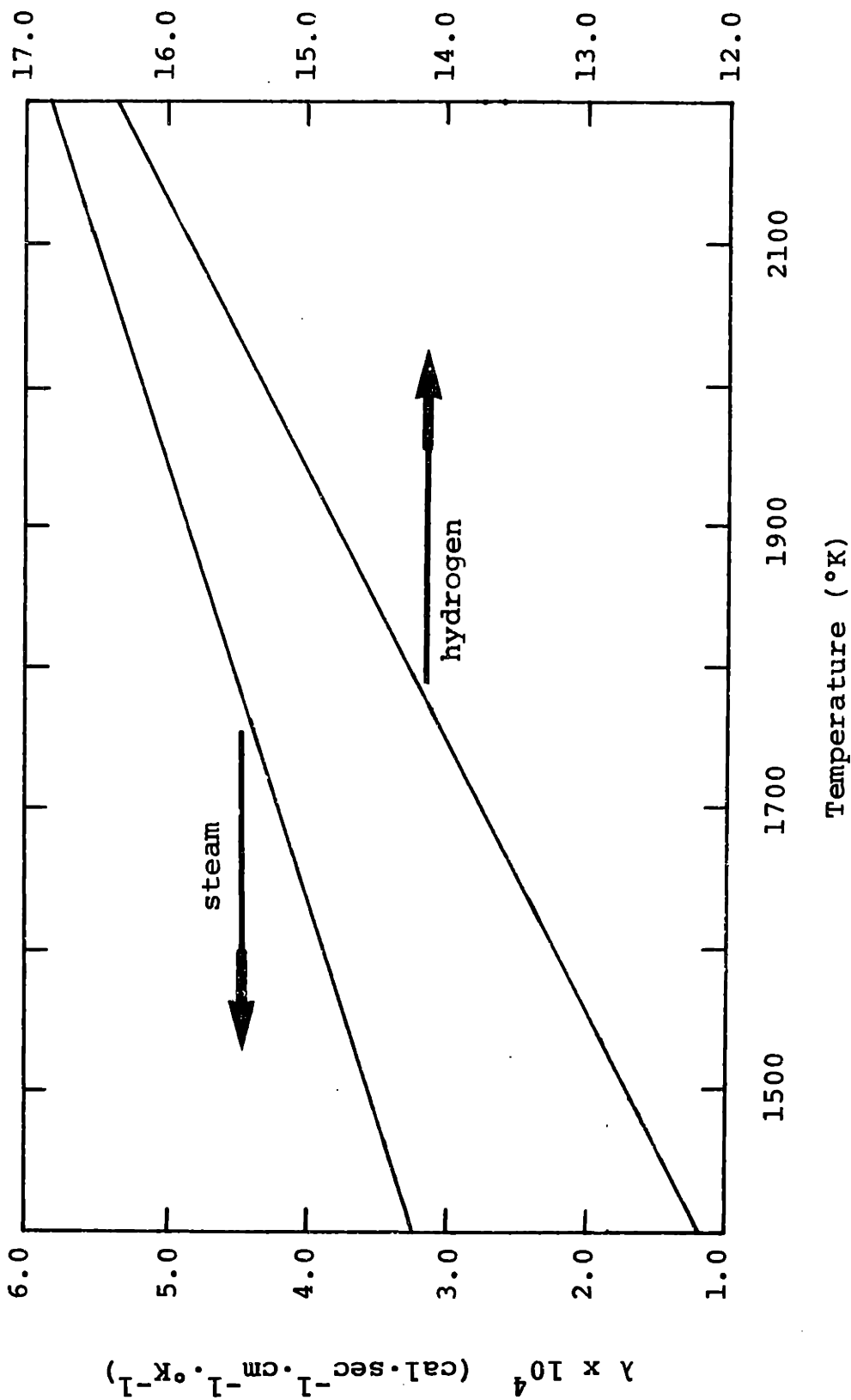


Figure G.1 Pure Component Thermal Conductivities (Steam and Hydrogen)

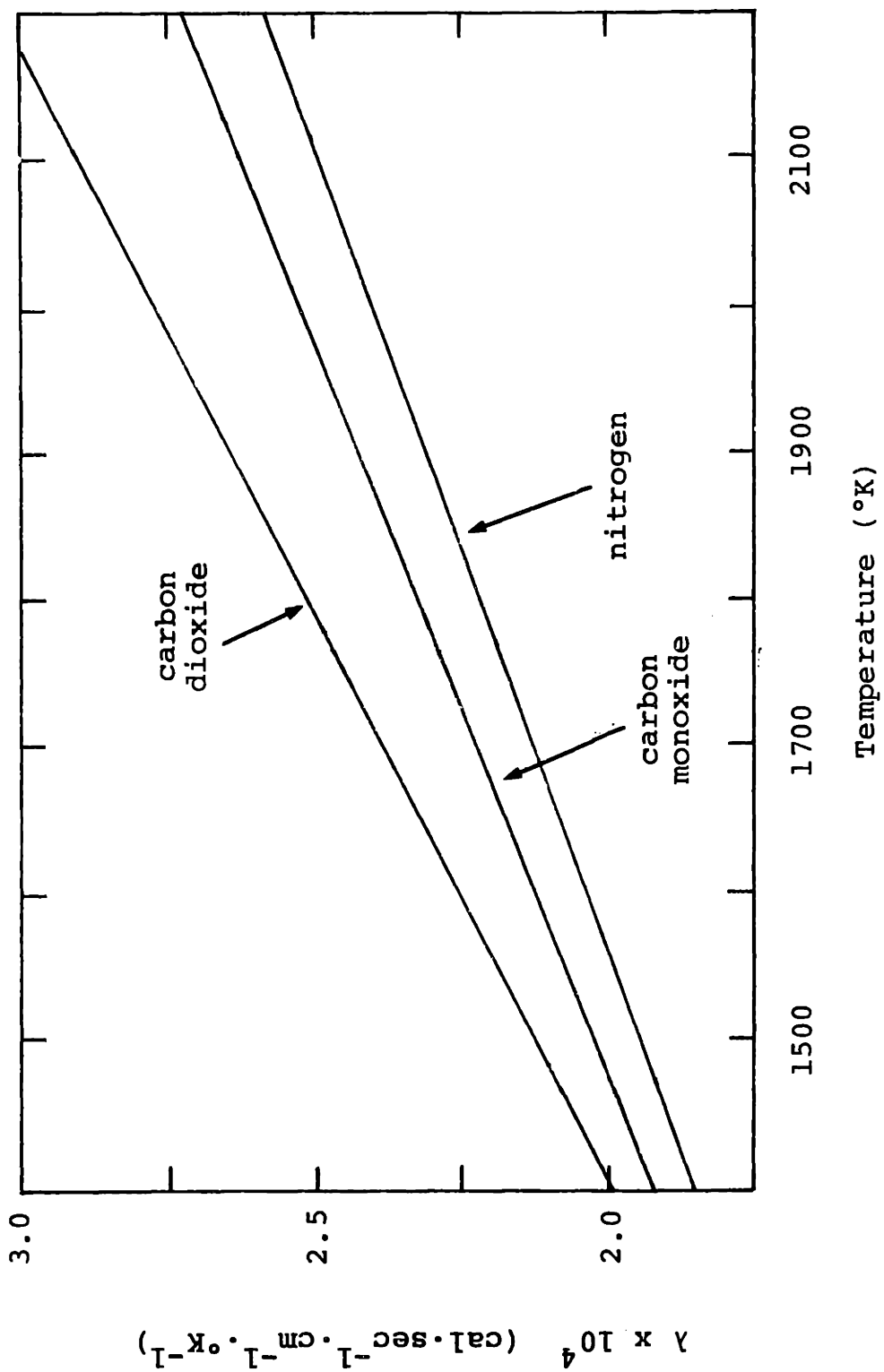


Figure G.2 Pure Component Thermal Conductivities  
( $\text{CO}_2$ ,  $\text{CO}$  and  $\text{N}_2$ )

$$\text{CO}_2 \quad 10.34 + 0.00274 T - 195500/T^2 \quad (\text{G.3})$$

$$\text{CO} \quad 6.60 + 0.00120 T \quad (\text{G.4})$$

$$\text{H}_2\text{O} \quad 8.22 + 0.00015 T + 1.34 \times 10^{-6} T^2 \quad (\text{G.5})$$

$$\text{H}_2 \quad 6.62 + 0.00081 T \quad (\text{G.6})$$

$$\text{N}_2 \quad 6.50 + 0.001 T \quad (\text{G.7})$$

where T is in degrees Kelvin.

Pure component thermal conductivities as a function of temperature are shown in Figure G.1 (steam and hydrogen) and Figure G.2 (carbon dioxide, carbon monoxide and nitrogen). Assuming main gas compositions as listed in Table D.1, equation (G.2) is used to estimate the main gas thermal conductivities shown in Figure G.3.

Noting the temperature dependence of viscosity (see equation (E.2)) and approximating that heat capacity is proportional to temperature raised to the first power (equations (G.3) through (G.7)), it is reasonable to approximate the temperature dependence of the main gas thermal conductivity (over the temperature range of Figure G.3) to be of the form:

$$\lambda \approx \lambda_1 + \lambda_2 T^{\frac{3}{2}} \quad (\text{G.8})$$

where  $\lambda_1$  and  $\lambda_2$  are constants which are different for each assumed main gas composition. The constants which best associate the data of Figure G.3 to equation (G.8) are:

$\lambda_1 \times 10^4$	$\lambda_2 \times 10^9$
$\left[ \frac{\text{cal}}{\text{cm sec } ^\circ\text{K}} \right]$	$\left[ \frac{\text{cal}}{\text{cm sec } ^\circ\text{K}^{\frac{5}{2}}} \right]$

CO<sub>2</sub> gasification:

P <sub>CO<sub>2</sub></sub> = 0.26 atm	1.040	1.80
P <sub>CO<sub>2</sub></sub> = 0.60 atm	0.987	1.97

H<sub>2</sub>O gasification:

P <sub>H<sub>2</sub>O</sub> = 0.34 atm	0.950	2.56
P <sub>H<sub>2</sub>O</sub> = 0.65 atm	0.925	3.94

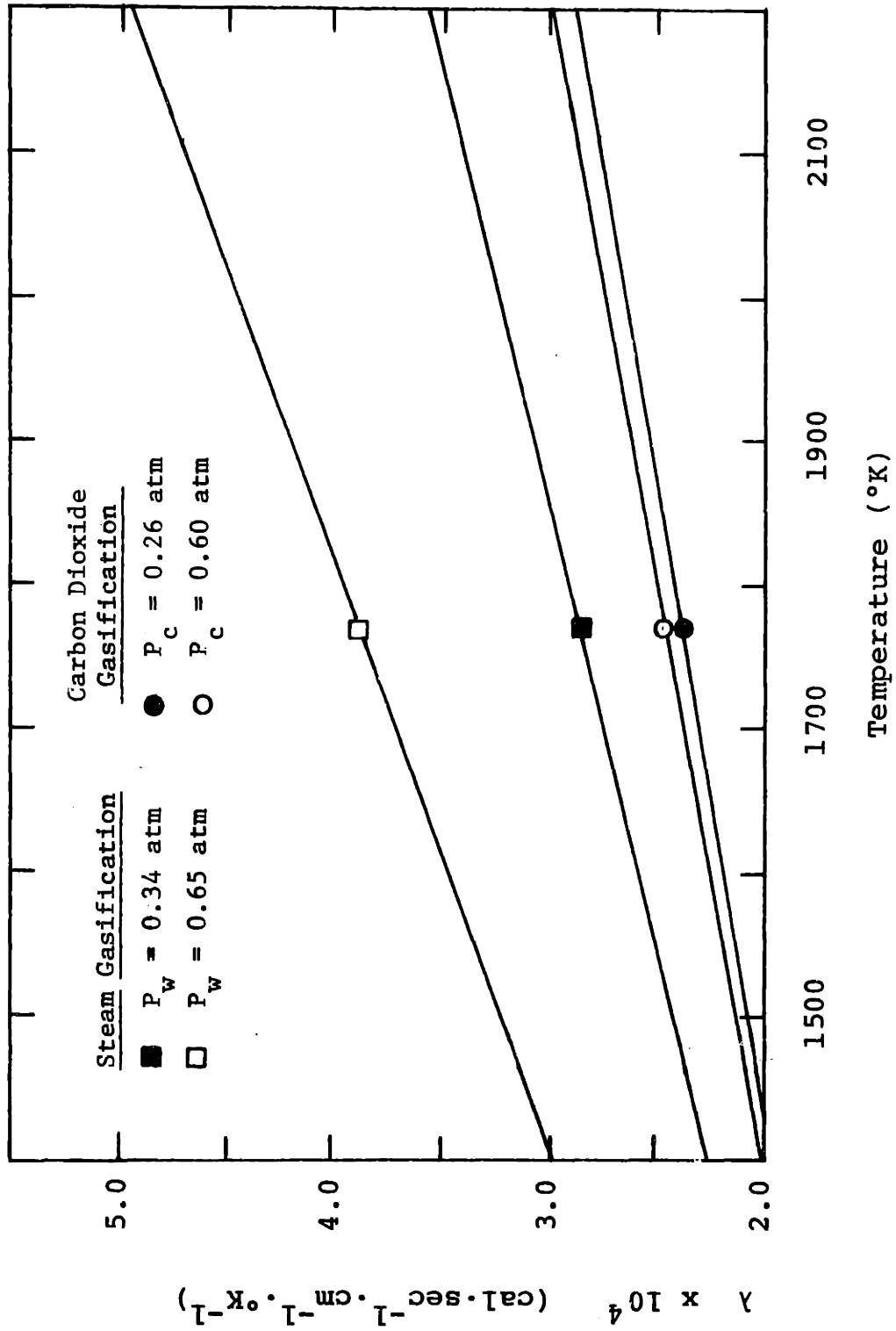


Figure G.3 Main Gas Thermal Conductivities

Appendix H

BULK DIFFUSION COEFFICIENTS

In order to facilitate the estimation of diffusion coefficients for the oxidizing component in the main gas stream, it is necessary to approximate the main gas as a binary mixture of the oxidizing gas (CO<sub>2</sub> or H<sub>2</sub>O) and nitrogen. Thus, the bulk diffusivity of a binary gas mixture, D<sub>12</sub> (units are cm<sup>2</sup>/sec) can be estimated from Satterfield<sup>67</sup> as a function of temperature (°K) by:

$$D_{12} = \frac{0.001858 T^{\frac{3}{2}} \left( \frac{1}{M_1} + \frac{1}{M_2} \right)^{\frac{1}{2}}}{P_{\text{tot}} r_{12}^2 I_D} \quad (\text{H.1})$$

where M<sub>1</sub> and M<sub>2</sub> are the molecular weights of components 1 and 2, P<sub>tot</sub> is the total system pressure (atm), r<sub>12</sub> is the collision diameter (Å) for species 1 and 2 and I<sub>D</sub> is the collision integral for diffusion. Values of I<sub>D</sub> are tabulated<sup>67</sup> as a function of the group κT/ε<sub>12</sub>, where κ is Boltzmann's constant (1.38 × 10<sup>-6</sup> erg/°K) and ε<sub>12</sub> is the energy of molecular interaction (°K) for species 1 and 2. The binary parameters r<sub>12</sub> and ε<sub>12</sub> are related to tabulated parameters for the individual species by:

$$r_{12} = \frac{1}{2} [(r_o)_1 + (r_o)_2] \quad (\text{H.2})$$

$$\epsilon_{12} = [\epsilon_1 \epsilon_2]^{\frac{1}{2}} \quad (\text{H.3})$$

Values of  $(r_o)_i$  and  $\epsilon_i$  are presented in Satterfield:<sup>67</sup>

<u>Component</u>	<u><math>\epsilon/\kappa</math> (<math>^{\circ}\text{K}</math>)</u>	<u><math>r_o</math> (<math>\text{\AA}</math>)</u>
$\text{CO}_2$	195.2	3.941
$\text{H}_2\text{O}$	809.1	2.641
$\text{N}_2$	71.4	3.798

Calculated values of  $r_{12}$  and  $\epsilon_{12}/\kappa$  for the oxidant-nitrogen mixtures are:

<u>Binary</u>	<u><math>r_{12}</math> (<math>\text{\AA}</math>)</u>	<u><math>\epsilon_{12}/\kappa</math> (<math>^{\circ}\text{K}</math>)</u>
$\text{CO}_2\text{-N}_2$	3.870	118.1
$\text{H}_2\text{O-N}_2$	3.220	240.4

Values for the collision integral  $I_D$  are:

<u><math>\kappa T/\epsilon_{12}</math></u>	<u><math>I_D</math></u>
6.0	0.8124
7.0	0.7896
8.0	0.7712
9.0	0.7556
10.0	0.7424
20.0	0.6640

Using equation (H.1) and the above data, a plot of  $D_{12}$  as a function of temperature (Figure H.1) can be constructed.



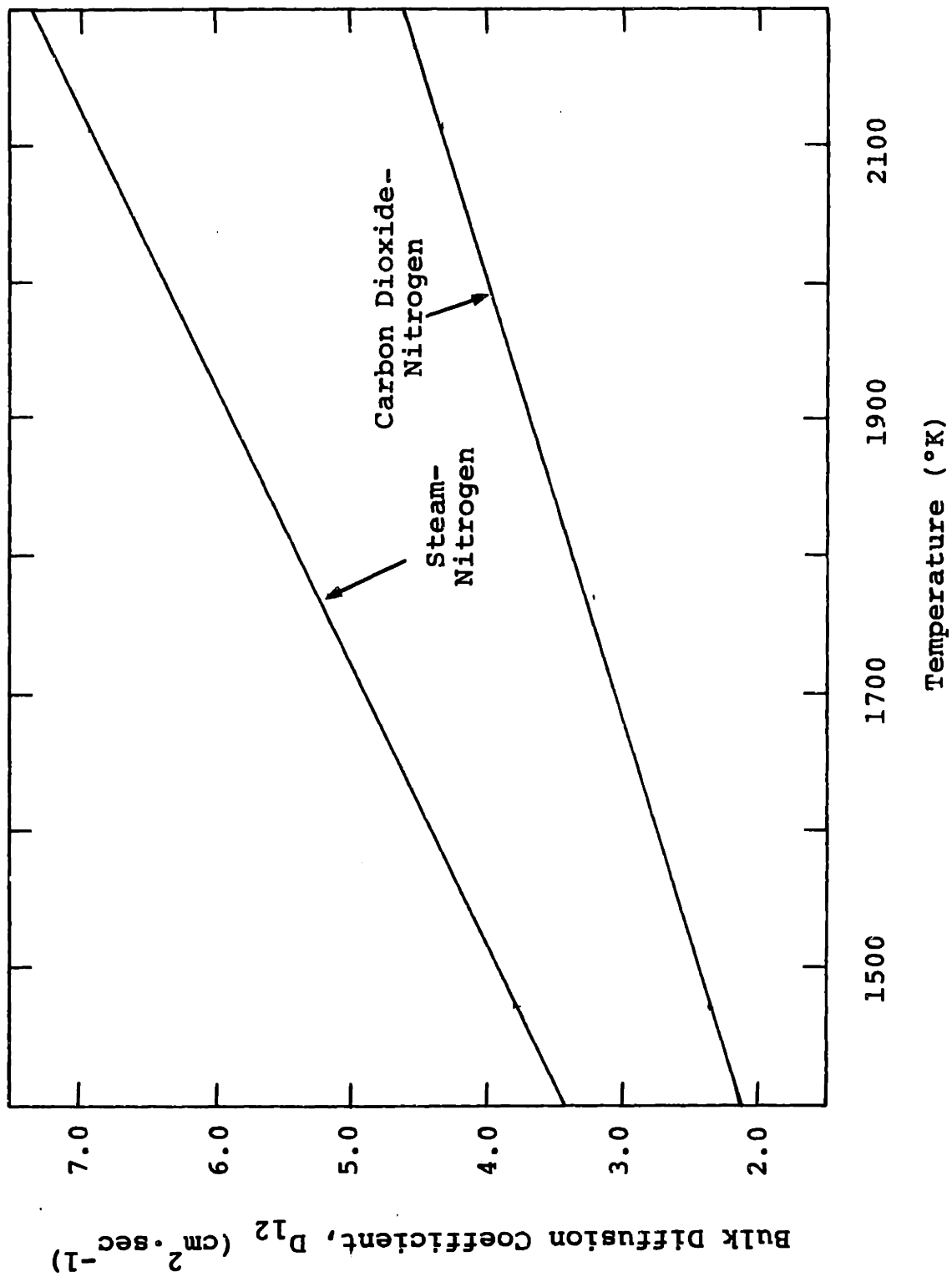


Figure H.1 Bulk Diffusion Coefficients  
For  $\text{CO}_2\text{-N}_2$  and  $\text{H}_2\text{O-N}_2$  Mixtures

Satterfield<sup>67</sup> suggests that for  $\epsilon_{12}/\kappa > 100$ ,  $D_{12}$  can be represented by a power law function of temperature, the exponent being approximately 1.65:

$$D_{12} = d T^m \quad (\text{H.2})$$

$$m \approx 1.65 \quad (\text{H.3})$$

The constants which best fit the data of Figure H.1 to equation (H.2) are:

	<u>m</u>	<u><math>d \times 10^5</math> (<math>\text{cm}^2 \text{ sec}^{-1} \text{ }^\circ\text{K}^{-m}</math>)</u>
$\text{CO}_2 - \text{N}_2$	1.67	1.241
$\text{H}_2\text{O} - \text{N}_2$	1.67	1.993

Appendix I  
PORE DIFFUSIVITIES <sup>16</sup>

Two mechanisms may characterize diffusion of gas molecules through particle pores. (Surface diffusion is neglected.)

Molecular, or bulk diffusion dominates if the pore radius is large relative to the molecular mean free path. Mass transport is determined by intermolecular collisions rather than interactions between the pore walls and diffusing molecules. The effective diffusivity for bulk diffusion is:

$$D_{12,eff} = \frac{\xi D_{12}}{\tau} \quad (I.1)$$

where  $\xi$  is the particle fractional porosity,  $\tau$  is the tortuosity factor and  $D_{12}$  is the bulk diffusion coefficient (Appendix H).

If the pore radius is small relative to the mean free path, Knudsen diffusion controls intraphase mass transport. Diffusion is determined mainly by collisions between the diffusing molecules and the pore walls. For Knudsen diffusion:

$$D_{K,eff} = \frac{\xi D_K}{\tau} \quad (I.2)$$

where  $D_K$  is the Knudsen diffusion coefficient:

$$D_K = 9700 r_p (T/M)^{1/2} \quad (I.3)$$

In equation (I.3),  $r_p$  is the pore radius (cm),  $T$  is the absolute particle temperature ( $^{\circ}$ K) and  $M$  is the molecular

weight of the diffusing species. An average pore radius may be calculated in terms of particle surface area and porosity:

$$\bar{r}_p = \frac{2\xi}{S_g \rho_p} \quad (\text{I.4})$$

Thus, the effective diffusivity becomes:

$$D_{K,eff} = 19,400 \frac{\xi^2}{\tau S_g \rho_p} (T/M)^{\frac{1}{2}} \text{ cm}^2/\text{sec} \quad (\text{I.5})$$

where  $S_g$  is in square centimeters per gram and  $\rho_p$  is in grams per cubic centimeter.

In the transition range between bulk diffusion control and Knudsen diffusion control, an effective diffusivity may be estimated as:

$$\frac{1}{D_{eff}} = \frac{1}{D_{12,eff}} + \frac{1}{D_{K,eff}} \quad (\text{I.6})$$

Effective diffusivities are calculated by equation (I.6) at each of the conditions listed in Tables 4.5 and 4.6. The following values are used:

$$\begin{aligned} \tau &= 2^{\frac{1}{2}} \\ \xi &= 0.72 \text{ (initial char)} \\ \rho_p &= 0.49 \text{ g/cm}^3 \text{ (initial char)} \\ M &= \begin{cases} 44 & \text{carbon dioxide} \\ 18 & \text{steam} \end{cases} \end{aligned}$$

Surface area data are discussed in section 4.3. Values for  $D_{12}$  are calculated by equation (H.2) and the data in Appendix H. Effective pore diffusivities are listed in Tables I.1 and I.2.

Table I.1

Pore Diffusion Coefficients  
For Char - Carbon Dioxide Systems

$T_O$ (°K)	$P_C$ (atm)	$T_S$ (°K)	$S_g$ (m <sup>2</sup> /g)	$D_{12}$	$D_{12,eff}$	$D_{K,eff}$	$D_{eff}$
1473	0.26	1441	230	2.27	1.15	0.0358	0.0347
1473	0.53	1434	230	2.25	1.14	0.0357	0.0346
1773	0.26	1684	175	2.94	1.49	0.0508	0.0492
1773	0.60	1661	175	2.88	1.46	0.0505	0.0488
2113	0.26	1935	135	3.71	1.88	0.0706	0.0681
2113	0.57	1880	135	3.54	1.79	0.0696	0.0670

Table I.2

Pore Diffusion Coefficients for Char - Steam Systems

$T_O$ (°K)	$P_W$ (atm)	$T_S$ (°K)	$S_g$ (m <sup>2</sup> /g)	Diffusion Coefficients (cm <sup>2</sup> /sec)			
				$D_{12}$	$D_{12,eff}$	$D_{K,eff}$	$D_{eff}$
1473	0.33	1440	300	3.75	1.90	0.0429	0.0419
1473	0.65	1407	300	3.61	1.83	0.0424	0.0414
1773	0.32	1679	220	4.85	2.46	0.0631	0.0616
1773	0.65	1546	220	4.22	2.14	0.0606	0.0589
2113	0.32	1910	135	6.01	3.05	0.110	0.106
2113	0.65	1845	135	5.67	2.87	0.108	0.104

Appendix J

PARTICLE TERMINAL VELOCITY

For a single, independent spherical particle falling in a gas, the terminal velocity (steady state velocity relative to the gas) is given by:<sup>8,61</sup>

$$\begin{aligned} u_{\text{term}} &= u_p - u_g \\ &= \left[ \frac{4 g d_p (\rho_p - \rho)}{3 \rho f} \right]^{\frac{1}{2}} \end{aligned} \quad (\text{J.1})$$

where  $d_p$  is the particle diameter,  $\rho_p$  is the particle bulk density,  $\rho$  is the gas density,  $g$  is the gravitational acceleration constant and  $f$  is the Fanning friction factor. If the particle Reynolds number based on  $u_{\text{term}}$  ( $Re_p = \rho u_{\text{term}} d_p / \mu$ , where  $\mu$  is the gas viscosity) indicates Stokes' Law flow ( $Re_p < 0.3$ ), then:

$$f \approx 24 / Re_p \quad (\text{J.2})$$

and

$$u_{\text{term}} = \frac{g d_p^2 (\rho_p - \rho)}{18 \mu} \quad (\text{J.3})$$

Hence,  $u_{\text{term}}$  is independent of the gas velocity.

Assuming values for  $d_p$  and  $\rho_p$ ,

$$d_p = 100 \mu\text{m} = 0.01 \text{ cm}$$

$$\rho_p = 0.43 \text{ g/cm}^3 \quad (\text{see Appendix N})$$

a particle terminal velocity can be calculated at each of the

experimental nominal temperatures, for each of the main gas compositions. Viscosity data are taken from Figure E.2, and gas densities are calculated using equation (F.2). Calculated values of  $u_{\text{term}}$  are listed in Table J.1. A check of the values in Table J.1 shows that use of equation (J.2) is justified.

To estimate the time ( $t^*$ ) required for a char particle to reach its terminal velocity, consider a force balance on a single, independent particle leaving the feeder tube:

$$\left[ \frac{\pi}{6} d_p^3 \rho_p \right] \frac{d}{dt} u_p = \left\{ \frac{\pi}{6} d_p^3 g (\rho_p - \rho) \right\} - \left\{ \frac{\pi}{8} d_p^2 \rho (u_p - u_g)^2 \delta \right\} \quad (\text{J.4})$$

where  $u_p$  is the particle velocity and  $u_g$  is the gas velocity. If  $t^*$  is small, then  $u_g \approx u_{g,\text{avg}}$ , the average gas velocity, for all  $t < t^*$ , so

$$\frac{d}{dt} u_p \approx \frac{d}{dt} (u_p - u_{g,\text{avg}}) \quad (\text{J.5})$$

Using equations (J.2) and (J.5), equation (J.4) can be rewritten as:

$$\frac{d}{dt} (u_p - u_{g,\text{avg}}) = g \left\{ \frac{\rho_p - \rho}{\rho_p} \right\} - \left\{ \frac{18 (u_p - u_{g,\text{avg}})^2 \mu}{d_p^2 \rho_p} \right\} \quad (\text{J.6})$$

Defining:

$$\Delta u = u_p - u_{g,\text{avg}} \quad (\text{J.7})$$

$$a = \left[ \frac{\rho_p - \rho}{\rho_p} \right] g \quad (\text{J.8})$$

and

$$b = \frac{18 \mu}{d_p^2 \rho_p} \quad (\text{J.9})$$



Table J.1  
Char Particle Terminal Velocities

Main Gas Composition	$u_{\text{term}}$ (cm/sec)		
	1473°K	1773°K	2113°K
CO <sub>2</sub> Gasification:			
$P_{\text{CO}_2} = 0.26 \text{ atm}$	4.49	4.01	3.62
$P_{\text{CO}_2} = 0.60 \text{ atm}$	4.39	3.90	3.50
H <sub>2</sub> O Gasification:			
$P_{\text{H}_2\text{O}} = 0.34 \text{ atm}$	4.72	4.21	3.80
$P_{\text{H}_2\text{O}} = 0.65 \text{ atm}$	4.97	4.39	3.91

equation (J.6) is rewritten as:

$$\frac{d}{dt} (\Delta u) + b(\Delta u) = a \quad (J.10)$$

The initial condition required to solve equation (J.10) is:

$$(\Delta u)_{t=0} \approx u_{\text{carr}} - u_{g,\text{avg}} = \Delta u_0 \quad (J.11)$$

where  $u_{\text{carr}}$  is the char feeder carrier gas average velocity at 298°K. The solution to (J.10) and (J.11) is:

$$\Delta u(t) = \frac{a}{b} + (\Delta u_0 - \frac{a}{b}) \cdot e^{-bt} \quad (J.12)$$

Obviously, for  $t \rightarrow \infty$ ,  $\Delta u \rightarrow \frac{a}{b} = u_{\text{term}}$  (see equation (J.3)).

For estimating  $t^*$ , assume that the main gas flow rate is set at 6 l/min STP (100 cm<sup>3</sup>/sec STP), from which values of  $u_{g,\text{avg}}$  may be calculated at each value of  $T_0$  (the reactor tube has a 1.0 inch I.D.):

<u><math>T_0</math> (°K)</u>	<u><math>u_{g,\text{avg}}</math> (cm/sec)</u>
1473	24
1773	29
2113	35

Also, the carrier gas flow rate is approximately 22 cm<sup>3</sup>/min, or 0.37 cm<sup>3</sup>/sec STP, so the carrier gas velocity at 298°K is (the feeder tube has a 1/16 inch I.D.) approximately 19 cm/sec. Defining  $t^*$  as the time required for 95 percent of the velocity changes to occur in:

$$\frac{\Delta u_0 - \Delta u(t^*)}{\Delta u_0 - u_{\text{term}}} = 0.95 \quad (J.13)$$

and, using equation (J.12):

$$0.95 = 1.0 - e^{-bt^*} \quad (\text{J.14})$$

so

$$t^* = -\frac{1}{b} \ln(0.05) \approx \frac{3}{b} = \frac{d_p^2 \rho_p}{6\mu} \quad (\text{J.15})$$

Using average values of  $\mu$  at each  $T_o$ ,  $t^*$  is estimated to be between 11 and 15 msec, or about 10 percent of the shortest experimental residence time at each temperature.

Appendix K

ASH CONTENT OF THE INITIAL CHAR

Using the procedure described in section 2.4, the ash content of the initial char was determined to be 20.5 percent by weight. The test results (Table K.1) are averaged by weight to obtain this value:

$$f_{\text{ash}}^{\circ} \cdot 100\% = \frac{\sum_{i=1}^6 W_i \% \text{ash}_i}{\sum_{i=1}^6 W_i} \quad (\text{K.1})$$

where  $W_i$  is the initial weight of char sample  $i$  in Table K.1,  $\% \text{ash}_i$  is its ash content, and  $f_{\text{ash}}^{\circ}$  is the calculated ash content of the initial char.

Table K.1

Results of Ash Determination Tests

<u>Test Number</u>	<u>Initial Weight (g)</u>	<u>Final Weight (g)</u>	<u>Ash Content (wt%)</u>
1.	0.4412	0.1048	23.75
2.	0.4785	0.1258	26.29
3.	0.3832	0.0821	21.61
4.	0.5689	0.1061	18.65
5.	0.8315	0.1516	18.23
6.	0.5721	0.1017	17.78

Appendix L

FITTING DATA TO LINEAR EQUATIONS BY  
THE METHOD OF LEAST SQUARES

Consider  $m$  sets of data:

$$y_i; \quad x_{i2}, x_{i3}, \dots, x_{ik} \quad (i=1, 2, \dots, m) \quad (L.1)$$

where  $x_{ij}$  are independent variables and  $y_i$  is the dependent (observed) variable. Draper and Smith<sup>18</sup> and Perry and Chilton<sup>61</sup> present the method of least squares to fit sets of data of the form (L.1) to the linear equation:

$$\hat{y}_i = B_1 + \sum_{j=2}^k B_j x_{ij} \quad (L.2)$$

where the parameters  $B_j$  are chosen to minimize S.S., the sum of the squares of the residuals,  $\epsilon_i$  (the differences between the observed values  $y_i$ , and the values predicted by equation (L.2),  $\hat{y}_i$ ):

$$\begin{aligned} \text{S.S.} &= \sum_{i=1}^m \epsilon_i^2 \\ &= \sum_{i=1}^m (y_i - \hat{y}_i)^2 \\ &= \sum_{i=1}^m (y_i - B_1 - \sum_{j=2}^k B_j x_{ij})^2 \end{aligned} \quad (L.3)$$

Using matrix notation, all data of the form (L.2) can be written as:

$$\vec{Y} = [X] \vec{B} + \vec{\epsilon} \quad (\text{L.4})$$

where  $\vec{Y}$  is the column vector containing elements  $y_i$  ( $i=1,2,\dots,m$ ),  $\vec{B}$  is the column vector containing elements  $B_j$  ( $j=1,2,\dots,k$ ),  $[X]$  is the independent variable matrix (dimensions  $m$  by  $k$ , with  $x_{i1} = 1$  for all  $i$ ) and  $\vec{\epsilon}$  is the column vector of residuals,  $\epsilon_i$ . To determine  $\vec{B}$ , consider the partial derivative of equation (L.3) with respect to  $B_n$ :

$$\frac{\partial}{\partial b_n} (\text{s.s.}) = 2 \left\{ \sum_{j=1}^k [B_j \sum_{i=1}^m (x_{ij} x_{in})] - \sum_{i=1}^m (y_i x_{in}) \right\} \quad (\text{L.5})$$

Setting the right side of equation (L.5) equal to zero, and repeating for  $n$  equal to each value of  $j$  ( $j=1,2,\dots,k$ ) results in a system of  $k$  linear equations in the undetermined parameters  $B_j$  ( $j=1,2,\dots,k$ ), which in matrix form is:

$$[X^{\dagger}X] \vec{B} = [X^{\dagger}Y] \quad (\text{L.6})$$

where  $[X^{\dagger}]$  is the matrix transpose of  $[X]$ ,  $[X^{\dagger}X]$  is the matrix product of  $[X^{\dagger}]$  and  $[X]$ , and  $[X^{\dagger}Y]$  is the matrix product of  $[X^{\dagger}]$  and  $\vec{Y}$ . The solution for the parameter vector is obtained by multiplying both sides of equation (L.6) by the inverse matrix of  $[X^{\dagger}X]$ :

$$\vec{B} = [X^{\dagger}X]^{-1} \cdot [X^{\dagger}Y] \quad (\text{L.7})$$

It can be shown that the sum of the residuals  $\epsilon_i$  equals zero:

$$\sum_{i=1}^m \epsilon_i = \sum_{i=1}^m (y_i - \hat{y}_i) = 0 \quad (\text{L.8})$$

Appendix M

EVALUATION OF  $I(T_o, \bar{E}, \bar{n}, L)$

The integral  $I(T_o, \bar{E}, \bar{n}, L)$ , used in calculation of apparent gasification rates, is given by:

$$I(T_o, \bar{E}, \bar{n}, L) = \int_{L_1}^L \frac{\theta_w^{-\bar{n}} \cdot [\exp(-\bar{E}_o/\theta_w)]}{[\theta_w \cdot u_{g,avg} \cdot u_g^*(0, z, 1)] + u_{term}} dz \quad (4.15)$$

The right side of equation (4.15) is evaluated numerically using Simpson's approximation for integration. Computer program INTEG (Appendix O) is used. The results are shown in Table M.1 and Table M.2.

It is found that  $I(T_o, \bar{E}, \bar{n}, L)$  may be linearized in the form:

$$\ln [I(T_o, \bar{E}, \bar{n}, L)] = I_1 \bar{E} + I_3 \bar{n} + I_4 \quad (4.17)$$

where  $I_1$ ,  $I_3$  and  $I_4$  are functions of  $T_o$ ,  $L$  and the main gas composition. Computer program LNI (Appendix O) is used to determine the linearization constants of equation (4.17), via the methods of Appendix I. These values are listed in Table M.3.



Table M.1

Numerical Integration of  $I(T_0, \bar{E}, \bar{n}, L)$  for CO<sub>2</sub> Gasification Experiments

( $\bar{E} = 0$  kcal/mole)

REACTION		CARBON DIOXIDE		REACTION		CARBON DIOXIDE		
NOM. TEMP.	1473. DEG K	NOM. TEMP.	1773. DEG K	NOM. TEMP.	1773. DEG K	NOM. TEMP.	2113. DEG K	
NOM. PRES.	0.26 ATM	NOM. PRES.	0.26 ATM	NOM. PRES.	0.26 ATM	NOM. PRES.	0.26 ATM	
KINEM. VISC.	2.00 SQ CM / SEC	KINEM. VISC.	2.69 SQ CM / SEC	KINEM. VISC.	2.69 SQ CM / SEC	KINEM. VISC.	3.55 SQ CM / SEC	
MAIN AVG. VEL.	26.22 CM/SEC	MAIN AVG. VEL.	31.33 CM/SEC	MAIN AVG. VEL.	31.33 CM/SEC	MAIN AVG. VEL.	36.85 CM/SEC	
TERM. VEL.	4.49 CM/SEC	TERM. VEL.	4.01 CM/SEC	TERM. VEL.	4.01 CM/SEC	TERM. VEL.	3.62 CM/SEC	
ACTIV. ENERGY	0 KCAL	ACTIV. ENERGY	0 KCAL	ACTIV. ENERGY	0 KCAL	ACTIV. ENERGY	0 KCAL	
EPSILON	0.000	EPSILON	0.000	EPSILON	0.000	EPSILON	0.000	
$\bar{N}$	INT(L2)	INT(L3)	INT(L2)	INT(L3)	INT(L2)	INT(L3)	INT(L2)	INT(L3)
0.00	7.39985E-02	1.51522E-01	6.26732E-02	1.26659E-01	0.00	5.36231E-02	9.57273E-02	1.10324E-01
0.25	7.49608E-02	1.55127E-01	6.34886E-02	1.31695E-01	0.25	5.43210E-02	9.64524E-02	1.12933E-01
0.50	7.59370E-02	1.58810E-01	6.43196E-02	1.34823E-01	0.50	5.50289E-02	9.71878E-02	1.15621E-01
0.75	7.69271E-02	1.62602E-01	6.51545E-02	1.38049E-01	0.75	5.57469E-02	9.79338E-02	1.18389E-01
1.00	7.79314E-02	1.66509E-01	6.60054E-02	1.41370E-01	1.00	5.64753E-02	9.86905E-02	1.21241E-01
1.25	7.89501E-02	1.70534E-01	6.68686E-02	1.44792E-01	1.25	5.72140E-02	9.94580E-02	1.24179E-01
1.50	7.99835E-02	1.74682E-01	6.77441E-02	1.48318E-01	1.50	5.79635E-02	1.02366E-02	1.27207E-01
1.75	8.10317E-02	1.78956E-01	6.86322E-02	1.51952E-01	1.75	5.87237E-02	1.05264E-02	1.30328E-01
2.00	8.20950E-02	1.83362E-01	6.95332E-02	1.55698E-01	2.00	5.94948E-02	1.08275E-02	1.33545E-01
<hr/>								
REACTION		CARBON DIOXIDE		REACTION		CARBON DIOXIDE		
NOM. TEMP.	1473. DEG K	NOM. TEMP.	1773. DEG K	NOM. TEMP.	1773. DEG K	NOM. TEMP.	2113. DEG K	
NOM. PRES.	0.60 ATM	NOM. PRES.	0.60 ATM	NOM. PRES.	0.60 ATM	NOM. PRES.	0.60 ATM	
KINEM. VISC.	1.74 SQ CM / SEC	KINEM. VISC.	2.36 SQ CM / SEC	KINEM. VISC.	2.36 SQ CM / SEC	KINEM. VISC.	3.12 SQ CM / SEC	
MAIN AVG. VEL.	26.75 CM/SEC	MAIN AVG. VEL.	30.20 CM/SEC	MAIN AVG. VEL.	30.20 CM/SEC	MAIN AVG. VEL.	35.74 CM/SEC	
TERM. VEL.	4.39 CM/SEC	TERM. VEL.	3.90 CM/SEC	TERM. VEL.	3.90 CM/SEC	TERM. VEL.	3.50 CM/SEC	
ACTIV. ENERGY	0 KCAL	ACTIV. ENERGY	0 KCAL	ACTIV. ENERGY	0 KCAL	ACTIV. ENERGY	0 KCAL	
EPSILON	0.000	EPSILON	0.000	EPSILON	0.000	EPSILON	0.000	
$\bar{N}$	INT(L2)	INT(L3)	INT(L2)	INT(L3)	INT(L2)	INT(L3)	INT(L2)	INT(L3)
0.00	7.39056E-02	1.51059E-01	6.35102E-02	1.34288E-01	0.00	5.57273E-02	9.57273E-02	1.14476E-01
0.25	7.48665E-02	1.54619E-01	6.43623E-02	1.37458E-01	0.25	5.64524E-02	9.64524E-02	1.17181E-01
0.50	7.58419E-02	1.58289E-01	6.52226E-02	1.40722E-01	0.50	5.71878E-02	9.71878E-02	1.19967E-01
0.75	7.68295E-02	1.62050E-01	6.61031E-02	1.44084E-01	0.75	5.79338E-02	9.79338E-02	1.22837E-01
1.00	7.78322E-02	1.65950E-01	6.69923E-02	1.47548E-01	1.00	5.86905E-02	9.86905E-02	1.25794E-01
1.25	7.88493E-02	1.69957E-01	6.78943E-02	1.51117E-01	1.25	5.94580E-02	9.94580E-02	1.28840E-01
1.50	7.98810E-02	1.74086E-01	6.88092E-02	1.54796E-01	1.50	6.02366E-02	1.02366E-02	1.31979E-01
1.75	8.09275E-02	1.78341E-01	6.97373E-02	1.58584E-01	1.75	6.10264E-02	1.05264E-02	1.35214E-01
2.00	8.19891E-02	1.82727E-01	7.06787E-02	1.62490E-01	2.00	6.18275E-02	1.08275E-02	1.38549E-01

Table M.1 continued ( $\bar{E} = 10$  kcal/mole)

REACTION		CARBON DIOXIDE		REACTION		CARBON DIOXIDE		REACTION		CARBON DIOXIDE	
NOM. TEMP.	1473. DEG K	NOM. TEMP.	1773. DEG K	NOM. TEMP.	1773. DEG K	NOM. TEMP.	1773. DEG K	NOM. TEMP.	2113. DEG K	NOM. TEMP.	2113. DEG K
NOM. PRES.	0.26 ATM	NOM. PRES.	0.26 ATM	NOM. PRES.	0.26 ATM	NOM. PRES.	0.26 ATM	NOM. PRES.	0.26 ATM	NOM. PRES.	0.26 ATM
KINEM. VISC.	2.00 SQ CM / SEC	KINEM. VISC.	2.69 SQ CM / SEC	KINEM. VISC.	2.69 SQ CM / SEC	KINEM. VISC.	2.69 SQ CM / SEC	KINEM. VISC.	3.55 SQ CM / SEC	KINEM. VISC.	3.55 SQ CM / SEC
MAIN AVG. VEL.	26.22 CM/SEC	MAIN AVG. VEL.	31.33 CM/SEC	MAIN AVG. VEL.	31.33 CM/SEC	MAIN AVG. VEL.	31.33 CM/SEC	MAIN AVG. VEL.	36.85 CM/SEC	MAIN AVG. VEL.	36.85 CM/SEC
TERM. VEL.	4.49 CM/SEC	TERM. VEL.	4.01 CM/SEC	TERM. VEL.	4.01 CM/SEC	TERM. VEL.	4.01 CM/SEC	TERM. VEL.	3.62 CM/SEC	TERM. VEL.	3.62 CM/SEC
ACTIV. ENERGY	10 KCAL	ACTIV. ENERGY	10 KCAL	ACTIV. ENERGY	10 KCAL	ACTIV. ENERGY	10 KCAL	ACTIV. ENERGY	10 KCAL	ACTIV. ENERGY	10 KCAL
EPSILON	3.416	EPSILON	2.838	EPSILON	2.838	EPSILON	2.838	EPSILON	2.381	EPSILON	2.381
$\bar{N}$	INT(L2)	INT(L3)	INT(L2)	INT(L3)	INT(L2)	INT(L3)	INT(L2)	INT(L3)	INT(L2)	INT(L3)	INT(L3)
0.00	2.02894E-03	3.66676E-03	3.19712E-03	5.74887E-03	3.19712E-03	5.74887E-03	3.19712E-03	5.74887E-03	4.36814E-03	8.11462E-03	8.11462E-03
0.25	2.05484E-03	3.68430E-03	3.19756E-03	5.87457E-03	3.19756E-03	5.87457E-03	3.19756E-03	5.87457E-03	4.42426E-03	8.29450E-03	8.29450E-03
0.50	2.08111E-03	3.76398E-03	3.23858E-03	6.00382E-03	3.23858E-03	6.00382E-03	3.23858E-03	6.00382E-03	4.48118E-03	8.47950E-03	8.47950E-03
0.75	2.10774E-03	3.84589E-03	3.28018E-03	6.13672E-03	3.28018E-03	6.13672E-03	3.28018E-03	6.13672E-03	4.53891E-03	8.66980E-03	8.66980E-03
1.00	2.13474E-03	3.93010E-03	3.32237E-03	6.27339E-03	3.32237E-03	6.27339E-03	3.32237E-03	6.27339E-03	4.59745E-03	8.86556E-03	8.86556E-03
1.25	2.16215E-03	4.01668E-03	3.36515E-03	6.41398E-03	3.36515E-03	6.41398E-03	3.36515E-03	6.41398E-03	4.65682E-03	9.06698E-03	9.06698E-03
1.50	2.18993E-03	4.10571E-03	3.40854E-03	6.55860E-03	3.40854E-03	6.55860E-03	3.40854E-03	6.55860E-03	4.71704E-03	9.27424E-03	9.27424E-03
1.75	2.21811E-03	4.19728E-03	3.45255E-03	6.70739E-03	3.45255E-03	6.70739E-03	3.45255E-03	6.70739E-03	4.77811E-03	9.48755E-03	9.48755E-03
2.00	2.24668E-03	4.29147E-03	3.49718E-03	6.86050E-03	3.49718E-03	6.86050E-03	3.49718E-03	6.86050E-03	4.84006E-03	9.70711E-03	9.70711E-03
-----											
REACTION	CARBON DIOXIDE		REACTION	CARBON DIOXIDE		REACTION	CARBON DIOXIDE		REACTION	CARBON DIOXIDE	
NOM. TEMP.	1473. DEG K	1473. DEG K	NOM. TEMP.	1773. DEG K	1773. DEG K	NOM. TEMP.	1773. DEG K	NOM. TEMP.	2113. DEG K	NOM. TEMP.	2113. DEG K
NOM. PRES.	0.60 ATM	0.60 ATM	NOM. PRES.	0.60 ATM	0.60 ATM	NOM. PRES.	0.60 ATM	NOM. PRES.	0.60 ATM	NOM. PRES.	0.60 ATM
KINEM. VISC.	1.74 SQ CM / SEC	1.74 SQ CM / SEC	KINEM. VISC.	2.36 SQ CM / SEC	2.36 SQ CM / SEC	KINEM. VISC.	2.36 SQ CM / SEC	KINEM. VISC.	3.12 SQ CM / SEC	KINEM. VISC.	3.12 SQ CM / SEC
MAIN AVG. VEL.	26.75 CM/SEC	26.75 CM/SEC	MAIN AVG. VEL.	30.20 CM/SEC	30.20 CM/SEC	MAIN AVG. VEL.	30.20 CM/SEC	MAIN AVG. VEL.	35.74 CM/SEC	MAIN AVG. VEL.	35.74 CM/SEC
TERM. VEL.	4.39 CM/SEC	4.39 CM/SEC	TERM. VEL.	3.90 CM/SEC	3.90 CM/SEC	TERM. VEL.	3.90 CM/SEC	TERM. VEL.	3.50 CM/SEC	TERM. VEL.	3.50 CM/SEC
ACTIV. ENERGY	10 KCAL	10 KCAL	ACTIV. ENERGY	10 KCAL	10 KCAL	ACTIV. ENERGY	10 KCAL	ACTIV. ENERGY	10 KCAL	ACTIV. ENERGY	10 KCAL
EPSILON	3.416	3.416	EPSILON	2.838	2.838	EPSILON	2.838	EPSILON	2.381	EPSILON	2.381
$\bar{N}$	INT(L2)	INT(L3)	$\bar{N}$	INT(L2)	INT(L3)	$\bar{N}$	INT(L2)	INT(L3)	$\bar{N}$	INT(L2)	INT(L3)
0.00	2.02652E-03	3.59641E-03	0.00	3.30016E-03	6.00192E-03	0.00	3.30016E-03	6.00192E-03	0.00	4.53975E-03	8.42176E-03
0.25	2.05239E-03	3.67363E-03	0.25	3.34243E-03	6.13305E-03	0.25	3.34243E-03	6.13305E-03	0.25	4.59804E-03	8.60828E-03
0.50	2.07861E-03	3.75299E-03	0.50	3.38530E-03	6.26787E-03	0.50	3.38530E-03	6.26787E-03	0.50	4.65718E-03	8.80011E-03
0.75	2.10521E-03	3.83457E-03	0.75	3.42877E-03	6.40650E-03	0.75	3.42877E-03	6.40650E-03	0.75	4.71715E-03	8.99743E-03
1.00	2.13218E-03	3.91843E-03	1.00	3.47285E-03	6.54907E-03	1.00	3.47285E-03	6.54907E-03	1.00	4.77797E-03	9.20041E-03
1.25	2.15953E-03	4.00466E-03	1.25	3.51756E-03	6.69371E-03	1.25	3.51756E-03	6.69371E-03	1.25	4.83963E-03	9.40925E-03
1.50	2.18727E-03	4.09332E-03	1.50	3.56291E-03	6.84656E-03	1.50	3.56291E-03	6.84656E-03	1.50	4.90222E-03	9.62415E-03
1.75	2.21540E-03	4.18430E-03	1.75	3.60889E-03	7.00175E-03	1.75	3.60889E-03	7.00175E-03	1.75	4.96567E-03	9.84531E-03
2.00	2.24393E-03	4.27830E-03	2.00	3.65553E-03	7.16145E-03	2.00	3.65553E-03	7.16145E-03	2.00	5.03002E-03	1.00729E-02

Table M.1 continued ( $\bar{E} = 20 \text{ kcal/mole}$ )

REACTION		CARBON DIOXIDE		REACTION		CARBON DIOXIDE		REACTION		CARBON DIOXIDE	
N	INT(L2)	INT(L3)	N	INT(L2)	INT(L3)	N	INT(L2)	INT(L3)	N	INT(L2)	INT(L3)
0.00	5.58180E-05	8.8924E-05	0.00	1.59408E-04	2.62231E-04	0.00	3.556414E-04	6.05716E-04	0.00	3.556414E-04	6.05716E-04
0.25	5.65176E-05	9.01174E-05	0.25	1.61419E-04	2.67544E-04	0.25	3.60935E-04	6.18307E-04	0.25	3.60935E-04	6.18307E-04
0.50	5.72268E-05	9.18968E-05	0.50	1.63458E-04	2.72998E-04	0.50	3.65519E-04	6.31237E-04	0.50	3.65519E-04	6.31237E-04
0.75	5.79459E-05	9.37222E-05	0.75	1.65526E-04	2.78596E-04	0.75	3.70167E-04	6.44519E-04	0.75	3.70167E-04	6.44519E-04
1.00	5.86749E-05	9.55950E-05	1.00	1.67622E-04	2.84344E-04	1.00	3.74880E-04	6.58163E-04	1.00	3.74880E-04	6.58163E-04
1.25	5.94141E-05	9.75166E-05	1.25	1.69748E-04	2.90245E-04	1.25	3.79659E-04	6.72181E-04	1.25	3.79659E-04	6.72181E-04
1.50	6.01639E-05	9.94866E-05	1.50	1.71903E-04	2.96306E-04	1.50	3.84506E-04	6.86585E-04	1.50	3.84506E-04	6.86585E-04
1.75	6.09233E-05	1.01512E-04	1.75	1.74089E-04	3.02531E-04	1.75	3.89420E-04	7.01387E-04	1.75	3.89420E-04	7.01387E-04
2.00	6.16938E-05	1.03590E-04	2.00	1.76305E-04	3.08926E-04	2.00	3.94404E-04	7.16603E-04	2.00	3.94404E-04	7.16603E-04
-----											
REACTION		CARBON DIOXIDE		REACTION		CARBON DIOXIDE		REACTION		CARBON DIOXIDE	
N	INT(L2)	INT(L3)	N	INT(L2)	INT(L3)	N	INT(L2)	INT(L3)	N	INT(L2)	INT(L3)
0.00	5.57551E-05	8.81597E-05	0.00	1.66637E-04	2.75832E-04	0.00	3.70430E-04	6.28767E-04	0.00	3.70430E-04	6.28767E-04
0.25	5.64537E-05	8.98883E-05	0.25	1.68739E-04	2.79376E-04	0.25	3.75127E-04	6.41825E-04	0.25	3.75127E-04	6.41825E-04
0.50	5.71619E-05	9.16612E-05	0.50	1.70870E-04	2.85066E-04	0.50	3.79889E-04	6.55235E-04	0.50	3.79889E-04	6.55235E-04
0.75	5.78799E-05	9.34798E-05	0.75	1.73031E-04	2.90907E-04	0.75	3.84718E-04	6.69010E-04	0.75	3.84718E-04	6.69010E-04
1.00	5.86078E-05	9.53453E-05	1.00	1.75222E-04	2.96903E-04	1.00	3.89615E-04	6.83159E-04	1.00	3.89615E-04	6.83159E-04
1.25	5.93459E-05	9.72599E-05	1.25	1.77443E-04	3.03061E-04	1.25	3.94561E-04	6.97697E-04	1.25	3.94561E-04	6.97697E-04
1.50	6.00942E-05	9.92244E-05	1.50	1.79695E-04	3.09384E-04	1.50	3.99616E-04	7.12634E-04	1.50	3.99616E-04	7.12634E-04
1.75	6.08529E-05	1.01240E-04	1.75	1.81979E-04	3.15878E-04	1.75	4.04723E-04	7.27984E-04	1.75	4.04723E-04	7.27984E-04
2.00	6.16222E-05	1.03310E-04	2.00	1.84295E-04	3.22550E-04	2.00	4.09901E-04	7.43762E-04	2.00	4.09901E-04	7.43762E-04

Table M.1 continued ( $\bar{E} = 30$  kcal/mole)

REACTION		CARBON DIOXIDE		REACTION		CARBON DIOXIDE		REACTION		CARBON DIOXIDE	
N	INT(L2)	INT(L3)	N	INT(L2)	INT(L3)	N	INT(L2)	INT(L3)	N	INT(L2)	INT(L3)
0.00	1.54066E-06	2.22197E-06	0.00	8.06744E-06	1.21859E-05	0.00	2.91285E-05	4.58318E-05	0.00	2.91285E-05	4.58318E-05
0.25	1.55962E-06	2.26199E-06	0.25	8.16747E-06	1.24153E-05	0.25	2.94932E-05	4.67265E-05	0.25	2.94932E-05	4.67265E-05
0.50	1.57883E-06	2.30296E-06	0.50	8.26907E-06	1.26504E-05	0.50	2.98629E-05	4.76442E-05	0.50	2.98629E-05	4.76442E-05
0.75	1.59831E-06	2.34491E-06	0.75	8.37207E-06	1.28913E-05	0.75	3.02378E-05	4.85853E-05	0.75	3.02378E-05	4.85853E-05
1.00	1.61805E-06	2.38786E-06	1.00	8.47649E-06	1.31382E-05	1.00	3.06179E-05	4.95508E-05	1.00	3.06179E-05	4.95508E-05
1.25	1.63806E-06	2.43184E-06	1.25	8.58235E-06	1.33914E-05	1.25	3.10033E-05	5.05414E-05	1.25	3.10033E-05	5.05414E-05
1.50	1.65835E-06	2.47689E-06	1.50	8.68966E-06	1.36509E-05	1.50	3.13939E-05	5.15577E-05	1.50	3.13939E-05	5.15577E-05
1.75	1.67891E-06	2.52303E-06	1.75	8.79846E-06	1.39170E-05	1.75	3.17901E-05	5.26007E-05	1.75	3.17901E-05	5.26007E-05
2.00	1.69975E-06	2.57029E-06	2.00	8.90875E-06	1.41899E-05	2.00	3.21917E-05	5.36713E-05	2.00	3.21917E-05	5.36713E-05
-----											
REACTION		CARBON DIOXIDE		REACTION		CARBON DIOXIDE		REACTION		CARBON DIOXIDE	
N	INT(L2)	INT(L3)	N	INT(L2)	INT(L3)	N	INT(L2)	INT(L3)	N	INT(L2)	INT(L3)
0.00	1.53902E-06	2.21707E-06	0.00	8.43342E-06	1.27275E-05	0.00	3.02750E-05	4.75848E-05	0.00	3.02750E-05	4.75848E-05
0.25	1.55795E-06	2.25696E-06	0.25	8.53817E-06	1.29669E-05	0.25	3.06540E-05	4.85129E-05	0.25	3.06540E-05	4.85129E-05
0.50	1.57714E-06	2.29779E-06	0.50	8.64436E-06	1.32122E-05	0.50	3.10382E-05	4.94647E-05	0.50	3.10382E-05	4.94647E-05
0.75	1.59659E-06	2.33960E-06	0.75	8.75201E-06	1.34636E-05	0.75	3.14277E-05	5.04410E-05	0.75	3.14277E-05	5.04410E-05
1.00	1.61630E-06	2.38240E-06	1.00	8.86113E-06	1.37213E-05	1.00	3.18226E-05	5.14423E-05	1.00	3.18226E-05	5.14423E-05
1.25	1.63629E-06	2.42623E-06	1.25	8.97176E-06	1.39855E-05	1.25	3.22230E-05	5.24659E-05	1.25	3.22230E-05	5.24659E-05
1.50	1.65654E-06	2.47112E-06	1.50	9.08392E-06	1.42563E-05	1.50	3.26289E-05	5.35241E-05	1.50	3.26289E-05	5.35241E-05
1.75	1.67707E-06	2.51710E-06	1.75	9.19762E-06	1.45340E-05	1.75	3.30405E-05	5.46059E-05	1.75	3.30405E-05	5.46059E-05
2.00	1.69789E-06	2.56421E-06	2.00	9.31289E-06	1.48187E-05	2.00	3.34378E-05	5.57162E-05	2.00	3.34378E-05	5.57162E-05

Table M.1 continued ( $\bar{E} = 40$  kcal/mole)

REACTION		CARBON DIOXIDE		REACTION		CARBON DIOXIDE		REACTION		CARBON DIOXIDE	
NOM. TEMP.	1479. DEG K	NOM. TEMP.	1779. DEG K	NOM. TEMP.	1779. DEG K	NOM. TEMP.	2119. DEG K	NOM. TEMP.	2119. DEG K	NOM. TEMP.	2119. DEG K
NOM. PRES.	0.26 ATM	NOM. PRES.	0.26 ATM	NOM. PRES.	0.26 ATM	NOM. PRES.	0.26 ATM	NOM. PRES.	0.26 ATM	NOM. PRES.	0.26 ATM
KINEM. VISC.	2.00 SQ CM / SEC	KINEM. VISC.	2.69 SQ CM / SEC	KINEM. VISC.	2.69 SQ CM / SEC	KINEM. VISC.	3.55 SQ CM / SEC	KINEM. VISC.	3.55 SQ CM / SEC	KINEM. VISC.	3.55 SQ CM / SEC
MAIN AVG. VEL.	26.22 CM/SEC	MAIN AVG. VEL.	31.33 CM/SEC	MAIN AVG. VEL.	31.33 CM/SEC	MAIN AVG. VEL.	36.85 CM/SEC	MAIN AVG. VEL.	36.85 CM/SEC	MAIN AVG. VEL.	36.85 CM/SEC
TERM. VEL.	4.49 CM/SEC	TERM. VEL.	4.01 CM/SEC	TERM. VEL.	4.01 CM/SEC	TERM. VEL.	3.62 CM/SEC	TERM. VEL.	3.62 CM/SEC	TERM. VEL.	3.62 CM/SEC
ACTIV. ENERGY	40 KCAL	ACTIV. ENERGY	40 KCAL	ACTIV. ENERGY	40 KCAL	ACTIV. ENERGY	40 KCAL	ACTIV. ENERGY	40 KCAL	ACTIV. ENERGY	40 KCAL
EPSILON	13.666	EPSILON	11.354	EPSILON	11.354	EPSILON	9.527	EPSILON	9.527	EPSILON	9.527
$\bar{N}$	INT(L2)	INT(L3)	INT(L2)	INT(L3)	INT(L2)	INT(L3)	INT(L2)	INT(L3)	INT(L2)	INT(L3)	INT(L3)
0.00	4.26611E-08	5.70983E-08	4.09178E-07	5.75667E-07	4.09178E-07	5.75667E-07	2.38437E-06	3.51091E-06	2.38437E-06	3.51091E-06	3.51091E-06
0.25	4.31765E-08	5.80484E-08	4.14285E-07	5.85778E-07	4.14285E-07	5.85778E-07	2.41384E-06	3.57544E-06	2.41384E-06	3.57544E-06	3.57544E-06
0.50	4.36988E-08	5.90192E-08	4.19259E-07	5.96123E-07	4.19259E-07	5.96123E-07	2.44372E-06	3.64193E-06	2.44372E-06	3.64193E-06	3.64193E-06
0.75	4.42282E-08	6.00113E-08	4.24403E-07	6.06707E-07	4.24403E-07	6.06707E-07	2.47401E-06	3.70922E-06	2.47401E-06	3.70922E-06	3.70922E-06
1.00	4.47646E-08	6.10252E-08	4.29616E-07	6.17539E-07	4.29616E-07	6.17539E-07	2.50471E-06	3.77857E-06	2.50471E-06	3.77857E-06	3.77857E-06
1.25	4.53082E-08	6.20617E-08	4.34899E-07	6.28624E-07	4.34899E-07	6.28624E-07	2.53583E-06	3.84962E-06	2.53583E-06	3.84962E-06	3.84962E-06
1.50	4.58591E-08	6.31212E-08	4.40255E-07	6.39971E-07	4.40255E-07	6.39971E-07	2.56738E-06	3.92241E-06	2.56738E-06	3.92241E-06	3.92241E-06
1.75	4.64174E-08	6.42044E-08	4.45683E-07	6.51587E-07	4.45683E-07	6.51587E-07	2.59936E-06	3.99701E-06	2.59936E-06	3.99701E-06	3.99701E-06
2.00	4.69832E-08	6.53121E-08	4.51186E-07	6.63480E-07	4.51186E-07	6.63480E-07	2.63178E-06	4.07348E-06	2.63178E-06	4.07348E-06	4.07348E-06
-----											
REACTION		CARBON DIOXIDE		REACTION		CARBON DIOXIDE		REACTION		CARBON DIOXIDE	
NOM. TEMP.	1479. DEG K	NOM. TEMP.	1779. DEG K	NOM. TEMP.	1779. DEG K	NOM. TEMP.	2119. DEG K	NOM. TEMP.	2119. DEG K	NOM. TEMP.	2119. DEG K
NOM. PRES.	0.60 ATM	NOM. PRES.	0.60 ATM	NOM. PRES.	0.60 ATM	NOM. PRES.	0.60 ATM	NOM. PRES.	0.60 ATM	NOM. PRES.	0.60 ATM
KINEM. VISC.	1.74 SQ CM / SEC	KINEM. VISC.	2.36 SQ CM / SEC	KINEM. VISC.	2.36 SQ CM / SEC	KINEM. VISC.	3.12 SQ CM / SEC	KINEM. VISC.	3.12 SQ CM / SEC	KINEM. VISC.	3.12 SQ CM / SEC
MAIN AVG. VEL.	26.75 CM/SEC	MAIN AVG. VEL.	30.20 CM/SEC	MAIN AVG. VEL.	30.20 CM/SEC	MAIN AVG. VEL.	35.74 CM/SEC	MAIN AVG. VEL.	35.74 CM/SEC	MAIN AVG. VEL.	35.74 CM/SEC
TERM. VEL.	4.39 CM/SEC	TERM. VEL.	3.90 CM/SEC	TERM. VEL.	3.90 CM/SEC	TERM. VEL.	3.50 CM/SEC	TERM. VEL.	3.50 CM/SEC	TERM. VEL.	3.50 CM/SEC
ACTIV. ENERGY	40 KCAL	ACTIV. ENERGY	40 KCAL	ACTIV. ENERGY	40 KCAL	ACTIV. ENERGY	40 KCAL	ACTIV. ENERGY	40 KCAL	ACTIV. ENERGY	40 KCAL
EPSILON	13.666	EPSILON	11.354	EPSILON	11.354	EPSILON	9.527	EPSILON	9.527	EPSILON	9.527
$\bar{N}$	INT(L2)	INT(L3)	INT(L2)	INT(L3)	INT(L2)	INT(L3)	INT(L2)	INT(L3)	INT(L2)	INT(L3)	INT(L3)
0.00	4.26193E-08	5.69880E-08	4.27768E-07	6.01359E-07	4.27768E-07	6.01359E-07	2.47832E-06	3.64583E-06	2.47832E-06	3.64583E-06	3.64583E-06
0.25	4.31331E-08	5.79359E-08	4.38001E-07	6.11913E-07	4.38001E-07	6.11913E-07	2.50894E-06	3.71278E-06	2.50894E-06	3.71278E-06	3.71278E-06
0.50	4.36547E-08	5.89031E-08	4.48304E-07	6.22711E-07	4.48304E-07	6.22711E-07	2.53999E-06	3.78135E-06	2.53999E-06	3.78135E-06	3.78135E-06
0.75	4.41833E-08	5.98922E-08	4.43680E-07	6.33758E-07	4.43680E-07	6.33758E-07	2.57146E-06	3.85158E-06	2.57146E-06	3.85158E-06	3.85158E-06
1.00	4.47190E-08	6.09031E-08	4.49128E-07	6.45064E-07	4.49128E-07	6.45064E-07	2.60336E-06	3.92352E-06	2.60336E-06	3.92352E-06	3.92352E-06
1.25	4.52618E-08	6.19363E-08	4.54631E-07	6.56534E-07	4.54631E-07	6.56534E-07	2.63570E-06	3.99722E-06	2.63570E-06	3.99722E-06	3.99722E-06
1.50	4.58120E-08	6.29925E-08	4.60248E-07	6.68477E-07	4.60248E-07	6.68477E-07	2.66848E-06	4.07274E-06	2.66848E-06	4.07274E-06	4.07274E-06
1.75	4.63695E-08	6.40724E-08	4.65921E-07	6.80801E-07	4.65921E-07	6.80801E-07	2.70170E-06	4.15013E-06	2.70170E-06	4.15013E-06	4.15013E-06
2.00	4.69345E-08	6.51766E-08	4.71672E-07	6.93013E-07	4.71672E-07	6.93013E-07	2.73939E-06	4.22945E-06	2.73939E-06	4.22945E-06	4.22945E-06

Table M.1 continued ( $\bar{E} = 50$  kcal/mole)

REACTION			CARBON DIOXIDE			REACTION			CARBON DIOXIDE		
NOM. TEMP.	NOM. PRES.	KINEM. VISC.	NOM. TEMP.	NOM. PRES.	KINEM. VISC.	NOM. TEMP.	NOM. PRES.	KINEM. VISC.	NOM. TEMP.	NOM. PRES.	KINEM. VISC.
MAIN AVG. VEL.	TERM. VEL.	ACTIV. ENERGY	MAIN AVG. VEL.	TERM. VEL.	ACTIV. ENERGY	MAIN AVG. VEL.	TERM. VEL.	ACTIV. ENERGY	MAIN AVG. VEL.	TERM. VEL.	ACTIV. ENERGY
EPSILON			EPSILON			EPSILON			EPSILON		
	INT(L2)	INT(L3)		INT(L2)	INT(L3)		INT(L2)	INT(L3)		INT(L2)	INT(L3)
0.00	1.18497E-09	1.49439E-09	0.00	2.07995E-08	2.73876E-08	0.00	1.95483E-07	2.71942E-07	0.00	1.95483E-07	2.71942E-07
0.25	1.19903E-09	1.51769E-09	0.25	2.10501E-08	2.80419E-08	0.25	1.97869E-07	2.76662E-07	0.25	1.97869E-07	2.76662E-07
0.50	1.21328E-09	1.54129E-09	0.50	2.13042E-08	2.85060E-08	0.50	2.00287E-07	2.81490E-07	0.50	2.00287E-07	2.81490E-07
0.75	1.22771E-09	1.56538E-09	0.75	2.15616E-08	2.89801E-08	0.75	2.02738E-07	2.86429E-07	0.75	2.02738E-07	2.86429E-07
1.00	1.24234E-09	1.58997E-09	1.00	2.18222E-08	2.94646E-08	1.00	2.05222E-07	2.91482E-07	1.00	2.05222E-07	2.91482E-07
1.25	1.25719E-09	1.61505E-09	1.25	2.20868E-08	2.99597E-08	1.25	2.07739E-07	2.96651E-07	1.25	2.07739E-07	2.96651E-07
1.50	1.27217E-09	1.64066E-09	1.50	2.23547E-08	3.04657E-08	1.50	2.10291E-07	3.01941E-07	1.50	2.10291E-07	3.01941E-07
1.75	1.28738E-09	1.66679E-09	1.75	2.26262E-08	3.09830E-08	1.75	2.12877E-07	3.07355E-07	1.75	2.12877E-07	3.07355E-07
2.00	1.30279E-09	1.69346E-09	2.00	2.29013E-08	3.15117E-08	2.00	2.15498E-07	3.12897E-07	2.00	2.15498E-07	3.12897E-07
-----											
REACTION			CARBON DIOXIDE			REACTION			CARBON DIOXIDE		
NOM. TEMP.	NOM. PRES.	KINEM. VISC.	NOM. TEMP.	NOM. PRES.	KINEM. VISC.	NOM. TEMP.	NOM. PRES.	KINEM. VISC.	NOM. TEMP.	NOM. PRES.	KINEM. VISC.
MAIN AVG. VEL.	TERM. VEL.	ACTIV. ENERGY	MAIN AVG. VEL.	TERM. VEL.	ACTIV. ENERGY	MAIN AVG. VEL.	TERM. VEL.	ACTIV. ENERGY	MAIN AVG. VEL.	TERM. VEL.	ACTIV. ENERGY
EPSILON			EPSILON			EPSILON			EPSILON		
	INT(L2)	INT(L3)		INT(L2)	INT(L3)		INT(L2)	INT(L3)		INT(L2)	INT(L3)
0.00	1.18386E-09	1.49199E-09	0.00	2.17452E-08	2.86234E-08	0.00	2.03193E-07	2.82437E-07	0.00	2.03193E-07	2.82437E-07
0.25	1.19790E-09	1.51508E-09	0.25	2.20073E-08	2.92977E-08	0.25	2.05672E-07	2.87935E-07	0.25	2.05672E-07	2.87935E-07
0.50	1.21213E-09	1.53863E-09	0.50	2.22728E-08	2.97822E-08	0.50	2.08185E-07	2.93445E-07	0.50	2.08185E-07	2.93445E-07
0.75	1.22654E-09	1.56266E-09	0.75	2.25418E-08	3.02772E-08	0.75	2.10732E-07	2.97470E-07	0.75	2.10732E-07	2.97470E-07
1.00	1.24115E-09	1.58718E-09	1.00	2.28145E-08	3.07830E-08	1.00	2.13313E-07	3.02713E-07	1.00	2.13313E-07	3.02713E-07
1.25	1.25594E-09	1.61219E-09	1.25	2.30908E-08	3.12998E-08	1.25	2.15929E-07	3.08077E-07	1.25	2.15929E-07	3.08077E-07
1.50	1.27094E-09	1.63779E-09	1.50	2.33708E-08	3.18281E-08	1.50	2.18580E-07	3.13566E-07	1.50	2.18580E-07	3.13566E-07
1.75	1.28613E-09	1.66378E-09	1.75	2.36545E-08	3.23680E-08	1.75	2.21267E-07	3.19184E-07	1.75	2.21267E-07	3.19184E-07
2.00	1.30152E-09	1.69038E-09	2.00	2.39421E-08	3.29200E-08	2.00	2.23991E-07	3.24933E-07	2.00	2.23991E-07	3.24933E-07

Table M. 2  
 Numerical Intergration of  $I(T_0, \bar{E}, \bar{n}, L)$  for Steam Gasification Experiments  
 ( $\bar{E} = 0$  kcal/mole)

STEAM				REACTION				STEAM				REACTION				STEAM				REACTION			
NOM. TEMP.				NOM. TEMP.				NOM. TEMP.				NOM. TEMP.				NOM. TEMP.				NOM. TEMP.			
NOM. PRES.				NOM. PRES.				NOM. PRES.				NOM. PRES.				NOM. PRES.				NOM. PRES.			
KINEM. VISC.				KINEM. VISC.				KINEM. VISC.				KINEM. VISC.				KINEM. VISC.				KINEM. VISC.			
MAIN AVG. VEL.				MAIN AVG. VEL.				MAIN AVG. VEL.				MAIN AVG. VEL.				MAIN AVG. VEL.				MAIN AVG. VEL.			
TERM. VEL.				TERM. VEL.				TERM. VEL.				TERM. VEL.				TERM. VEL.				TERM. VEL.			
ACTIV. ENERGY				ACTIV. ENERGY				ACTIV. ENERGY				ACTIV. ENERGY				ACTIV. ENERGY				ACTIV. ENERGY			
EPSILON				EPSILON				EPSILON				EPSILON				EPSILON				EPSILON			
N				N				N				N				N				N			
INT(L2)				INT(L3)				INT(L2)				INT(L3)				INT(L2)				INT(L3)			
0.00	7.60618E-02	1.56331E-01	1.56331E-01	0.00	6.42314E-02	1.32464E-01	1.32464E-01	0.00	5.46258E-02	1.12787E-01	1.12787E-01	0.00	5.46258E-02	1.12787E-01	1.12787E-01	0.00	5.46258E-02	1.12787E-01	1.12787E-01				
0.25	7.70518E-02	1.60026E-01	1.60026E-01	0.25	6.51285E-02	1.35599E-01	1.35599E-01	0.25	5.53373E-02	1.15460E-01	1.15460E-01	0.25	5.53373E-02	1.15460E-01	1.15460E-01	0.25	5.53373E-02	1.15460E-01	1.15460E-01				
0.50	7.80559E-02	1.63832E-01	1.63832E-01	0.50	6.59776E-02	1.38829E-01	1.38829E-01	0.50	5.60590E-02	1.18213E-01	1.18213E-01	0.50	5.60590E-02	1.18213E-01	1.18213E-01	0.50	5.60590E-02	1.18213E-01	1.18213E-01				
0.75	7.90743E-02	1.67752E-01	1.67752E-01	0.75	6.68388E-02	1.42155E-01	1.42155E-01	0.75	5.67911E-02	1.21049E-01	1.21049E-01	0.75	5.67911E-02	1.21049E-01	1.21049E-01	0.75	5.67911E-02	1.21049E-01	1.21049E-01				
1.00	8.01074E-02	1.71790E-01	1.71790E-01	1.00	6.77124E-02	1.45582E-01	1.45582E-01	1.00	5.75336E-02	1.23971E-01	1.23971E-01	1.00	5.75336E-02	1.23971E-01	1.23971E-01	1.00	5.75336E-02	1.23971E-01	1.23971E-01				
1.25	8.11553E-02	1.75951E-01	1.75951E-01	1.25	6.85985E-02	1.49113E-01	1.49113E-01	1.25	5.82869E-02	1.26981E-01	1.26981E-01	1.25	5.82869E-02	1.26981E-01	1.26981E-01	1.25	5.82869E-02	1.26981E-01	1.26981E-01				
1.50	8.22183E-02	1.80239E-01	1.80239E-01	1.50	6.94974E-02	1.52752E-01	1.52752E-01	1.50	5.90509E-02	1.30084E-01	1.30084E-01	1.50	5.90509E-02	1.30084E-01	1.30084E-01	1.50	5.90509E-02	1.30084E-01	1.30084E-01				
1.75	8.32966E-02	1.84658E-01	1.84658E-01	1.75	7.04093E-02	1.56502E-01	1.56502E-01	1.75	5.98260E-02	1.33281E-01	1.33281E-01	1.75	5.98260E-02	1.33281E-01	1.33281E-01	1.75	5.98260E-02	1.33281E-01	1.33281E-01				
2.00	8.43904E-02	1.89213E-01	1.89213E-01	2.00	7.13343E-02	1.60368E-01	1.60368E-01	2.00	6.06123E-02	1.36577E-01	1.36577E-01	2.00	6.06123E-02	1.36577E-01	1.36577E-01	2.00	6.06123E-02	1.36577E-01	1.36577E-01				

---

STEAM				REACTION				STEAM				REACTION				STEAM				REACTION			
NOM. TEMP.				NOM. TEMP.				NOM. TEMP.				NOM. TEMP.				NOM. TEMP.				NOM. TEMP.			
NOM. PRES.				NOM. PRES.				NOM. PRES.				NOM. PRES.				NOM. PRES.				NOM. PRES.			
KINEM. VISC.				KINEM. VISC.				KINEM. VISC.				KINEM. VISC.				KINEM. VISC.				KINEM. VISC.			
MAIN AVG. VEL.				MAIN AVG. VEL.				MAIN AVG. VEL.				MAIN AVG. VEL.				MAIN AVG. VEL.				MAIN AVG. VEL.			
TERM. VEL.				TERM. VEL.				TERM. VEL.				TERM. VEL.				TERM. VEL.				TERM. VEL.			
ACTIV. ENERGY				ACTIV. ENERGY				ACTIV. ENERGY				ACTIV. ENERGY				ACTIV. ENERGY				ACTIV. ENERGY			
EPSILON				EPSILON				EPSILON				EPSILON				EPSILON				EPSILON			
N				N				N				N				N				N			
INT(L2)				INT(L3)				INT(L2)				INT(L3)				INT(L2)				INT(L3)			
0.00	7.29442E-02	1.50109E-01	1.50109E-01	0.00	6.18529E-02	1.27664E-01	1.27664E-01	0.00	5.25752E-02	1.08752E-01	1.08752E-01	0.00	5.25752E-02	1.08752E-01	1.08752E-01	0.00	5.25752E-02	1.08752E-01	1.08752E-01				
0.25	7.38635E-02	1.53654E-01	1.53654E-01	0.25	6.26580E-02	1.30689E-01	1.30689E-01	0.25	5.32603E-02	1.11332E-01	1.11332E-01	0.25	5.32603E-02	1.11332E-01	1.11332E-01	0.25	5.32603E-02	1.11332E-01	1.11332E-01				
0.50	7.48264E-02	1.57312E-01	1.57312E-01	0.50	6.34782E-02	1.33805E-01	1.33805E-01	0.50	5.39552E-02	1.13989E-01	1.13989E-01	0.50	5.39552E-02	1.13989E-01	1.13989E-01	0.50	5.39552E-02	1.13989E-01	1.13989E-01				
0.75	7.58030E-02	1.61079E-01	1.61079E-01	0.75	6.43041E-02	1.37014E-01	1.37014E-01	0.75	5.46601E-02	1.16726E-01	1.16726E-01	0.75	5.46601E-02	1.16726E-01	1.16726E-01	0.75	5.46601E-02	1.16726E-01	1.16726E-01				
1.00	7.67937E-02	1.64961E-01	1.64961E-01	1.00	6.51449E-02	1.40320E-01	1.40320E-01	1.00	5.53751E-02	1.19546E-01	1.19546E-01	1.00	5.53751E-02	1.19546E-01	1.19546E-01	1.00	5.53751E-02	1.19546E-01	1.19546E-01				
1.25	7.77996E-02	1.68960E-01	1.68960E-01	1.25	6.59978E-02	1.43727E-01	1.43727E-01	1.25	5.61094E-02	1.22452E-01	1.22452E-01	1.25	5.61094E-02	1.22452E-01	1.22452E-01	1.25	5.61094E-02	1.22452E-01	1.22452E-01				
1.50	7.88180E-02	1.73081E-01	1.73081E-01	1.50	6.68429E-02	1.47238E-01	1.47238E-01	1.50	5.68361E-02	1.25447E-01	1.25447E-01	1.50	5.68361E-02	1.25447E-01	1.25447E-01	1.50	5.68361E-02	1.25447E-01	1.25447E-01				
1.75	7.98320E-02	1.77328E-01	1.77328E-01	1.75	6.77405E-02	1.50856E-01	1.50856E-01	1.75	5.75824E-02	1.28534E-01	1.28534E-01	1.75	5.75824E-02	1.28534E-01	1.28534E-01	1.75	5.75824E-02	1.28534E-01	1.28534E-01				
2.00	8.09010E-02	1.81706E-01	1.81706E-01	2.00	6.86308E-02	1.54586E-01	1.54586E-01	2.00	5.83395E-02	1.31715E-01	1.31715E-01	2.00	5.83395E-02	1.31715E-01	1.31715E-01	2.00	5.83395E-02	1.31715E-01	1.31715E-01				

Table M.2 continued ( $\bar{E} = 10$  kcal/mole)

REACTION		STEAM		REACTION		STEAM		REACTION		STEAM	
N	INT(L2)	INT(L3)	N	INT(L2)	N	INT(L2)	N	INT(L2)	N	INT(L2)	INT(L3)
0.00	2.08524E-03	3.71798E-03	0.00	3.23825E-03	0.00	5.91560E-03	0.00	4.44938E-03	0.00	8.29190E-03	
0.25	2.11188E-03	3.79807E-03	0.25	3.27977E-03	0.25	6.04522E-03	0.25	4.50699E-03	0.25	8.47608E-03	
0.50	2.13889E-03	3.88039E-03	0.50	3.32188E-03	0.50	6.17850E-03	0.50	4.56461E-03	0.50	8.66552E-03	
0.75	2.16629E-03	3.96500E-03	0.75	3.36488E-03	0.75	6.31556E-03	0.75	4.62345E-03	0.75	8.86038E-03	
1.00	2.19407E-03	4.05200E-03	1.00	3.40788E-03	1.00	6.45952E-03	1.00	4.68313E-03	1.00	9.06086E-03	
1.25	2.22225E-03	4.14145E-03	1.25	3.45180E-03	1.25	6.60151E-03	1.25	4.74366E-03	1.25	9.26713E-03	
1.50	2.25082E-03	4.23343E-03	1.50	3.49634E-03	1.50	6.75067E-03	1.50	4.80505E-03	1.50	9.47939E-03	
1.75	2.27980E-03	4.32804E-03	1.75	3.54152E-03	1.75	6.90415E-03	1.75	4.86731E-03	1.75	9.69786E-03	
2.00	2.30919E-03	4.42536E-03	2.00	3.58734E-03	2.00	7.06207E-03	2.00	4.93046E-03	2.00	9.92273E-03	
-----											
REACTION		STEAM		REACTION		STEAM		REACTION		STEAM	
N	INT(L2)	INT(L3)	N	INT(L2)	N	INT(L2)	N	INT(L2)	N	INT(L2)	INT(L3)
0.00	1.99882E-03	3.56878E-03	0.00	3.11521E-03	0.00	5.69967E-03	0.00	4.28211E-03	0.00	7.99329E-03	
0.25	2.02436E-03	3.64579E-03	0.25	3.15516E-03	0.25	5.82469E-03	0.25	4.33719E-03	0.25	8.17104E-03	
0.50	2.05027E-03	3.72482E-03	0.50	3.19568E-03	0.50	5.95324E-03	0.50	4.39306E-03	0.50	8.35385E-03	
0.75	2.07644E-03	3.80612E-03	0.75	3.23678E-03	0.75	6.08543E-03	0.75	4.44972E-03	0.75	8.54190E-03	
1.00	2.10318E-03	3.88971E-03	1.00	3.27846E-03	1.00	6.22139E-03	1.00	4.50718E-03	1.00	8.73537E-03	
1.25	2.13020E-03	3.97565E-03	1.25	3.32079E-03	1.25	6.36125E-03	1.25	4.56546E-03	1.25	8.93444E-03	
1.50	2.15763E-03	4.06404E-03	1.50	3.36360E-03	1.50	6.50513E-03	1.50	4.62456E-03	1.50	9.13929E-03	
1.75	2.18539E-03	4.15494E-03	1.75	3.40707E-03	1.75	6.65314E-03	1.75	4.68451E-03	1.75	9.35014E-03	
2.00	2.21357E-03	4.24846E-03	2.00	3.45117E-03	2.00	6.80590E-03	2.00	4.74532E-03	2.00	9.56716E-03	



Table M.2 continued ( $\bar{E} = 20$  kcal/mole)

REACTION		STEAM		REACTION		STEAM		REACTION		STEAM	
NOM. TEMP.	DEG K	NOM. TEMP.	DEG K	NOM. TEMP.	DEG K	NOM. TEMP.	DEG K	NOM. TEMP.	DEG K	NOM. TEMP.	DEG K
NOM. PRES.	ATM	NOM. PRES.	ATM	NOM. PRES.	ATM	NOM. PRES.	ATM	NOM. PRES.	ATM	NOM. PRES.	ATM
KINEM. VISC.	SQ CM / SEC	KINEM. VISC.	SQ CM / SEC	KINEM. VISC.	SQ CM / SEC	KINEM. VISC.	SQ CM / SEC	KINEM. VISC.	SQ CM / SEC	KINEM. VISC.	SQ CM / SEC
MAIN AVG. VEL.	CM/SEC	MAIN AVG. VEL.	CM/SEC	MAIN AVG. VEL.	CM/SEC	MAIN AVG. VEL.	CM/SEC	MAIN AVG. VEL.	CM/SEC	MAIN AVG. VEL.	CM/SEC
TERM. VEL.	CM/SEC	TERM. VEL.	CM/SEC	TERM. VEL.	CM/SEC	TERM. VEL.	CM/SEC	TERM. VEL.	CM/SEC	TERM. VEL.	CM/SEC
ACTIV. ENERGY	KCAL	ACTIV. ENERGY	KCAL	ACTIV. ENERGY	KCAL	ACTIV. ENERGY	KCAL	ACTIV. ENERGY	KCAL	ACTIV. ENERGY	KCAL
EPSILON		EPSILON		EPSILON		EPSILON		EPSILON		EPSILON	
N	INT(L2)	N	INT(L3)	N	INT(L2)	N	INT(L3)	N	INT(L2)	N	INT(L3)
0.00	5.73594E-05	9.10509E-05	9.10509E-05	0.00	1.63485E-04	2.69688E-04	2.69688E-04	0.00	3.63006E-04	6.18668E-04	6.18668E-04
0.25	5.80788E-05	9.28419E-05	9.28419E-05	0.25	1.65549E-04	2.75164E-04	2.75164E-04	0.25	3.67614E-04	6.31555E-04	6.31555E-04
0.50	5.88082E-05	9.46790E-05	9.46790E-05	0.50	1.67642E-04	2.80785E-04	2.80785E-04	0.50	3.72286E-04	6.44790E-04	6.44790E-04
0.75	5.95477E-05	9.65636E-05	9.65636E-05	0.75	1.69764E-04	2.86555E-04	2.86555E-04	0.75	3.77024E-04	6.58385E-04	6.58385E-04
1.00	6.02974E-05	9.84971E-05	9.84971E-05	1.00	1.71916E-04	2.92480E-04	2.92480E-04	1.00	3.81829E-04	6.72352E-04	6.72352E-04
1.25	6.10576E-05	1.00481E-04	1.00481E-04	1.25	1.74098E-04	2.98563E-04	2.98563E-04	1.25	3.86700E-04	6.86701E-04	6.86701E-04
1.50	6.18283E-05	1.02517E-04	1.02517E-04	1.50	1.76310E-04	3.04811E-04	3.04811E-04	1.50	3.91641E-04	7.01447E-04	7.01447E-04
1.75	6.26097E-05	1.04607E-04	1.04607E-04	1.75	1.78554E-04	3.11229E-04	3.11229E-04	1.75	3.96650E-04	7.16601E-04	7.16601E-04
2.00	6.34021E-05	1.06752E-04	1.06752E-04	2.00	1.80828E-04	3.17821E-04	3.17821E-04	2.00	4.01731E-04	7.32178E-04	7.32178E-04
-----											
N	INT(L2)	N	INT(L3)	N	INT(L2)	N	INT(L3)	N	INT(L2)	N	INT(L3)
0.00	5.49787E-05	8.73722E-05	8.73722E-05	0.00	1.57264E-04	2.59779E-04	2.59779E-04	0.00	3.49340E-04	5.96250E-04	5.96250E-04
0.25	5.56885E-05	8.90925E-05	8.90925E-05	0.25	1.59250E-04	2.65505E-04	2.65505E-04	0.25	3.53777E-04	6.08683E-04	6.08683E-04
0.50	5.63979E-05	9.08571E-05	9.08571E-05	0.50	1.61264E-04	2.70475E-04	2.70475E-04	0.50	3.58275E-04	6.21452E-04	6.21452E-04
0.75	5.70769E-05	9.26673E-05	9.26673E-05	0.75	1.63306E-04	2.76039E-04	2.76039E-04	0.75	3.62836E-04	6.34570E-04	6.34570E-04
1.00	5.77958E-05	9.45245E-05	9.45245E-05	1.00	1.65377E-04	2.81752E-04	2.81752E-04	1.00	3.67462E-04	6.48045E-04	6.48045E-04
1.25	5.85247E-05	9.64304E-05	9.64304E-05	1.25	1.67577E-04	2.87619E-04	2.87619E-04	1.25	3.72153E-04	6.61891E-04	6.61891E-04
1.50	5.92537E-05	9.83864E-05	9.83864E-05	1.50	1.69806E-04	2.93644E-04	2.93644E-04	1.50	3.76909E-04	6.76119E-04	6.76119E-04
1.75	6.00130E-05	1.00393E-04	1.00393E-04	1.75	1.71765E-04	2.99833E-04	2.99833E-04	1.75	3.81733E-04	6.90742E-04	6.90742E-04
2.00	6.07727E-05	1.02454E-04	1.02454E-04	2.00	1.73954E-04	3.06191E-04	3.06191E-04	2.00	3.86624E-04	7.05772E-04	7.05772E-04

Table M.2 continued ( $\bar{E} = 30$  kcal/mole)

REACTION		STEAM		REACTION		STEAM		REACTION		STEAM	
NOM. TEMP.	DEG K	NOM. TEMP.	DEG K	NOM. TEMP.	DEG K	NOM. TEMP.	DEG K	NOM. TEMP.	DEG K	NOM. TEMP.	DEG K
KINEM. VISC.	SO CM / SEC	KINEM. VISC.	SO CM / SEC	KINEM. VISC.	SO CM / SEC	KINEM. VISC.	SO CM / SEC	KINEM. VISC.	SO CM / SEC	KINEM. VISC.	SO CM / SEC
MAIN AVG. VEL.	CM/SEC	MAIN AVG. VEL.	CM/SEC	MAIN AVG. VEL.	CM/SEC	MAIN AVG. VEL.	CM/SEC	MAIN AVG. VEL.	CM/SEC	MAIN AVG. VEL.	CM/SEC
TERM. VEL.	CM/SEC	TERM. VEL.	CM/SEC	TERM. VEL.	CM/SEC	TERM. VEL.	CM/SEC	TERM. VEL.	CM/SEC	TERM. VEL.	CM/SEC
ACTIV. ENERGY	KCAL	ACTIV. ENERGY	KCAL	ACTIV. ENERGY	KCAL	ACTIV. ENERGY	KCAL	ACTIV. ENERGY	KCAL	ACTIV. ENERGY	KCAL
EPSILON		EPSILON		EPSILON		EPSILON		EPSILON		EPSILON	
INT(L2)	INT(L3)	INT(L2)	INT(L3)	INT(L2)	INT(L3)	INT(L2)	INT(L3)	INT(L2)	INT(L3)	INT(L2)	INT(L3)
0.00	1.58300E-06	2.28777E-06	0.00	8.27261E-06	1.25259E-05	0.00	2.96642E-05	0.00	2.96642E-05	0.00	4.67917E-05
0.25	1.60250E-06	2.32906E-06	0.25	8.37547E-06	1.27623E-05	0.25	3.00360E-05	0.25	3.00360E-05	0.25	4.77071E-05
0.50	1.62225E-06	2.37133E-06	0.50	8.47975E-06	1.30043E-05	0.50	3.04128E-05	0.50	3.04128E-05	0.50	4.86459E-05
0.75	1.64228E-06	2.41461E-06	0.75	8.58546E-06	1.32527E-05	0.75	3.07949E-05	0.75	3.07949E-05	0.75	4.96089E-05
1.00	1.66258E-06	2.45982E-06	1.00	8.69262E-06	1.35071E-05	1.00	3.11823E-05	1.00	3.11823E-05	1.00	5.05988E-05
1.25	1.68316E-06	2.50431E-06	1.25	8.80126E-06	1.37679E-05	1.25	3.15751E-05	1.25	3.15751E-05	1.25	5.16103E-05
1.50	1.70402E-06	2.55079E-06	1.50	8.91140E-06	1.40353E-05	1.50	3.19733E-05	1.50	3.19733E-05	1.50	5.26504E-05
1.75	1.72516E-06	2.59840E-06	1.75	9.02306E-06	1.43094E-05	1.75	3.23770E-05	1.75	3.23770E-05	1.75	5.37177E-05
2.00	1.74659E-06	2.64718E-06	2.00	9.13626E-06	1.45906E-05	2.00	3.27864E-05	2.00	3.27864E-05	2.00	5.48132E-05
-----											
REACTION		STEAM		REACTION		STEAM		REACTION		STEAM	
NOM. TEMP.	DEG K	NOM. TEMP.	DEG K	NOM. TEMP.	DEG K	NOM. TEMP.	DEG K	NOM. TEMP.	DEG K	NOM. TEMP.	DEG K
KINEM. VISC.	SO CM / SEC	KINEM. VISC.	SO CM / SEC	KINEM. VISC.	SO CM / SEC	KINEM. VISC.	SO CM / SEC	KINEM. VISC.	SO CM / SEC	KINEM. VISC.	SO CM / SEC
MAIN AVG. VEL.	CM/SEC	MAIN AVG. VEL.	CM/SEC	MAIN AVG. VEL.	CM/SEC	MAIN AVG. VEL.	CM/SEC	MAIN AVG. VEL.	CM/SEC	MAIN AVG. VEL.	CM/SEC
TERM. VEL.	CM/SEC	TERM. VEL.	CM/SEC	TERM. VEL.	CM/SEC	TERM. VEL.	CM/SEC	TERM. VEL.	CM/SEC	TERM. VEL.	CM/SEC
ACTIV. ENERGY	KCAL	ACTIV. ENERGY	KCAL	ACTIV. ENERGY	KCAL	ACTIV. ENERGY	KCAL	ACTIV. ENERGY	KCAL	ACTIV. ENERGY	KCAL
EPSILON		EPSILON		EPSILON		EPSILON		EPSILON		EPSILON	
INT(L2)	INT(L3)	INT(L2)	INT(L3)	INT(L2)	INT(L3)	INT(L2)	INT(L3)	INT(L2)	INT(L3)	INT(L2)	INT(L3)
0.00	1.51731E-06	2.19477E-06	0.00	7.93731E-06	1.20625E-05	0.00	2.85459E-05	0.00	2.85459E-05	0.00	4.50860E-05
0.25	1.53590E-06	2.23442E-06	0.25	8.03629E-06	1.22903E-05	0.25	2.89038E-05	0.25	2.89038E-05	0.25	4.59691E-05
0.50	1.55484E-06	2.27501E-06	0.50	8.13664E-06	1.25238E-05	0.50	2.92666E-05	0.50	2.92666E-05	0.50	4.68475E-05
0.75	1.57404E-06	2.31657E-06	0.75	8.23836E-06	1.27631E-05	0.75	2.96344E-05	0.75	2.96344E-05	0.75	4.78036E-05
1.00	1.59350E-06	2.35912E-06	1.00	8.34148E-06	1.30083E-05	1.00	3.00074E-05	1.00	3.00074E-05	1.00	4.87565E-05
1.25	1.61323E-06	2.40270E-06	1.25	8.44603E-06	1.32598E-05	1.25	3.03855E-05	1.25	3.03855E-05	1.25	4.97343E-05
1.50	1.63323E-06	2.44734E-06	1.50	8.57201E-06	1.35176E-05	1.50	3.07689E-05	1.50	3.07689E-05	1.50	5.07376E-05
1.75	1.65350E-06	2.49307E-06	1.75	8.67946E-06	1.37819E-05	1.75	3.11576E-05	1.75	3.11576E-05	1.75	5.17673E-05
2.00	1.67406E-06	2.53992E-06	2.00	8.78840E-06	1.40530E-05	2.00	3.15518E-05	2.00	3.15518E-05	2.00	5.28242E-05

Table M.2 continued ( $\bar{E} = 40$  kcal/mole)

REACTION		STEAM		REACTION		STEAM		REACTION		STEAM	
NOM. TEMP.	DEG K	NOM. TEMP.	DEG K	NOM. TEMP.	DEG K	NOM. TEMP.	DEG K	NOM. TEMP.	DEG K	NOM. TEMP.	DEG K
NOM. PRES.	ATM	NOM. PRES.	ATM	NOM. PRES.	ATM	NOM. PRES.	ATM	NOM. PRES.	ATM	NOM. PRES.	ATM
KINEM. VISC.	SO CM / SEC	KINEM. VISC.	SO CM / SEC	KINEM. VISC.	SO CM / SEC	KINEM. VISC.	SO CM / SEC	KINEM. VISC.	SO CM / SEC	KINEM. VISC.	SO CM / SEC
MAIN AVG. VEL.	CM/SEC	MAIN AVG. VEL.	CM/SEC	MAIN AVG. VEL.	CM/SEC	MAIN AVG. VEL.	CM/SEC	MAIN AVG. VEL.	CM/SEC	MAIN AVG. VEL.	CM/SEC
TERM. VEL.	CM/SEC	TERM. VEL.	CM/SEC	TERM. VEL.	CM/SEC	TERM. VEL.	CM/SEC	TERM. VEL.	CM/SEC	TERM. VEL.	CM/SEC
ACTIV. ENERGY	KCAL	ACTIV. ENERGY	KCAL	ACTIV. ENERGY	KCAL	ACTIV. ENERGY	KCAL	ACTIV. ENERGY	KCAL	ACTIV. ENERGY	KCAL
EPSILON		EPSILON		EPSILON		EPSILON		EPSILON		EPSILON	
INT(L2)	INT(L3)	INT(L2)	INT(L3)	INT(L2)	INT(L3)	INT(L2)	INT(L3)	INT(L2)	INT(L3)	INT(L2)	INT(L3)
0.00	4.3281E-09	5.87598E-08	5.91456E-07	0.00	4.19547E-07	5.91456E-07	5.91456E-07	0.00	2.42798E-06	2.42798E-06	3.58300E-06
0.25	4.43580E-08	5.97394E-08	4.24664E-07	0.25	4.24664E-07	6.01866E-07	6.01866E-07	0.25	2.45802E-06	2.45802E-06	3.64899E-06
0.50	4.48951E-08	6.07404E-08	4.29892E-07	0.50	4.29892E-07	6.12518E-07	6.12518E-07	0.50	2.48847E-06	2.48847E-06	3.71658E-06
0.75	4.54392E-08	6.17694E-08	4.35170E-07	0.75	4.35170E-07	6.23416E-07	6.23416E-07	0.75	2.51934E-06	2.51934E-06	3.78581E-06
1.00	4.59907E-08	6.28089E-08	4.40519E-07	1.00	4.40519E-07	6.34369E-07	6.34369E-07	1.00	2.55063E-06	2.55063E-06	3.85674E-06
1.25	4.65496E-08	6.3877E-08	4.45941E-07	1.25	4.45941E-07	6.45398E-07	6.45398E-07	1.25	2.58234E-06	2.58234E-06	3.92940E-06
1.50	4.71160E-08	6.49704E-08	4.51437E-07	1.50	4.51437E-07	6.57669E-07	6.57669E-07	1.50	2.61449E-06	2.61449E-06	4.00386E-06
1.75	4.76900E-08	6.60876E-08	4.57008E-07	1.75	4.57008E-07	6.69632E-07	6.69632E-07	1.75	2.64709E-06	2.64709E-06	4.08017E-06
2.00	4.82718E-08	6.72300E-08	4.62654E-07	2.00	4.62654E-07	6.81880E-07	6.81880E-07	2.00	2.68013E-06	2.68013E-06	4.15839E-06
0.00	4.20039E-08	5.63581E-08	4.03532E-07	0.00	4.03532E-07	5.69444E-07	5.69444E-07	0.00	2.33633E-06	2.33633E-06	3.45167E-06
0.25	4.25119E-08	5.72983E-08	4.08476E-07	0.25	4.08476E-07	5.79477E-07	5.79477E-07	0.25	2.36524E-06	2.36524E-06	3.51532E-06
0.50	4.30267E-08	5.82595E-08	4.13487E-07	0.50	4.13487E-07	5.89742E-07	5.89742E-07	0.50	2.39455E-06	2.39455E-06	3.58050E-06
0.75	4.35485E-08	5.92416E-08	4.18565E-07	0.75	4.18565E-07	6.00246E-07	6.00246E-07	0.75	2.42427E-06	2.42427E-06	3.64727E-06
1.00	4.40772E-08	6.02454E-08	4.23713E-07	1.00	4.23713E-07	6.10996E-07	6.10996E-07	1.00	2.45439E-06	2.45439E-06	3.71567E-06
1.25	4.46130E-08	6.12714E-08	4.28930E-07	1.25	4.28930E-07	6.21999E-07	6.21999E-07	1.25	2.48492E-06	2.48492E-06	3.78575E-06
1.50	4.51561E-08	6.23204E-08	4.34218E-07	1.50	4.34218E-07	6.33261E-07	6.33261E-07	1.50	2.51587E-06	2.51587E-06	3.85757E-06
1.75	4.57064E-08	6.33931E-08	4.39579E-07	1.75	4.39579E-07	6.44792E-07	6.44792E-07	1.75	2.54725E-06	2.54725E-06	3.93117E-06
2.00	4.62641E-08	6.44898E-08	4.45012E-07	2.00	4.45012E-07	6.56598E-07	6.56598E-07	2.00	2.57906E-06	2.57906E-06	4.00661E-06

Table M.2 continued ( $\bar{E} = 50$  kcal/mole)

REACTION		STEAM		REACTION		STEAM		REACTION		STEAM	
NOM. TEMP.	DEG K	NOM. TEMP.	DEG K	NOM. TEMP.	DEG K	NOM. TEMP.	DEG K	NOM. TEMP.	DEG K	NOM. TEMP.	DEG K
NOM. PRES.	ATM	NOM. PRES.	ATM	NOM. PRES.	ATM	NOM. PRES.	ATM	NOM. PRES.	ATM	NOM. PRES.	ATM
KINEM. VISC.	SO CM / SEC	KINEM. VISC.	SO CM / SEC	KINEM. VISC.	SO CM / SEC	KINEM. VISC.	SO CM / SEC	KINEM. VISC.	SO CM / SEC	KINEM. VISC.	SO CM / SEC
MAIN AVG. VEL.	CM/SEC	MAIN AVG. VEL.	CM/SEC	MAIN AVG. VEL.	CM/SEC	MAIN AVG. VEL.	CM/SEC	MAIN AVG. VEL.	CM/SEC	MAIN AVG. VEL.	CM/SEC
TERM. VEL.	CM/SEC	TERM. VEL.	CM/SEC	TERM. VEL.	CM/SEC	TERM. VEL.	CM/SEC	TERM. VEL.	CM/SEC	TERM. VEL.	CM/SEC
ACTIV. ENERGY	KCAL	ACTIV. ENERGY	KCAL	ACTIV. ENERGY	KCAL	ACTIV. ENERGY	KCAL	ACTIV. ENERGY	KCAL	ACTIV. ENERGY	KCAL
EPSILON		EPSILON		EPSILON		EPSILON		EPSILON		EPSILON	
0.00	1.21724E-09	1.53734E-09	1.53734E-08	0.00	2.13241E-08	2.83323E-08	1.99040E-07	0.00	1.99040E-07	2.77422E-07	2.77422E-07
0.25	1.23170E-09	1.56120E-09	2.15819E-08	0.25	2.15819E-08	2.87997E-08	2.01471E-07	0.25	2.01471E-07	2.82248E-07	2.82248E-07
0.50	1.24635E-09	1.58554E-09	2.18420E-08	0.50	2.18420E-08	2.92773E-08	2.03935E-07	0.50	2.03935E-07	2.87189E-07	2.87189E-07
0.75	1.26118E-09	1.61037E-09	2.21061E-08	0.75	2.21061E-08	2.97639E-08	2.06432E-07	0.75	2.06432E-07	2.92232E-07	2.92232E-07
1.00	1.27621E-09	1.63570E-09	2.23738E-08	1.00	2.23738E-08	3.02640E-08	2.08963E-07	1.00	2.08963E-07	2.97397E-07	2.97397E-07
1.25	1.29144E-09	1.66156E-09	2.26450E-08	1.25	2.26450E-08	3.07739E-08	2.11529E-07	1.25	2.11529E-07	3.02683E-07	3.02683E-07
1.50	1.30687E-09	1.68795E-09	2.29199E-08	1.50	2.29199E-08	3.12931E-08	2.14129E-07	1.50	2.14129E-07	3.08091E-07	3.08091E-07
1.75	1.32251E-09	1.71488E-09	2.31985E-08	1.75	2.31985E-08	3.18267E-08	2.16765E-07	1.75	2.16765E-07	3.13627E-07	3.13627E-07
2.00	1.33839E-09	1.74237E-09	2.34808E-08	2.00	2.34808E-08	3.23710E-08	2.19436E-07	2.00	2.19436E-07	3.19293E-07	3.19293E-07
-----											
0.00	1.16651E-09	1.47421E-09	2.05090E-08	0.00	2.05090E-08	2.72722E-08	1.91519E-07	0.00	1.91519E-07	2.67202E-07	2.67202E-07
0.25	1.16036E-09	1.49710E-09	2.07564E-08	0.25	2.07564E-08	2.77226E-08	1.93856E-07	0.25	1.93856E-07	2.71895E-07	2.71895E-07
0.50	1.19440E-09	1.52046E-09	2.10072E-08	0.50	2.10072E-08	2.81828E-08	1.96228E-07	0.50	1.96228E-07	2.76614E-07	2.76614E-07
0.75	1.20863E-09	1.54429E-09	2.12614E-08	0.75	2.12614E-08	2.86530E-08	1.98632E-07	0.75	1.98632E-07	2.81482E-07	2.81482E-07
1.00	1.22305E-09	1.56861E-09	2.15189E-08	1.00	2.15189E-08	2.91335E-08	2.01068E-07	1.00	2.01068E-07	2.86462E-07	2.86462E-07
1.25	1.23764E-09	1.59343E-09	2.17799E-08	1.25	2.17799E-08	2.96245E-08	2.03538E-07	1.25	2.03538E-07	2.91559E-07	2.91559E-07
1.50	1.25243E-09	1.61875E-09	2.20444E-08	1.50	2.20444E-08	3.01264E-08	2.06041E-07	1.50	2.06041E-07	2.96774E-07	2.96774E-07
1.75	1.26742E-09	1.64461E-09	2.23124E-08	1.75	2.23124E-08	3.06394E-08	2.08578E-07	1.75	2.08578E-07	3.02112E-07	3.02112E-07
2.00	1.28261E-09	1.67100E-09	2.25841E-08	2.00	2.25841E-08	3.11639E-08	2.11150E-07	2.00	2.11150E-07	3.07576E-07	3.07576E-07

Table M.3

Linearization of  $I(T_o, \bar{E}, \bar{n}, L)$

$$\ln I \approx I_1 \bar{E} + I_3 \bar{n} + I_4$$

REACTION -----	TEMP. (K) -----	PRES. (ATM) -----	SEP IN (CM) -----	LINEARIZATION CONSTANTS		
				I1 -----	I3 -----	I4 -----
STEAM	1473	0.34	11.4	-0.3590	0.04963	-2.579
STEAM	1473	0.34	15.2	-0.3693	0.07749	-1.881
STEAM	1773	0.34	11.4	-0.2984	0.05003	-2.746
STEAM	1773	0.34	15.2	-0.3076	0.08003	-2.037
STEAM	2113	0.34	11.4	-0.2505	0.05035	-2.908
STEAM	2113	0.34	15.2	-0.2587	0.08225	-2.192
STEAM	1473	0.65	11.4	-0.3591	0.04965	-2.621
STEAM	1473	0.65	15.2	-0.3693	0.07754	-1.922
STEAM	1773	0.65	11.4	-0.2984	0.05005	-2.784
STEAM	1773	0.65	15.2	-0.3077	0.08012	-2.074
STEAM	2113	0.65	11.4	-0.2505	0.05037	-2.946
STEAM	2113	0.65	15.2	-0.2588	0.08232	-2.228
CARBON DIOXIDE	1473	0.26	11.4	-0.3590	0.04947	-2.608
CARBON DIOXIDE	1473	0.26	15.2	-0.3689	0.07645	-1.920
CARBON DIOXIDE	1773	0.26	11.4	-0.2984	0.04987	-2.772
CARBON DIOXIDE	1773	0.26	15.2	-0.3073	0.07894	-2.073
CARBON DIOXIDE	2113	0.26	11.4	-0.2504	0.05019	-2.927
CARBON DIOXIDE	2113	0.26	15.2	-0.2584	0.08111	-2.220
CARBON DIOXIDE	1473	0.60	11.4	-0.3590	0.04945	-2.609
CARBON DIOXIDE	1473	0.60	15.2	-0.3689	0.07637	-1.923
CARBON DIOXIDE	1773	0.60	11.4	-0.2984	0.04984	-2.728
CARBON DIOXIDE	1773	0.60	15.2	-0.3073	0.07888	-2.030
CARBON DIOXIDE	2113	0.60	11.4	-0.2504	0.05016	-2.889
CARBON DIOXIDE	2113	0.60	15.2	-0.2584	0.08103	-2.183

Appendix N

PHYSICAL CHANGES DURING GASIFICATION

A discussion of the physical changes in the char particles (surface area, density) as a result of partial gasification in carbon dioxide and steam, is found in section 4.3. The data used to prepare Figures 4.5 through 4.7 are found in Tables N.1 and N.2.

Table N.1

Physical Properties of Char Samples  
After Partial Gasification in Carbon Dioxide

Run Number <sup>†</sup>	d.a.f. Wt. Loss (x·100%)	T <sub>o</sub> (°K)	S <sub>g</sub> (m <sup>2</sup> /g)*	ρ <sub>p</sub> (g/cm <sup>3</sup> )*
C-02	16.1	1773	175	0.39
C-03	13.1	1773	170	0.41
C-05	29.5	1773	170	0.38
C-06	30.1	1773	167	0.36
C-14	- 1.0	1473	118	-
C-15	- 1.5	1473	209	-
C-21	12.8	1473	219	0.47
C-22	7.9	1473	230	0.42
C-23	8.4	1473	255	0.41
C-24	5.8	1473	231	0.42
C-29	9.7	1773	148	-
C-31	19.3	1773	193	0.42
C-33	20.5	1773	180	0.43
C-35	31.1	1773	178	0.36
C-36	30.4	1773	175	0.45
C-38	41.1	1773	161	-
C-61	62.8	2113	120	-
C-67	25.6	2113	151	-

<sup>†</sup> Corresponds to run codes of Table A.1

\* Analysis by Phillips Petroleum Company, Bartlesville, Oklahoma

Table N.2

Physical Properties of Char Samples  
After Partial Gasification in Steam

Run Number <sup>†</sup>	d.a.f. Wt. Loss (x·100%)	T <sub>o</sub> (°K)	S <sub>g</sub> (m <sup>2</sup> /g) <sup>*</sup>	ρ <sub>p</sub> (g/cm <sup>3</sup> ) <sup>*</sup>
S-01	7.7	1473	270	0.44
S-02	8.1	1473	277	0.46
S-05	1.0	1473	173	-
S-09	41.9	1773	219	0.36
S-10	44.1	1773	217	0.36
S-11	50.0	1773	215	0.40
S-12	23.2	1773	223	0.45
S-14	22.5	1773	223	0.45
S-19	32.6	1773	220	0.37
S-20	33.8	1773	232	0.35
S-21	37.0	1773	232	-
S-22	30.4	1473	369	0.37
S-24	27.5	1473	351	0.44
S-26	11.2	1473	274	0.43
S-27	13.7	1473	293	0.44
S-32	9.4	1473	263	-
S-35	71.3	1773	175	-
S-37	49.6	1773	273	-
S-42	26.8	1773	201	-
S-43	81.7	1773	248	0.28
S-44	75.2	1773	203	0.35
S-55	78.2	2113	121	-
S-61	28.8	2113	155	-

<sup>†</sup> Corresponds to run codes of Table B.1

<sup>\*</sup> Analysis by Phillips Petroleum Company, Bartlesville, Oklahoma



Appendix O

LISTING OF COMPUTER PROGRAMS

Several computer programs were written to perform the calculations of Chapter 4. The FORTRAN computer language was used. Computer work was done on the IBM 1130 Computer System in the Chemical Engineering Department at the Massachusetts Institute of Technology. The programs, and source decks for executing them, are listed in this Appendix.

<u>Program Name</u>	<u>Purpose</u>
INTEG	Numerical integration of equation (4.15), for each test atmosphere and the following values of $\bar{E}$ and $\bar{n}$ : E = 0, 10, 20, 30, 40, 50 kcal/mole n = 0.25, 0.50, 0.75, ..., 2.00
LNI	Fits the results of INTEG to the form of equation (4.17)
AVFIT	Determines apparent kinetic parameters, based on char weight loss experimental data (section 4.2).
INVRS	Inverts matrices
MULT	Multiplies matrices

INTEG - p.1

```

// FOR
**NAME INTEG
**IOCS(DISK,CARD,1132PRINTER)

C THIS PROGRAM NUMERICALLY INTEGRATES THE INTEGRAL DESIGNATED
C I(I,T,E,N,L) IN THE CALCULATIONS OF STEAM AND CO2 GASIFICATION
C REACTION KINETICS.
C SIMPSON'S APPROXIMATION IS USED FOR NUMERICAL INTEGRATION.
C THE EVALUATED INTEGRALS WILL BE STORED IN THE ARRAYS
C INT2(I,N,J) AND INT3(I,N,J).
C INT2 CONTAINS THE INTEGRALS WITH L2 (11.4 CM) AS THE
C UPPER LIMIT OF INTEGRATION.
C INT3 CONTAINS THE INTEGRALS WITH L3 (15.2 CM) AS THE
C UPPER LIMIT OF INTEGRATION.
C THE SUBSCRIPTS FOR INT2 AND INT3 ARE
C ; DESIGNATES WHICH SET OF DATA IS USED.
C I = 01 H2O 1473 DEG K 0.34 ATM
C I = 02 H2O 1773 DEG K 0.34 ATM
C I = 03 H2O 2113 DEG K 0.34 ATM
C I = 04 H2O 1473 DEG K 0.65 ATM
C I = 05 H2O 1773 DEG K 0.65 ATM
C I = 06 H2O 2113 DEG K 0.65 ATM
C I = 07 CO2 1473 DEG K 0.26 ATM
C I = 08 CO2 1773 DEG K 0.26 ATM
C I = 09 CO2 2113 DEG K 0.26 ATM
C I = 10 CO2 1473 DEG K 0.6 ATM
C I = 11 CO2 1773 DEG K 0.6 ATM
C I = 12 CO2 2113 DEG K 0.6 ATM
C N INDICATES THE ORDER OF REACTION USED IN THE INTEGRATION
C ORDER = 0.75 * (N-1)
C J INDICATES THE ACTIVATION ENERGY (KCAL) ASSUMED
C ACTIV. ENERGY = 10 * (J-1)
C INTEG CAN BE FOLLOWED BY PROGRAM LNI, WHICH FITS EACH
C SET OF INTEGRALS TO AN EXPRESSION OF THE FORM
C LN I(T,L,E,N) = I1(T,L)*E + I3(T,L)*N + I4(T,L).

REAL NU(I,2)
REAL INT2(12,9,6), INT3(12,9,6)
DIMENSION T(12)
DIMENSION UAVG(12), UTERM(12)
C THE ARRAYS INT2, INT3, AND T WILL LATER BE STORED ON FILES.
C DEFINE FILE 2(12,108,0,IN2),3(12,108,0,IN3),4(1,24,0,ITEMP)

C STATEMENT FUNCTIONS
C THETA T(2) / T=NOV
C USTAR DIMENSIONLESS MAIN GAS CENTERLINE VELOCITY
C FOR ISOTHERMAL REACTOR AT T=NOV.
C USTAR = U(R=0.2,THETA=1) / U-AVG
C GRAND THE INTEGRAND OF I(E,L,T,N), WHERE
C E ACTIVATION ENERGY
C T NOMINAL TEMPERATURE
C N ORDER OF REACTION
C L UPPER LIMIT OF INTEGRATION

```

INTEG - p.2

```

THETA(Z) = 1.0 - ((1.083E-04)*(Z**2.7097))
USTAR(Z,XNU,UAVG) = 2.0 - ((0.5939)*(EXP(-14.9375*XNU*Z/(UAVG*2.54
1*2.54))))

```

```

GRAND(Z,XNU,UAVG,EPS,UTERM,ORDER)=(THETA(Z)**(-1.0*ORDER))*EXP(-1.
10*EPS/THETA(Z))/(USTAR(Z,XNU,UAVG)*UAVG*THETA(Z)+UTERM)

```

C R IS THE GAS CONSTANT (CAL/MOLE DEG K)  
R=1.987

C H IS THE WIDTH OF THE INTERVAL USED FOR NUMERICAL INTEGRATION.  
H=7.62/40.

C READ IN RUN DATA AND PHYSICAL PROPERTY DATA  
C NU KINEMATIC VISCOSITY (SQ CM/SEC)  
C UTERM PARTICLE TERMINAL VELOCITY RELATIVE TO THE MAIN GAS (CM/SEC)  
C UAVG MAIN GAS STREAM AVERAGE VELOCITY AT T-NOM (CM/SEC)  
C T T-NOM

```

DO 100 I=1,12
READ(2,50)NU(I),UTERM(I),UAVG(I),T(I)
50 FORMAT(2F5.2,F6.2,F6.1)
DO 100 N=1,9
ORDER=0.25*FLOAT(N-1)
DO 100 J=1,6
ACT=10.0*FLOAT(J-1)
EPS=ACT*1000./(R*T(I))

```

C BEGIN NUMERICAL INTEGRATION FOR CONDITIONS I,N,J  
TOTAL=0.0  
Z=7.62

C SET L=2 FOR INTEGRATION TO UPPER LIMIT OF L2

```

L=2
70 TOTAL=TOTAL+1.0*GRAND(Z,NU(I),UAVG(I),EPS,UTERM(I),ORDER)
DO 80 K=1,9
Z=Z+H
TOTAL=TOTAL+4.0*GRAND(Z,NU(I),UAVG(I),EPS,UTERM(I),ORDER)
Z=Z+H
TOTAL=TOTAL+2.0*GRAND(Z,NU(I),UAVG(I),EPS,UTERM(I),ORDER)
80 CONTINUE

```

```

Z=Z+H
TOTAL=TOTAL+4.0*GRAND(Z,NU(I),UAVG(I),EPS,UTERM(I),ORDER)
Z=Z+H
TOTAL=TOTAL+1.0*GRAND(Z,NU(I),UAVG(I),EPS,UTERM(I),ORDER)
IF(L.EQ.3) GO TO 90
Determine INT2(I,N,J)
INT2(I,N,J)=TOTAL*H/3.0

```

C SET L=3 TO CONTINUE INTEGRATION TO UPPER LIMIT OF L3

```

L=3
GO TO 70
Determine INT3(I,N,J)
90 INT3(I,N,J)=TOTAL*H/3.0
100 CONTINUE

```

```

C          PRINT OUT RESULTS
DO 790 L=1,2
11=6*L-5
12=6*L-4
13=6*L-3
14=6*L-2
15=6*L-1
16=6*L
DO 780 J=1,6
  IACT=(J-1)*10
  ACT=FLOAT(IACT)
  EPS1=1000.*ACT/(R*T(I1))
  EPS2=1000.*ACT/(R*T(I2))
  EPS3=1000.*ACT/(R*T(I3))
  WRITE(3,605)
  FORMAT(11)
  WRITE(3,606)
  FORMAT(11111)
605  IF(L-1)610,610,620
606  WRITE(3,615)
610  FORMAT(1,2('REACTION',9X,'STEAM',20X), 'REACTION',9X,'STEAM')
615  P1=0.34
      P2=0.65
      GO TO 630
620  WRITE(3,625)
625  FORMAT(1,2('REACTION',9X,'CARBON DIOXIDE',11X), 'REACTION',9X,'CA
      RRON DIOXIDE')
      P1=0.26
      P2=0.6
630  WRITE(3,640)T(I1),T(I2),T(I3)
640  FORMAT(1X,2('NOM. TEMP.',7X,F5.0,' DEG K',15X), 'NOM. TEMP.',7X,F5.
      0,' DEG K')
      WRITE(3,645)P1,P1,P1
645  FORMAT(1X,2('NOM. PRES.',6X,F4.2,' ATM',16X), 'NOM. PRES.',6X,F
      4.2,' ATM')
      WRITE(3,650)NU(I1),NU(I2),NU(I3)
650  FORMAT(1X,2('KINEM. VISC.',5X,F4.2,' SO CM / SEC',8X), 'KINEM. VIS
      IC.',5X,F4.2,' SO CM / SEC')
      WRITE(3,660)UAVG(I1),UAVG(I2),UAVG(I3)
660  FORMAT(1X,2('MAIN AVG. VEL.',3X,F5.2,' CM/SEC',13X), 'MAIN AVG. VEL
      1.',3X,F5.2,' CM/SEC')
      WRITE(3,670)UTERM(I1),UTERM(I2),UTERM(I3)
670  FORMAT(1X,2('TERM. VEL.',7X,F4.2,' CM/SEC',13X), 'TERM. VEL.',7X,F
      4.2,' CM/SEC')
      WRITE(3,680)IACT,IACT,IACT
680  FORMAT(1X,2('ACTIV. ENERGY',4X,I2,' KCAL',15X), 'ACTIV. ENERGY',
      4X,I2,' KCAL')
      WRITE(3,690)EPS1,EPS2,EPS3
690  FORMAT(1X,2('EPSILON',9X,F7.3,19X), 'EPSILON',9X,F7.3)

```

INTEG - p.4

```
WRITE(3,700)
700 FORMAT(/,1X,2(' N',0X,'INT(L2)',0X,'INT(L3)',0X),' N',0X,'INT(L2)',
1,0X,'INT(L3)',/)
DO 730 N=1,9
ORDER=0.25*FLOAT(N-1)
WRITE(3,720)ORDER,INT2(11,N,J),INT3(11,N,J),ORDER,INT2(12,N,J),INT
13(12,N,J),ORDER,INT2(13,N,J),INT3(13,N,J)
720 FORMAT(1X,2(F4.2,3X)E13.5,3X)E13.5,2,3X)E13.5,2X)E13.5)
730 CONTINUE
WRITE(3,740)
740 FORMAT(/,1X,2('-----',6X),'-----',6X),/)
1
IF(L=11750,750,760
750 WRITE(3,615)
GO TO 770
760 WRITE(3,625)
770 WRITE(3,640)T(14),T(15),T(16)
WRITE(3,645)P2,P2,P2
WRITE(3,650)NU(14),NU(15),NU(16)
WRITE(3,660)UAVG(14),UAVG(15),UAVG(16)
WRITE(3,670)UTERM(14),UTERM(15),UTERM(16)
WRITE(3,680)IACI,IACI,IACI
WRITE(3,690)EPS1,EPS2,EPS3
WRITE(3,700)
DO 775 N=1,9
ORDER=0.25*FLOAT(N-1)
775 WRITE(3,720)ORDER,INT2(14,N,J),INT3(14,N,J),ORDER,INT2(15,N,J),INT
15(15,N,J),ORDER,INT2(16,N,J),INT3(16,N,J)
780 CONTINUE
790 CONTINUE
WRITE(3,605)
C STORE INT2, INT3 AND T ON FILES
C FOR USE BY PROGRAM LNI
WRITE(2,1)INT2
WRITE(3,1)INT3
WRITE(4,1)I
CALL EXIT
END
// DUP WS UA INTEG
*STORE
// DUP UA MD002 0012
*DFILE UA MD003 0012
*DFILE UA MD004 0001
```

LNI - P.1

```

// FOR
NAME LNI
*TOCSIDISK,CARD,1132PRINTER)

C LNI IS USED FOLLOWING PROGRAM INTEG. TO FIT EACH
C SET OF INTEGRALS TO THE EQUATION
C LN I(T,L,E,N) = I1(T,L,E + I3(T,L,N) * I4(T,L)
C THIS LINEARIZATION OF I(T,L,E,N) IS GENERALLY ACCURATE
C TO WITHIN +/- 3 PERCENT.
C BY USING THIS LINEARIZATION OF I(T,L,E,N), THE INTEGRATED
C POWER-LAW KINETIC RATE EQUATION BECOMES LINEAR
C IN THE 3 UNKNOWN OBSERVED KINETIC PARAMETERS
C 1. ARRHENIUS FREQUENCY FACTOR, A
C 2. ACTIVATION ENERGY, E
C 3. ORDER OF REACTION, N

REAL L2,L3
REAL INT2(12,9,6), INT3(12,9,6)
INTEGER FLAG
DIMENSION T(12)
DIMENSION XTRX2(3,3)
DIMENSION XTRY2(3), XTRY3(3)
DIMENSION XKIN2(3,3)
DIMENSION B2(3), B3(3)
THE FILES CONTAIN THE ARRAYS INT2, INT3 AND T
FROM PROGRAM INTEG.
DEFINE FILE 2(12,1080),IN2)3(12,1080),IN3)4(1,24,0),ITEMP)

C READ INT2, INT3, AND T FROM THE DISK
C READ(2,1)INT2
C READ(3,1)INT3
C READ(4,1)T

C SET-UP OUTPUT PAGE
WRITE(9,990)
990 FORMAT(1)
WRITE(9,905)
905 FORMAT(1)
WRITE(9,910)
910 FORMAT(17X,'LINEAR APPROXIMATION FOR I(T,L,E,N) / I6X,'LN I = I1(L
1,1)*E + I3(L,T)*N + I4(L,T) / I6X,'
2-----)
WRITE(9,920)
920 FORMAT(17X,'TEMP. PRES. SEP.'N,9X,'LINEARIZATION CONSTANTS')
930 FORMAT(1X,'REACTION',10X,'(K) (ATM) (CM)',6X,'I1',7X,'I3',8X
1,14)
WRITE(9,940)
940 FORMAT(17X,'',9X,'
1-----)

```

LNI - p.2

```

C THE METHOD TO BE USED TO DETERMINE I1, I3 AND I4
C WILL BE A LEAST-SQUARES FIT.
C CONSIDER  $Y(I) = B(1) + B(2)*X(I,2) + B(3)*X(I,3)$  FOR
C EACH OF I SETS OF POINTS.
C Y IS THE DEPENDENT (OBSERVED) VARIABLE.
C X(2) AND X(3) ARE THE INDEPENDENT VARIABLES.
C R(1), B(2) AND R(3) ARE THE LEAST-SQUARE FIT
C PARAMETERS THAT BEST CORRELATE Y AND X IN THE EQUATION.
C FOR THIS APPLICATION
C Y IS LN ( I*(1+E*N) )
C X(2) IS E (ACTIVATION ENERGY, KCAL)
C X(3) IS N (ORDER OF REACTION)
C R IS THE COLUMN VECTOR OF LENGTH 3, CONTAINING
C THE LEAST-SQUARE FIT PARAMETERS.
C B(1) IS I4(T,L)
C R(2) IS I1(T,L)
C B(3) IS I3(T,L)
C THE SOLUTION FOR R IS GIVEN BY
C  $B = INVERSE(X-TRANPOSE * X) * (X-TRANPOSE * Y)$ 
C THE CORRESPONDING ARRAYS IN THIS PROGRAM ARE
C XTRX2 X-TRANPOSE * X
C XKIN2 INVERSE OF X-TRANPOSE * X
C XTRY2 X-TRANPOSE * Y, FOR CORRELATING INT2
C XTRY3 X-TRANPOSE * Y, FOR CORRELATING INT3
C R2 LEAST-SQUARE FIT PARAMETERS FOR INT2
C R3 LEAST-SQUARE FIT PARAMETERS FOR INT3

C I CORRESPONDS TO SETS OF DATA, AS EXPLAINED IN INTEG.
C H2O GASIFICATION, I = 1 THRU 6
C CO2 GASIFICATION, I = 7 THRU 12
C DO 900 I=1,12

C INITIALIZE VECTORS
C DO R05 J=1,9
C XTRY2(I)=0.0
C XTRY3(I)=0.0
C 805 CONTINUE

C K CORRESPONDS TO THE ORDER OF REACTION N = 0.25 * (K-1).
C FOR H2O GASIFICATION, INTEGRALS FOR N (ORDER OF REACTION)
C BETWEEN 0.0 AND 2.0 WILL BE CORRELATED.
C FOR CO2 GASIFICATION, INTEGRALS FOR N
C BETWEEN 0.0 AND 1.0 WILL BE CORRELATED.
C M WILL INDICATE THIS.
C M=5
C IF(I,LE,6)M=9
C DO R20 K=1,M
C ORDER=0.25*FLOAT(K-1)

C J CORRESPONDS TO THE ACTIVATION ENERGY E, KCAL = 10 * (J-1)
C DO R20 J=1,5
C E=10.0*FLOAT(J-1)

```

LNI - p.3

```
C      COMPIL XTRY2 AND XTRY3
      Y2=ALOG(INT2(I,K,J))
      Y3=ALOG(INT3(I,K,J))
      XTRY2(1)=XTRY2(1)+Y2
      XTRY3(1)=XTRY3(1)+Y3
      XTRY2(2)=XTRY2(2)+Y2+E
      XTRY3(2)=XTRY3(2)+Y3+E
      XTRY2(3)=XTRY2(3)+Y2+ORDER
      XTRY3(3)=XTRY3(3)+Y3+ORDER
      820
```

```
C      COMPIL XTRX2
      IF (I.GE.7)GO TO 825
      XTRX2(1,1)=54.
      XTRX2(1,2)=1350.
      XTRX2(1,3)=54.
      XTRX2(2,2)=49500.
      XTRX2(3,3)=76.5
      XTRX2(2,3)=1350.
      GO TO 826
      825 XTRX2(1,1)=30.
      XTRX2(1,2)=750.
      XTRX2(1,3)=15.
      XTRX2(2,2)=27500.
      XTRX2(3,3)=11.25
      XTRX2(2,3)=375.
      826 CONTINUE
      XTRX2(2,1)=XTRX2(1,2)
      XTRX2(3,1)=XTRX2(1,3)
      XTRX2(3,2)=XTRX2(2,3)
```

```
C      COMPUTE XXIN2
      CALL INVS(XTRX2,XXIN2,3,FLAG)
      COMPUTE B2 AND B3
      CALL MULT(XXIN2,XTRY2,82,3,3,1)
      CALL MULT(XXIN2,XTRY3,83,3,3,1)
```



LNI - p.4

```

C      PRINT OUT RESULTS
      ITEM=IFIX(T(1))
      L2=11.4
      L3=15.2
      IF(1.0E-7)GO TO 860
      P1=0.34
      P2=0.65
      PRES=P2
      IF(1.0E-3)PRES=P1
      WRITE(3,840)ITEM,PRES,L2,B2(2),B2(3),B2(1)
      WRITE(3,840)ITEM,PRES,L3,B3(2),B3(3),B3(1)
840  FORMAT(' STEAM',12X,14.4X,F4.2,4X,F4.1,4X,F7.6,3X,F7.5,3X,F6.3)
      IF(1.0E-6) WRITE(3,850)
850  FORMAT(/)
      GO TO 900
860  P1=0.26
      P2=0.6
      PRES=P2
      IF(1.0E-9)PRES=P1
      WRITE(3,870)ITEM,PRES,L2,B2(2),B2(3),B2(1)
      WRITE(3,870)ITEM,PRES,L3,B3(2),B3(3),B3(1)
870  FORMAT(' CARBON DIOXIDE',3X,14.4X,F4.2,4X,F4.1,4X,F7.6,4X,F7.5,3X,
1F6.3)
900  CONTINUE
      WRITE(3,990)
      CALL EXIT
      END

```

// DUP WS UA LNI \*STORE

Deck for INTEG/LNI

```
// JOB
// XEQ INTEG      01
*FILES(2,MD002),(3,MD003),(4,MD004)
2.44 4.72 24.75 1473.    P1 STEAM
3.29 4.21 29.79 1773.    P1 STEAM
4.35 3.80 35.46 2113.    P1 STEAM
2.82 4.97 25.59 1473.    P2 STEAM
3.84 4.39 30.73 1773.    P2 STEAM
5.14 3.91 36.62 2113.    P2 STEAM
2.00 4.49 26.22 1473.    P1 CARBON DIOXIDE
2.69 4.01 31.33 1773.    P1 CARBON DIOXIDE
3.55 3.62 36.85 2113.    P1 CARBON DIOXIDE
1.74 4.39 26.75 1473.    P2 CARBON DIOXIDE
2.36 3.90 30.20 1773.    P2 CARBON DIOXIDE
3.12 3.50 35.74 2113.    P2 CARBON DIOXIDE
// XEQ LNI      01
*FILES(2,MD002),(3,MD003),(4,MD004)
// *END JOB
```

AVFIT - P.1

```

// FOR
*IOCSIDISK,CARD,1132PRINTER)
*NAME AVFIT
C
C THIS PROGRAM FINDS THE LEAST SQUARE FIT FOR THE OBSERVED
C KINETIC PARAMETERS A, N, E
C IN THE (INTEGRATED) RATE EQUATION
C  $-\ln(1.0 - X(L)/1.0 - X(L)) = A * (C^{**N}) * I(T, E, N, L)$ 
C WHERE X IS THE D.A.F. FRACTIONAL CONVERSION OF THE CHAR
C C IS THE PULK PHASE CONCENTRATION OF H2O OR CO2 (MOLE/CC)
C L IS THE FEEDER-TO-COLLECTOR SEPARATION (CM)
C N IS THE ORDER OF REACTION
C E IS THE ACTIVATION ENERGY (KCAL)
C A IS THE ARRHENIUS FREQUENCY FACTOR
C  $I(T, E, N, L)$  IS THE INTEGRAL WHICH ACCOUNTS FOR THE
C NON-ISOTHERMIVITY ALONG THE REACTOR AXIS AND
C THE DEVELOPMENT OF THE MAIN GAS VELOCITY PROFILE.
C I IS LINEARIZED IN THE FORM
C  $\ln I = I1(T, L)*E + I3(T, L)*N + I4(T, L)$ 
C
C BY TAKING THE NATURAL LOGARITHM OF THE INTEGRATED RATE EQUATION
C AND RE-ARRANGING TERMS, THE EQUATION IS SEEN TO BE OF THE FORM
C  $Y = B(0) + B(1)*X(1) + B(2)*X(2)$ 
C WHERE B(0), B(1), B(2) ARE THE PARAMETERS TO BE DETERMINED
C X(1), X(2) ARE THE INDEPENDENT VARIABLES, AND
C Y IS THE DEPENDENT (OBSERVED) VARIABLE.
C FOR THIS ANALYSIS
C B(0) = LN(A)
C B(1) = ORDER OF REACTION, N
C B(2) = ACTIVATION ENERGY, E (KCAL)
C X(1) = LN(C) + I3(L, T)
C X(2) = I1(L, T)
C Y = LN (-LN((1-X(L))/(1-X(L1)))) - I4
C
REAL MSRFG
REAL INT1(3,2,3), INT3(3,2,3), INT4(3,2,3)
REAL I1(15), I3(15), I4(15)
REAL MSSGE(60)
INTEGER T(15)
INTEGER TNOM(15), PNOM(15), LNOM(15)
DIMENSION R(3)
DIMENSION CONC(15,2)
DIMENSION P(15)
DIMENSION NO(15)
DIMENSION RESID(15), RESO(15)
DIMENSION SEP(15)
DIMENSION WT(15,3)
DIMENSION XTR(3,3), XTRY(3), XXINV(3,3)
DIMENSION XHAT(15)
DIMENSION Y(15), YHAT(15)
COMMON A, ORDER, ACTIV, MSSGE

```

AVFIT - p.2

```

C      R IS THE GAS CONSTANT (CC*ATH/(MOLE*DEG K))
      P=82.057

C      CODE IS THE 1-LETTER DESIGNATION FOR THE REACTION.
C      S = STEAM
C      C = CARBON DIOXIDE
      READ(2,5)CODE
      5 FORMAT(A1)

C      MSGGE IS A 3-CARD MESSAGE TO BE PRINTED AS A HEADING.
      READ(7,6)YSSGE
      6 FORMAT(20A4)

C      READ IN THE CONSTANTS I1, I3, I4 FOR THE EQUATION
      LN I = I1(L,T)*E + I3(L,T)*N + I4(L,T)
      DO 20 I=1,17
      READ(2,15)IT,IP,IL,C1,C3,C4
      15 FORMAT(5X,I1,2X,I1,2X,I1,8X,3F10.5)
      IT REPRESENTS THE NOMINAL TEMPERATURE
      IP REPRESENTS THE NOMINAL PRESSURE
      IL REPRESENTS THE NOMINAL FEEDER-COLLECTOR SEPARATION
      (SEE COMMENTS IN SECTION WHERE RUN DATA ARE READ IN)
      INT1(IT,IP,IL)=C1
      INT3(IT,IP,IL)=C3
      INT4(IT,IP,IL)=C4
      20 CONTINUE

C      M WILL BE THE NUMBER OF RUNS (OR DATA POINTS) BEING ANALYZED.
C      INITIALIZE YSUM AND Y50, WHERE
C      YSUM IS THE SUM OF ALL Y(I)      I=1,2,...,M
C      Y50 IS THE SUM OF TERMS Y(I)**2  I=1,2,...,M
      YSUM=0.
      Y50=0.

C      READ IN RUN DATA
      V=0
      M=M+1
      READ(2,40)NO(M),TNOM(M),PNOM(M),P(M),LNOM(M),WT(M,1),WT(M,2)
      40 FORMAT(12,2I2X,I1),F5.2,2X,I1,2F5.1)
      NO(M) IS THE RUN NUMBER FROM THE MAIN DATA LISTINGS.
      (NO IS SET TO 99 FOR DATA POINTS.)
      IF(NO(M).EQ.0) GO TO 50
      TNOM(M) INDICATES THE NOMINAL TEMPERATURE (DEG K) OF RUN M
      IF(TNOM(M).EQ.1) T(M)=1473
      IF(TNOM(M).EQ.2) T(M)=1773
      IF(TNOM(M).EQ.3) T(M)=2113
      LNOM(M) INDICATES THE FEEDER-COLLECTOR SEPARATION (CM) FOR RUN M
      IF(LNOM(M).EQ.2) SEP(M)=11.6
      IF(LNOM(M).EQ.3) SEP(M)=15.2

```

AVFIT - p.3

```

C      P(M) IS THE OXIDANT PARTIAL PRESSURE (ATM) IN RUN M.
C      CONC(M,1)=P(M)/(R*T(M))
C      CONC(M,2) IS THE NATURAL LOG OF CONC(M,1)
C      WT(M,1) IS THE D.A.F. PERCENT WEIGHT LOSS FOR RUN M (T.P.L)
C      WT(M,2) IS THE AVERAGE PERCENT D.A.F. WEIGHT LOSS AT (T.P.L1)
C      DEFINE WT(M,3)
C      WT(M,3)=(100.-WT(M,1))/(100.-WT(M,2))

C      ASSOCIATE THE PROPER CONSTANTS I1,I3,I4 FOR EACH RUN
C      NOM1=INOM(Y)
C      NOM2=PNOM(M)
C      NOM3=LNOW(M)
C      I1(M)=INT1(NOM1,NOM2,NOM3)
C      I3(M)=INT3(NOM1,NOM2,NOM3)
C      I4(M)=INT4(NOM1,NOM2,NOM3)

C      DEFINE Y(M)
C      Y(M)=1.0*ALOG(WT(M,3))
C      Y(M)=ALOG(Y(M))-I4(M)
C      CONTINUE CALCULATING YSUM, YSO
C      YSUM=YSUM+Y(M)
C      YSO=YSO+Y(M)*Y(M)
C      READ IN DATA FOR THE NEXT RUN
C      GO TO 30

C      DEFINE M AS THE TOTAL NUMBER OF RUNS BEING CONSIDERED
C      M=M-1
C      YEAR IS THE AVERAGE VALUE OF Y(I)
C      YBAR=YSUM/FLOAT(M)

C      ARRAY X(M,3) IS THE INDEPENDENT VARIABLE MATRIX
C      X(I,1) = 1.0 FOR ALL I      I=1,2,...,M
C      X(I,2) = LN(C) + I3(I)
C      X(I,3) = I1(I)
C      Y IS THE COLUMN VECTOR OF Y(I)      I=1,2,...,M
C      XTRY(3) IS THE MATRIX PRODUCT OF X-TRANPOSE * Y
C      XTRY(1) = YSUM
C      XTRY(2) IS THE SUM OF TERMS, Y(I)*X(I,2)
C      XTRY(3) IS THE SUM OF TERMS, Y(I)*X(I,3)
C      XTRX(3,3) IS THE MATRIX PRODUCT OF X-TRANPOSE * X
C      XTRX(1,1) = M
C      XTRX(1,2) = XTRX(2,1) IS THE SUM OF TERMS, X(I,2)
C      XTRX(1,3) = XTRX(3,1) IS THE SUM OF TERMS, X(I,3)
C      XTRX(2,2) IS THE SUM OF TERMS, X(I,2)**2
C      XTRX(3,3) IS THE SUM OF TERMS, X(I,3)**2
C      XTRX(2,3) = XTRX(3,2) IS THE SUM OF TERMS, X(I,2)*X(I,3)

```

AVFIT - p.4

```
C      XXINV IS THE MATRIX INVERSE OF XTRX
C      THE COLUMN VECTOR B(3) OF LEAST SQUARE FIT PARAMETERS
C      IS GIVEN BY
C      B = INVERSE (X-TRANPOSE * X) * (X-TRANPOSE * Y)
C
C      INITIALIZE XTRX AND XTRY
DO 60 I=1,3
  XTRY(I)=0.0
DC 60 J=1,3
60 XTRX(I,J)=0.0
C
C      CALCULATE THE TERMS IN XTRX AND XTRY
DO 70 I=1,N
  XTRX(1,2)=XTRX(1,2)+CONC(I,2)+I3(I)
  XTRX(1,3)=XTRX(1,3)+I1(I)
  XTRX(2,2)=XTRX(2,2) + (CONC(I,2)+I3(I))**2.
  XTRX(2,3)=XTRX(2,3) + (CONC(I,2)+I3(I))*I1(I)
  XTRX(3,3)=XTRX(3,3)+I1(I)**2.
  XTRY(2)=XTRY(2) + (CONC(I,2)+I3(I))*Y(I)
  XTRY(3)=XTRY(3)+I1(I)*Y(I)
70 CONTINUE
  XTRX(1,1)=FLOAT(M)
  XTRX(2,1)=XTRX(1,2)
  XTRX(3,1)=XTRX(1,3)
  XTRX(3,2)=XTRX(2,3)
  XTRY(1)=YSUM
C      CALCULATE XXINV
CALL INVR(XTRX,XXINV,3,IFLAG)
IF(IFLAG.EQ.1)GO TO 1000
C      CALCULATE THE PARAMETER VECTOR B
CALL MULT(XXINV,XTRY,R,3,3,1)
C
C      DEFINE THE KINETIC PARAMETERS
C      A      ARRHENIUS FREQUENCY FACTOR ( (SEC**--1)*(MOLE/CC)**--N )
C      ORDER OF REACTION
C      ACTIV ACTIVATION ENERGY (KCAL)
A=EXP(R(1))
ORDER=R(2)
ACTIV=B(3)
```

AVFIT - p.5

```

C      BEGIN LINEAR REGRESSION ANALYSIS
C      YHAT(I) IS THE VALUE OF Y(I) PREDICTED BY THE LEAST SQUARE FIT MODEN.
C      HAT IS THE SUM OF TERMS, YHAT(I)      I=1,2,...,M
C      HATSO IS THE SUM OF TERMS, YHAT(I)**2
C      RESID(I) IS THE RESIDUAL (Y - YHAT) OF RUN I
C      RESQ(I) IS THE SQUARE OF RESID(I)
C      RSUM IS THE SUM OF TERMS, RESQ(I)
C      R2SUM IS THE SUM OF TERMS, RESQ(I)
C      XHAT(I) IS THE PREDICTED D.A.F. PERCENT WEIGHT LOSS
C      AT THE CONDITIONS (T,P,L) OF RUN I

C      INITIALIZE SUMMATIONS
      HAT=0.0
      HATSO=0.0
      RSUM=0.0
      R2SUM=0.0
C      COMPUTE REGRESSION SUMS
      DO 190 I=1,M
      YHAT(I) = B(1) + B(2)*(CONC(I,2)+I3(I)) + B(3)+I1(I)
      RESID(I)=Y(I)-YHAT(I)
      RESQ(I)=RESID(I)**2.0
      HAT=HAT+YHAT(I)
      HATSO=HATSO+YHAT(I)**2.0
      RSUM=RSUM+RESQ(I)
      R2SUM=R2SUM+RESQ(I)
C      CALCULATE XHAT(I)
      XHAT(I)=YHAT(I)+I4(I)
      XHAT(I)=1.0*EXP(XHAT(I))
      XHAT(I)=EXP(XHAT(I))*100.-WT(I,2)
      XHAT(I)=1.0*XHAT(I)+100.
190 CONTINUE

C      CALCULATE TERMS FOR THE ANALYSIS OF VARIANCE TABLE
C      THE TOTAL SUM OF SQUARES (UNCORRECTED FOR THE MEAN, YBAR) IS YSQ.
C      WITH M DEGREES OF FREEDOM.
C      SS AVG IS THE CORRECTION FOR THE MEAN (1 DEGREE OF FREEDOM).
C      SS AVG=M*YBAR**2.
C      SS IS THE TOTAL (CORRECTED) SUM OF SQUARES (M-1 DEGREES OF FREEDOM)
      M=M-1
      SS=YSQ-SSAVG
C      SSREG (SUM OF SQUARES DUE TO REGRESSION, 2 DEGREES OF FREEDOM),
C      IS THE SUM OF TERMS, (YHAT(I)-YBAR)**2, WHICH EQUALS HATSO-SSAVG.
      SSREG=HATSO-SSAVG
C      WSREG IS THE MEAN SQUARE DUE TO REGRESSION
      WSREG=SSREG/2.
C      THE SUM OF SQUARES ABOUT THE REGRESSION IS R2SUM,
C      WITH M-3 DEGREES OF FREEDOM (SUM OF RESIDUALS SQUARED).
      M=M-3
      S2=(R2SUM/MM)

```

```

C THE F RATIO IS THE QUOTIENT,
C W.S. DUE TO REGRESSION / M.S. ABOUT THE REGRESSION
C F=MSREG/S2
C R2 (READ R SQUARED), IS THE RATIO
C S.S. DUE TO REGRESSION / S.S. (TOTAL, CORRECTED)
C R2 CLOSE TO UNITY INDICATES A GOOD FIT TO THE REGRESSION MODEL.
C R2=SSREG/S5

```

```

C PRINT TABLE OF RUN DATA
C WRITE(3,199)
C WRITE(3,198)
C WRITE(3,200)MSGGE
C WRITE(3,291)
C WRITE(3,200)
C WRITE(3,220)
C FORMAT(1):
C 198 FORMAT(///)
C 290 FORMAT(21X,20A4)
C 291 FORMAT(' ',20X,'
1-----')
C 200 FORMAT(///)
C 201 X MAT,7X,Y,10X,Y MAT,7X,RESIDUAL,1)
C 220 FORMAT(
1-----')
C DO 370 I=1,M
C WRITE(3,360) CODE,NO(I),T(I),P(I),CONC(I,1),SEP(I),WT(I,1),WT(I,2)
C 1),XHAT(I),Y(I),YHAT(I),RESID(I)
C 360 FORMAT(3X,2X,A1,'-',12,17,F6.2,2X,E11.3,F7.1,F6.1,F7.1,F9.2,3(2X,E
11.3))
C 370 CONTINUE

```

```

C PRINT LEAST-SQUARE FIT OBSERVED KINETIC PARAMETERS
C WRITE(3,550)M
C WRITE(3,551)
C WRITE(3,570)A
C WRITE(3,580)ORDER
C WRITE(3,590)ACTIV
C 550 FORMAT(///20X,'BEST PARAMETER FIT - ',13,' POINTS ')
C 551 FORMAT(20X,'-----')
C 570 FORMAT(26X,'PRE-EXP FACTOR',6X,E11.9,' ((G/SEC*G)*(MOLE/CC)**-N)
1),)
C 580 FORMAT(26X,'ORDER OF RXN',8X,E11.3)
C 590 FORMAT(26X,'ACTIV. ENERGY',7X,E11.3,' KCAL/MOLE')

```



```

C      PRINT ANALYSIS OF VARIANCE TABLE
      WRITE(3,410)
      WRITE(3,415)
      WRITE(3,420)
      WRITE(3,430)
      WRITE(3,440)
      410 FORMAT(///'36X,' ANALYSIS OF VARIANCE TABLE')
      415 FORMAT(36X,'-----'//)
      420 FORMAT(14X,'SOURCE OF',8X,'DEGREES OF')
      430 FORMAT(14X,'VARIATION',10X,'FREEDOM',6X,'SUM OF SQUARES',5X,'MEAN
      1 SQUARE',7X,'F RATIO')
      440 FORMAT(18X,'-----',8X,'-----',5X,'-----',5X,'-----
      1-----',7X,'-----'//)
      WRITE(3,450)M,YSC
      WRITE(3,460)SSAVG
      WRITE(3,470)MM,SS
      WRITE(3,480)SSREG,MSREG,F
      WRITE(3,490)MM,R2SUM,S2
      450 FORMAT(12X,' TOTAL (UNCORRECTED)',7X,I2, 9X,E15.7)
      460 FORMAT(12X,' MEAN (B(0))',16X,I1,9X,E15.7)
      470 FORMAT(12X,' TOTAL (CORRECTED)',9X,I2, 9X,E15.7)
      480 FORMAT(12X,' REGRESSION (R/R(0))',8X,I2,9X,E15.7,4X,E11.3,5X,E11.
      13)
      490 FORMAT(12X,' RESIDUAL',18X,I2,9X,E15.7,4X,E11.3/)
      WRITE(3,500)R2
      500 FORMAT(12X,' R SQUARED = ',F7.3)
      1000 CALL EXIT
      END

// DUP      WS UA AVFIT
*STORE

```

Deck for AVFIT (CO<sub>2</sub> Gasification)

```

// JOB
// XEQ AVFIT 01
*LOCALAVFIT,INVR,S,MULT
CARBON DIOXIDE

      C02 GASIFICATION OF FOSTER-WHEELER CHAR
      NOMINAL TEMPERATURES OF RUNS - 1473, 1773, 2113 DEG K
      (EXCLUDES RUNS C-10*16)
C02 T1 P1 L2 -0.3590 0.04947 -2.60R
C02 T1 P1 L3 -0.3689 0.07645 -1.920
C02 T1 P2 L2 -0.3590 0.04945 -2.609
C02 T1 P2 L3 -0.3689 0.07637 -1.923
C02 T2 P1 L2 -0.2984 0.04987 -2.772
C02 T2 P1 L3 -0.3073 0.07894 -2.073
C02 T2 P2 L2 -0.2984 0.04984 -2.728
C02 T2 P2 L3 -0.3073 0.07888 -2.030
C02 T3 P1 L2 -0.2504 0.05019 -2.927
C02 T3 P1 L3 -0.2584 0.08111 -2.220
C02 T3 P2 L2 -0.2504 0.05016 -2.889
C02 T3 P2 L3 -0.2584 0.08103 -2.183
99 T1 P1 0.26 L2 1.8 -1.5
99 T1 P1 0.26 L3 4.2 -1.5
99 T1 P2 0.53 L2 7.3 4.8
99 T1 P2 0.53 L3 12.9 4.8
99 T2 P1 0.26 L2 23.8 14.5
99 T2 P1 0.26 L3 29.4 14.5
99 T2 P2 0.60 L2 22.9 11.5
99 T2 P2 0.60 L3 33.4 11.5
99 T3 P1 0.26 L2 41.2 20.9
99 T3 P1 0.26 L3 48.5 20.9
99 T3 P2 0.57 L2 44.6 25.0
99 T3 P2 0.57 L3 64.0 25.0
00
// *END JOB

```

(LAST RUN DATA CARD)

// \*ENDJOB

Deck for AVFIT (Steam Gasification)

```

// JOR
// XEQ AVFIT 01
*LOCALAVFIT,INVR,MULT
STEAM
          STEAM GASIFICATION OF FOSTER-WHEELER CHAR
          NOMINAL TEMPERATURES OF RUNS - 1473, 1773, 2113 DEG K
          (EXCLUDES RUNS S-33,34,39,41,58)
H20 T1 P1 L2      -0.3590      0.04963      -2.579
H20 T1 P1 L3      -0.3693      0.07749      -1.881
H20 T1 P2 L2      -0.3591      0.04965      -2.621
H20 T1 P2 L3      -0.3693      0.07754      -1.922
H20 T2 P1 L2      -0.2984      0.05003      -2.746
H20 T2 P1 L3      -0.3076      0.08003      -2.037
H20 T2 P2 L2      -0.2984      0.05005      -2.784
H20 T2 P2 L3      -0.3077      0.08012      -2.074
H20 T3 P1 L2      -0.2505      0.05035      -2.908
H20 T3 P1 L3      -0.2587      0.08225      -2.192
H20 T3 P2 L2      -0.2505      0.05037      -2.946
H20 T3 P2 L3      -0.2588      0.08232      -2.228
99 T1 P1 0.33 L2  4.5  1.1
99 T1 P1 0.33 L3  7.5  1.1
99 T1 P2 0.65 L2 11.6  5.0
99 T1 P2 0.65 L3 26.6  5.0
99 T2 P1 0.32 L2 34.5 22.4
99 T2 P1 0.32 L3 44.9 22.4
99 T2 P2 0.65 L2 51.2 27.2
99 T2 P2 0.65 L3 72.2 27.2
99 T3 P1 0.32 L2 55.7 31.9
99 T3 P1 0.32 L3 66.7 31.9
99 T3 P2 0.65 L2 59.6 28.5
99 T3 P2 0.65 L3 78.1 28.5
00
// *END JOR
(LAST RUN DATA CARD)

```

INVRS

```

// FOR
SUBROUTINE INVRS(A,AINV,N,IFLAG)
C INVRS CALCULATES AINV, THE INVERSE OF MATRIX A.
C THE SUBROUTINE IS SET TO HANDLE UP TO A 3 X 3 MATRIX, BUT
C CAN BE ADJUSTED TO HANDLE ANY N X N MATRIX THAT IS
C INVERTIBLE, BY CHANGING THE DIMENSION STATEMENT.
INTEGER COL,ROW
DIMENSION A(3*3), AINV(3*3)
TEST=1.0E-05
IFLAG=0
DO 20 I=1,N
DO 20 J=1,N
20 AINV(I,J)=0.0
DO 30 I=1,N
30 AINV(I,1)=1.0
DO 200 COL=1,N
MAX=ARS(A(COL,COL))
MAX=COL
DO 50 ROW=COL,N
CHECK=ARS(A(ROW,COL))
IF(CHECK=MAX)50,50,40
40 MAX=ROW
50 CONTINUE
60 IF(A*MAX-TEST)60,60,80
60 WRITE(3,70)MAX
70 FORMAT(//3(' MATRIX NOT INVERTIBLE'//)E12.4)
IFLAG=1
RETURN
80 IF(MAX=COL)110,110,90
90 DO 100 K=1,N
HOLD=A(MAX,K)
A(MAX,K)=A(COL,K)
A(COL,K)=HOLD
HOLD=AINV(MAX,K)
AINV(MAX,K)=AINV(COL,K)
100 AINV(COL,K)=HOLD
110 CONTINUE
DIV=A(COL,COL)
DO 120 K=1,N
A(COL,K)=A(COL,K)/DIV
120 AINV(COL,K)=AINV(COL,K)/DIV
DO 150 ROW=1,N
IF(ROW=COL)130,150,130
130 IF(A(ROW,COL))140,150,140
140 XMULT=A(ROW,COL)
DO 145 K=1,N
A(ROW,K)=A(ROW,K)-XMULT*A(COL,K)
145 AINV(ROW,K)=AINV(ROW,K)-XMULT*AINV(COL,K)
150 CONTINUE
200 CONTINUE
RETURN
END
// DUP
*STORE WS UA INVRS

```

MULT

```

// FOR
C SUBROUTINE MULT (X,Y,XY,M,N,P)
C MULT CALCULATES XY, THE MATRIX PRODUCT OF
C AN M X N MATRIX X, AND AN N X P MATRIX Y.
C XY IS OF DIMENSION M X P.
C THE SUBROUTINE CAN HANDLE X AND Y UP TO DIMENSIONS 3 X 3.
C BUT CAN BE ADJUSTED TO HANDLE LARGER MATRICES BY
C CHANGING THE DIMENSION STATEMENTS.
C INTEGER P
C DIMENSION X(3,3)
C DIMENSION Y(3,3)
C DIMENSION XY(3,3)
C DO 60 I=1,M
C DO 60 J=1,P
C SUM = 0.0
C DO 50 K=1,N
C SUM=SUM+X(I,K)*Y(K,J)
50 XY(I,J)=SUM
60 CONTINUE
RETURN
END

// DUP
*STORE WS UA MULT
    
```

LITERATURE REFERENCES

1. Abramowitz, M. and Stegun, I.A. (editors), Handbook Of Mathematical Functions, U.S. Dept. of Commerce (1972).
2. Austin, L.G. and Walker, P.L., Jr., "Effect of Carbon Monoxide in Causing Nonuniform Gasification of Graphite by Carbon Dioxide," AIChE J., 9(3), 303 (1963).
3. Balzhiser, R.E., Samuels, M.R. and Eliassen, J.D., Chemical Engineering Thermodynamics, Prentice-Hall, Englewood, N.J. (1972).
4. Banchik, I.N., "The Winkler Process for the Production of Low-BTU Gas From Coal," Proc. 2nd Clean Fuels Coal Symp., Institute of Gas Technology, Chicago (1975).
5. Berger, J., Siemieniowska, T. and Tomkow, K., "Development of Porosity in Brown-Coal Chars on Activation with Carbon Dioxide," Fuel, 55(1), 9 (1976).
6. Biederman, D.L., Miles, A.J., Vastola, F.J. and Walker, P.L., Jr., "Carbon - Carbon Dioxide Reaction: Kinetics at Low Pressures and Hydrogen Inhibition," Carbon, 14(6), 351 (1976).
7. Binford, J.S. and Eyring, H., "Kinetics of the Steam - Carbon Reaction," J. Phys. Chem., 60(4), 486 (1956).
8. Bird, R.B., Stewart, W.E. and Lightfoot, E.N., Transport Phenomena, John Wiley & Sons, New York (1960).
9. Blackwood, J.D., "The Kinetics of Carbon Gasification," The Industrial Chemist, 36, 55, 129, 171 (1960).
10. Blake, J.H., Bopp, G.R., Jones, J.F., Miller, M.G. and Tambo, W., "Aspects of the Reactivity of Porous Carbons with Carbon Dioxide," Fuel, 46, 115 (1967).
11. Blakeley, J.P. and Overholser, L.G., "Oxidation of ATJ Graphite by Low Concentrations of Water Vapor and Carbon Dioxide in Helium," Carbon, 3, 269 (1965).
12. Blyholder, G. and Eyring, H., "Kinetics of the Steam - Carbon Reaction," J. Phys. Chem., 63, 693 (1959).

13. Bonner, F. and Turkevich, J., "Study of the Carbon Dioxide-Carbon Reaction Using  $C^{14}$  as a Tracer," J. Am. Chem. Soc., 73(2), 561 (1951).
14. Brown, F., "The Exchange of  $C^{14}$  Between Elementary Carbon and its Oxides," J. Chem. Soc., Faraday Trans., 48, 1005 (1952).
15. Bush, T.W., Dershowitz, M.S., Howard, J.B., Sarofim, A.F. and Serio, M.A., "Gasification of Coal Char with Carbon Dioxide and Steam at 1200-1800°C," Research Report to Phillips Petroleum Co., Bartlesville, Oklahoma (1978).
16. Carberry, J.J., Chemical and Catalytic Reaction Engineering, McGraw-Hill, New York (1976).
17. Clement, J.K., Adams, L.H. and Haskins, C.N., "Essential Factors in the Formation of Producer Gas," U.S. Bur. Mines Bull., 7 (1911).
18. Draper, N.H. and Smith, H., Applied Regression Analysis, John Wiley & Sons, New York (1966).
19. Dupree, W.G., Jr., and West, J.A., United States Energy Through the Year 2000, U.S. Dep. Inter. (1972).
20. Dutta, S., Wen, C.Y. and Belt, R.J., "Reactivity of Coal Char. 1. In Carbon Dioxide Atmosphere," Ind. Eng. Chem., Process Des. Dev., 16(1), 20 (1977).
21. Enzer, H., Dupree, W. and Miller, S., Energy Perspectives, U.S. Dep. Inter. (1975).
22. Ergun, S., "Kinetics of the Reaction of Carbon Dioxide with Carbon," J. Phys. Chem., 60(4), 480 (1956).
23. Ergun, S., "Kinetics of the Reactions of Carbon Dioxide and Steam with Coke," U.S. Bur. Mines Bull., 598 (1962).
24. Fink, C., Curran, G. and Sudbury, J., "CO<sub>2</sub> Acceptor Process Pilot Plant - 1974", Proc. 2nd Clean Fuels Coal Symp., Institute of Gas Technology, Chicago (1975).
25. Fleer, A.W. and White, A.H., "Catalytic Reactions of Carbon with Steam-Oxygen Mixtures," Ind. Eng. Chem., 28, 1301 (1936).

26. Gadsby, J., Hinshelwood, C.N., Sykes, F.R.S. and Sykes, K.W., "The Kinetics of the Reactions of the Steam - Carbon System," Proc. R. Soc. London, Ser. A, 187, 129 (1946).
27. Gadsby, J., Long, F.J., Sleightholm, P. and Sykes, K.W., "The Mechanism of the Carbon Dioxide - Carbon Reaction," Proc. R. Soc. London, Ser. A, 193, 357 (1948).
28. Gan, H., Nandi, S.P. and Walker, P.L., Jr., "Nature of the Porosity in American Coals," Fuel, 51(4), 272 (1972).
29. Given, P.H., "The Distribution of Hydrogen in Coals and Its Relation to Coal Structure," Fuel, 39, 147 (1960).
30. Goring, G.E., Curran, G.P., Tarbox, R.P. and Gorin, E., "Effect of High Temperature Pretreatment on Reactivity of Low Temperature Char to Steam and Carbon Dioxide," Ind. Eng. Chem., 44(5), 1051 (1952).
31. Goring, G.E., Curran, G.P., Tarbox, R.P. and Gorin, E., "Effect of Pressure and Carbon Burnoff on Rate of Interaction of Low Temperature Char with Steam-Hydrogen Mixtures at 1600°F," Ind. Eng. Chem., 44(5), 1057 (1952).
32. Gray, J.A. and Yavorsky, P.M., "The Hydrane Process," Proc. 2nd Clean Fuels Coal Symp., Institute of Gas Technology, Chicago (1975).
33. Gray, M.D. and Kimber, G.M., "Reaction of Charcoal Particles with Carbon Dioxide and Water at Temperatures up to 2800°K," Nature, 214 (May 20, 1967).
34. Gulbransen, E.A., Andrew, K.F. and Brassart, F.A., "Reaction of Graphite with Carbon Dioxide at 1000-1600°C Under Flow Conditions," Carbon, 2, 421 (1965).
35. Harris, L.R. and Yust, C.S., "Transmission Electron Microscope Observations of Porosity in Coal," Fuel, 55(3), 233 (1976).
36. Haynes, W.P. and Forney, A.J., "The Synthane Process," Proc. 2nd Clean Fuels Coal Symp., Institute of Gas Technology, Chicago (1975).
37. Hippo, E. and Walker, P.L., Jr., "Reactivity of Heat-Treated Coals in Carbon Dioxide at 900°C," Fuel, 54, 245 (1975).



38. Hirsch, P.B., "X-ray Scattering from Coals," Proc. R. Soc. London, Ser. A, 226, 143 (1954).
39. Hunt, B.E., Mori, S., Katz, S. and Peck, R.E., "Reaction of Carbon with Steam at Elevated Temperatures," Ind. Eng. Chem., 45, 677 (1953).
40. Jenkins, R.G., Nandi, S.P. and Walker, P.L., Jr., "Reactivity of Heat-Treated Coals in Air at 500°C," Fuel, 52(4), 288 (1973).
41. Johnstone, H.F., Chen, C.Y. and Scott, D.S., "Kinetics of the Steam - Carbon Reaction in Porous Graphite Tubes," Ind. Eng. Chem., 44(7), 1564 (1952).
42. Jolley, L.J. and Pohl, A.J., "Effects of Reactivity and Some Other Variables on Gasification of Coke with Steam," J. Inst. Fuel, 26, 33 (1953).
43. Kayembe, N. and Pulsifer, A.H., "Kinetics and Catalysis of the Reaction of Coal Char and Steam," Fuel, 55, 211 (1976).
44. Kobayashi, H., "Devolatilization of Pulverized Coal at High Temperatures," Ph.D. Thesis, Dept. of Chemical Engineering, Massachusetts Institute of Technology (1976).
45. Laine, N.R., Vastola, F.J. and Walker, P.L., Jr., "The Importance of Active Surface Area in the Carbon - Oxygen Reaction," J. Phys. Chem., 67, 2030 (1963).
46. Langhaar, H.L., "Steady Flow in the Transition Length of a Straight Tube," J. Appl. Mech., A55 (June, 1942).
47. Laurendeau, N.M., "Heterogeneous Kinetics of Coal Char Gasification and Combustion," Prog. Energy Combust. Sci., 4, 221 (1978).
48. Lewis, W.K., Gilliland, E.R. and McBride, G.T., Jr., "Gasification of Carbon by Carbon Dioxide in Fluidized Powder Bed," Ind. Eng. Chem., 41, 1213 (1949).
49. Linares, A., Mahajan, O.P. and Walker, P.L., Jr., "Reactivities of Heat Treated Coals in Steam," Am. Chem. Soc. Div. Fuel Chem. Prepr., 22(1), 1 (1977).
50. Long, F.J. and Sykes, K.W., "The Catalysis of the Oxidation of Carbon," J. Chim. Phys., 47, 361 (1950).

51. Long, F.J. and Sykes, K.W., "The Mechanism of the Steam - Carbon Reaction," Proc. R. Soc. London, Ser. A, 193, 377 (1948).
52. Mandel, G., "Gasification of Coal Char In Oxygen and Carbon Dioxide at High Temperatures," M.S. Thesis, Dept. of Chemical Engineering, Massachusetts Institute of Technology (1977).
53. Mayers, M.A., "The Rate of Oxidation of Graphite by Steam," J. Am. Chem. Soc., 56, 1879 (1934).
54. Mayers, M.A., "The Rate of Reduction of Carbon Dioxide by Graphite," J. Am. Chem. Soc., 56, 70 (1934).
55. Mayers, M.A., "The Reduction of Carbon Dioxide by Graphite and Coke," J. Am. Chem. Soc., 61, 2053 (1939).
56. Menster, M. and Ergun, S., "A Study of the Carbon Dioxide-Carbon Reaction by Oxygen Exchange," U.S. Bur. Mines Bull., 664 (1973).
57. Meyer, L., "The Surface Reaction of Graphite with Oxygen, Carbon Dioxide and Water Vapour at Low Pressures," J. Chem. Soc., Faraday Trans., 34, 1056 (1938).
58. Overholser, L.G. and Blakeley, J.P., "Oxidation of Graphite by Low Concentrations of Water Vapor and Carbon Dioxide in Helium," Carbon, 2, 385 (1965).
59. Patel, J.G. and Loeding, J.W., "IGT U-GAS Process," Proc. 2nd Clean Fuels Coal Symp., Institute of Gas Technology, Chicago (1975).
60. Perry, H., "Coal Conversion Technology," Chem. Eng., 81, 88 (1974).
61. Perry, R.H. and Chilton, C.H. (editors), Chemical Engineers' Handbook, 5th edition, McGraw-Hill, New York (1973).
62. Petersen, E.E., Walker, P.L., Jr., and Wright, C.C., "Surface Area Development Within Artificial Graphite Rods Reacted with Carbon Dioxide from 900° to 1300°C," Ind. Eng. Chem., 47(8), 1629 (1955).
63. Pilcher, J.M., Walker, P.L., Jr. and Wright, C.C., "Kinetic Study of the Steam - Carbon Reaction," Ind. Eng. Chem., 47, 1742 (1955).

64. Reddy, G.N., "Environmental Aspects of Coal Conversion Plant Siting and Cost of Pollution Control," 3rd Intl. Conf. Coal Gasification and Liquefaction, Pittsburgh (1976).
65. Reif, A.E., "The Mechanism of the Carbon Dioxide - Carbon Reaction," J. Phys. Chem., 56(6), 785 (1952).
66. Salvador, L.A. and Holmgren, J.D., "Westinghouse Coal Gasification System," Proc. 5th Conf. Coal Gasification, Liquefaction and Conversion to Electricity, Pittsburgh (1978).
67. Satterfield, C.N., Mass Transfer in Heterogeneous Catalysis, Dept. of Chemical Engineering, Massachusetts Institute of Technology (1970).
68. Schora, F.C., "Progress in HYGAS Process," Coal Processing Technology, 2, 114 (1975).
69. Strange, J.F. and Walker, P.L., Jr., "Carbon - Carbon Dioxide Reaction: Langmuir-Hinshelwood Kinetics at Intermediate Pressures," Carbon, 14(6), 345 (1976).
70. Strickland-Constable, R.F., "The Interaction of Carbon Filaments at High Temperatures with Nitrous Oxide, Carbon Dioxide and Water Vapour," J. Chem. Soc., Faraday Trans., 43, 769 (1947).
71. Thomas, J.M. and Thomas, W.J., Introduction to the Principles of Heterogeneous Catalysis, Academic Press, London (1967).
72. Turkdogan, E.T. and Vinters, J.V., "Kinetics of Oxidation of Graphite and Charcoal in Carbon Dioxide," Carbon, 7, 101 (1969).
73. Turkdogan, E.T., Olsson, R.G. and Vinters, J.V., "Pore Characteristics of Carbons," Carbon, 8, 545 (1970).
74. Tyler, R.J. and Smith, I.W., "Reactivity of Petroleum Coke to Carbon Dioxide Between 1030 and 1180°K," Fuel, 54(2), 99 (1955).
75. U.S. Dept. of Energy, Coal Gasification, quarterly report (Oct.-Dec., 1977).

76. U.S. Dept. of Energy, Monthly Energy Review (Oct., 1978).
77. U.S. Dept. of Energy, "Summary Data Inputs and Forecasts for 1985 and 1990," Energy Information Administration, Annual Report to Congress, v.2 Appendix (1978).
78. Van Heek, K.H., Jüntgen, H. and Peters, W., "Fundamental Studies on Coal Gasification in the utilization of Thermal Energy from Nuclear High-Temperature Reactors," J. Inst. Fuel, 46, 249 (1973).
79. Verma, A., "From Coal to Gas," Chemtech, 378 (June, 1978).
80. Von Fredersdorff, C.G. and Elliott, M.A., "Coal Gasification," in Chemistry of Coal Utilization, H.H. Lowry, editor, John Wiley & Sons, New York (1963).
81. Walker, P.L., Jr. and Hippo, E.J., "Factors Affecting Reactivity of Coal Chars," Am. Chem. Soc. Div. Fuel. Chem. Prepr., 20(3), 45 (1975).
82. Walker, P.L., Jr., and Kini, K.A., "Measurement of Ultrafine Surface Area of Coals," Fuel, 44, 453 (1965).
83. Walker, P.L., Jr. and Raats, E., "Changes in Physical Properties of Graphitized Carbon Rods Upon Gasification with Carbon Dioxide," J. Phys. Chem., 60(3), 364 (1956).
84. Walker, P.L., Jr. and Raats, E., "Effect of Gas Diffusion in Graphitized Carbon Rods on their Gasification Rate with Carbon Dioxide," J. Phys. Chem., 60(3), 370 (1956).
85. Walker, P.L., Jr., Foresti, R.J. and Wright, C.C., "Surface Area Studies of Carbon - Carbon Dioxide Reaction," Ind. End. Chem., 45(8), 1703 (1953).
86. Walker, P.L., Jr., Rusinko, F., Jr. and Austin, L.G., "Gas Reactions of Carbon," in Adv. Catal., D.D. Eley, P.W. Selwood and P.B. Weisz, editors, 11, 133, Academic Press, New York (1959).
87. Warner, B.R., "Mechanism of the Steam - Carbon Reaction," J. Phys. Chem., 65(8), 1447 (1943).
88. Wen, C.Y. and Wu, N.T., "An Analysis of Slow Reactions in a Porous Particle," AIChE J., 22(6), 1012 (1976).

89. Wicke, E., "Contributions to the Combustion Mechanism of Carbon," Proc. Intl. Symp. Combust., 5, 245 (1955).
90. Zielke, C.W. and Gorin E., "Kinetics of Carbon Gasification," Ind. Eng. Chem., 49(3), 396 (1957).
91. \_\_\_\_, "Ash in the Analysis Sample of Coal and Coke," 1978 Annual Book of ASTM Standards, Part 26, Designation D3174-73, Am. Soc. Test. Mater., Philadelphia (1978).